NISTIR 8175

Applied and Computational Mathematics Division

Summary of Activities for Fiscal Year 2016

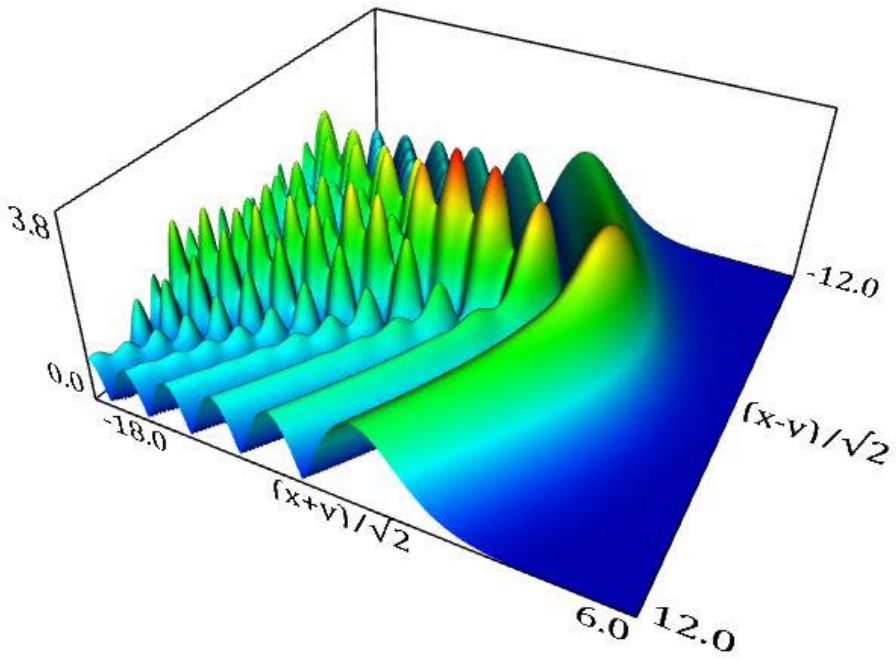

This publication is available free of charge from:
https://doi.org/10.6028/NIST.IR.8175

National Institute of Standards and Technology
U.S. Department of Commerce

NISTIR 8175

Applied and Computational Mathematics Division

Summary of Activities for Fiscal Year 2016

Ronald F. Boisvert, Editor
Applied and Computational Mathematics Division
Information Technology Laboratory

This publication is available free of charge from:
https://doi.org/10.6028/NIST.IR.8175

March 2017

U.S. Department of Commerce
Wilbur L. Ross, Jr., Secretary

National Institute of Standards and Technology
Kent Rochford, Acting NIST Director and Under Secretary of Commerce for Standards and Technology

Abstract

This report summarizes recent technical work of the Applied and Computational Sciences Division of the Information Technology Laboratory at the National Institute of Standards and Technology (NIST). Part I (Overview) provides a high-level overview of the Division's activities, including highlights of technical accomplishments during the previous year. Part II (Features) provides further details on three projects of particular note this year. This is followed in Part III (Project Summaries) by brief synopses of all technical projects active during the past year. Part IV (Activity Data) provides listings of publications, technical talks, and other professional activities in which Division staff members have participated. The reporting period covered by this document is October 2015 through December 2016.

For further information, contact Ronald F. Boisvert, Mail Stop 8910, NIST, Gaithersburg, MD 20899-8910, phone 301-975-3812, email boisvert@nist.gov, or see the Division's web site at https://www.nist.gov/itl/math/.

Cover Visualization: Visualization of the hyperbolic umbilic canonical integral function $\mathbf{\Psi^{(H)}(x, y, 3)}$ from the NIST Digital Library of Mathematical Functions (DLMF), http:/dlmf.nist.gov/36.3.F12b.webgl. For more information on DLMF visualizations, see page 94.

Section Visualizations: The word cloud found at the start of each Part of this document was created using Wordle, http://www.wordle.net/, using the text of this document as input.

Acknowledgements: Thanks to Lochi Orr for assisting in the compilation of Parts III and IV of this document. Thanks also to Brian Cloteaux and Michael Frey who each carefully read the manuscript and offered many corrections and suggestions for improvement.

Disclaimer: Certain commercial entities, equipment, or materials are identified in this document in order to describe an experimental procedure or concept adequately. Such identification is not intended to imply recommendation or endorsement by the National Institute of Standards and Technology, nor is it intended to imply that the entities, materials, or equipment are necessarily the best available for the purpose.

Contents

Part I

Overview

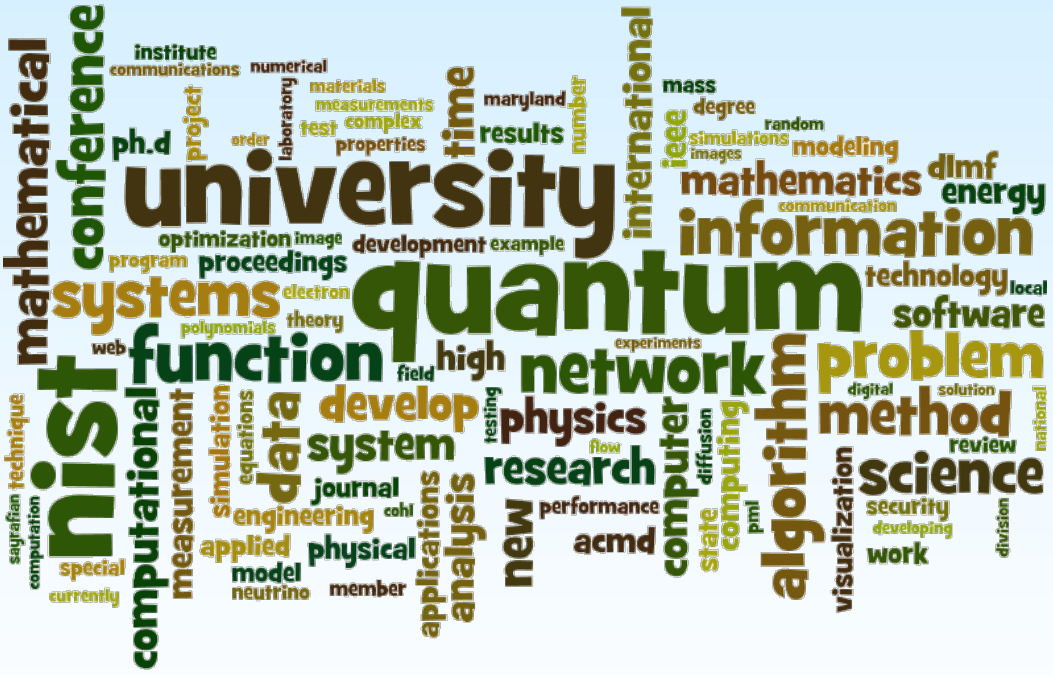

Introduction

Founded in 1901, the National Institute of Standards and Technology (NIST) is a non-regulatory federal agency within the U.S. Department of Commerce. NIST's mission is to promote U.S. innovation and industrial competitiveness by advancing measurement science, standards, and technology in ways that enhance economic security and improve our quality of life. The NIST Laboratory program is broad ranging, with research efforts encompassing physics, electrical engineering, nanotechnology, materials science, chemistry, bioscience, engineering, fire research, and information technology.

The Information Technology Laboratory (ITL) is one of seven major laboratories and user facilities at NIST. ITL's overarching purpose is to cultivate trust in information technology and metrology. This is accomplished primarily through the development of measurements, tests and guidance to support innovation in and deployment of information technology by industry and government, as well as in the application of advanced mathematics, statistics and computer science to help assure the quality of measurement science more broadly.

The Applied and Computational Mathematics Division (ACMD) is one of seven technical Divisions in ITL. ACMD's overarching purpose is to cultivate trust and confidence in NIST measurement science, as well as in computational science and engineering more broadly. To do so, ACMD provides leadership within NIST in the use of applied and computational mathematics to solve science and engineering problems arising in measurement science and related applications. In that role ACMD staff members

- perform research and development in applied mathematics and computational science and engineering, including analytical and numerical methods, high performance computing and visualization;
- engage in peer-to-peer collaborations to apply such techniques and tools to NIST problems;
- develop and disseminate mathematical reference data, software, and related tools; and
- work with internal and external groups to develop standards, tests, reference implementations, and other measurement technologies for scientific computation on current and future architectures.

Division staff is organized into four groups:

Mathematical Analysis and Modeling Group (*Timothy Burns, Leader*)

Performs research and maintains expertise in applied mathematics, mathematical modeling, and numerical analysis for application to measurement science.

Mathematical Software Group (*Michael Donahue, Leader*)

Performs research and maintains expertise in the methodology and application of mathematical algorithms and software in support of computational science within NIST as well as in industry and academia.

Computing and Communications Theory Group (*Ronald Boisvert, Acting Leader; Isabel Beichl and Xiao Tang, Project Leaders*)

Performs research and maintains expertise in the fundamental mathematics, physics, and measurement science necessary to enable the development and analysis of current and future computing and communications systems.

High Performance Computing and Visualization Group (*Judith Terrill, Leader*)

Performs research and maintains expertise in the methodologies and tools of high performance scientific computing and visualization for use in measurement science.

The technical work of the Division is organized into six thematic areas; these are described in the sidebar. Project descriptions in Part III of this document are organized according to these broad themes.

Division Thematic Areas

Broad Areas

Mathematics of Metrology. Mathematics plays an important role in the science of metrology. Mathematical models are needed to understand how to design effective measurement systems, and to analyze the results they produce. Mathematical techniques are used to develop and analyze idealized models of physical phenomena to be measured, and mathematical algorithms are necessary to find optimal system parameters. Finally, mathematical and statistical techniques are needed to transform measured data into useful information. The goal of this work is to develop fundamental mathematical methods and tools necessary for NIST to continue as a world-class metrology institute, and to apply them in measurement science.

High Performance Computing and Visualization. Computational capability is advancing rapidly, with the result that modeling and simulation can be done with greatly increased fidelity (e.g., higher resolution and more complex physics). However, developing the necessary large-scale parallel applications remains highly challenging, requiring expertise that application scientists rarely have. In addition, the hardware landscape is changing rapidly, so new algorithmic techniques must constantly be developed. We are developing such expertise for application to NIST problems. Such computations, as well as modern laboratory experiments, often produce large volumes of scientific data, which cannot be readily comprehended without some form of visual analysis. We are developing the infrastructure necessary for advanced visualization of scientific data, including the use of 3D immersive environments and applying this to NIST problems. One of our goals is to develop the 3D immersive environment into a true interactive measurement laboratory.

Current Focus Areas

Advanced Materials. Delivering technical support to the nation's manufacturing industries as they strive to out-innovate and out-perform the international competition has always been a top priority at NIST. Mathematical modeling, computational simulation, and data analytics are key enablers of emerging manufacturing technologies. This is most clearly evident in the Materials Genome Initiative, an interagency program with the goal of significantly reducing the time from discovery to commercial deployment of new materials through the use of modeling, simulation, and informatics. ACMD's role in advanced manufacturing centers on the development and assessment of modeling and simulation tools, with emphasis on uncertainty quantification, as well as support of NIST Laboratory efforts in such areas as materials modeling and smart manufacturing.

Quantum Information. An emerging discipline at the intersection of physics and computer science, quantum information science is likely to revolutionize 21st century science and technology in the same way that lasers, electronics, and computers did in the 20th century. By encoding information into quantum states of matter, one can, in theory, exploit the unique properties of quantum systems to enable phenomenal increases in information storage and processing capability, as well as communication channels with high levels of security. Although many of the necessary physical manipulations of quantum states have been demonstrated experimentally, scaling these up to enable fully capable quantum computers remains a grand challenge. We engage in (a) theoretical studies to understand the power of quantum computing, (b) collaborative efforts with the multi-laboratory experimental quantum science program at NIST to characterize and benchmark specific physical implementations of quantum information processing, and (c) demonstration and assessment of technologies for quantum communication.

Foundations of Measurement Science for Information Systems. Modern information systems are astounding in their complexity. Software applications are built from thousands of interacting components. Computer networks interconnect millions of independently operating nodes. Large-scale networked applications provide the basis for services of national scope, such as financial transactions and power distribution. In spite of our increasing reliance on such systems, our ability to build far outpaces our ability to ensure security and reliability. Protocols controlling individual nodes can lead to unexpected macroscopic behavior. Local power anomalies propagate in unexpected ways leading to large-scale outages. Computer system vulnerabilities are exploited in viral attacks resulting in widespread loss of data and system availability. The actual resilience of our critical infrastructure is largely unknown. Measurement science has long provided a basis for the understanding and control of physical systems. Such deep understanding and insight is lacking for complex information systems. We seek to develop the mathematical foundations needed for a true measurement science for complex networked information systems.

Mathematical Knowledge Management. We work with researchers in academia and industry to develop technologies, tools, and standards for representation, exchange, and use of mathematical data. Of particular concern are semantic-based representations which can provide the basis for interoperability of mathematical information processing systems. We apply this to the development and dissemination of reference data for applied mathematics. The centerpiece of this effort is the Digital Library of Mathematical Functions, a freely available interactive and richly linked online resource, providing essential information on the properties of the special functions of applied mathematics, the foundation of mathematical modeling in all of science and engineering.

Highlights

In this section we identify some of the major accomplishments of the Division during the past year. We also provide news related to ACMD staff.

Technical Accomplishments

ACMD has made significant technical progress on many fronts during the past year. Here we highlight a few notable technical accomplishments. Further details are provided in Part II (Features) and Part III (Project Summaries).

Mathematics of Metrology. Many problems in geoscience, environmental forensics, and in other measurement science applications require that one determine the previous state of a system given knowledge of the current state. If one has a model of the time-evolution of the system, then one can solve this problem by running the model backward in time. While this works in some cases, it fails for dissipative systems. In this case the problem is inherently ill-posed; many previous states could have led to the current one. Numerically, the symptom is that explicit marching schemes consistent with such problems are necessarily unconditionally unstable, i.e., small errors are explosively magnified. ACMD has developed a useful strategy to stabilize such ill-posed marching computations. While these stabilized schemes are slightly inconsistent, they nevertheless lead to useful results for numerous challenging nonlinear backward dissipative problems. See page 22.

Heating, ventilation and air conditioning (HVAC) systems in large buildings require very complex control systems. Computational models are important for studying such HVAC systems in order to guide the development of such control algorithms. The NIST Engineering Lab has such a model which has worked well for small-scale buildings, but has experienced numerical difficulties, such as convergence failure in its core nonlinear equation solver, when scaling to larger systems. ACMD has investigated the use of more sophisticated solvers and preconditioners to allow EL models to be extended to challenging scenarios in the simulation of realistic large-scale systems. See page 45.

Advanced Materials. ACMD continues to support the micromagnetics modeling community through the development of standardized benchmarks and reference software. This past year our reference software, the Object Oriented Micromagnetics Framework (OOMMF) was made available at nanoHUB[1], a gateway for nanotechnology research. At nanoHUB, users can test-drive OOMMF without having to install it on their own system. In related work, ACMD researchers have developed a capability to perform extremely high spatial resolution simulations using parallel calculations utilizing the high memory bandwidth available in modern commodity computer hardware. These simulations, which manage a billion degrees of freedom, are key to developing quantitative measures of error in micromagnetic calculations. See page 50.

Our collaborative work with the NIST Materials Measurement Laboratory (MML) is leading to new and more reliable methods of determining fundamental material properties. ACMD models of diffusion couples, for example, are supporting the work of MML scientists who are developing experimental techniques for measuring diffusion coefficients in alloys. See page 52.

High Performance Computing and Visualization. We are working closely with the NIST Engineering Lab to improve measurement science for cement and concrete. Of recent interest, has been the development of standard reference materials (SRMs) for calibrating rheometers that measure the flow properties of fresh concrete. We have developed sophisticated models for the flow of concrete, a challenging problem due to the multiple length scales involved as well as the fact that the resulting fluid is non-Newtonian. In addition, the complexity of the system, and the need for high fidelity simulations, requires the use of leadership class supercomputers. Our model is highly parallel, and has been shown to scale efficiently to more than 130 000 processors on Argonne National Laboratory's Blue Gene/Q system, on which we have received grants of computer time to carry out this research. Our simulations, and the sophisticated immersive visualizations

[1] https://nanohub.org/

that support their analysis, are leading to two new SRMs, one for cement, and one for mortar. These will be the first SRMs developed at NIST using supercomputers. See page 60.

Quantum Information. Quantum theory has properties that seem surprising and strange from the perspective of classical physics and everyday intuition. The most profound divide between classical physics and quantum physics is that classical physics obeys the principle of local realism, but quantum physics does not. Since the mid 1960s, when John Bell proposed an experimental test of this property, physicists have performed a series of experiments suggesting violation of local realism, but all have suffered from loopholes, and thereby have not definitively ruled out this principle. Early this fiscal year ACMD researchers participated in a loophole-free test of local realism, rejecting the hypothesis that the universe obeys local realism with a very high level of statistical significance and ending a decades long quest of foundational physics. This work received a great deal of attention, including being named as number nine in the top 25 science stories of 2015 by *Science News*, as well as being the subject of a Department of Commerce Gold Medal awarded in 2016. See page 73.

Public-key cryptosystems enable the transmission of sensitive information over the Internet by providing functionalities such as digital signatures, encryption, and key exchange. As such, they have become part of the infrastructure for electronic commerce. However, most public-key cryptosystems in use today are vulnerable to attack using quantum computers. While large quantum computers have not yet been built, they are believed to be a future threat to information security. ACMD staff are part of a NIST team taking steps to standardize new cryptosystems that are secure against quantum attacks. An important preliminary assessment of so-called post-quantum cryptosystems was released this year, as well as a formal call for proposals to be considered for future NIST standardization. See page 77.

Foundations of Measurement Science for Information Systems. We continue our fundamental investigations of how network structure influences performance (such as resilience to failure) in a variety of applications. For example, examining the system-level security of complex networks is hindered by the fact that security measures adopted by organizations (nodes in the network) produce either positive or negative effects on other participants in the network, leading to so-called interdependent security. We recently completed a study of how properties of the underlying network structure, such as correlations in node degrees (termed assortivity), affect the strategic choices made by network nodes, and how this in turn influences the network-level security. See page 80.

Real-world data suitable for testing algorithms for analyzing large-scale networks is in short supply. An alternate approach is to develop methods for generating "random" instances of networks with prescribed properties, such as a given degree sequence. (The degree of a node in a network is the number of other nodes to which it has direct connections. A degree sequence is a list of the degrees of all the nodes in a network.) Unfortunately, the problem of creating a uniformly sampled random graph for a given degree sequence using a reasonable amount of time and space is a difficult problem. ACMD has developed greatly improved methods for doing this. And, in the process, we have discovered new diagnostics for establishing when a degree sequence is *graphic*, i.e., it has a realization in some graph. See page 87.

Mathematical Knowledge Management. The NIST Digital Library of Mathematical Functions (DLMF), first released in 2010, is a major publicly accessible reference on the properties of the special functions of applied mathematics. At this writing Google Scholar already identifies more than 2 900 citations to the DLMF in the technical literature. This year ACMD took its first steps in developing significant extensions to the technical material in the DLMF, engaging external experts to develop additional material for the Orthogonal Polynomials and Painlevé Transcendent chapters, as well as a new chapter on Orthogonal Polynomials of Several Variables. See page 93.

Technology Transfer and Community Engagement

The volume of technical output of ACMD remains high. During the last 15 months, Division staff members were (co-)authors of 45 articles appearing in peer-reviewed journals, 28 papers in conference proceedings, and 7 published in other venues. Eleven additional papers were accepted for publication, while 33 others

are undergoing review. Division staff gave 43 invited technical talks and presented 53 others in conferences and workshops.

ACMD continues to maintain an active website with a variety of information and services, most notably the Digital Library of Mathematical Functions, though legacy services that are no longer actively developed, like the Guide to Available Mathematical Software, the Matrix Market, and the SciMark Java benchmark still see significant use. During calendar year (CY) 2016, the division web server satisfied more than 6 million requests for pages during nearly 1.2 million user visits. Another indication of the successful transfer of our technology is references to our software in refereed journal articles. For example, our software system for nano-magnetic modeling (OOMMF) was cited in 157 such papers published in CY 2016 alone; see page 50.

Members of the Division are also active in professional circles. Staff members hold a total of 17 editorial positions in peer-reviewed journals. For example, Barry Schneider is an Associate Editor-in-Chief and Isabel Beichl is an Editorial Board Member for IEEE's *Computing in Science and Engineering.* Staff members are also active in conference organization, serving on 17 organizing/steering/program committees. Of note, ACMD played an important role as sponsor or (co-)organizer of several significant events this year, including the following:

- *Numerical Reproducibility at Exascale*, at SC15[2], Austin, TX. November 20, 2015 and at SC16[3], Salt Lake City, UT, November 18, 2016. (M. Mascagni and Walid Keyrouz, Co-Organizers)

  A cornerstone of the scientific method is experimental reproducibility. As computation has grown into a powerful tool for scientific inquiry, the assumption of computational reproducibility has been at the heart of numerical analysis in support of scientific computing. With ordinary CPUs, supporting a single, serial, computation, the ability to document a numerical result has been a straightforward process. However, as computer hardware continues to develop, it is becoming harder to ensure computational reproducibility, or to even completely document a given computation. These two workshops explored the current state of computational reproducibility in high performance computing, and sought to organize solutions at different levels.

- *Inference on Networks: Algorithms, Phase Transitions, New Models and New Data*, Santa Fe Institute, NM, December 14-18, 2015.

  A NIST grant provided partial funding for this event. Networks provide a rigorous representation for both modeling and understanding the structure and function of complex systems. Over the past 10 years, researchers working in statistical inference and statistical physics have developed powerful new algorithms for understanding network data, and have revealed new phenomena in the behavior of these algorithms. This workshop brought together experts in network science, statistical inference, and statistical physics to present recent advances in inference on networks and to organize future efforts on developing a deeper mathematical understanding of probability on networks, message-passing algorithms, and random matrices, on developing new models to handle new sources of rich data, and on applying these ideas to key questions in complex systems.

- *6th International Conference on Quantum Cryptography (QCrypt)*[4], Washington, DC, September 12-16, 2016. (Yi-Kai Liu, Steering Committee Chair and Lead Organizer)

  Quantum cryptography aims to achieve security from fundamental physical principles, such as the quantum mechanical phenomena of entanglement and Heisenberg's uncertainty principle. In the last few years, significant progress has been made in the theoretical understanding of quantum cryptography, and its technological feasibility has been demonstrated experimentally. The main goals of QCrypt are to represent the previous year's best results and to support the building of a research community in quantum cryptography. More than 200 researchers participated.

[2] http://www.nist.gov/itl/ssd/is/numreprod2015.cfm

[3] http://www.cs.fsu.edu/~nre/

[4] http://2016.qcrypt.net/

Figure 1. *ACMD staff members engage in a variety of outreach efforts throughout the year. In November 2016 Anthony Kearsley (center) and Ryan Evans (far right) host a visit to NIST by Professor Luis Melara (second from right) and students from his undergraduate Partial Differential Equations course at Shippensburg University (PA). Melara, a former NIST NRC Postdoctoral Associate in ACMD, is also the Editor-in-Chief of the SIAM Undergraduate Research Online journal.*

- *Circumventing Turing's Achilles Heel*, Santa Fe Institute, NM, November 14-15, 2016.

  A NIST grant provided partial funding for this event. Subject to the limitations of finite memory, time, and processor speed, today's general-purpose computers are (near) Turing complete; that is, capable of computing anything that is computable. But it's exactly that strength that makes our computer and network systems so vulnerable to attack: If outsiders can gain control of your system, then, in principle, they can use it for whatever tasks they are clever enough to trick your system into executing. This SFI Working Group explored strategies for retaining the hardware and software advantages of general purpose computers, while denying those same general purpose capabilities to outside attackers.

Service within professional societies is also prevalent among our staff. For example, Barry Schneider served as Past Chair of the Division of Computational Physics of the American Physical Society (APS). Geoffrey McFadden serves as Member-at-Large of the Council of the Society for Industrial and Applied Mathematics (SIAM). Faculty appointee Michael Mascagni is a Member of the Board of Directors of the International Association for Mathematics and Computers in Simulation (IMACS). Ronald Boisvert continues to serve as a member of the Publications Board of the Association for Computing Machinery (ACM). Staff members are also active in a variety of working groups. For example, Ronald Boisvert and Andrew Dienstfrey serve as members of the International Federation for Information Processing (IFIP) Working Group 2.5 on Numerical Software, Donald Porter is a member of the Tcl Core Team, Bruce Miller is a member of W3C's Math Working Group, and Sandy Ressler is a member of the Web3D Consortium. Barry

Schneider represents NIST on the High End Computing (HEC) Interagency Working Group of the Federal Networking and Information Technology Research and Development (NITRD) Program. Further details can be found in Part IV of this report.

Staff News

The past year saw a few staffing changes. Among these are the following.

Arrivals

Lochi Orr joined ACMD on December 14, 2015 to provide administrative support to the Mathematical Analysis and Modeling Group and the Mathematical Software Group. Lochi, who has a degree in Criminal Justice, was most recently employed by the Drug Enforcement Administration in Baltimore.

Sean Colbert-Kelly, a former NIST/NRC Postdoctoral Associate, returned to ACMD on January 11, 2016. Sean, who was previously an NRC Postdoc in ACMD, is currently supported by the NIST Fellows postdoc program. (The NIST Director has reserved funding that allows each NIST Fellow to employ one postdoc.) Sean is working with NIST Fellow and ACMD staff member Geoffrey McFadden.

Ryan Evans began a two-year appointment as a NIST/NRC Postdoctoral Associate in August 2016. He comes to us from the University of Delaware, where he received a PhD in applied mathematics. At NIST he is working with advisor Anthony Kearsley on the modeling of multiple-component surface-volume reactions with optical biomolecular sensors.

Charles Baldwin joined ACMD's quantum information research team in Boulder in early October 2016 as an NIST/NRC Postdoctoral Associate. Charles recently completed a PhD in Physics at the University of New Mexico, and is working with ACMD's Scott Glancy on the development of new, practical methods for quantum state tomography.

Departures

Diane O'Leary and **G. W. (Pete) Stewart**, faculty appointees in ACMD from the Computer Science Department at the University of Maryland, departed from NIST in 2016 to pursue full-time retirement activities after a combined service in excess of 55 years.

Students

During FY 2015 ACMD supported the work of 44 student interns, including 10 graduate students, 10 undergraduates, and 24 high school students. See Table 1 and Table 2 in the Appendix for a complete listing. ACMD staff members are also quite active in the education of graduate students, serving both as Ph.D. advisers and as members of thesis committees. For a complete list, see page 122.

Recognition

Division staff garnered a variety of professional recognitions during the past year. Several ACMD staff were recognized with DOC/NIST awards at the December 2015 NIST Awards Ceremony:

- **Manny Knill** was honored with the 2015 Samuel Wesley Stratton Award "for pioneering research in the field of quantum information science and engineering." The Stratton Award, one of the most prestigious awards conferred by NIST, was first presented in 1962. It is granted for outstanding scientific or engineering achievements in support of NIST objectives.
- **Kamran Sayrafian** received a 2015 Department of Commerce (DOC) Bronze Medal "for leadership in the advancement of body-area network technologies that will enable innovations in personal health care delivery and telemedicine."

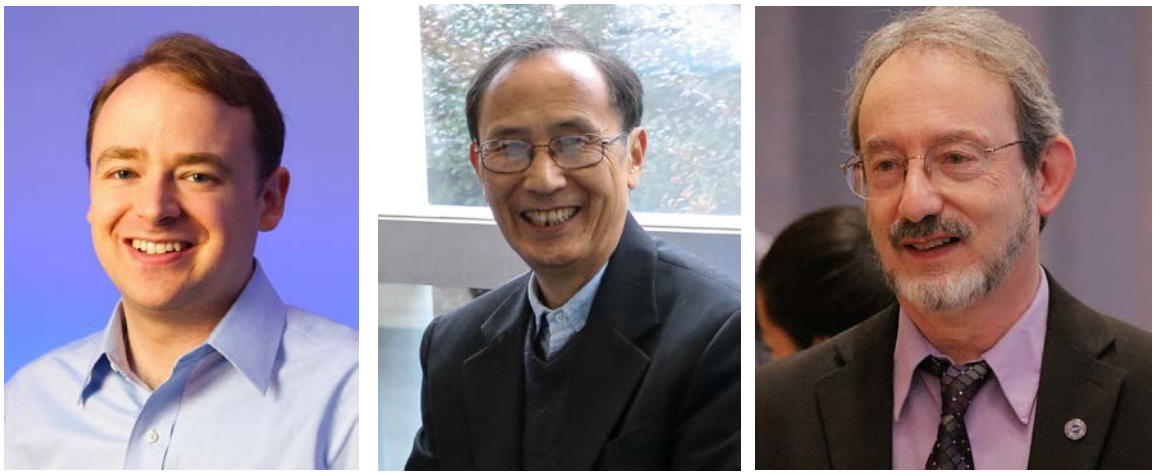

Figure 2. *ACMD award winners this year included (l ot r): Stephen Jordan (Sigma Xi Katherine Gebbie Young Investigator Award), Xiao Tang (APS Fellow) and Ronald Boisvert (AAAS Fellow).*

- **Barry Hershman**, **Paulina Kuo**, **Oliver Slattery** and **Xiao Tang** also received a 2015 DOC Bronze medal. They were cited "for the development of upconversion single photon detectors and spectrometers for use in quantum information research and measurement science."

The landmark loophole-free Bell test performed at the NIST Boulder Laboratories in November 2015 was the subject of a 2016 Department of Commerce Gold Medal awarded to the NIST Physical Measurement Laboratory and Information Technology Laboratory. ACMD staff members **Manny Knill** and **Scott Glancy**, as well as ACMD postdoc **Peter Bierhorst** were part of the team whose work was honored by the Department.

Stephen Jordan was named co-winner of the 2016 Katharine Gebbie Young Investigator Award. Sponsored by NIST's chapter of Sigma Xi, this award recognizes exceptional fundamental science in support of the NIST mission by a researcher with less than 10 years of professional experience. Jordan was cited for his groundbreaking research in quantum algorithms, which are providing insight into the potential power of future computers which exploit the principles of quantum mechanics. The award was conferred in ceremonies held in Gaithersburg on May 25, 2016.

Two Division staff members were elevated to Fellow status in external professional organizations:

- **Ronald Boisvert** was elected a Fellow of the American Association for the Advancement of Science (AAAS) "for distinguished contributions to the fields of mathematical software and computational science, excellence in public administration of science, and service to the computing profession." The honor will be conferred at the AAAS Annual Meeting in Boston in February 2017.
- **Xiao Tang** was elected a Fellow of the American Physical Society (APS). He was cited "for outstanding contributions in optical technologies and systems, with application to quantum communications, spectrometry, and digital preservation." He was nominated by the APS Topical Group on Quantum Information, and will be inducted at the APS Meeting in March 2017. Tang joins three current ACMD staff members with this honor: Manny Knill, Geoffrey McFadden, and Barry Schneider.

ACMD staff were cited for several distinctions as part of ITL's 2016 awards program:

- **Amanda Streib, Noah Streib, Isabel Beichl,** and **Francis Sullivan** received the ITL Outstanding Journal Paper Award for their paper "Stratified Sampling for the Ising Model: A Graph-theoretic Approach" published in *Computer Physics Communications*, Volume 191, June 2015, pp. 1–8

Figure 3. *Peter Bierhorst received the 2016 ITL Outstanding Associate Award for his contributions to the landmark loop-hole free Bell test performed at NIST in late 2015.*

- **Gunay Dogan, Javier Bernal** and Charles Hagwood received the ITL Outstanding Conference Paper Award for their paper "A Fast Algorithm for Elastic Shape Distances between Closed Planar Curves" presented at the 2015 IEEE Conference on Computer Vision and Pattern Recognition (CVPR), Boston, MA, June 7-12, 2015.
- **Peter Bierhorst** was named ITL Outstanding Associate of Year for excellence in advancing the understanding of quantum correlations and applying that understanding to experiments in the foundations of physics.
- **Barry Hershman** received the ITL Outstanding Technical Support Award for outstanding and resourceful support of quantum communications research and development and exemplary service as Division Safety Representative.

There were several other external distinctions of note. **Brian Cloteaux** was honored with a 2016 Gold Nugget Award by the University of Texas at El Paso and the UTEP Alumni Association. The awards program is aimed at identifying alumni "whose achievements stand out as monuments to dedication, integrity and hard work." In July 2016 **Jeffery Fong** was guest of honor at the 50th anniversary celebration of the Smith Mountain Dam in southwestern Virginia. Fong was the lead designer and engineer for the project for New York's EBASCO Services, where he worked before coming to NIST (in 1966).

Finally, two existing ACMD staff members completed their studies this year and received their Ph.D. degrees. **Oliver Slattery**, a member of ACMD's quantum communications team, was awarded his degree in physics from the University of Limerick in December 2015. Ollie's research focused on the development of single-photon sources, detectors, spectrometer and interfaces for quantum communication systems. **Wesley Griffin** of ACMD's High Performance Computing and Visualization Group received his degree in computer science from the University of Maryland Baltimore County in August 2016. In his dissertation Wes developed perception-based image quality metrics to evaluate texture compression algorithms in computer graphics.

Part II

Features

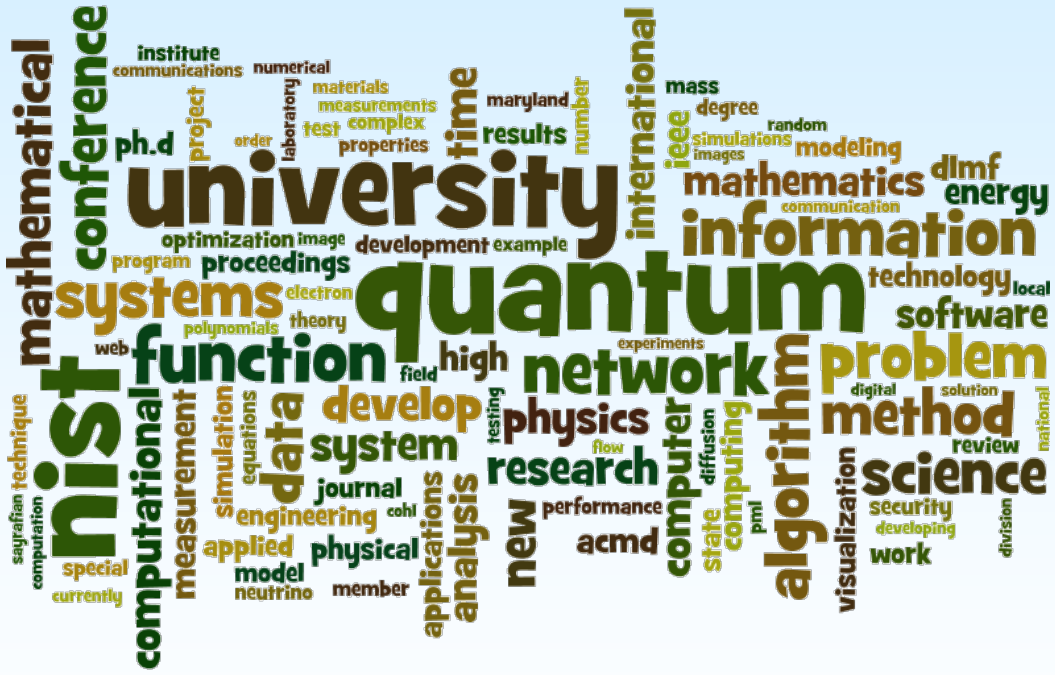

Identification of Nearly-Coincident Events in Calorimetric Sensors

Major advances in particle physics in recent years have come from measuring the incidence of solar neutrinos and comparing to predictions from solar models. These have prompted experiments now under construction, with NIST participation, to measure neutrino mass precisely, possibly leading to revised theories of the evolution of the universe. Improved microcalorimeter technology, with applications in x-ray line metrology, nuclear forensics, exotic atom science, and synchrotron and tabletop absorption and emission spectroscopy, are more immediate benefits of the collaboration.

Bradley Alpert

Experimental confirmation by the Super-Kamiokande Collaboration in 1998 and the Sudbury Neutrino Observatory Collaboration in 2001/2002 of oscillations between three flavors ν_e, ν_μ and ν_τ of neutrino, resolved the forty-year-old solar neutrino problem, demonstrating according to quantum theory that neutrinos have mass. This has created urgency to determine the scale of neutrino mass, which may be a key to advancing cosmology and modifying the Standard Model of particle physics. Several experiments, prompted by this impetus, pose major challenges to a variety of advanced measurement technologies. NIST microcalorimeters and experiment analysis are playing a central role in one of these experiments.

Solar Neutrinos. Energy production by the Sun proceeds by fusion, involving several nuclear reactions of which the dominant one according to the standard solar model can be written schematically as

$$p + p \rightarrow {}^2H^+ + e^+ + \nu_e(E_\nu) + E$$

in which two protons (hydrogen nuclei, $p = {}^1H^+$) combine to produce a deuterium nucleus (one proton and one neutron), a positron (anti-electron), an electron neutrino, and released energy E. The neutrino—a solar pp neutrino—has the potential to be observed at one of several deep underground detectors built for this purpose, provided its energy E_ν is large enough. The first detector, constructed by Raymond Davis at the Homestake gold mine in Lead, South Dakota, and consisting of large vats of perchloroethylene C_2Cl_4, observed the reaction

$$\nu_e + {}^{37}Cl \rightarrow e^- + {}^{37}Ar$$

over more than twenty years until 1985. This victory for solar neutrino capture recorded, however, less than one-third the number of incidents predicted by the standard solar model (Figure 4). There were several possible explanations for this deficiency, dubbed the *solar neutrino problem*, including the relatively high 0.814 MeV energy minimum for detection. The second solar neutrino detector, beginning in 1987 at the Kamiokande zinc mine in Japan, recorded solar neutrino arrival direction and timing, but at the cost of yet higher 7.3 MeV minimum energy and, like the Homestake detector, had as its neutrino source primarily the much less frequent solar reaction

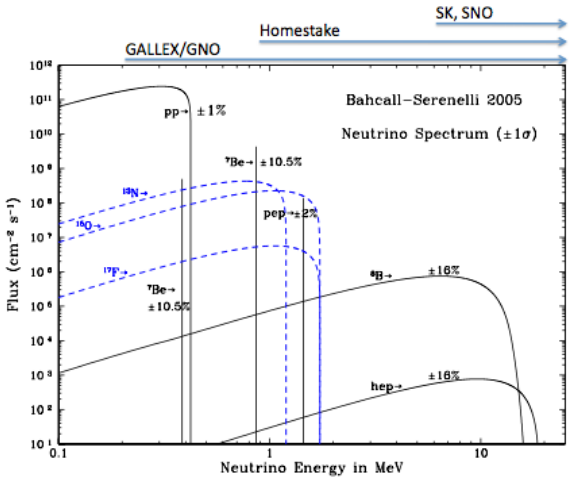

Figure 4. *Neutrino fluxes (with uncertainies) as predicted by the Bahcall-Serenelli solar model, in $cm^{-2}s^{-1}MeV^{-1}$ ($cm^{-2}s^{-1}$ for the lines). Arrows above the plot show the energy ranges accessible to the experiments [1, 2].*

$$^8B \rightarrow {}^8Be + e^+ + \nu_e(E_\nu) + E$$

capable of generating neutrinos with sufficient energy E_ν. By contrast, the pp neutrino energy does not exceed 0.420 MeV. Additional detectors, built at the Baksan Neutrino Laboratory under a mountain in the Caucasus (SAGE) and under the 2900-meter tall Gran Sasso d'Italia (Gallex/GNO), based on the gallium reaction

$$\nu_e + {}^{71}Ga \rightarrow e^- + {}^{71}Ge$$

that should detect neutrinos with energies as low as 0.233 MeV, which includes many of the pp neutrinos, deepened the mystery of the solar neutrino problem by detecting almost none! For discussions, see [3, 4].

The results of all these experiments, which seemed at odds with an increasingly detailed and otherwise well-supported standard solar model, left little apparent alternative to spontaneous oscillations between ν_e, ν_μ and ν_τ neutrino flavors, theorized as a possibility by Bruno Pontecorvo as early as 1957. The limitation to detecting just the electron neutrino ν_e, rather than the muon neutrino ν_μ or tau neutrino ν_τ, finally was remedied in part

by the Super-Kamiokande Collaboration (SK) and decisively by the Sudbury Neutrino Observatory Collaboration (SNO) which started observing in 1999. These observations discovered the missing neutrinos as ν_μ and ν_τ flavors, resolved the solar neutrino problem, and transformed understanding of neutrino physics [2, 5].

Neutrino Mass Experiments. Atmospheric, solar, accelerator, and reactor neutrino measurements provide compelling evidence that neutrino flavors are superpositions of mass eigenstates and that neutrinos in flight oscillate between flavors. But as a sort of interference experiment, they provide evidence only of differences, not absolute values, of squared mass [6]. Other present evidence yields the rather broad range

$$0.01 \text{ eV}/c^2 \leq m_\beta \leq 2.05 \text{ eV}/c^2$$

where m_β is the electron-flavor-weighted neutrino mass [7]. Theories of possible evolution of the universe consistent with this range, but not with certain reductions of it, have accelerated physicists' race to measure neutrino mass.

<u>*Tritium.*</u> The most-studied reaction enabling direct—that is model-free—measurement of the electron (anti-) neutrino mass is the β-decay of tritium

$$^3\text{H} \rightarrow {}^3\text{He}^+ + \text{e}^-(E) + \bar{\nu}_e(E_\nu)$$

in which the difference in mass between tritium and its helium and electron daughters is $mc^2 = Q = E + E_\nu = 18.6$ keV. Here the neutrino escapes, but the remaining energy E carried kinetically by the electron, is measured. The precise shape of the spectrum of E especially near the endpoint Q, is determined by the minimum value of E_ν, that is, by the rest mass of $\bar{\nu}_e$. Measurements of tritium β-decay began in the 1940s and have been conducted in the 1990s at Los Alamos, Zürich, Tokyo, Beijing, Livermore, Mainz, and Troitsk [6]. Magnetic spectrometers were developed in the early work; more recently, applied electrostatic spectrometers have been constructed. Large experiments currently underway are KATRIN (Karlsruhe Tritium Neutrino project) [6] and Project 8 [7, 8]. The latter employs a highly novel approach that uses a cyclotron to measure a frequency shift due to individual, mildly relativistic daughter electrons.

<u>*Holmium.*</u> Another reaction that may allow neutrino mass measurement, proposed in 1982 by de Rujula and Lusignoli [9], is electron capture by holmium, in which an electron from the atom's K or L shell merges with a proton of the nucleus to become a neutron,

$$^{163}\text{Ho} \rightarrow \nu_\text{e}(E_\nu) + {}^{163}\text{Dy}^\text{h} \downarrow {}^{163}\text{Dy} + E_\text{c}.$$

Here superscript h indicates a hole in an electron shell of the daughter atom dysprosium, which is filled by electrons shifting orbitals, resulting in photon radiation

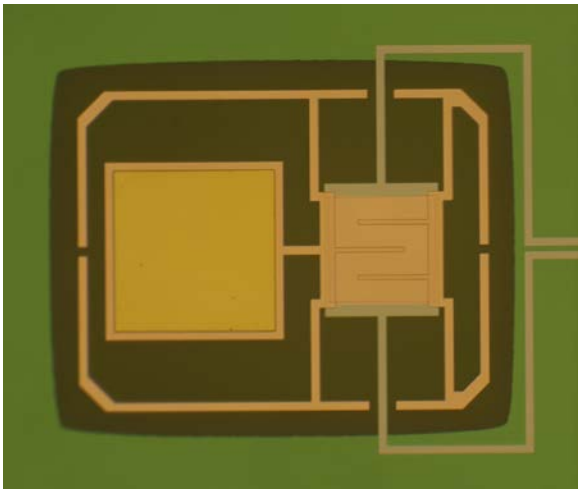

Figure 5. *Prototype transition-edge sensor (TES) microcalorimeter, designed and fabricated at NIST for the HOLMES experiment [10]. The square pad to the left would receive and encase a deposit of ^{163}Ho and distribute the heat of photons from electron captures to the TES on the right. Skeleton-like wires from the TES increase heat transfer to the silicon-nitride substrate, while the wire passing vertically through the TES conducts electric current to measure photon energy from the sharp resistance change with temperature.*

of E_c. The subscript of E_c is chosen to denote absorption and measurement by a calorimeter. This alternative to tritium β-decay was proposed due to a lower $Q = E_\nu + E_\text{c}$ reported in 1982 by two groups as 2.58 ± 0.10 keV and 2.30 ± 0.15 keV. The lower value than for tritium ensures that more of the spectrum of E_c will be influenced by the minimum value of E_ν hence by $m(\nu_\text{e})$ [9]. Recently, a Penning trap measurement has determined a Q-value of $2833 \pm 30_\text{stat} \pm 15_\text{sys}$ eV [11].

During the past several years low-temperature microcalorimeters have been developed that enable exquisitely precise measurement of energies of single photons (x-ray or gamma ray), over wide frequency bands, with high detection efficiency. Transition-edge-sensor (TES) microcalorimeters developed at NIST achieve energy resolution of 2 eV (full-width-at-half-maximum, or FWHM) at 6 keV [12]. Another technology, metallic magnetic calorimeters (MMC), developed at Kirchhoff Institute for Physics, Heidelberg, Germany, achieves similar energy resolution [13]. These detector resolutions for individual photons, accumulated over many observations, in principle are adequate to establish distinctions in the shape of the emission spectrum well below 0.1 eV. ECHo is an experiment to measure neutrino mass from ^{163}Ho electron capture and is using MMCs for energy measurement [14]. HOLMES is a second experiment based on the same nuclear decay, but employing TESs (Figure 5) for energy measurement [15].

<u>*Strategies.*</u> There are many challenges for each of the experiments, engaging dozens of specialists. In all the mass measurement efforts, for a very large proportion of

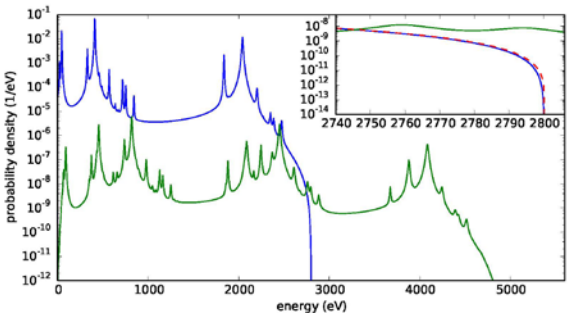

Figure 6. *De-excitation spectrum from ^{163}Ho electron capture, based on energy endpoint Q = 2800 eV and neutrino mass $m(\nu_e)$ = 0 eV, is shown (blue) along with its self convolution (green), the spectrum of a piled-up pair. Latter is scaled by the relative probability 3.00×10^{-4} of pile-up from an event rate of 300 /s and time resolution of 1 μs. Inset focuses on energies of interest near Q and adds single-event spectrum for Q = 2801, $m(\nu_e)$ = 1 eV (red, dashed) [16]. In an experiment, just the sum of single-event and pile-up spectra is observable.*

nuclear decays the neutrino departs with much or most of the energy. Remaining, measurable energy then is far from the endpoint *Q* of the spectrum and provides little or no information about the neutrino mass. Therefore, each experiment has some strategy to restrict attention to the highest energies, which are seen in such a small fraction of events that they must be extracted from ~ 10^{14} decays [17]. A second issue for the electron capture experiments is that the ^{163}Dy de-excitation spectrum, dependent on the neutrino mass, is not sufficiently well-known to enable appropriate $m(\nu_e)$ inference; rather, it is a topic of active theoretical work [18-23]. Another very significant challenge for the ^{163}Ho experiments is the isotope generation in a nuclear reactor and subsequent separation from other isotopes. Finally, due to the requirement for such a large number of decays, there is a need for both large arrays of detectors and high decay rates per detector, increasing the probability of pairs of nearly simultaneous events being mistaken for one event (see Figure 6). ECHo expects to reduce undetected coincident arrivals through the very fast MMC detector response to each event, at the price of considerable challenge to achieving highly multiplexed readout of the detectors. HOLMES use of TES detectors, with proven multiplexing but slower response, necessitates better signal analysis [16].

To detect nearly-simultaneous events, which produce detector responses (pulses) that pile up and can be mistaken for single events, a two-pronged approach was adopted: first, x-ray fluorescence from known sources will be used to develop a single-event pulse model for each detector and, not incidentally, enable energy calibration across the array of detectors, and second, the pulse model will be exploited to reject double-event pulses. A workhorse of numerical linear algebra, the singular value decomposition, is employed to construct the single-pulse model. For a single event, pulse shape variability with magnitude, sub-sample arrival time, and readout baseline, are all encoded in several singular vectors and their coefficients, and further reduced by regression to a low-order polynomial in three variables. Typicality, or lack thereof, in this representation enables distinguishing single events from event pairs in the training data and the model is iteratively refined by iterative rejection of outliers. On the ^{163}Ho data, rejection of event pairs is determined by the norm of the residual under the refined model. Simulations based on ordinary differential equations to model TES microcalorimeter response, correlated Gaussian noise, the ^{163}Dy de-excitation spectrum, and exaggerated pile-up incidence, predict that this approach will succeed in satisfying the HOLMES experiment specification of 1 μs time resolution [16].

Experimenters will tend to adopt whatever tools are expected to be effective and ECHo researchers have expressed considerable interest in the pile-up detection algorithms developed for HOLMES.

References

[1] J. N. Bahcall, A. M. Serenelli and S. Basu, New Solar Opacities, Abundances, Helioseismology, and Neutrino Fluxes. *The Astrophysical Journal* **621** (2005), L85–L88.

[2] Scientific Background on the Nobel Prize in Physics 2015: Neutrino Oscillations, http://www.nobelprize.org/nobel_prizes/physics/laureates/2015/advanced-physicsprize2015.pdf, accessed January 28, 2017.

[3] B. Schwarzschild, Solar Neutrino Update: Three Detectors Tell Three Stories, *Physics Today* **43**:10 (1990), 17.

[4] B. Schwarzschild. Gallex Data Can't Quite Lay the Solar Neutrino Problem to Rest, *Physics Today* **45**:8 (1992), 17.

[5] J. N. Bahcall, Solving the Mystery of the Missing Neutrinos,http://www.nobelprize.org/nobel_prizes/themes/physics/bahcall/index.html, first published April 28, 2004, accessed January 28, 2017.

[6] G. Drexlin, V. Hannen, S. Mertens and C. Weinheimer, Current Direct Neutrino Mass Experiments, *Advances in High Energy Physics* **2013** (2013), 293986.

[7] D. M. Asner, et al., Single-electron Detection and Spectroscopy via Relativistic Cyclotron Radiation, *Physical Review Letters* **114** (2015),162501.

[8] B. Monreal and J. A. Formaggio, Relativistic Cyclotron Radiation Detection of Tritium Decay Electrons as a New Technique for Measuring the Neutrino Mass, *Physical Review D* **80** (2009), 051301(R).

[9] A. de Rújula and M. Lusignoli. Calorimetric Measurements of ^{163}Holmium Decay as Tools to Determine the Electron Neutrino Mass, *Physics Letters B* **118** (1982), 429–434.

[10] J. P. Hays-Wehle, D. R. Schmidt, J. N. Ullom and D. S. Swetz, Thermal Conductance Engineering for High-Speed TES Microcalorimeters. *Journal of Low Temperature Physics* **184** (2016), 492.

[11] S. Eliseev et al., Direct Measurement of the Mass Difference of ^{163}Ho and ^{163}Dy Solves the Q-Value Puzzle for the Neutrino Mass Determination, *Physical Review Letters* **115** (2015), 062501.

[12] Joel N. Ullom and Douglas A. Bennett, Review of Superconducting Transition-Edge Sensors for X-Ray and Gamma-Ray Spectroscopy, *Superconductor Science and Technology* **28** (2015), 084003.

[13] A. Fleischmann et al., Metallic Magnetic Calorimeters, *AIP Conference Proceedings* **1185** (2009), 571.

[14] L. Gastaldo et al., The Electron Capture ^{163}Ho Experiment ECHo. *Journal of Low Temperature Physics* **176** (2014), 876–884.

[15] B. Alpert et al., The Electron Capture Decay of ^{163}Ho to Measure the Electron Neutrino Mass with Sub-Ev Sensitivity, *European Physical Journal C* **75** (2015), 112.

[16] B. Alpert et al., Algorithms for Identification of Nearly-Coincident Events in Calorimetric Sensors, *Journal of Low Temperature Physics* **184** (2015), 263.

[17] A. Nucciotti, The Use of Low Temperature Detectors for Direct Measurements of the Mass of the Electron Neutrino, *Advances in High Energy Physics* **2016** (2016), 9153024.

[18] A. Faessler, L. Gastaldo and F. Šimkovic, Electron Capture in ^{163}Ho, Overlap Plus Exchange Corrections and Neutrino Mass, *Journal of Physics G: Nuclear and Particle Physics* **42** (2015), 015108.

[19] A. Faessler and F. Šimkovic, Improved Description of One- and Twohole Excitations After Electron Capture in 163Ho and the Determination of the Neutrino Mass, *Physical Review C* **91** (2015), 045505.

[20] A. Faessler, C. Enss, L. Gastaldo and F. Šimkovic, Determination of the Neutrino Mass by Electron Capture in ^{163}Ho and the Role of the Three-hole States in ^{163}Dy, *Physical Review C* **91** (2015), 064302.

[21] A. de Rújula. Two Old Ways to Measure the Electron-Neutrino Mass, 2013, arXiv:1305.4857.

[22] A. De Rújula and M. Lusignoli. The Calorimetric Spectrum of the Electron-Capture Decay of ^{163}Ho: A Preliminary Analysis of the Preliminary Data, 2015, arXiv:1510.05462v2.

[23] A. De Rújula and M. Lusignoli, The Calorimetric Spectrum of the Electron-Capture Decay of ^{163}Ho: The Spectral Endpoint Region, *Journal of High Energy Physics* **2016** (2016), 15.

Participants

Bradley Alpert (ACMD); Douglas Bennett, Joseph Fowler, James Hays-Wehle, Gene Hilton, John (Ben) Mates, Carl Reintsema, Dan Schmidt, Daniel Swetz, Joel Ullom (NIST PML); Marco Balata, Michele Biasotti, Corrado Boragno, Chiara Brofferio, Valentina Ceriale, Dario Corsini, Matteo De Gerone, Marco Faverzani, Elena Ferri, Flavio Gatti, Andrea Giachero, Maurizio Lusignoli, Matteo Maino, Stefano Nisi, Riccardo Nizzolo, Angelo Nucciotti, Gianluigi Pessina, Giulio Pizzigoni, Andrei Puiu, Stefano Ragazzi, Monica Sisti, Francesco Terranova (INFN); Peter Day (JPL); Rugard Dressler, Stephan Heinitz, Dorothea Schumann (Paul Scherrer Institut); Ulli Köster (Institut Laue-Langevin); Maria Ribeiro Gomes (University of Lisbon)

Relocation Algorithms for Autonomous Cells on Wheels in Public Safety Networks

Lack of network availability or limited access to communication services are among the challenges that public safety officials and first responders could face during disasters or emergencies. Networking infrastructure can partially (or sometimes fully) breakdown during such events. At the same time, unusual peaks in public traffic could lead to much higher blocking probability or service interruptions for critical communication. Inadequate communication among emergency responders or public safety personnel could put lives at risks. The use of mobile infrastructures, commonly referred to as cells on wheels, offers a possible solution. These mobile cells can complement the existing undamaged infrastructure or enable a temporary emergency network by themselves. Given the limited capacity of each cell, variable and spatially non-uniform traffic across the disaster area can make a big impact on the network performance. Not only can judicious deployment of cells help to meet coverage and capacity demands, but intelligent relocation strategies can optimally match the network resources to potentially changing traffic demands. Assuming that each cell can autonomously change its location, in this project, we aim to develop decentralized relocation algorithms for autonomous cells on wheels that adapts network coverage in order to increase the supported user traffic.

Kamran Sayrafian

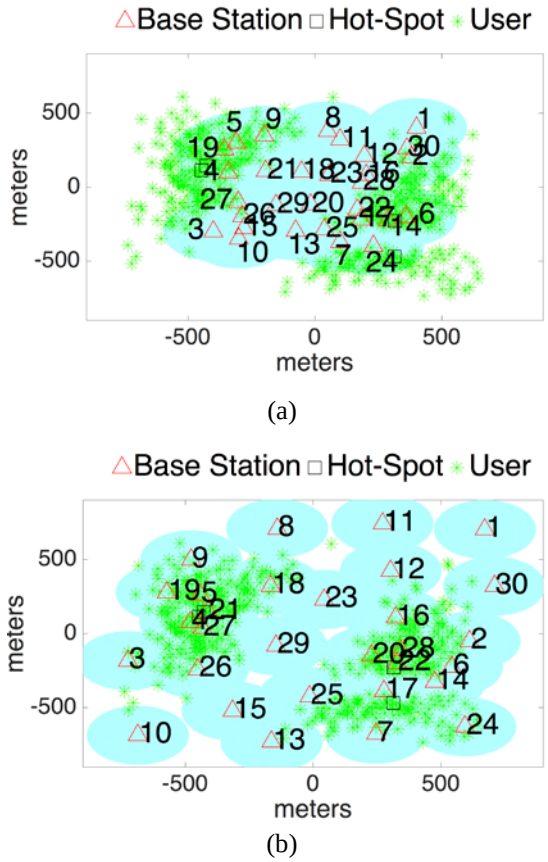

Figure 7. *Example Scenario: (a) Initial location of base stations; (b) Final location of base stations after execution of the algorithm. Base stations are denoted in red, their coverage areas in blue, and users by green asterisks.*

Emergency scenarios such as natural or man-made disasters are typically characterized by unusual peaks in communications demand from both people in the disaster area as well as the first responders and public safety personnel [1]. Traffic hotspots that typically involve vital life-saving information are a major challenge for the communication network covering the disaster area. The exact location and magnitude of these traffic hot-spots within a disaster area are usually unknown *a priori*. As the sizes of possible emergency incidents are unpredictable, estimating the capacity requirements to meet the resulting excess traffic is nearly impossible. Designing a communication network for peak traffic is clearly inefficient, and prohibitively expensive, due to the large peak-to-average traffic ratio [1]. In addition, an over-provisioned network infrastructure itself may be subject to breakdowns or be the target of attack, and therefore not be able to address peak communication needs during emergencies. A reasonable solution to this problem is to use a set of mobile base stations that can be quickly deployed to service the excess traffic during disaster recovery.

Portable cell sites, also referred to as a *cell on wheels* (COW) can be used to augment the remaining communication infrastructure, keeping first responders connected to their command centers. Cellular antennas that are attached to a pneumatic mast on a COW provide additional mobile connection points. By properly deploying these mobile connection points, one can create a temporary network to enable public safety personnel and agencies to maintain communication connectivity throughout their operation.

Base station deployment (i.e., the positioning problem) has been studied in the past [2]. It has been shown that the identification of the globally optimum base station deployment in a network is far too complex to be solved computationally (i.e., it is an NP-hard problem)

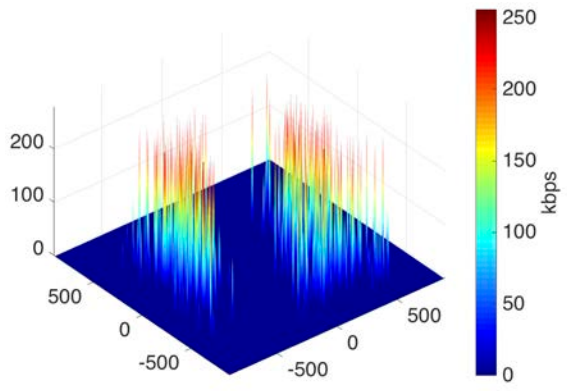

Figure 8. *Distribution of traffic demand in the first scenario.*

[3]. In practice, most of the system parameters required to find such an optimal solution are unknown. In addition, the optimal positions could change due to variations in traffic demand or its spatial distribution. Thus, it is natural to assume that optimal adaptive positioning of mobile base stations based on instantaneous traffic distribution is also an NP-hard problem.

In [4], a portable self-configurable cellular system is proposed to assist with damaged or destroyed network infrastructure in emergencies or other natural disasters. However, the deployment phase was not considered to be autonomous or adaptive. In this project, we aim to develop adaptive self-deployment algorithms to autonomously relocate base stations and maximize network coverage subject to their capacity limits. We assume that each base station has access to information about the location of its neighboring base stations and their capacity demand. Our proposed strategy makes use of the location and capacity demand of each base station and the base stations in its neighborhood. It applies an adaptation of a simulation optimization algorithm presented in [5, 6], which makes use of a feasible direction method to carry out constrained optimization. The basic strategy of the algorithm in [5] is to generate a sequence of feasible and improving solutions. If the magnitude of the constraint function is less than a lower threshold, it means the constraint is well satisfied; then, the variables change in order to improve the objective function. If the constraint function is not satisfied and it is greater than an upper threshold, the variables change in order to satisfy the constraint.

Intuitively, our proposed algorithm aims to maximize network coverage while ensuring that base stations are not over-utilized. Each base station tries to increase its local coverage when the capacity constraints of itself and its neighbors are satisfied. We refer to this phase as the *coverage improvement phase*. On the other hand, if the capacity constraint of a base station is not satisfied (i.e., an overload situation), it makes a request for help by sending a signal to the neighboring base stations to ask them to get closer. We refer to this phase as the *load balancing phase*. In this phase, the neighboring base stations relocate closer to the overloaded base stations if they have available capacity. Because of their moves, some traffic in the coverage area of the overloaded base station can be offloaded onto the neighboring base stations. The sequence of these relocations is expected to improve the overall traffic support throughout the target area. As several neighboring base stations could be in similar situations with varying degrees of excess traffic, the algorithm uses the concept of a virtual force to determine the final direction in which an under-loaded base station should move.

As an example for the operation of our algorithm, consider an initial random deployment of mobile base stations at the center of a 400m × 400m target field. Figure 7(a) shows the initial positions of the base stations (marked by red triangles) along with initial user distribution (marked by green asterisk). Figure 8 displays the traffic demand and its spatial distribution over the region. Given this initial deployment, base stations 4, 6, 19 and 24 encounter high traffic demands beyond their capacity limits. With the execution of our proposed relocation algorithm, base stations that have available capacity relocate closer to traffic hot-spots. When the capacities of base stations meet the traffic demand within their coverage area, they will continue relocating to expand network coverage within the target field. In this way, traffic hot-spots that were originally outside the coverage area of the initial deployment will get an opportunity to be discovered. The above process continues until all base stations can meet their respective traffic demands and maximum network coverage is achieved. Figure 7(b) shows the final base station positions after 30 time-steps. Figure 9 shows how network coverage and the total supported user traffic evolve during the execution of our proposed algorithm. As observed, our proposed algorithm results in increasing

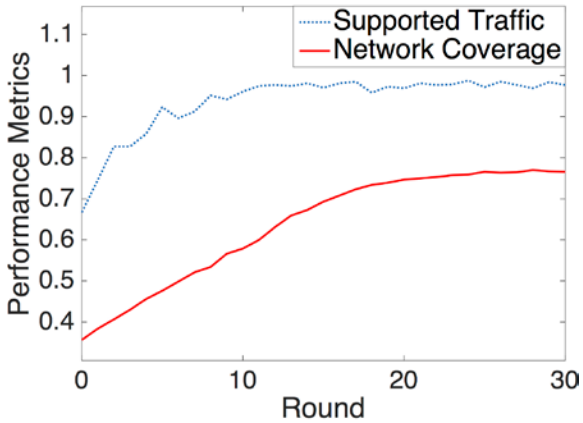

Figure 9. *Network coverage and supported traffic during execution of our proposed adaptive algorithm*

the supported user traffic from 66 % to 96 % as well as improving the network coverage from 35 % to 77 %. Further results can be found in [7].

The execution of our algorithm will effectively adapt the overall network coverage to maximize the supported user traffic. Simulation results show that substantial gain in performance can be achieved under typical usage scenarios. Further research is required to study the impact of various system parameters on the overall performance and convergence speed of the algorithm. We have initially assumed that the base stations can move toward any direction without any restrictions. If there are obstacles or prohibited areas within the target field, the relocation algorithm has to consider additional constraints. Also, new strategies will be required if the overall network consists of a combination of mobile and static base stations. We plan to investigate these scenarios in the future.

References

[1] The Public Safety Nationwide Interoperable Broadband Network: A New Model for Capacity, Performance and Cost, Federal Communications Commission, June 2010.

[2] S. Hurley, Planning Effective Cellular Mobile Radio Networks, *IEEE Transactions on Vehicular Technology*, **51**:2 (2002), 243–253.

[3] R. Mathar and T. Niessen, Optimum Positioning of Base Stations for Cellular Radio Networks, *Wireless Networks* **6**:6 (2000), 421–428.

[4] D. Abusch-Magder, P. Bosch, T. E. Klein, P. A. Polakos, L. G. Samuel and H. Viswanathan, 911-Now: A Network On Wheels for Emergency Response and Disaster Recovery Operations, *Bell Labs Technical Journal* **11**:4 (2007), 113–133.

[5] S. Bashyam and M. C. Fu, Optimization of (*s*, *s*) Inventory Systems with Random Lead Times and a Service Level Constraint, *Management Science* **44**:12-part-2 (1998), S243–S256.

[6] H. Mahboubi, K. Moezzi, A. G. Aghdam, K. Sayrafian and V. Marbukh, Distributed Deployment Algorithms for Improved Coverage in a Network of Wireless Mobile Sensors, *IEEE Transactions on Industrial Informatics* **10**:1 (2014), 163–174.

[7] L. Rabieekenari, K. Sayrafian and J. S. Baras, Autonomous Relocation Strategies for Cells on Wheels in Public Safety Networks, in *Proceedings of the 14th Annual IEEE Consumer Communications & Networking Conference* (IEEE CCNC 2017), Las Vegas, NV, January 8-11, 2017, to appear.

Participants

Kamran Sayrafian (ACMD); Ladan Rabieekenari, John S. Baras (Univeristy of Maryland)

Compensated Explicit Schemes in Ill-Posed Time-Reversed Evolution Equations

Initial value problems for time dependent partial differential equations (PDEs) arise in various branches of continuum physics. Given the initial state of a physical system at time t=0, its progressive future evolution up to some fixed time T > 0 can routinely be predicted by numerical computation of the associated PDE system using a stepwise time-marching scheme with time steps of Δt > 0. However, in certain cases, the following inverse problem *may be of major interest. Given the observed state of the physical system at time T > 0, can one reconstruct its past evolution from some unknown previous state at time t=0? A related control theory question might be to find an initial state at time t=0 that would achieve a desired final state at some given time T > 0. Ideally, such questions might easily be answered by marching backward from a given state at T > 0, using negative time steps Δt < 0.*

One important example of such time reversal is the recovery of the history of groundwater contaminant plumes, by solving an advection diffusion equation backward in time. Another rich source of time reversed diffusion equations lies in the deconvolution problems that pervade measurement science. Commonly, the true physical signal must be deconvolved from the Gaussian-like point spread functions that typically characterize many measuring instruments. Such deconvolution problems can be reformulated into mathematically equivalent backward diffusion equations. That approach has produced high quality reconstructions in galactic scale Hubble telescope imagery, as well as in nanoscale scanning electron microscopy.

Unfortunately, although highly desirable because of their simplicity, stepwise schemes marching backward in time cannot be used on PDE systems involving dissipation. These are ill-posed initial value problems, and marching schemes consistent with such problems are necessarily unconditionally unstable, *leading to explosive noise amplification. Recently, a useful strategy has been developed that can stabilize such ill-posed marching computations. These stabilized schemes are slightly inconsistent, yet lead to useful results in numerous challenging nonlinear backward dissipative problems.*

Alfred Carasso

Compensated explicit schemes constitute a significant ACMD intervention, one that permits effective numerical computation of multidimensional nonlinear dissipative evolution equations, backward in time [1, 2]. While generally considered intractable, such ill-posed retrospective problems are of great interest in such fields as environmental forensics [3-5], geophysics [6-8], and image deblurring [9-11]. Numerous other types of ill-posed partial differential equation (PDE) problems are discussed in [12-14].

The initial focus in this ongoing research project was on stabilizing the $O(\Delta t)$ accurate pure explicit marching scheme, by applying easily synthesized linear smoothing operators at each time step, based on positive real powers of the negative Laplacian, to quench the instability. This was successfully used in nonlinear backward parabolic equations in [1, 2]. Subsequently, a stabilized pure explicit scheme was successfully used in ill-posed time-reversed viscoelastic wave propagation [15]. While compensated explicit schemes can be applied to interesting classes of nonlinear problems, the analysis of stability is restricted to linear problems involving selfadjoint spatial operators. However, even in that simplified case, non-trivial analysis involving 3×3 systems of PDEs is often necessary to obtain the requisite energy inequalities.

Stabilized Leapfrog Scheme. Stabilizing the Richardson $O(\Delta t)^2$ accurate leapfrog scheme is of considerable computational interest, but presents challenging difficulties. In well-posed linear wave propagation problems, the leapfrog scheme requires a Courant stability condition on the time step Δt. However, even when the Courant condition is obeyed, the leapfrog scheme becomes unstable in nonlinear wave propagation problems [16, 17]. For parabolic equations, the leapfrog scheme is unconditionally unstable even in well-posed forward linear problems!!! Nevertheless, the leapfrog scheme can be stabilized for linear forward or backward parabolic equations by appropriate use of compensating smoothing operators at each time step. Unfortunately, as in wave propagation equations, the stabilized compensated leapfrog scheme becomes unstable in nonlinear parabolic equations.

In atmospheric and oceanic computations, leapfrog nonlinear instability is routinely suppressed by applying the Robert-Asselin-Williams (RAW) post-processing technique [18-20]. Remarkably, as shown in [21], the same post-processing technique can also be usefully applied in the nonlinear ill-posed parabolic case. Thus, the compensated leapfrog scheme in [21], coupled with RAW filtering, can solve nonlinear backward parabolic equations explicitly with $O(\Delta t)^2$ accuracy. This is surely a noteworthy achievement.

Coupled Hyperbolic Parabolic Systems Backward in Time. Beginning with coupled sound and heat flow discussed in [16], there has been growing interest in

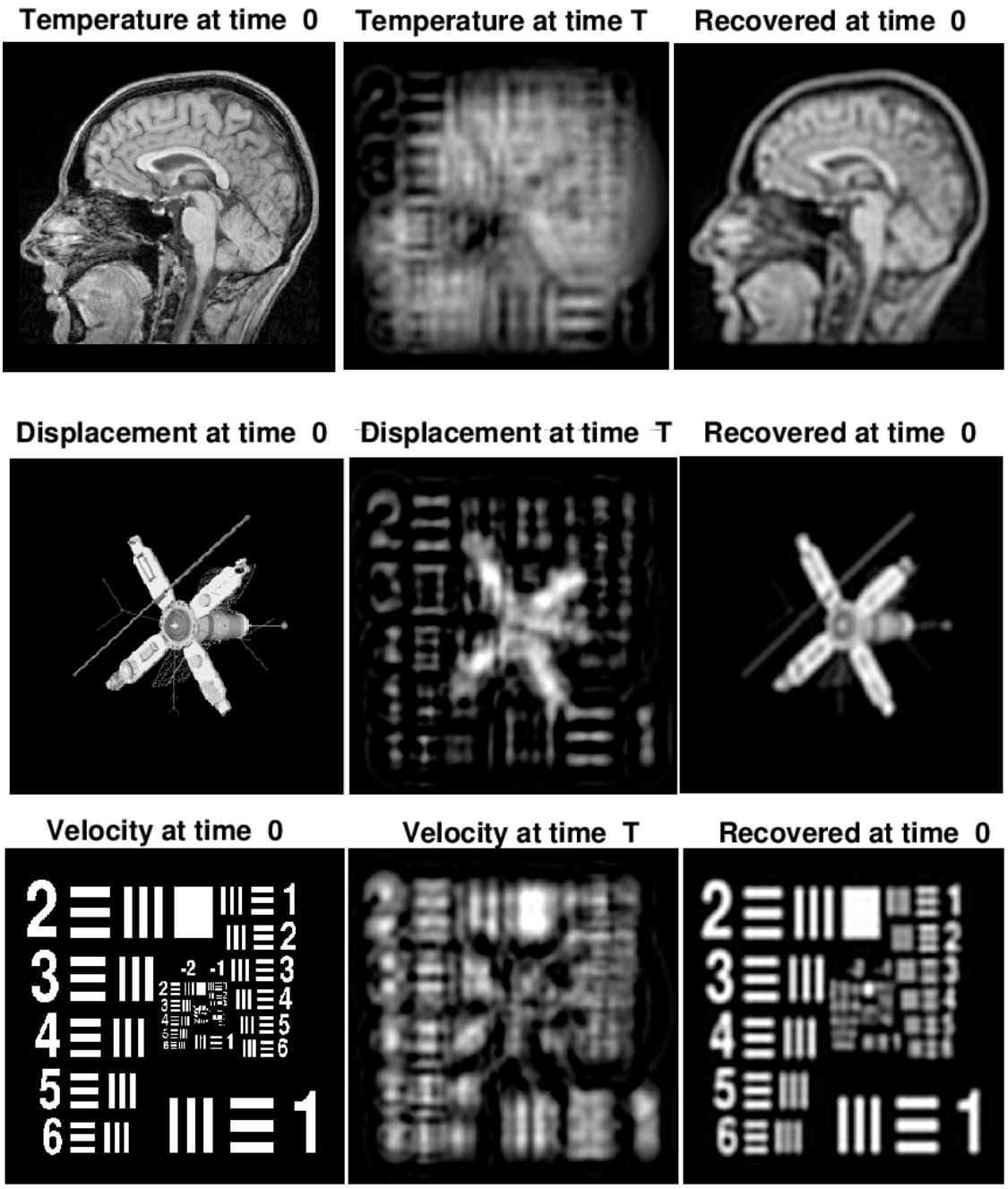

Figure 10. *Backward Recovery in Thermoelastic Plate. Using data at positive time T, shown in middle column, the stabilized explicit scheme aims at reconstructing the true initial data at time 0, shown in the leftmost column. The actual recovered data is shown in the rightmost column.*

coupled hyperbolic parabolic systems. Heightened interest in the semigroup properties of such systems was fueled by the equations for dynamic thermoelasticity which lead to holomorphic semigroups [22-25], whereas this is not true in coupled sound and heat flow. Hyperbolic-parabolic systems typically result in a system of three first order in time partial differential equations, involving linear or nonlinear spatial differential operators of second or higher order. In such systems, the three distinct initial values propagate and influence one another in ways that are not easily anticipated, and generally result in unrecognizable data at time $T > 0$. An intriguing question is whether the seriously distorted data at time $T > 0$ uniquely reflect the initial values. Can these data be used in a backward in time calculation to reconstruct the initial values? Important analytical studies of backward

in time uniqueness and backward stability in linear thermoelasticity may be found in [26-28]. However, very little seems to be known regarding the possibility of effective numerical computation of such backward problems.

Time Reversed Thermoelastic Wave Propagation. In a significant advance, a methodology was devised for constructing compensated explicit schemes for the equations of coupled sound and heat flow discussed in [13] and [16], and the thermoelastic plate equations discussed in [23], together with proofs of stability of these schemes in the L^2 norm. Numerous computational experiments were performed to validate the theory. A striking example of backward-in-time reconstruction for the plate equations in [23], is shown in Figure 10, using images of recognizable objects as input data at time $t = 0$. Such images are defined by highly nonsmooth intensity data that provide challenging tests for any ill-posed reconstruction method. Here, the input data in the leftmost column produce the severely distorted results at the positive time T, shown in the middle column. Using these data in the compensated explicit scheme running backward in time, produces the results in the rightmost column.

References

[1] A. S. Carasso, Compensating Operators and Stable Backward in Time Marching in Nonlinear Parabolic Equations, *International Journal of Geomathematics* **5** (2014), 1-16.

[2] A. S. Carasso, Stable Explicit Time-Marching in Well-Posed or Ill-Posed Nonlinear Parabolic Equations, *Inverse Problems in Science and Engineering* **24** (2016), 1364-1384.

[3] R. N. Singh, Advection Diffusion Equation Models in Near-Surface Geophysical and Environmental Sciences, *Journal of the Indian Geophysical Union* **17** (2013), 117-127.

[4] J Atmadja and A. C. Bagtzoglou, State of the Art Report on Mathematical Methods for Groundwater Pollution Source Identification, *Environmental Forensics* **2** (2001), 205-214.

[5] J. Atmadja and A. C. Bagtzoglou, Pollution Source Identification in Heterogeneous Porous Media, *Water Resources Research* **37** (2001), 2113-2125.

[6] Ismail-Zadeh, et al., Inverse Problem of Thermal Convection: Numerical Approach and Application to Mantle Plume Restoration, *Physics of the Earth and Planetary Interiors* **145** (2004), 99-114.

[7] A. Ismail-Zadeh et al., Three Dimensional Forward and Backward Numerical Modeling of Mantle Plume Evolution: Effects of Thermal Diffusion, *Journal of Geophysical Research* **111** (2006), B06401.

[8] A. Ismail-Zadeh et al., Numerical Techniques for Solving the Inverse Retrospective Problem of Thermal Evolution of the Earth Interior, *Computers and Structures* **87** (2009), 802-811.

[9] G. Gilboa et al., Forward-and-Backward Diffusion Processes for Adaptive Image Enhancement and Denoising, *IEEE Transactions on Image Processing* **11** (2002), 669-703.

[10] A. S. Carasso, D. S. Bright and A. E. Vladar. APEX Method and Real-Time Blind Deconvolution of Scanning Electron Microscope Imagery, *Optical Engineering* **41** (2002), 2499-2514.

[11] A. S. Carasso, Bochner Subordination, Logarithmic Diffusion Equations, And Blind Deconvolution of Hubble Space Telescope Imagery and Other Scientific Data, *SIAM Journal on Imaging Science* **3** (2010), 954-980.

[12] M. M. Lavrentiev, *Some Improperly Posed Problems of Mathematical Physics*, Springer-Verlag, New York, 1967.

[13] R. Lattès and J. L. Lions, *The Method of Quasi-Reversibility*, American Elsevier, New York, 1969.

[14] K. A. Ames and B. Straughan, *Non-Standard and Improperly Posed Problems*, Academic Press, New York, 1997.

[15] A. S. Carasso, Stable Explicit Marching Scheme in Ill-Posed Time-Reversed Viscous Wave Equations, *Inverse Problems in Science and Engineering* **24** (2016), 1454-1474.

[16] R. D. Richtmyer and K. W. Morton, *Difference Methods for Initial Value Problems*, 2nd ed., Wiley, New York, 1967.

[17] B. Fornberg, On the Instability of Leapfrog and Crank-Nicolson Approximations of a Nonlinear Partial Differential Equation, *Mathematics of Computation* **27** (1973), 45-57.

[18] R. Asselin, Frequency Filter for Time Domain Integrations, *Monthly Weather Review* **100** (1972), 487-490.

[19] P. D. Williams, A Proposed Modification to the Robert-Asselin Time Filter, *Monthly Weather Review* **137**, (2009), 2358-2546.

[20] Y. Li and C. Trenchea, A Higher Order Robert-Asselin Type Time-Filter, *Journal of Computational Physics* **259** (2014), 23-32.

[21] A. S. Carasso, Stabilized Richardson Leapfrog Scheme in Explicit Stepwise Computation of Forward or Backward Nonlinear Parabolic Equations, in review.

[22] D. L. Russell, A General Framework for The Study of Indirect Damping Mechanisms in Elastic Systems, *Journal of Mathematical Analysis and Applications* **173** (1993), 339-358.

[23] Z. Liu and M. Renardy, A Note on the Equations of a Thermoelastic Plate, *Applied Mathematics Letters* **8** (1995), 1-6.

[24] J. E. Muñoz Rivera and Y. Shibata, A Linear Thermoelastic Plate Equation with Dirichlet Boundary Condition, *Mathematical Methods in the Applied Sciences* **20** (1997), 915-932.

[25] Z. Liu and S. Zheng, *Semigroups Associated with Dissipative Systems*, Chapman and Hall/CRC, New York, (1999).

[26] K. A. Ames and L. E. Payne, Stabilizing Solutions of the Equations of Dynamical Linear Thermoelasticity Backward in Time, *Stability and Applied Analysis of Continuous Media* **1** (1991), 243-260.

[27] I. Lasiecka, M. Renardy and R. Triggiani, Backward Uniqueness for Thermoelastic Plates with Rotational Forces, *Semigroup Forum* **62** (2001), 217-242.

[28] M. Ciarletta, On the Uniqueness and Continuous Dependence of Solutions in Dynamical Thermoelasticity Backward in Time, *Journal of Thermal Stresses* **25** (2002), 969-984.

Participants

Alfred Carasso (ACMD)

Grover Search and the No-Signaling Principle

From an information processing point of view, two of the key properties of quantum physics are the no-signaling principle and the lower bound on the complexity of search problems. That is, despite admitting stronger-than-classical correlations, quantum mechanics does not imply faster-than-light signaling, and despite a form of exponential parallelism, quantum mechanics does not allow exponentially hard computational problems to be solved efficiently by brute-force search. Recently, we investigated the degree to which these two properties are connected. We examined various deviations from quantum mechanics, for which we drew inspiration from the literature on the black hole information paradox. We found that in these models, the physical resources required to send a faster-than-light signal closely tracked the resources needed to speed up quantum search algorithms. Thus, the impossibility of performing exponentially large searches in polynomial time appears to be remarkably robust, depending not in a sensitive way on the complete formalism of quantum mechanics, but rather determined by more foundational principles such as the impossibility of transmitting signals faster than light.

Stephen Jordan

Quantum mechanics has many counterintuitive features that have consequences for information transmission and processing. In particular, the principle of superposition says that, as in the famous "Schrodinger's cat" thought experiment, systems can be put into superpositions over distinct classical states. More quantitatively, the state of a quantum system is described by a vector of complex numbers called amplitudes, one associated with each distinguishable state. The probability of observing the system in a given state is then given by the absolute square of the associated amplitude. Thus, for a system of n quantum bits ("qubits") the quantum state is a list of 2^n amplitudes, one for each possible length-n bit string. For ordinary macroscopic objects (such as cats) stray interactions with the environment quickly wash out any detectable effects of quantum superposition. However, in carefully controlled laboratory environments quantum superpositions of increasingly large and complex systems have been demonstrated. Many labs around the world are now intensifying such efforts with the goal of building large scale quantum computers.

The exponentially high dimension of quantum state vectors provided one of the first hints which led Richard Feynman and others to suggest in the 1980s that quantum systems with many degrees of freedom might serve as computers with exponentially more power than conventional classical computers. These intuitions were borne out by subsequent developments, such as Peter Shor's spectacular 1994 discovery of a quantum algorithm to factor n-digit integers using only of order n^3 steps. The fastest known classical algorithm for integer factorization uses a number of steps that grows nearly exponentially in n. Another key development was the 1995 discovery by Lov Grover of a quantum algorithm to search an unstructured database of size N using only of order $\sqrt{N}$ queries, whereas of order N queries would be needed classically.

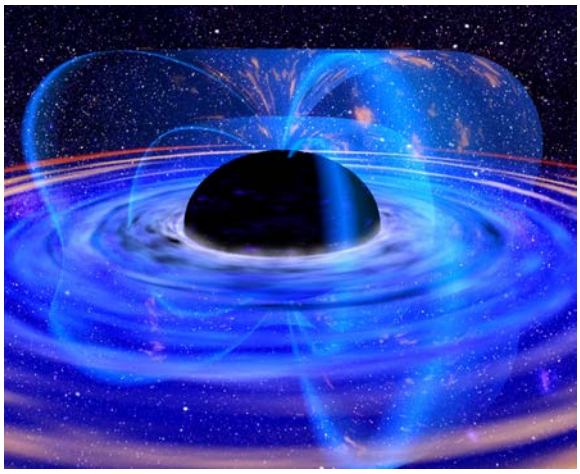

Figure 11. *Artist's rendering of a black hole. The black hole information paradox has interesting implications for quantum algorithms, and vice versa.* (Credit: Dana Berry, NASA)

Although the exponentially high dimensional state space of quantum mechanics is a necessary ingredient for the exponential computational speedups achievable by quantum algorithms, quantum computers do not achieve their advantages simply by performing exponentially many different computations in parallel via superposition. In fact, prior to Grover's discovery of a quadratic quantum speedup for search, Bennett et al. proved that quantum computers are incapable of greater than quadratic speedup for unstructured search problems [1]. That is, Grover's algorithm is as good as it gets for quantum speedup of brute force search.

Entanglement is another counterintuitive feature of quantum mechanics, of a subtler but perhaps even more fundamental nature than superposition. Quantum entanglement manifests itself as correlations between the outcomes of measurements performed on separated systems that are not achievable by any local classical process. The canonical example of this is the CHSH game. In this game, two parties, conventionally called Alice and Bob, are widely separated to prevent communication. They are each independently at random given

one of two possible instructions I_{Alice}, $I_{Bob} \in \{0,1\}$ and they reply with one of two possible responses R_{Alice}, $R_{Bob} \in \{0,1\}$. The goal of the game is to achieve $R_{Alice} \oplus R_{Bob} = I_{Alice} \wedge I_{Bob}$. It can be proven that, in a classical world, if Alice and Bob cannot communicate (so that Alice does not know I_{Bob} at the moment she has to produce R_{Alice} and Bob does not know I_{Alice} at the moment he has to produce R_{Alice}) the highest achievable probability for winning this game is 75 %. An optimal classical strategy is simply for Alice and Bob each to respond with 0 every time. However, if Alice and Bob share an entangled quantum state they can use it to win the game with probability approximately 85 %.

Although originally a thought experiment, the CHSH game can now be implemented in laboratories. The ultimate version of this experiment is to separate Alice and Bob sufficiently widely that the experiment is completed in less time than it would take for light to travel from Alice to Bob or vice-versa. This was recently achieved using high speed photonics at NIST [2]. According to special relativity, no signal can travel faster than light, and therefore such separation guarantees no communication between Alice and Bob. If signals did travel faster than light, then this would allow transmission of signals backward in time, with all the associated paradoxes. Although measurements on entangled quantum states allow certain correlations that are stronger than those achievable classically, the correlations are not strong enough to allow signals to be sent faster than light. The impossibility of faster-than-light signaling is in fact provable within the axioms of quantum mechanics, and is known as the no-signaling theorem. (Alternatively, attempts have been made to regard the no-signaling principle as an axiom, which combined with other operational principles, might allow quantum mechanics to be derived.)

The no-signaling principle and the Grover search lower bound are two of the key properties of quantum physics as it relates to information science. That is, despite admitting stronger-than-classical correlations, quantum mechanics does not imply superluminal signaling, and despite a form of exponential parallelism, quantum mechanics does not imply polynomial-time brute force solution of exponentially hard search and optimization problems. In recent work [3] we investigated the degree to which these two properties are connected. To clarify the relationships between these features we examined various deviations from the axioms of quantum mechanics. What we found was that, in every case, the physical resources required to send a superluminal signal scale polynomially with the resources needed to speed up Grover's algorithm. Hence the no-signaling principle is equivalent to the inability to efficiently perform exponential-size brute force search within the classes of theories analyzed. Put differently, the impossibility of performing exponentially large searches in polynomial time appears to be remarkably robust, depending not in a sensitive way on the complete Hilbert-space formalism of quantum mechanics, but rather determined by more foundational operational principles such as the impossibility of superluminal signaling.

To obtain physically motivated examples of modifications to the axioms of quantum mechanics, we drew upon the literature on the black hole information paradox. According to quantum mechanics, the time evolution of state vectors is always reversible; information is never destroyed. According to general relativity, information can never escape from a black hole. Calculations by Hawking indicate that black holes should gradually evaporate through the emission of thermal radiation. So, if information falls into a black hole, and the black hole evaporates, but information cannot escape from the black hole, then where did the information go? Many resolutions have been proposed to this apparent conflict between quantum mechanics and general relativity without any consensus emerging. Several of the proposed resolutions work by modifying the axioms of quantum mechanics such as by allowing nonlinear time-evolution of the state-vector.

Work by Abrams and Lloyd in 1998 showed that, generically, nonlinear time-evolution of quantum state-vectors allows polynomial-time solution to exponential size search problems [4]. So, does this suggest that black holes could, in principle, be used to perform exponentially difficult computations beyond the reach even of "standard" quantum computers? Our results throw some cold water on this possibility. Specifically, we find that if the nonlinearities are strong enough to yield efficient solution to exponentially large search problems, then they are also strong enough to allow nonnegligably large instantaneous information transmission capacity over arbitrarily large distances, in violation of well-established principles of special relativity.

References

[1] C. H. Bennett, E. Bernstein, G. Brassard and U. Vazirani, Strengths and Weaknesses of Quantum Computing, *SIAM J. on Computing* **26** (1997), 1510-1523.

[2] L. K. Shalm, et al., Strong Loophole-free Test of Local Realism, *Physical Review Letters* **115** (2015), 150402.

[3] N. Bao, A. Bouland and S. P. Jordan, Grover Search and the No-signaling Principle, *Physical Review Letters* **117** (2016) 120501.

[4] D. S. Abrams and S. Lloyd, Nonlinear Quantum Mechanics Implies Polynomial-Time Solution for NP-Complete and #P Problems, *Physical Review Letters* **81** (1998), 3992.

Participants

Stephen Jordan (ACMD); Ning Bao (Caltech); Adam Bouland (MIT)

Taking the CAVE on the Road Using 360º Video

ACMD's High Performance Computing and Visualization Group (HPCVG) operates an immersive virtual environment (IVE) in support of its mission to develop advanced visualization of scientific data in support of NIST measurement science. This work includes developing the 3D immersive environment into an interactive measurement laboratory. HPCVG collaborates with researchers across NIST to apply the IVE and virtual measurement techniques to both experimental and simulation data. One drawback to our IVE, known as the CAVE, is that it is very difficult to provide the sense of immersion except by physically visiting the CAVE installation. This makes it difficult to publicize the visualizations that HPCVG has developed.

This past year we integrated 360° video generation into our visualization pipeline, allowing us to generate video clips of immersive visualizations. These 360° clips allow the viewer to turn around and see the data from different orientations. They can be uploaded to YouTube for easy public viewing. At the NIST/ITL/ACMD booth at the 2016 Supercomputing Conference we provided a GearVR Head-Mounted Display loaded with several 360° videos of immersive visualizations. This configuration let us provide booth visitors a sense of the immersion offered by the CAVE.

Wesley Griffin

An immersive virtual environment (IVE) is a type of virtual reality (VR) system in which the viewer is typically standing and the viewer's body position and orientation are part of the viewing experience. There are three key components to the system needed to provide immersion.

1. Multiple large screens to encompass as much of the user's field of view as possible. We have found that projecting an image onto the floor significantly improves immersion.
2. Stereoscopic displays providing 3D viewing through synchronized glasses.
3. Head tracking of the user. A six-degree-of-freedom tracker, placed on the glasses, reports real-time position and orientation of the user's head.

Combined, these three components enable 3D rendering of data as if it is occupying the same physical space as the user.

This type of IVE/VR system is commonly referred to as a CAVE™ [1, 2, 3]. A CAVE (CAVE Automatic Virtual Environment[5]) is just one type of IVE/VR system. CAVEs vary in configuration from two to six screens, (three are installed at NIST), where the user is placed inside a fully projected cube. All IVE/VR systems have trade-offs. A CAVE can be thought of as a small room, and thus provides a physical space for multiple people to meet, collaborate, and interact with the data. Figure 12 shows the three-screen CAVE installed at NIST and Figure 13 shows a scientist using the CAVE for data visualization.

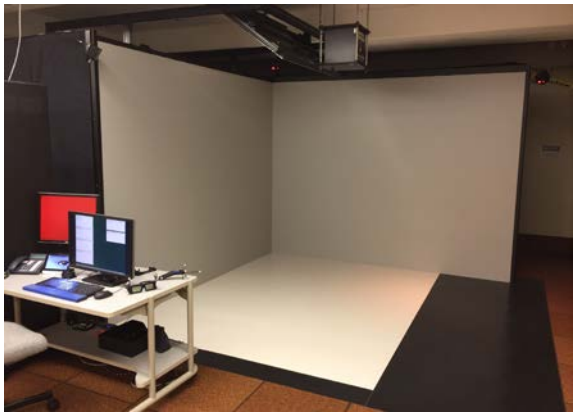

Figure 12. *The HPCVG CAVE facility.*

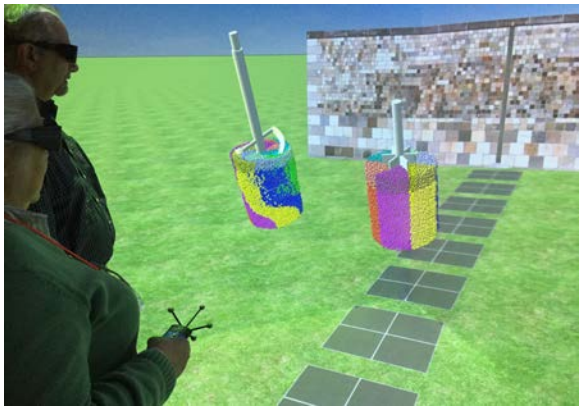

Figure 13. *Scientists using the CAVE facility.*

The CAVE has proven to be very effective at allowing scientists to visualize data, while providing a versatile space for collaborative working sessions and visitor demonstrations. One drawback to the CAVE, however, is that it is very difficult to provide the sense of immersion except by physically visiting the CAVE installation. This makes it difficult to publicize the immersive visualizations HPCVG has developed.

In contrast to the CAVE, a different type of VR system is the head-mounted display (HMD). An HMD

[5] Yes, this is indeed a recursive acromym.

system is a pair of small displays that are mounted together into a goggle-style form factor and worn on the head. The user is completely immersed in the virtual world through isolation from the physical world. Head-mounted display systems have seen significant recent growth in popularity due to a drastic reduction in cost. Traditional HMD systems require a separate computer to drive the displays; however, cell-phones are proving remarkably capable of being used for HMDs. The Samsung GearVR [4] is one example of this type of self-contained HMD.

360° Video. 360° video is a specially encoded video file that a 360° video player can present in a manner that allows the viewer to "look around" the video file. This YouTube video[6] is an example of a 360° video. The YouTube player understands the special encoding, and using the mouse, the viewer can rotate the scene around in the video player. This example is a "test pattern" where the viewer is standing inside a box and each face of the box is labelled: Front, Left, Right, Back, Down, and Top. This method of representing a surrounding environment is called a cubemap.

Cube maps are one approach to rendering a 360° view of a scene. Essentially, the scene camera is positioned at the center of a cube and the virtual world is then rendered on the inside face of the cube to form six images that surround the viewer. Figure 14 shows the cube faces "unfolded" into a linear form. Each of the six faces is labelled. As we discuss later, we were able to modify our CAVE rendering software to render all six faces of the cube.

While it is possible to reconstruct a projected view directly from the cube map representation, video playback is simpler if one projects the 360° view into a single, linear 2D image. The most commonly accepted form of this projection is the equirectangular projection. Figure 15 shows the six cube faces from above encoded in this way. During playback, this image is re-projected back into an image based on the viewer's orientation. The mathematics behind this projection is straightforward; however, we found encoding many frames of video to be time consuming. Thus, we implemented a custom stitching program that is described later.

Software Development. Our High End Visualization (HEV) software is a mix of open-source and custom software that we have developed to build visualization applications that run both on our desktops and in the CAVE. We have deliberately focused on a modular software architecture and this approach allowed us to add support for rendering cubemaps relatively easily.

HEV software uses a dynamic shared object (DSO) [5] to isolate the specific characteristics of display devices. A desktop DSO is loaded when running

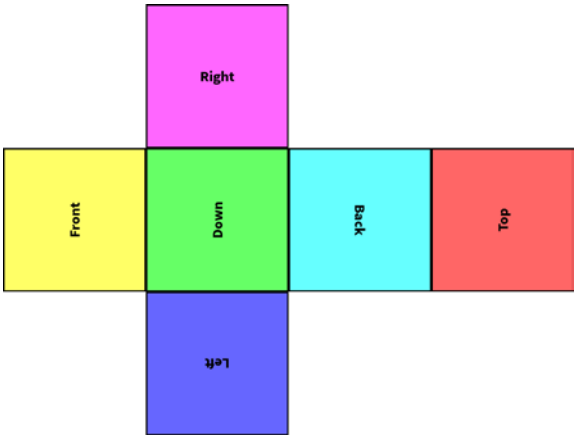

Figure 14. *A cube "unwrapped into a 2D image.*

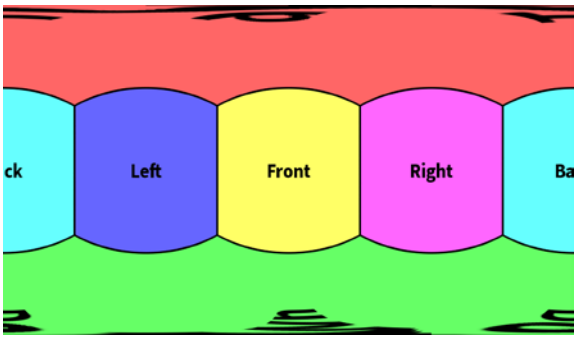

Figure 15. *Equirectangular stitching of cube into a 2D image.*

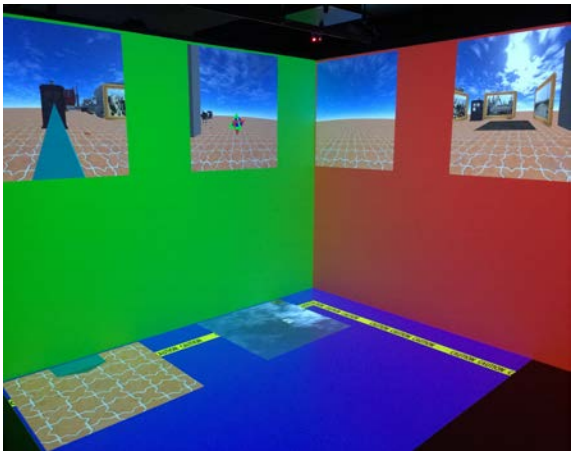

Figure 16. *CAVE with six views displayed.*

applications on the desktop, and a DSO tailored to our specific CAVE is used for CAVE applications. Our first step for generating the six images needed per cubemap was to create a Cube Map DSO.

The Cube Map DSO is a variation of the CAVE DSO. Instead of rendering one full screen view for the three (Front, Left, Down) screens, the variation displays two views per screen: Front Screen for front and back

[6] https://youtu.be/AiYIuK3eR_U

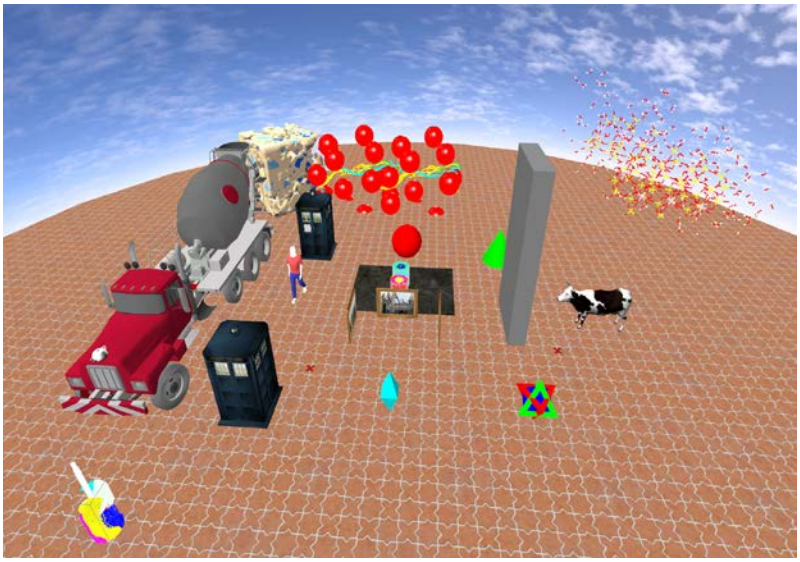

Figure 17. *Diorama prototype.*

Figure 18. *Signposts for explanation.*

views; Left Screen for left and right view; Down Screen for down and top view. With this DSO, we simply run the application and perform six screen grabs to generate the six images needed for a Cube map. Figure 16 illustrates this.

Due to the resolution of the screen displays, rendering two views per screen limits the cube map images to 512 × 512 pixels. To move to higher resolutions, we created another display DSO utilizing off-screen rendering. This off-screen DSO allows us to generate the six cube map images at the desirable 1024 × 1024 resolution. Higher resolutions are also possible when needed.

After HEV has rendered the cube map frames we need some method to stitch the individual cube map faces for each video frame into a single equirectangular projected frame. The projection math is straight-forward and we describe it more fully, along with several other projection methods in a paper currently being written [6]. This paper describes a student project by Vinay K. Sriram, who studied several different methods of re-sampling the cube map faces, and also several different methods of projection. He implemented all the approaches in a program [7] and used two objective image comparison metrics: CIELAB ΔE color differencing and the Structural Similarity Index Metric to evaluate the results.

From that initial implementation, we quickly discovered the need for higher speed when stitching the frames. To enable this, we hard-coded several components of the stitching algorithm, making use of Correlated Multi-Jittered Sampling [8] with 16 samples per pixel for sampling from the cube map faces. Once the parameters were fixed, we vectorized the equirectangular projection algorithm using the Intel AVX instruction set. We also added multi-threading to stitch as many frames as CPU cores in parallel. These changes resulted in a 15-fold speedup over the initial implementation that stitched one frame per CPU core in parallel but was not vectorized.

Our HEV software also includes an animated path capability allowing the user to move through an environment following a predefined set of locations. We combined this capability with the cube map rendering and frame grabbing to create a desired set frames. To aid in crafting a path, we developed a simple path editor and preview capability. Using the CAVE, the user goes into the diorama and walks around marking specific locations of interest. Using these “bread crumbs,” the path software generates a smooth path. The designer can preview and edit the path before running it with cube map frame grabbing enabled.

Results. We demonstrated a prototype 360° video and described our initial attempts at the Immersive Visualization for Science and Research Birds of a Feature (BoF) at the ACM SIGGRAPH Conference in July, 2016 [9]. The demonstration was very successful and we received quite a bit of interest from the BoF attendees in 360° video. The GearVR was extremely

useful in providing a sense of immersion for the video.

This prototype was a virtual environment which included several of our existing application visualizations. Individually, the applications exist as data floating in front of the user standing in the CAVE. In the CAVE the user can rotate, scale, fly though and manipulate the data in ways specific to the application. For the 360º prototype, the multiple visualizations exist in a shared space, much like the rides on a carnival mid-way. To enhance this paradigm, a ground plane and blue sky with moving clouds were added. Figure 17 is an image of the prototype diorama. When displayed in the CAVE, the user can explore and view the animated visualization on a human scale.

As we worked with the prototype diorama and the resulting 360° videos, we noted that using a traditional audio track would not be entirely effective, since in a 360° video the user controls where and when to look. Thus, audio track narration wouldn't necessarily correspond with what the users see. Our solution was to create signposts in the environment, shown in Figure 18, with written information describing that view, much like an information panel on a museum exhibit.

Our final goal for the year was to take several videos showcasing our cement visualizations to the Supercomputing Conference (SC) in November 2016. ACMD organizes a booth each year in the SC Exhibit Hall, and we felt the 360° videos viewed with a GearVR would provide booth visitors with a sense of the immersive quality of our visualization work. The following videos were well received there:

- Two Pipe Flow Comparison[7]. This visualization compares the flow of suspensions in a pipe. In one case the matrix fluid (fluid with immersed solids) is Newtonian (constant viscosity). In the other case, the matrix fluid is shear thinning (i.e., viscosity decreases with increasing shear rate or velocity gradient). Several results can be seen. First, the shear thinning fluid flows faster. Second, all the action is near the pipe wall, where the flow velocity changes very rapidly, such that viscosity becomes much lower. In both cases, the solid density is greater near the tube central axis, with this effect enhanced in the Newtonian case.
- Spiral Rheometer[8]. Rheometers are often used to evaluate the rheological properties of complex suspensions, such as concrete. This visualization illustrates the flow of a suspension in a rheometer with a double spiral-shaped impeller. Our study showed that such an impeller did a better job of mixing the suspension than other impellers typically used in industry (e.g., vane-shaped impeller). Because of this, the measurements were based on a more representative sample of the concrete (e.g., less sedimentation and migration away from the blade).
- Cement Fibers[9]. Fibers are often added to mortar and concrete to improve their tensile properties, making them more resistant to cracking. This project was carried out to study the effect of fiber stiffness on a mortar's flow properties (viscosity). Comparisons were made between the flow of very stiff fibers (e.g., those made out of steel) and very flexible fibers (e.g., shredded rubber tires) in a mortar. It was observed that the more flexible the fibers are, the more likely they are to become entangled and not disperse well. Thus, the mortar becomes more viscous and less homogeneous due to the fiber entanglements.

References

[1] C. Cruz-Neira, D. J. Sandin, T. A. DeFanti, R. V. Kenyon, and J. C. Hart. The CAVE: Audio Visual Experience Automatic Virtual Environment, *Communications of the ACM* **35**:6 (1992), 64-72.

[2] C. Cruz-Neira, D. J. Sandin and T. A. DeFanti. Surround-Screen Projection-based Virtual Reality: The Design and Implementation of the CAVE, in *SIGGRAPH'93: Proceedings of the 20th Annual Conference on Computer Graphics and Interactive Techniques*, Anaheim, CA, August 2-6, 1993, 135-142.

[3] CAVE (CAVE Automatic Virtual Environment) is a trademark owned by the University of Illinois at Chicago (UIC) Board of Trustees. Mechdyne Corporation is licensed to manufacture and distribute the product.

[4] Samsung, GearVR, Accessed July 2016, http://www.samsung.com/us/explore/gear-vr/.

[5] Wikipedia, Dynamic Loading, Accessed December 2016, https://en.wikipedia.org/wiki/Dynamic_loading.

[6] V. K. Sriram and W. Griffin, Implementation of a Sampling-Agnostic Software Framework for Converting Between Texture Map Representations of Virtual Environments, in progress.

[7] V. Sriram. cubemap-stitch, https://github.com/usnistgov/cubemap-stitch.

[8] A. Kensler, Correlated Multi-Jittered Sampling, Pixar Technical Memo 13-01, March, 2013.

[9] W. Griffin, S. Satterfield, S. Ressler and J. Terrill. 360 Video from a Virtual Six-Sided Cave, Immersive Visualization for Science and Research, SIGGRAPH Birds of a Feather, Anaheim CA, US, July 25, 2016.

Participants

William George, Wesley Griffin, Steve Satterfield, Sandy Ressler, Vinay Sriram and Judith Terrill (ACMD)

[7] https://www.youtube.com/watch?v=hLVIBP-7QcQ

[8] https://www.youtube.com/watch?v=ux_pFExlj9c

[9] https://www.youtube.com/watch?v=5YzDc0LsyXA

Part III

Project Summaries

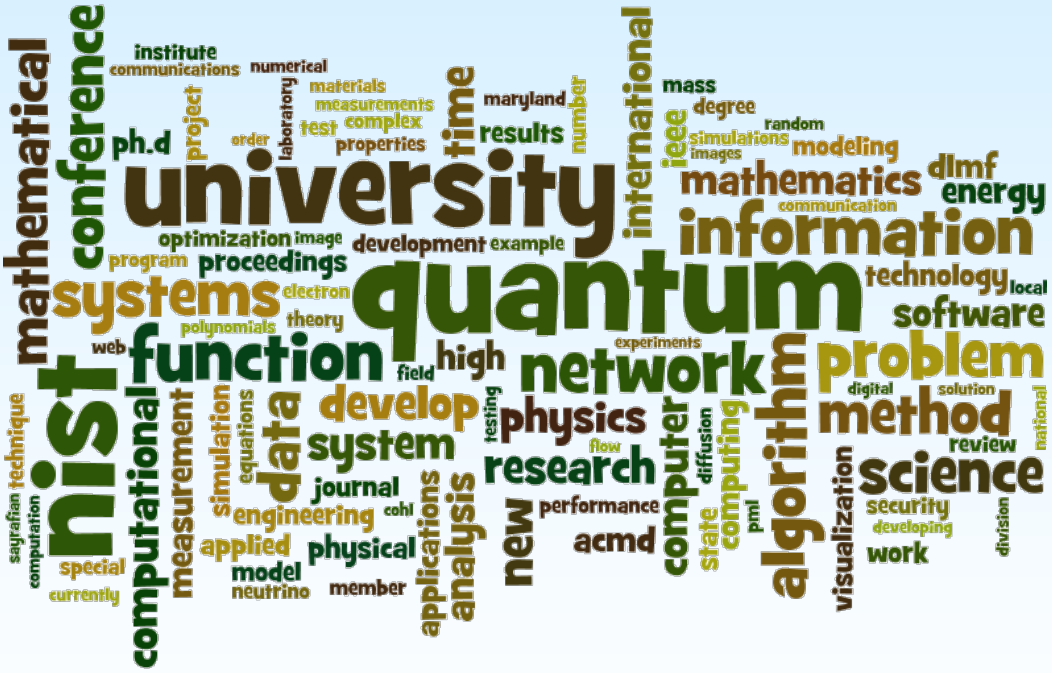

Mathematics of Metrology

Mathematics plays an important role in the science of metrology. Mathematical models are needed to understand how to design effective measurement systems, and to analyze the results they produce. Mathematical techniques are used to develop and analyze idealized models of physical phenomena to be measured, and mathematical algorithms are necessary to find optimal system parameters. Finally, mathematical and statistical techniques are needed to transform measured data into useful information. The goal of this work is to develop fundamental mathematical methods and analytical tools necessary for NIST to continue as a world-class metrology institute, and to apply them to critical measurement science applications.

Molecular Movies: Imaging Femtosecond Motion during Electrochemical Transitions

Bradley Alpert
Joel Ullom et al. (NIST PML)
Chris Cromer et al. (NIST PML)
Ralph Jimenez et al. (NIST PML)

Vital to the development of next-generation nanomaterials, including photovoltaics and industrial catalysts, is an understanding gained through measurement of electron release, transport, and transfer in engineered nanostructures. This project, now beyond its five-year support by the NIST Innovations in Measurement Science (IMS) program, completed its reports of the first demonstration of time-resolved x-ray emission and time-resolved x-ray absorption measurements with a table-top laboratory set-up. The apparatus enables experiments to capture the motion of electrons, atoms, and molecules on femtosecond time scales and with picometer spatial resolution.

The combination of table-top pulsed x-ray lasers, developed at JILA, with transition-edge sensor (TES) microcalorimeter spectroscopy, intensively developed and refined in the NIST Quantum Electronics and Photonics Division, enables these new measurement capabilities. The integration of these components, accompanied by significant increase in detector array sizes, to achieve large increases in temporal and spatial resolution while maintaining extraordinary TES energy resolution, continues to demand new data modeling and processing techniques. These techniques will overcome current limitations by resolving temporal overlap in photon detection while achieving energy resolution of temporally isolated arrivals, improving efficiency in elimination of low-frequency background noise, and extending multiplexing and reducing cross talk in extracting the signals from 0.1 K to room temperatures.

Wiener filtering, long used among astronomers for estimating amplitudes of pulses of known shape contaminated with noise of known frequency content, is suitable for measuring isolated pulses. Novel processing approaches have been developed, characterized,

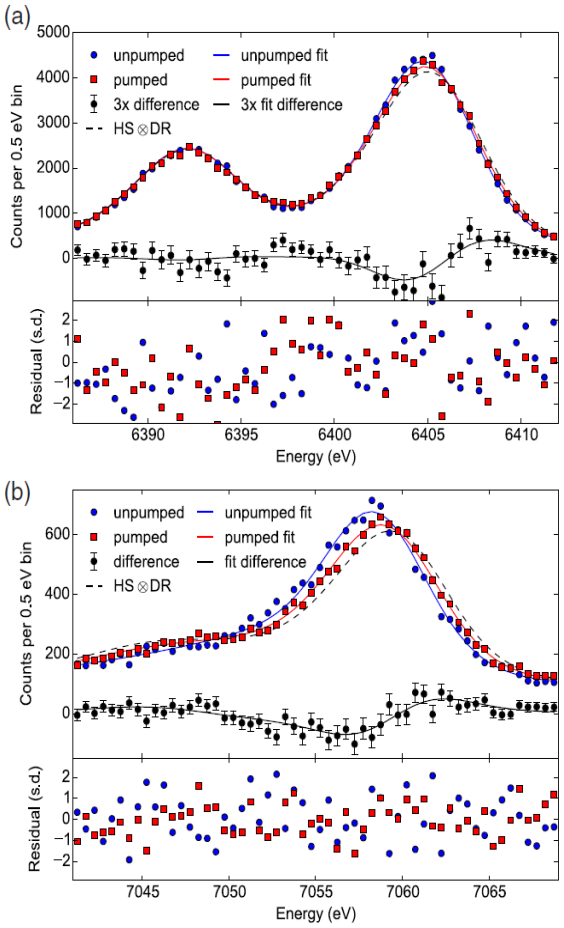

Figure 19. *X-ray emission spectra of [Fe(bpy)_3]$^{2+}$ less than 6 ps after photoexcitation. (a) Fe Kα (b) Fe Kβ. Pumped and unpumped measurements are shown as red and blue markers, respectively. The dashed black lines are the reference high-spin spectra convolved with the detector response (DR) function. The solid red and blue curves are fits to the data that use a linear combination of high-spin and low-spin reference data convolved with the DR. The black markers show the difference between the pumped and unpumped data with 1-σ error bars and the solid black line is the difference between the two fit curves. The lower axes show residuals between the data and the two fit curves. Error values are calculated assuming Poisson statistics in each energy bin. This data set is acquired over 12.5 h of integration.*

and are being extended, that rely on this knowledge but are suitable for overlapping pulses.

Analysis efforts this year focused on preserving the extraordinary energy resolution of TES detectors at high event rates, when nonlinear detector response significantly degrades energy resolution under existing processing methods. This potential capability would enable a variety of types of calorimetric sensors to function with much higher throughput. Current methods under investigation include the use and extension of manifold learning algorithms.

[1] L. Miaja-Avila, G. C. O'Neil, Y. I. Joe, B. K. Alpert, N. H. Damrauer, W. B. Doriese, S. M. Fatur, J. W. Fowler, G. C. Hilton, R. Jimenez, C. D. Reintsema, D. R. Schmidt, K. L. Silverman, D. S. Swetz, H. Tatsuno and J. N. Ullom, Ultrafast Time-resolved Hard X-Ray Emission Spectroscopy on a Tabletop, *Physical Review X* **6** (2016), 031047.

[2] G. C. O'Neil, L. Miaja-Avila, Y. Il Joe, B. K. Alpert, M. Balasubramanian, S. Dodd, W. B. Doriese, J. W. Fowler, W. K. Fullagar, G. C. Hilton, R. Jimenez, B. Ravel, C. D. Reintsema, D. R. Schmidt, K. L. Silverman, D. S. Swetz, J. Uhlig and J. N. Ullom, Ultrafast Time-resolved X-ray Absorption Spectroscopy of Ferrioxalate Photolysis with a Laser Plasma X-ray Source and Microcalorimeter Array, in review.

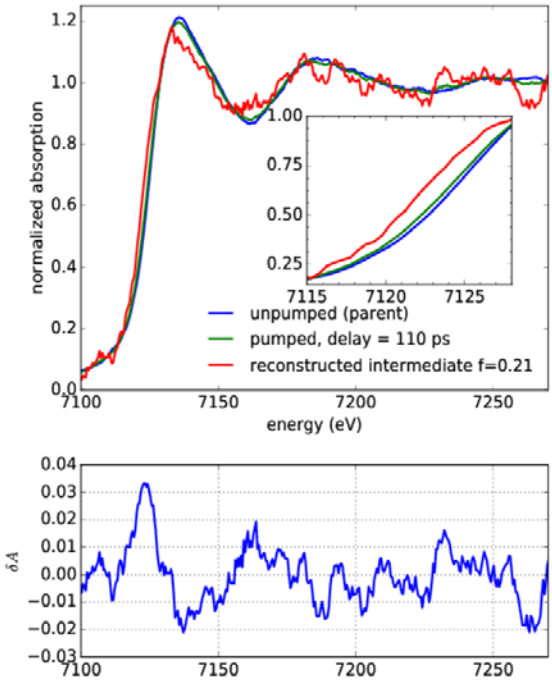

Figure 20. *Normalized absorption spectra of aqueous ferrioxalate at large negative delay (unpumped), at 100 ps delay, and the reconstructed intermediate spectrum at 100 ps. Shown with 5 eV moving average applied. (inset) The edge region expanded to how the edge shift more clearly. Axis units and legend colors apply to both the surrounding figure and the inset. (bottom). The difference ΔA in the normalized absorption between the pumped and unpumped spectrum is shown with a 5 eV moving average applied. A given 5 eV bin has absorption difference uncertainty of ~0.005. However, because of the moving average, the uncertainty on each point shown is not independent.*

A Thousand-Fold Performance Leap in Ultrasensitive Cryogenic Detectors

Bradley Alpert
Joel Ullom et al. (NIST PML)
Lawrence Hudson et al. (NIST PML)
Terrence Jach (NIST MML)

Small arrays of ultrasensitive cryogenic detectors developed at NIST have driven breakthroughs in x-ray materials analysis, nuclear forensics, and astrophysics. They have played a part in prominent international science collaborations in recent years. Despite these successes, NIST's existing cryogenic sensor technology is inadequate for new applications such as in-line industrial materials analysis, energy resolved x-ray imaging, and next-generation astrophysics experiments, which all require faster sensors, much larger arrays, or both. Support under the NIST Innovations in Measurement Science (IMS) program was awarded to develop both capabilities in pursuit of 1000-fold increase in sensor throughput, through completely new sensor readout (microwave multiplexer) enabling much larger detector arrays and through major new, higher throughput, processing capabilities.

A major project connected to the NIST IMS effort is HOLMES, underway in Italy to measure the mass of the electron neutrino. This experiment, which will use NIST-developed microcalorimeters, SQUID amplifiers, and microwave multiplexer readout, relies on extreme statistics for the spectrum produced by the decay of ^{163}Ho. A principal source of error for microcalorimeter characterization of this spectrum is expected to be due to undetected near-simultaneous ^{163}Ho decay events (pile-ups). Improvements in processing that will allow better detection of nearly coincident pulse pairs has significantly altered the design space for the detectors of the experiment.

Alpert's novel pile-up detection algorithm using NIST detector response models convinced the Italian team, led by Angelo Nucciotti, to consider a region of the detector design space (for slower pulse rise) previously believed unusable for HOLMES. The resulting detectors will have reduced pulse rise (or arrival time) distortion and the readout electronics specifications will be less extreme, enabling arrays containing more detectors and therefore potentially higher statistics and more precise characterization of the neutrino mass.

Additional, related project work on detector multiplexing, pulse processing, and spectrum analysis methods have led to improved energy resolution and decreased uncertainty of positions and shapes of fluorescence lines of certain lanthanide metals and the initial demonstration of potential for standard reference data based on microcalorimeter measurements.

[1] B. Alpert, E. Ferri, D. Bennett, M. Faverzani, J. Fowler, A. Giachero, J. Hays-Wehle, M. Maino, A. Nucciotti, A. Puiu, D. Swetz and J. Ullom, Algorithms for Identification of Nearly-Coincident Events in Calorimetric Sensors, *Journal of Low Temperature Physics* **184** (2016), 263-273.

[2] K. M. Morgan, B. K. Alpert, D. A. Bennett, E. V. Denison, W. B. Doriese, J. W. Fowler, J. D. Gard, G. C. Hilton, K. D. Irwin, Y. I. Joe, G. C. O'Neil, C. D. Reintsema, D. R. Schmidt, J. N. Ullom and D. S. Swetz, Code-division-multiplexed Readout of Large Arrays of TES Microcalorimeters, *Applied Physics Letters* **109** (2016), 112604.

[3] J. W. Fowler, B. K. Alpert, W. B. Doriese, Y. I. Joe, G. C. O'Neil, J. N. Ullom and D. S. Swetz, The Practice of Pulse Processing, *Journal of Low Temperature Physics* **184** (2016), 374-381.

[4] J. W. Fowler, B. K. Alpert, W. B. Doriese, J. Hays-Wehle, Y.-I. Joe, K. M. Morgan, G. C. O'Neil, C. D. Reintsema, D. R. Schmidt, J. N. Ullom and D. S. Swetz, When Optimal Filtering Isn't, *IEEE Transactions on Applied Superconductivity*, to appear.

[5] J. W. Fowler, B. K. Alpert, W. B. Doriese, G. C. Hilton, L. T. Hudson, T. Jach, Y.-I. Joe, K. M. Morgan, G.C. O'Neil, C. D. Reintsema, D. R. Schmidt, D. S. Swetz, C. Szabo-Foster and J. N. Ullom, A Reassessment of Absolute X-ray Line Energies for Lanthanide Metals, in review.

Numerical Assessment of NIST Mass Spectral Search Identification and Similarity Algorithms

Anthony J. Kearsley
Arun S. Moorthy (MML)
William E. Wallace (MML)
Stephen E. Stein (MML)

http://chemdata.nist.gov

Mass spectrometry is a commonly employed analytical chemistry technique. A chemical (or biological) sample is fragmented into its constituent molecular ions and a mass spectrum describing the abundance of each molecular ion in the sample is generated. An example mass spectrum detailing the abundance (*y*-axis) of each molecular ion at mass-charge locations (*x*-axis) in a Fentanyl sample is shown as Figure 21. In theory, knowing the mass-charge locations and abundances of molecular ions from a mass spectrum is adequate for an analytical chemist to determine the identity of a chemical sample. However, the chemical complexity of many samples of interest often introduces unexpected fragmentation behavior. As such, identification of a chemical compound by interpretation of its mass spectrum alone is not always possible.

An alternative compound identification strategy using mass spectrometry is library searching. Given a curated library containing mass spectra of known compounds, one should be able to find a spectrum with similar features to the spectrum of their unknown compound, and thus postulate the identity of their unknown sample. Numerous library search algorithms (modified similarity measures) are currently employed by mass spectrometrists [1, 2, 3, 4], and additional ones are being developed [5]. These methods search the unknown spectrum against a library of known spectra and generate a hit list of possible matching compounds. All published library search algorithm testing/verification studies to date have ensured that (i) the instrument/system used to fragment the unknown produces a sufficiently accurate spectrum (free of contamination, appropriately de-convoluted noise), and (ii) a spectrum sufficiently similar to the unknown exists in the curated library. Somewhat unsurprisingly, the qualitative difference between the hit lists (ordering of possible matches) generated using the various search algorithms currently employed is unsubstantial, and so the development and/or adoption of new algorithms has been limited.

In this testing/verification study we address an important question: How do the available library search algorithms perform in identifying compounds when their spectra contain varying degrees of noise? In answering this question, we will be able to better understand the limitations of existing search algorithms and create novel tools better suited for real mass spectral data. Our findings will be useful in quantifying the identification uncertainty of current library search algorithms implemented in the NIST MS Search software and, subsequently, be of significant value across numerous applications where compound identification using mass spectra is a key process (e.g. food/pharmaceutical development, forensics).

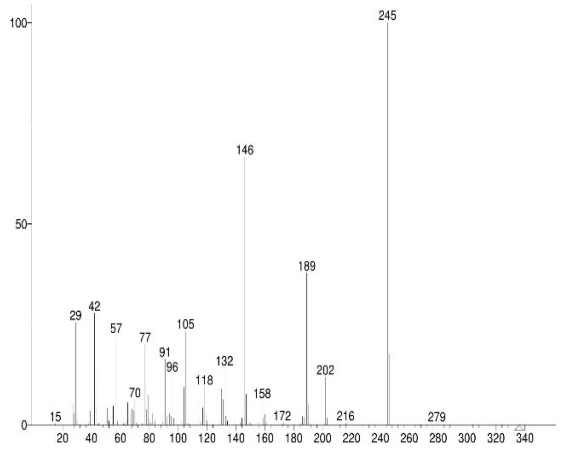

Figure 21. *Mass spectrum of Fentanyl (NIST No. 250541) exported from NIST Mass Spectral Search Program 2.2. The x-axis describes the mass-charge (mass) and the y-axis describes the abundance of molecular ions in the sample.*

[1] S. E. Stein and D. R. Scott, Optimization and Testing of Mass Spectral Library Search Algorithms for Compound Identification, *Journal of the American Society for Mass Spectrometry* **5:**9 (1994), 859–866.

[2] S. E. Stein, Estimating Probabilities of Correct Identification from Results of Mass Spectral Library Searches, *Journal of the American Society for Mass Spectrometry* **5:**4 (1994), 316–323.

[3] F. McLafferty, R. Hertel and R. Villwock, Probability Based Matching of Mass Spectra: Rapid Identification of Specific Compounds in Mixtures, *Organic Mass Spectrometry* **9**:7 (1974), 690–702.

[4] M. A. Bodnar Willard, R. Waddell Smith and V. L. McGuffin, Statistical Approach to Establish Equivalence of Unabbreviated Mass Spectra, *Rapid Communications in Mass Spectrometry* **28**:1 (2014), 83–95.

[5] W. E. Wallace, et al., Improved Clustering of Fentanyl-Like Spectra Using the Ms/Ms Hybrid Search, in preparation.

Biomolecular Metrology

Ryan M. Evans
Anthony Kearsley
Arvind Balijepali (NIST PML)

Heterogeneous effects of medicine on various sub-populations have motivated an interest in precision medicine; i.e., medicine tailored to one's genetic sequence [2]. Creating precision medicine involves measuring protein-ligand interactions at concentrations well below the sensitivity of current state-of-the-art technology such as nuclear magnetic resonance (NMR) [5], or mass spectrometry [4]. Measurements are further obstructed by the need for precise control of the *in vitro* environment necessary for proteins to function [1]. In response, NIST scientists are developing a novel nanoscale electronics instrument capable of measuring protein-ligand interactions at very low concentrations in physiologically realistic environments.

A schematic of the instrument is depicted in Figure 22. The device is partitioned into two regions: a biological region and an electronics region. The biological region consists of a well which contains a buffer fluid, and the electronics region consists of a semiconductor channel; the two regions are separated by a biochemical gate. While ligand molecules are injected into the well, electrons are flowing from source to drain in the semiconductor channel adjacent to the biochemical gate. Ligand binding with receptors immobilized on the biochemical gate modulates current flow through the semiconductor channel. The result of this process is a time-dependent current signal, which can be used to extract reaction rate constants associated with a given biochemical process.

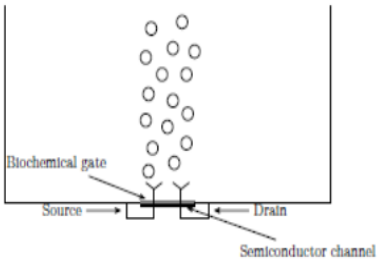

Figure 22. *This schematic of a nanoscale electronics instrument shows ligand molecules diffusing through a buffer fluid in the biological region, to bind with receptors immobilized on a biochemical gate on the floor of the instrument.*

Extracting the rate constants relies on an accurate mathematical model of this process. To this end, we have modeled the experiment with a diffusion equation for the unbound ligand concentration $C(x,y,t)$ in the well, nonlinearly coupled through a diffusive flux condition to a partial differential equation (PDE) describing evolution of the bound ligand concentration $B(x,t)$ on the biochemical gate. The nonlinear coupling between $C(x,y,t)$ and $B(x,t)$ along with the disparate time scales for reaction and diffusion render analysis and simulation of our model a nontrivial task. Nevertheless, using techniques from asymptotic and complex analysis, we have reduced this coupled PDE system to a single nonlinear integro-differential equation (IDE). Further, we have developed a numerical approximation to the solution of this IDE. These results are being included in a paper in progress [3]. In the future, we will use these results to determine instrument sensitivity, and for parameter estimation.

[1] Realizing the Potential of Stratified Medicine, Technical Report, The Academy of Medical Sciences, July 2013.

[2] M. De Palma and D. Hanahan, The Biology of Personalized Cancer Medicine: Facing Individual Complexities Underlying Hallmark Capabilities, *Molecular Oncology* **6**:2 (2012), 111-127.

[3] A. Balijepali, R. M. Evans and A. J. Kearsley. Diffusion-limited Reaction in Nanoscale Electronics, in preparation.

[4] J. Gault, et al., High-resolution Mass Spectrometry of Small Molecules Bound to Membrane Proteins, *Nature Methods* **13** (2016) 333-336.

[5] B. S. Perrinet et al., High-resolution Structures and Orientations of Antimicrobial Peptides and Piscidin 1 and Piscidin 3 in Fluid Bilayers Reveal Tilting, Kinking, and Bilayer Immersion, *Journal of the American Chemical Society* **136** (2014), 3491-3504.

Modeling and Optimization in Cryobiology

Daniel Anderson
James Benson (Northern Illinois University)
Adam Higgins (Oregon State University)
Anthony Kearsley

Mathematical modeling plays an important role in understanding the behavior of cells, tissues, and organs undergoing cryopreservation. Uses of such models range from explanation of phenomena, exploration of potential theories of damage or success, development of equipment, and refinement of optimal cryopreservation/cryoablation strategies. Cryobiology broadly impacts medicine, agriculture and forensics and is important in the fight to maintain earth's biodiversity.

Cryoprotocols, strategies used to cool and warm biospecimens, have a variety of objectives ranging from preserving the viability of a cell as in assisted reproduction, to locally destroying cells or tissue in cryosurgery, to optimally preserving chemical, genetic or proteomic information for archival and/or forensics applications. Mathematical and computational sciences play a critical role as a means of effectively and efficiently exploring these complex bio-chemical-physical systems and their overcrowded parameter spaces.

Cryopreservation procedures permit cells to be stored indefinitely using extremely cold temperatures to suspend all metabolic activities and therefore preserve the cell and cell function. Loosely speaking, there are two main types of cryopreservation procedures: equilibrium (conventional slow freezing) and non-equilibrium or ultra-rapid freezing (vitrification). Both procedures employ the use of cryoprotectants, chemicals behaving like antifreeze to prevent cellular damage during the freezing process. After proper freezing, cells should be able to be stored for an indefinite amount of time. This can be done, for example, by immersing them in liquid nitrogen, an extremely cold fluid with an approximate temperature of -196 C. Cryoprotectants must be removed later during thawing, when the water balance in the cell can be slowly restored, and normal activity in the cell should return.

Procedures exist for the freezing of single cells, tissue comprised of many cells, and entire organs. Size, amount of cytoplasm (or fluid) structural complexity change the freezing procedures employed. For example, cells with less cytoplasm, like sperm cells, are generally considered to be less difficult to freeze than those cells with more cytoplasm, like eggs. Slow freezing or equilibration has been successfully employed to freeze and store a wide range cells, but research is ongoing to optimize the cryobiology of cells. Recently we studied the use of optimization techniques to determine or improve the equilibration of cryoprotectant. We considered the case of cells and tissues with high concentrations of permeating chemicals known as cryoprotective agents, or CPAs. Despite their protective properties, CPAs can cause damage because of osmotically-driven cell volume changes, as well as chemical toxicity.

In this study, data was used to determine a toxicity cost function, a quantity that represents the cumulative damage caused by toxicity. We then used this cost function to define and numerically solve the optimal control problem for CPA equilibration, using human oocytes as representative cell type with high clinical relevance [1]. The resulting toxicity-optimal procedures are predicted to yield significantly less toxicity than conventional procedures. Results showed that toxicity is minimized during CPA addition by inducing the cell to swell to its maximum tolerable volume and then loading it with CPA while in the swollen state. This counterintuitive result is considerably different from the conventional stepwise strategy, which involves exposure to successively higher CPA concentrations to avoid excessive shrinkage. The procedures identified are a first step in deriving protocols that significantly reduce toxicity damage.

Over the last half century there has been a considerable amount of work in bio-heat and mass-transport, and these models and theories have been readily and repeatedly applied to cryobiology with much success. However, there are significant gaps between experimental and theoretical results that suggest missing links in models. One source for these potential gaps is that cryobiology is at the intersection of several very challenging aspects of transport theory: it couples multicomponent, moving boundary, multiphase solutions that interact through a semipermeable elastic membrane with multicomponent solutions in a second time-varying domain, during a two-hundred Kelvin temperature change with multi-molar concentration gradients and multi-atmosphere pressure changes. We have been developing mathematical and computational models built on first principles to describe coupled heat and mass transport in cryobiological systems to account for these various effects [2, 3]. Our efforts have advanced along three fronts: (1) we have examined concentration variable relationships, their impact on choices of Gibbs energy models, and their impact on chemical potentials, (2) we have subsequently developed heat and mass transport models that are coupled through phase-change and biological membrane boundary conditions, and (3) we have developed numerical methods for solving these multispecies multiphase free boundary problems.

[1] J. D. Benson, A. J. Kearsley and A. Z. Higgins, Mathematical Optimization Procedures for Cryoprotectant Equilibration using a Toxicity Cost Function, *Cryobiology*, **64**:3 (2012), 144-151.

[2] D.M. Anderson, J. D. Benson and A. J. Kearsley, Foundations of Modeling in Cryobiology I: Concentration,

Gibbs Energy, and Chemical Potential Relationships, *Cryobiology* **69**:3 (2014), 349-360.

[3] D. M. Anderson, J. D. Benson and A. J. Kearsley, Foundations of Modeling in Cryobiology II: Heat and Mass transport in Bulk and at Cell Membrane and Ice-liquid Interfaces, in review.

Clustering Nuclear Magnetic Resonance Images of Proteins

Ryan M. Evans
Anthony Kearsley
William Wallace (NIST MML)
Frank Delaglio (IBBR)
John Marino (IBBR)
Robert Brinson (IBBR)
Luke Arbogast (IBBR)

Many biologically based medicines are currently facing patent expiration [3], thus creating an opportunity for pharmaceutical companies to develop cost-effective alternatives to their name-brand counterparts. Typically referred to as *biosimilars*, these alternatives have the potential to significantly reduce patient costs by introducing competition into the marketplace [2]. However, before biosimilars are released to consumers, they must undergo a rigorous comparison with their name brand counterparts to ensure safety and efficacy [4].

Biosimilars differ from traditional generic drugs because their active ingredients are large biologically active molecules with intricate structure [2]. Hence, comparing biosimilars with their name-brand counterparts is a nontrivial task. Scientists have recently started using nuclear magnetic resonance (NMR) experiments as a basis for this comparison [1]. The result of such an NMR experiment is a highly detailed two-dimensional image, which can be studied to reveal the chemical structure underlying the biosimilar in question. Currently, analysis of NMR images is based upon a combination of principal component analysis (PCA) and visual inspection [1]. Though these are valuable, there is currently no established distance metric for measuring the difference between two NMR images.

We are currently developing a metric to compare NMR images of proteins. This metric is based upon the so-called earth mover's distance, and accounts for the topology and structure underlying NMR images. Moreover, we are working on combining this metric with a novel clustering algorithm that we have developed, to group NMR images according to their chemical structure. After validating our techniques on in-house NMR protein images, we will then apply these techniques to images from a large inter-laboratory study. Should our techniques prove effective on NMR images from this inter-laboratory study, we would like to implement these techniques to aid NIST researchers in developing standard reference biological medicines.

[1] H. Ghasriani, D. J. Hodgson, R. G. Brinson, I. McEwen, L. F. Buhse, S. Kozlowski, J. P. Marino, Y. Aubin and D. A. Keire. Precision and Robustness of 2D-NMR for Structure Assessment of Filgrastim Biosimilars, *Nature Biotechnology* **34**:2 (2016), 139-141.

[2] H. Ledford, et al., First Biosimilar Drug Set to Enter US Market, *Nature* **517**:7534 (2015), 253-254.

[3] N. Udpa and R. Million, Monoclonal Antibody Biosimilars, *Nature Reviews Drug Discovery* **15** (2015), 13-14.

[4] U.S. Food and Drug Administration, *Quality Considerations in Demonstrating Biosimilarity of a Therapeutic Protein to a Reference Product*, April 2015.

Traceable Simulation of Magnetic Resonance Imaging

Zydrunas Gimbutas
Andrew Dienstfrey
Steve Russek (NIST PML)
Katy Keenan (NIST PML)
Karl Stupic (NIST PML)
Michael Boss (NIST PML)

Magnetic resonance imaging (MRI) is maturing as a quantitative biomedical imaging technology. For example, imaging facilities routinely report tumor volumes in units of mm^3, blood perfusion in units of ml g^{-1} min^{-1}, apparent diffusion coefficient in mm^2 s^{-1}, and temperature in K. However, as of a few years ago the use of SI units for these technologies was potentially unwarranted as SI traceability chains supporting these MRI measurement modalities were unclear if not non-existent. More recently NIST and partner institutions have made substantial investments to develop such traceability chains. In the medical community, standard reference artifacts are referred to as *phantoms* and NIST now supports several phantoms providing SI-traceable calibration artifacts for MRI scanners.

MRI is governed by solutions to the Bloch equations,

$$\frac{d\mathbf{M}}{dt} = \gamma \mathbf{M} \times \mathbf{B} - \frac{M_x \hat{x} + M_y \hat{y}}{T_2} + \frac{(M_0 - M_z)\hat{z}}{T_1} + D\nabla^2 \mathbf{M}$$

Here **M** the magnetic moment arising from collections of nuclear spins, the gyromagnetic ratio γ is a physical constant, and **B** is the forcing magnetization. The quantities of medical interest are T_1, T_2 and D. The first two are tissue-dependent relaxation times. Experimental estimation of these times provides a two-parameter characterization of the material exhibiting the signal. This is the source of MRI's unparalleled capabilities for *in vivo* soft-tissue imaging. Moreover, D is an effective diffusion constant that reflects a combination of tissue

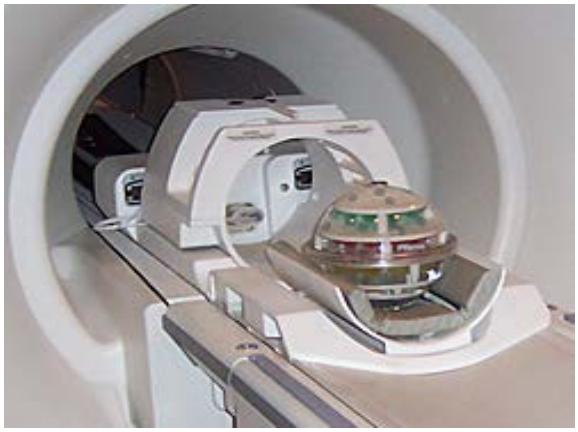

Figure 23. *NIST-developed MRI phantom.*

porosity and anatomical structure. Refined control of the forcing function **B** using combinations of linear gradients and RF fields allows one to map distributions of T_1, T_2 and D. The details are numerous. The point emphasized here is that, while extremely challenging, predictive quantitative simulation of this imaging modality is nevertheless possible.

Virtual prototyping is highly desirable to improve the fundamental understanding of MRI capabilities resulting in significant reductions in time and costs to develop new scan technologies. A growing number of computer codes are available which claim to do just this. While there is uniform agreement on the potential for quantitative MRI simulation, neither NIST nor any other national metrology institution is currently positioned to certify the accuracy of such claims.

We developed an elementary MRI simulator to serve as the foundation for what we ultimately expect to become the computational reference for this community. The NIST Bloch solver is parallelizable via OpenMP and includes several commonly used MRI sequences such as the gradient echo (GE) and spin echo (SE) sequence families, in both one and two dimensions, optionally combined with the inversion recover (IR) step. We have preliminarily validated the simulation results with the measurements of simple T_1 and T_2 array phantoms as provided by the MRI group at NIST, which will serve as a template for the future computational benchmark problems.

In addition to virtual prototyping, there exist many research opportunities directly arising from experimental MRI signals analysis. In medical practice, quantitative measurement of T_1 and T_2 is useful for a wide range of assessments including: iron distribution in the brain which may serve as a biomarker for traumatic brain injury, treatment monitoring for heart attacks, and multiple sclerosis [9]. The tradeoffs associated with this are time, cost, and accuracy. Together with the MRI measurement group at NIST, we are investigating T_1 and T_2 curve mapping techniques that use complex MRI signal data. The new schemes compare favorably to the existing techniques that use only the magnitude of reconstructed MRI signal. For given accuracy, we expect reduction in the number of MRI scans to be collected due to reduced numerical ranks of the fitting curves and possible use of model linearization. We have also discussed possibilities of developing nonlinear gradient and phase error correction schemes for the current NIST MRI measurement system.

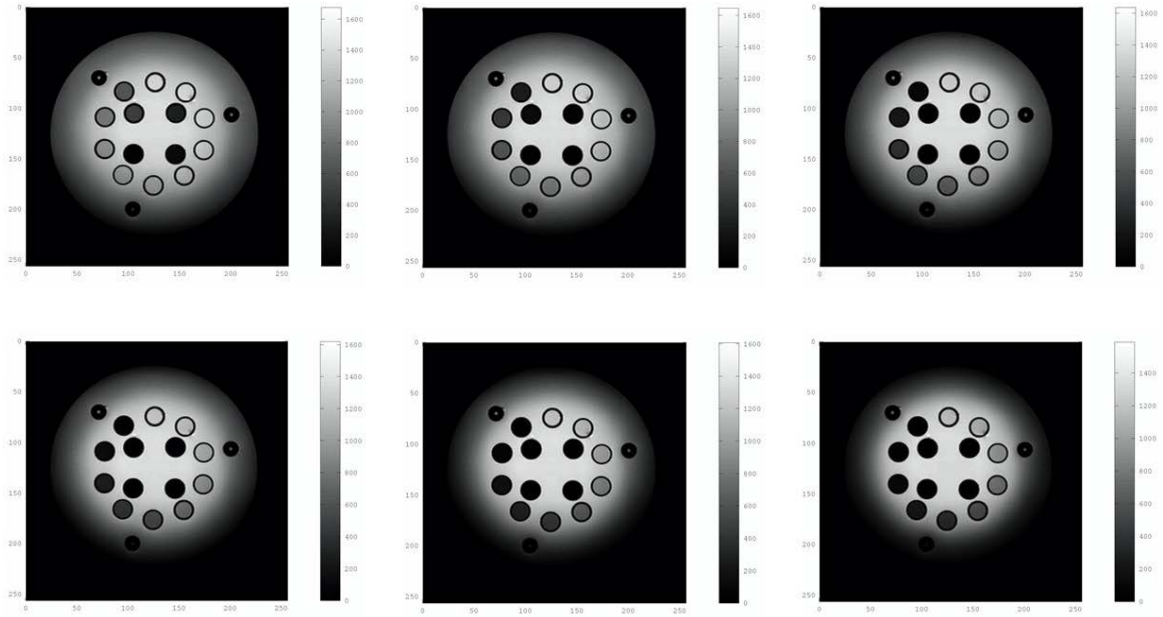

Figure 24. *MR scan of NIST T2 array. Each sphere is loaded with MnCl2 solution of different concentrations resulting in a known collection of true T2 values. The signal intensity progresses from light to dark following an exponential decay law.*

In 2017, we will combine the NIST Bloch solver and the T_1 and T_2 curve mapping techniques to create a new NIST MRI and NMR measurement service. It is proposed that the proton spin relaxation times T_1 and T_2 of the solutions used in MRI phantoms can be quantified at a specified field strength and temperature. The measurement system uncertainties can be assessed by simulating distortions and nonuniformities in the magnet DC field and the probe RF field, temperature error, electronics noise, and detector timing errors.

[1] Z. Gimbutas and A. Dienstfrey, "MRI Simulators and their Performance," NIST Workshop on Standards for Quantitative MRI, Boulder, CO, July 14-17, 2014.

[2] N. Stikov, et al., On the Accuracy of T1 Mapping: Searching for Common Ground, *Magnetic Resonance in Medicine* **73**:2 (2015), 514-522.

[3] P. B. Kingsley, Signal Intensities and T1 Calculations in Multiple-Echo Sequences with Imperfect Pulses, *Concepts in Magnetic Resonance* **11**:1 (1999), 29-49.

[4] P. B. Kingsley, Methods of Measuring Spin-Lattice (T1) Relaxation Times: An Annotated Bibliography, *Concepts in Magnetic Resonance* **11**:4 (1999), 243-276.

[5] H. Benoit-Cattin, G. Collewet, H. Saint-Jaimes and C. Odet, The SIMRI Project: A Versatile and Interactive MRI Simulator, *Journal of Magnetic Resonance* **173**:1 (March 2005), 97-115.

[6] T. H. Jochimsen and M. von Mengershausen, ODIN - Object-oriented Development Interface for NMR, *Journal of Magnetic Resonance* **170**:1 (September 2004), 67-78.

[7] T. Stocker, K. Vahedipour and D. Pugfelder, High-Performance Computing MRI Simulations, *Magnetic Resonance in Medicine* **64**:1 (July 2010), 186-193.

[8] H.-L. Cheng, et al, Practical Medical Applications of Quantitative MR Relaxometry, *Journal of Magnetic Resonance Imaging* **36** (2012), 805-824.

Heavy Tailed Distributions and Enhancement of State of the Art Imagery

Alfred S. Carasso
Dale E Newbury (NIST MML)
Andras E. Vladar (NIST MML)

Non-Gaussian heavy-tailed distributions continued to play a significant role in ACMD image enhancement. Low exponent Lévy stable densities, associated with fractional diffusion equations, were unexpectedly successful in improving new kinds of scanning electron microscope images of an aluminum-copper eutectic alloy. As in [1], progressive fractional diffusion smoothing coupled with adaptive histogram equalization, produced the remarkable deblurring shown in the top row of Figure 25.

On October 19 2015, NASA published an exciting new Hubble Space Telescope image of the elliptic barred spiral galaxy NGS4639. Using the blind deconvolution methodology in [2], based on Linnick densities and ill-posed time-reversed logarithmic diffusion equations, produced the enhanced image shown in the bottom row of Figure 25.

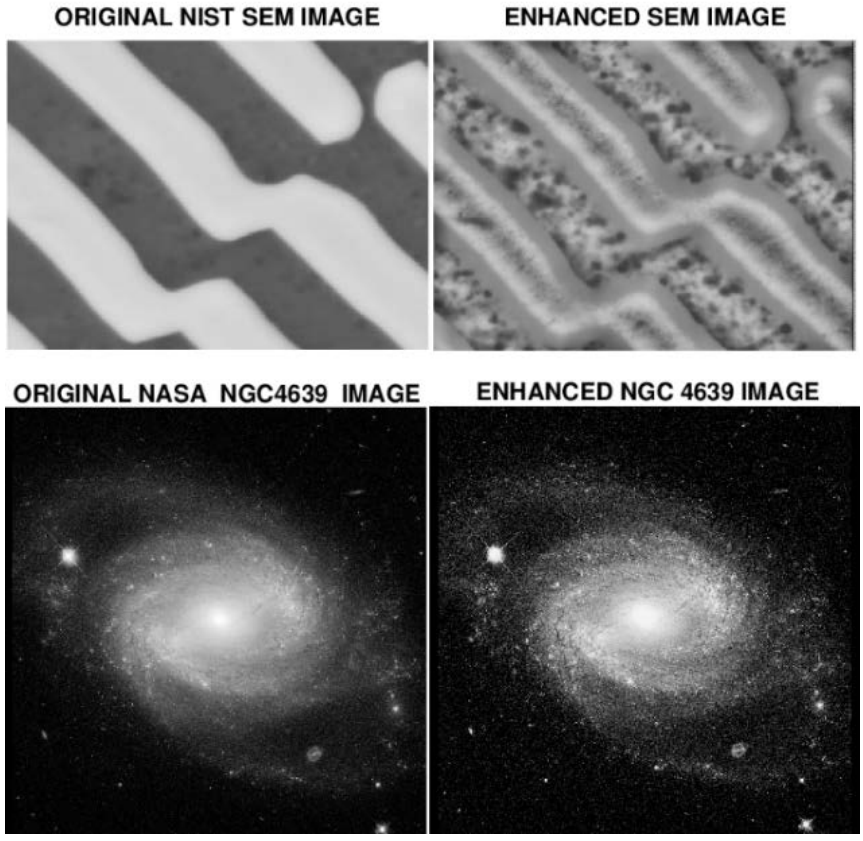

Figure 25. *From the nanoscale to the galactic scale. Non-Gaussian heavy-tailed Levy and Linnick densities associated with fractional or logarithmic diffusion equations deblurred these images.*

[1] A. S. Carasso and A. E. Vladar, Recovery of Background Structures in Nanoscale Helium Ion Microscope Imaging, *Journal of Research of the NIST* **119** (2014), 683-701.

[2] A. S. Carasso, Bochner Subordination, Logarithmic Diffusion Equations, and Blind Deconvolution of Hubble Space Telescope Imagery and Other Scientific Data, *SIAM Journal on Imaging Science* **3** (2010), 954-980.

Computational Tools for Shape Measurement and Analysis

Günay Doğan (Theiss Research)
Javier Bernal
Charles R. Hagwood (NIST ITL)

The main goal of this project is to develop efficient and reliable computational tools to detect geometric structures, such as curves, regions and boundaries, from given direct and indirect measurements, e.g., microscope images or tomographic measurements, as well as to evaluate and compare these geometric structures or shapes in a quantitative manner. This is important in many areas of science and engineering, where the practitioners obtain their data as images, and would like to detect and analyze the objects in the data. Examples are microscopy images for cell biology or micro-CT (computed tomography) images of microstructures in material science. In the fiscal year 2016, advances were made in the following two fronts of this project.

Shape Analysis. The goal of this project is to develop a useful shape distance or dissimilarity measure, and an efficient algorithm to compute this distance. The PIs have adopted the elastic shape distance measure [1] of Anuj Srivastava (faculty appointee in SED/ITL). This shape distance formulation has desirable properties, such as invariance with respect to translation, rotation and reparameterization, and it seems to match a human's intuition well on what the shape of an object is. However, it relies on a computationally expensive optimization. Hence, it is not suitable for large-scale shape analysis, a need in cell biology or forensics applications. Previously, the PIs developed a fast iterative algorithm to compute the shape distance, and reduced the time complexity to subquadratic in experiments (with respect to number of curve nodes) from the cubic time complexity of Srivastava's algorithm [2, 3].

In this FY, they focused on the dynamic programming component of the algorithm (used to compute optimal reparameterizations of curves), and reduced its time complexity from quadratic to linear. This algorithm leverages coarse solutions of problem to limit the search space of the optimization to only the relevant parts of the space and gradually obtains a refined solution (see Figure 26). To enable further savings in computation they reformulated the algorithms to work with nonuniformly sampled curves, which focus the curve nodes in areas of high curvature, rather than using a fine uniform sampling in all parts of the curve. This adaptive discretization of the curve dramatically reduces the number of variables in the optimization (see Figure 27).

Collaborations with NIST scientists were also carried out to apply the shape distance algorithm to important applications. They worked with Martin Herman (ITL) to apply the algorithm to shoeprint data. They measured the shape dissimilarity of possibly discriminative regions or features found in shoeprints, and performed statistical analyses using a GUI tool developed by NIST SHIP student Eve Fleisig (see Figure 28). They also worked with William Wallace (MML) to align chromatograms, a critical step for chemical composition analysis. They achieved superior performance, aligning chromatograms with up to 20 000 points in less than three minutes, a scenario previously impractical (see Figure 29). They wrote a paper describing the linear time dynamic programming algorithm [4] and presented it at the 2nd International Workshop on Differential Geometry in Computer Vision and Machine Learning.

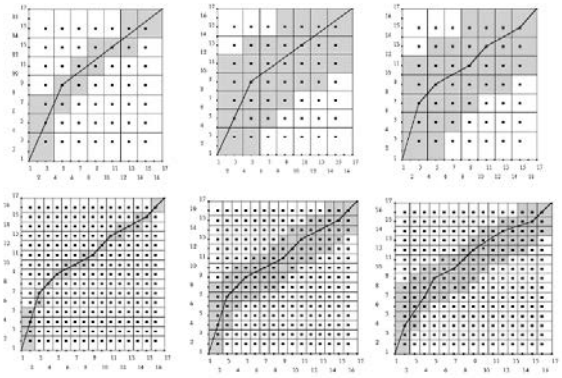

Figure 26. *Dynamic Programming using coarse-to-fine approach to achieve linear time complexity.*

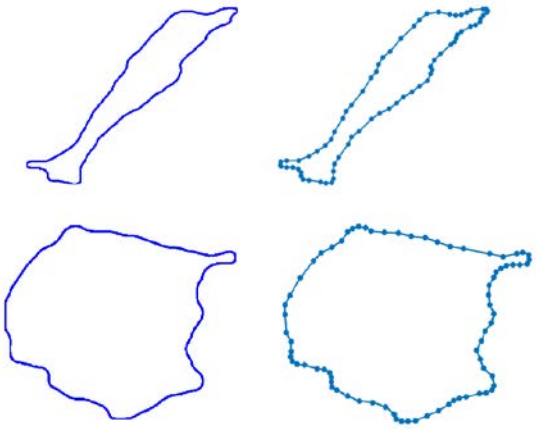

Figure 27. *Adaptive discretization of cell boundary curves from N=1024 nodes down to N=74 (top), N=78 (bottom).*

Image segmentation and meshing. G. Doğan has been developing algorithms for image segmentation, and meshing of segmented images. His segmentation algorithms build on a shape optimization framework, which is used to detect optimal region boundaries in microstructure images. This is done by minimizing specially designed image segmentation energies in this framework. He previously implemented edge-based and

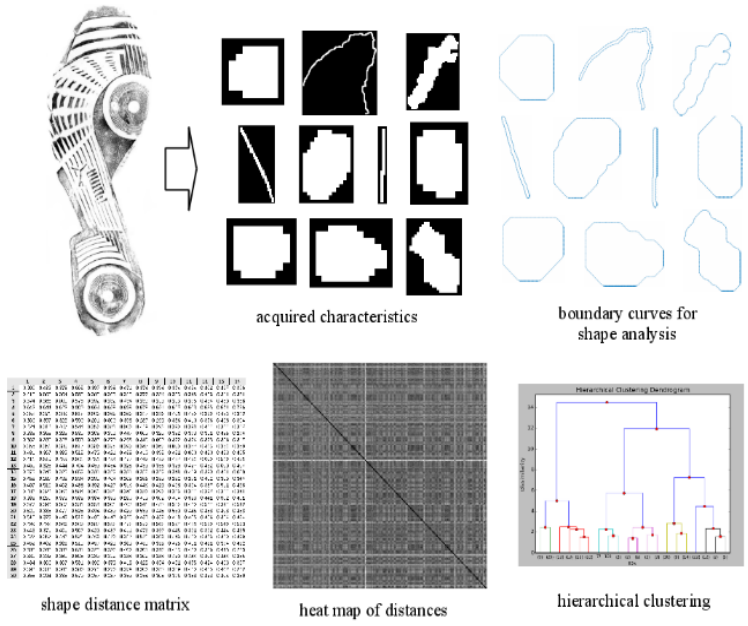

Figure 28. *Shape analysis of acquired characteristics from shoeprint images.*

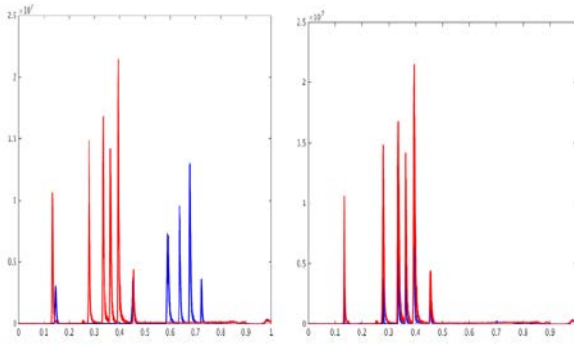

Figure 29. *Two spectral curves (left) of 20K nodes aligned (right) in 172 seconds using fast Dynamic Programming.*

region-based segmentation energies [5, 6]. In the last year he developed a new anisotropic boundary energy. The isotropic edge-based boundary energy has a curve-shortening bias, sometimes causing it to miss concavities of the regions to be detected. The anisotropic energy tries to align the normals of the curve with the extended image gradient, and in this way it can detect region concavities better by bending the curve towards them.

A typical user of the segmentation package usually does not have much image analysis experience, and thus can be overwhelmed by the multiple parameters necessary to be set to obtain a good segmentation. This can be a hurdle even for experienced specialists trying to get the optimal segmentations for varying input images. To simplify the process of tuning the segmentation parameters, G. Doğan implemented additional heuristic decisions to automate the definition of the edge-based segmentation energies, as well as methods to better control the step size in the iterations of the optimization.

He has also been working on interfacing the segmentation package with the ACMD materials modeling system OOF. Currently, his image-based meshing algorithm can be invoked by pressing a button on the OOF GUI. This algorithm takes a segmented microstructure image as input, and automatically creates a high-quality triangulation matching the phases and grains in the microstructure image.

G. Doğan has been developing a fast multigrid optimization algorithm with Harbir Antil and Stephen Nash of George Mason University for energy minimization. This algorithm is expected to provide significant computational savings for 3d shape optimization, which would have much higher computational cost. In this last year, they incorporated adaptivity to this algorithm, so that the optimization algorithm can examine the domain of the solution, and can refine the underlying mesh to increase resolution and accuracy, as opposed to using a uniformly-refined high-resolution mesh, which would have high computational cost.

[1] A. Srivastava, E. Klassen, S. Joshi and I. Jermyn, Shape Analysis of Elastic Curves in Euclidean Space, *IEEE Transactions on Pattern Analysis and Machine Intelligence* **33**:7 (2011), 1415-1428.

[2] G. Doğan, J. Bernal and C. R. Hagwood, Fast Algorithms for Shape Analysis of Planar Objects, in *Proceedings of the IEEE Conference on Computer Vision and Pattern Recognition (CVPR'15)*, Boston, MA, June 2015.

[3] G. Doğan, J. Bernal and C.R. Hagwood, FFT-based Alignment of 2d Closed Curves with Application to Elastic Shape Analysis, in *Proceedings of the 1st International Workshop on Differential Geometry in Computer Vision for Analysis of Shapes, Images and Trajectories (DiffCV'15)*, Swansea, United Kingdom, September 2015.

[4] J. Bernal, G. Doğan and C.R. Hagwood, Fast Dynamic Programming for Elastic Registration of Curves, in *Proceedings of the 2nd International Workshop on Differential Geometry in Computer Vision and Machine Learning (DiffCVML'16)*, Las Vegas, NV, July 1, 2016.

[5] G. Doğan, Fast Minimization of Region-Based Active Contours Using the Shape Hessian, in *Proceedings of 4th International Conference on Scale Space and Variational Methods in Computer Vision (SSVM)*, May 2015.

[6] G. Doğan, An Efficient Curve Evolution Algorithm for Multiphase Image Segmentation, in *Proceedings of the International Conference on Energy Minimization Methods in Computer Vision and Pattern Recognition (EMMCVPR)*, January 2015.

Numerical Methods for Improved HVACSIM+

Aaron Chen (Drexel University)
Anthony Kearsley
Amanda Pertzborn (NIST EL)
Shokouh Pourarian (Drexel University)
Jin Wen (Drexel University)

Buildings account for 82 % of the electrical energy consumption in the US, and approximately 84 % of the life cycle energy use of a building is associated with its operation rather than material and construction costs [2]. For this reason, optimal operational decisions are crucial to energy efficiency, especially considering a national push towards smart-grid applications and optimized power-grid use. For this to take place there is a need for buildings to interact with a smart electric grid as a function of energy demands. This poses a new computational challenge as optimal decision making for each building is governed by an automated cyber-physical system. As an example, heating, ventilation and air conditioning (HVAC) information provided to the building control system, as well as electrical pricing provided by the smart grid, can be used to make decisions about whether to use the power generated by solar panels in the building itself or to sell it to the utility for use elsewhere. This requires the development of algorithms for predicting usage, which in turn requires a large-scale HVAC simulation test bed that currently does not exist.

Previous work at NIST on this problem includes the development of HVACSIM+, a software package and computing environment for simulating HVAC systems originally developed in the 1980s [3]. However, in HVACSIM+ and in other software packages available currently, the limitations of numerical solvers employed are apparent: the user must be adept at formulating the problem to achieve a meaningful solution, the methods are too sensitive to initial estimates for the state of the system, and the size of the problems that can be solved is limited due to abundant use of dense storage. There are many instances where small scale building simulations work well but when coupled to larger systems of buildings there is a failure to converge [1].

As an example, in Figure 30 we see the residual associated with a system of nonlinear equations whose solution is sought to simulate an HVAC system over a period of 24 hours. This well studied example is usually solved in a reasonable amount of time using well-known nonlinear solution techniques. However, if one applies more realistic boundary conditions associated with hot weather (summer conditions), the existing methods fail to drive residuals to reasonable levels (see Figure 30). As part of an ongoing research effort we have investigated the use of more specialized solvers and preconditioners to identify particularly challenging scenarios and are applying these techniques when difficulties are detected. Figure 31 shows results from an improved method that succeeds in driving residuals to far more desirable levels over exactly the same time period and given exactly the same boundary conditions.

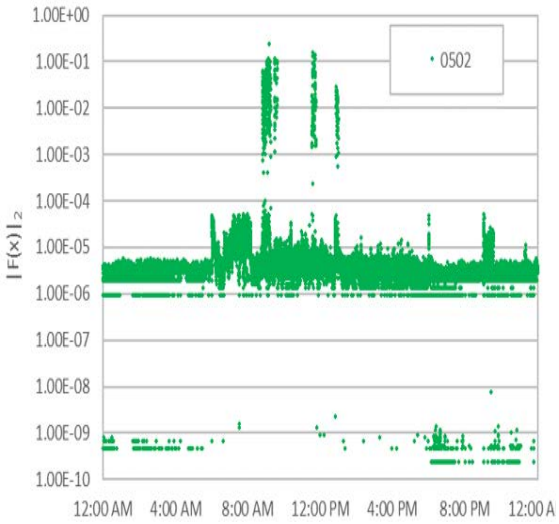

Figure 30. *Residual from a system of nonlinear equations whose solution simulates an HVAC system over a 24-hour period.*

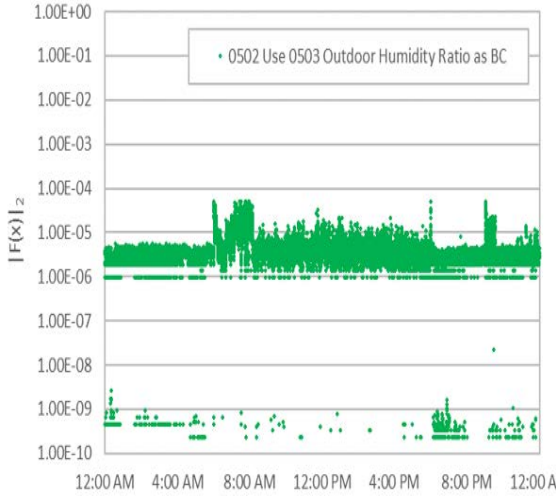

Figure 31. *Residuals from an improved method.*

[1] S. Pourarian, A. Kearsley, J. Wen and A. Pertzborn, Efficient and Robust Optimization for Building Energy Simulation, *Energy and Buildings* **122** (2016), 53-62.

[2] EEB Report, World Business Council for Sustainable Development, p. 11.

[3] C. D. Park, *HVACSIM+ User's Guide Update*, NIST Internal Report 7514, July 1, 2008.

Parallel Adaptive Refinement and Multigrid Finite Element Methods

William F. Mitchell
Eite Tiesinga (NIST PML)
Paul Julienne (NIST PML)
John Villarrubia (NIST PML)
Garnett Bryant (NIST PML)
Michael Gullans (NIST PML)

http://math.nist.gov/phaml

Finite element methods using adaptive refinement and multigrid techniques have been shown to be very efficient for solving partial differential equations (PDEs). Adaptive refinement reduces the number of grid points by concentrating the grid in the areas where the action is, and multigrid methods solve the resulting linear systems in an optimal number of operations. Recent research has considered *hp*-adaptive methods where adaptivity is in both the grid size and the polynomial order of approximation, resulting in exponential rates of convergence. W. Mitchell has been developing a code, PHAML, to apply these methods on parallel computers. The expertise and software developed in this project are useful for many NIST laboratory programs, including material design, semiconductor device simulation, the quantum physics of matter, and simulation of scanning electron microscopes.

We continue to expand the forms of *hp*-adaptivity available in PHAML. This year we extended the TYPEPARAM, PRIOR2P and BIGGER_ERRIND *hp*-adaptive strategies from 2D to 3D elliptic PDEs. We performed a numerical experiment [2, 3] to compare the performance of these strategies and four other *hp*-adaptive strategies on 3D problems, similar to the experiment performed a few years ago with 2D problems. The other four strategies were extended to 3D last year. We found the results for 3D problems to be similar to those for 2D problems in that the APRIORI strategy is best if there are singularities at known points, the COEF_DECAY strategy is a good general purpose approach, and all the other strategies have reasonable performance, standing out on particular types of problems.

We have created a web site [6] to make available a collection of standard benchmark PDEs that are suitable for benchmarking and testing adaptive mesh refinement algorithms and error estimators. We continue to add new PDEs to this collection to cover additional problem characteristics. This year we added 1D, 2D and 3D elliptic eigenvalue problems to the suite.

There are three major collaborative efforts with PML that apply PHAML to their physical models. First, in a collaboration with Eite Tiesinga and Paul Julienne, we are using PHAML to study the interaction of atoms and molecules held in an optical trap. In particular, we are using a 3D model to calculate the bound states, scattering properties and dynamics of two interacting dipolar molecules. We are also considering the use of absorbing (non-reflecting) boundary conditions on the surface of a quarter ellipse removed from a corner of a rectangle in 2D and an eighth of an ellipsoid removed from a corner of a cube in 3D. We have performed calculations to examine how the energy levels are effected by the eccentricity of the ellipse or ellipsoid. Figure 32 shows the real part of an example wave function in the vicinity of the removed ellipsoid along with the adaptive mesh. This one corresponds to the first eigenvalue whose real part is greater than 0.51 in a simulation of the interaction of trapped rubidium and cesium atoms.

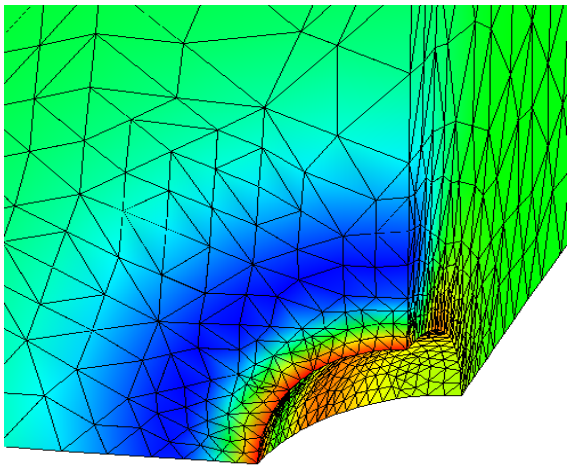

Figure 32. *Example wave function for the 3D absorbing boundary condition model of interacting trapped atoms.*

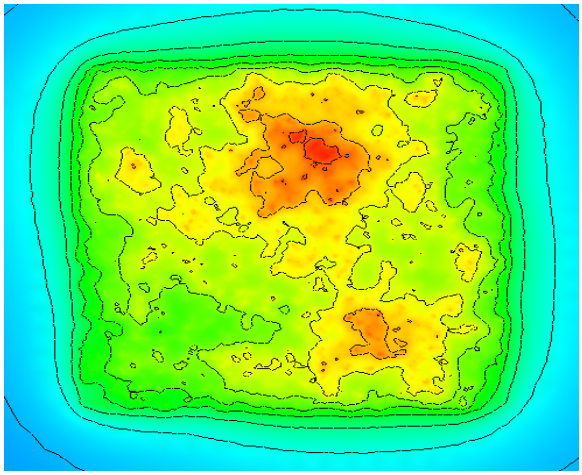

Figure 33. *The computed electric potential for a scanning electron microscope simulation with 10 500 randomly placed point charges.*

We are also collaborating with John Villarrubia to apply PHAML to the modeling of scanning electron microscope (SEM) images of samples containing a mixture of conducting and insulating regions. Villarrubia has a

code, JMONSEL, that models electron scattering in materials, secondary electron production, and detection. We have coupled this code with PHAML, which performs the finite element analysis needed to determine the electric fields that affect the image. This year we developed a new *a posteriori* error estimator suited to SEM simulations. The idea is to design an estimate that minimizes the error in the deflection of the electron path rather than minimizing some norm of the error in the electric potential. We also modified the high level adaptive strategy to attempt to place all local error estimates within a given interval.

We are currently performing experiments [4] to compare the performance of the adaptive meshes from the new error estimator and adaptive strategy with the fixed graded meshes currently used. For this experiment, we are using a simulation with randomly placed point charges in a parallelepiped within a layer of conducting material below a vacuum, for which a near-exact solution is known. This allows us to compute an error metric based on the trajectories of a collection of electrons using the computed electric field compared to using the near-exact electric field. Figure 33 shows the computed electric field at the interface between the conducting material and vacuum for a simulation with 5 000 negative charges and 5 500 positive charges using an adaptive mesh with 1.4 million tetrahedra.

Our collaboration with Garnett Bryant applies PHAML to the simulation of quantum dot structures. Nanoscale semiconductor quantum dot structures can be modified, controlled, and manipulated by applied electric fields that arise from the local strain in the quantum dots. In this collaboration, we are using PHAML to determine these applied fields and potentials down to the scale of the quantum dots. This year we performed some experiments to determine how large of a region we need to use as the truncation of the infinite domain. We found that, in general, truncating at four to eight times the extent of the charge density field gives adequate accuracy. With one of Bryant's postdocs, Michael Gullans, we have begun to use PHAML to model a single plasmon SET-donor-graphene device, which has applications to on-chip photodetection, optical signal processing and quantum computing with CMOS compatible devices. After setting up an initial model last year, this year we added graphene to the implementation of the model.

Future work will continue to enhance PHAML with additional capabilities, robustness and efficiency, improve the parallel implementation of PHAML with an emphasis on modern architectures such as the Intel Xeon Phi (Knight's Landing), continue the development of the adaptive mesh refinement benchmark suite, and continue NIST collaborations.

[1] W.F. Mitchell, 30 Years of Newest Vertex Bisection, in *Proceedings of the International Conference on Numerical Analysis and Applied Mathematics* 2015, AIP Conference Proceedings **1738** (2016), 020011.

[2] W.F. Mitchell, "Performance of Some *hp*-adaptive Strategies for 3D Elliptic Problems," Computation and Information Science and Engineering Conference, Portaria, Greece, June 2016.

[3] W.F. Mitchell, Performance of Some *hp*-adaptive Strategies for 3D Elliptic Problems," International Conference on Spectral and High Order Methods, Rio de Janeiro, Brazil, June 2016.

[4] W. F. Mitchell and J. S. Villarrubia, "Scanning Electron Microscope Simulation with Adaptive Finite Elements," SIAM Conference on Computational Science and Engineering, Atlanta, GA, March 2017, accepted.

[5] W. F. Mitchell, Performance of *hp*-Adaptive Strategies for 3D Elliptic Problems, in *Proceedings of the Computation and Information Science and Engineering Conference*, submitted.

[6] NIST Adaptive Mesh Refinement Benchmark Problems, http://math.nist.gov/amr-benchmark

Numerical Solutions of the Time Dependent Schrödinger Equation

Barry I. Schneider
Klaus Bartschat (Drake University)
Luca Argenti (Univeristy of Central Florida)

We have been collaborating with various scientists for several years to develop numerically robust methods for solving the time dependent Schrödinger equation. This has continued and a new collaborator, Luca Argenti, an Assistant Professor from the University of Central Florida, has joined the effort. In addition, a new NRC postdoctoral associate, Heman Gharibnejad will be joining NIST in January of 2017 to work on the hybrid Gaussian-FEDVR approach discussed below.

The approaches that have been developed are quite general, but the applications to date have concentrated on describing the single and double ionization of electrons exposed to intense, ultrafast, laser radiation in simple systems. These attosecond (10^{-18} sec) pulses provide a new window to study the electronic motion in atoms and molecules on their natural timescale. To put this in context, the motion of electrons responsible for chemical binding and electron transfer processes in nature have a characteristic timescale of about 100 attoseconds. (It takes an electron 152 attoseconds to go around the hydrogen atom). These processes can only be described using time dependent quantum mechanics and, where appropriate, need to be coupled to Maxwell's equations to describe macroscopic phenomena. At the end of the day, we wish to image quantum phenomena with sub-femtosecond temporal and sub-Angstrom spatial resolution. Eventually, one can contemplate producing "molecular movies" of this motion in much the same way as it is done in molecular dynamics simulations of heavy particle processes.

The basic methodology as applied to atoms and simple diatomic molecules, has been described in [1-3, 5-10], and [4] provides a detailed review of the work. The essential aspects have been development of the finite element discrete variable method (FEDVR) to spatially discretize the coordinates of the electrons, and use of the short iterative Lanczos method to propagate the wavefunction in time.

The method has been efficiently parallelized using MPI and scales linearly with the size of the FEDVR basis. Large scale calculations have been performed on several atoms and molecules using resources provided by the NSF Extreme Science and Engineering Discovery Environment (XSEDE). The group has received a competitively awarded allocation of more than 3.5 million service units for the current fiscal year.

We have begun a study to employ a mixed basis of Gaussian functions at short range and FEDVR functions at long range to extend our methods to complex polyatomic molecules. This approach has several important advantages over using a single basis over all of space. First, the use of nuclear centered Gaussians preserves the local atomic symmetry around each nucleus and avoids the poor convergence of using a single-center FEDVR basis at all distances. Second, once the electron is far enough away from the nuclear cusps, a single center expansion converges quickly and, importantly, can represent the electrons out to very large distances using an approach that is very amenable to domain decomposition. The major issue is to compute the one and two electron integrals between the two types of basis functions. During the current year, a new and efficient formalism, using transition density matrices, has been developed so that optimal use can be made of existing quantum chemistry codes to extract the information required to compute the additional integrals. This needs to be implemented and tested. This will be a major part of the responsibility of the new postdoctoral associate.

[1] J. Feist, S. Nagele, R. Pazourek, E. Persson, B. I. Schneider, L. A. Collins and J. Burgdörfer, Nonsequential Two-Photon Double Ionization of Helium, *Physical Review A* **77** (2008), 043420.

[2] X. Guan, K. Bartschat and B. I. Schneider, Dynamics of Two-photon Ionization of Helium in Short Intense XUV Laser Pulses, *Physical Review A* **77** (2008), 043421.

[3] X. Guan, K. Bartschat, and B. I. Schneider, Two-photon Double Ionization of H_2 in Intense Femtosecond Laser Pulses, *Physical Review A* **82** (2010), 041407.

[4] B. I. Schneider, J. Feist, S. Nagele, R. Pazourek, S. Hu, L. Collins and J. Burgdörfer, Recent Advances in Computational Methods for the Solution of the Time-Dependent Schrödinger Equation for the Interaction of Short, Intense Radiation with One and Two Electron Systems, in *Dynamic Imaging, Theoretical and Numerical Methods Series: CRM Series in Mathematical Physics XV*, (A. Bandrauk and M. Ivanov eds.), 2011.

[5] X. Guan, E. Secor, K. Bartschat, B. I. Schneider, Double-slit Interference Effect in Electron Emission from H_2^+ Exposed to X-Ray Radiation, *Physical Review A* **85** (2012), 043419.

[6] X. Guan, K. Bartschat, B. I. Schneider, L. Koesterke, Resonance Effects in Two-Photon Double Ionization of H_2 by Femtosecond XUV Laser Pulses, *Physical Review A* **88** (2013) 043402.

[7] J. Feist, O. Zatsarinny, S. Nagele, R. Pazourek, J. Burgdörfer, X. Guan, K. Bartschat and B. I., Time Delays for Attosecond Streaking in Photoionization, *Physical Review A* **89** (2014), 033417.

[8] X. Guan, K. Bartschat, B. I. Schneider, and L. Koesterke, Alignment and pulse-duration effects in two-photon double ionization of H_2 by femtosecond XUV laser pulses, *Physical Review A* **90** (2014), 043416.

[9] B. I. Schneider, L. A. Collins, X. Guan, K. Bartschat and D. Feder, Time-Dependent Computational Methods for Matter Under Extreme Conditions, *Advances in Chemical Physics* **157**, Proceedings of the 240 Conference: Science's Great Challenges, (A. Dinner, ed.), John Wiley and Sons, Inc., 2015.

[10] B. I. Schneider, X. Guan and K. Bartschat, Time Propagation of Partial Differential Equations Using the Short Iterative Lanczos Method and Finite-Element Discrete Variable Representation, *Advances in Quantum Chemistry* **72** (2016), A Tribute to Frank E. Harris.

[11] B. I. Schneider, How Novel Algorithms and Access to High Performance Computing Platforms Are Enabling Scientific Progress in Atomic and Molecular Physics, *IOP Journal of Physics Conference Series* **759** (2016).

Testing the Expansion Hypothesis

Bert W. Rust
Maria V. Pruzhinskaya (U. Blaise Pascal, France)

In 1974 Bert Rust made the first test of the expansion hypothesis of cosmology using measured Type Ia supernova light curves [1]. He found that the apparent expansion rate was significantly greater than that predicted by the conventional Big Bang theory. In 1976 de Vaucouleurs and Pence [2] confirmed Rust's result at an even higher level of statistical significance.

We have repeated the test using a sample of light curves assembled by Pskovskii [3] which covers a smaller range of redshifts, but displays better estimates of the rate of change in the supernovae luminosity declines. The results for this test are displayed in Figure 34, where Pskovskii's "photometric class" parameter β was introduced "to measure the rate at which the star fades in blue light (magnitudes per 100d) during its fast post maximum decline." The black (average) line is the prediction for a static Euclidean universe and the red regression line is the prediction for an expanding universe in a 4-dimensional Minkowski space-time $R_1 \times R_3$. The

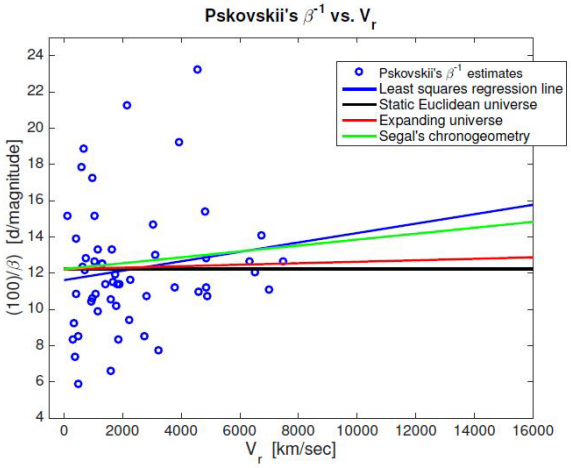

Figure 34. *Analysis of Segal's chronogeometry.*

green regression line is the prediction for I. E. Segal's chronogeometry theory [4] which applies in Einstein's Universe $R_1 \times S_3$.

Segal derived his theory with no assumptions about general relativity or any other gravitational theory. He showed that only two 4-dimensional space times are consistent with the causality principle, the Einstein Universe and its tangent Minkowski space-time. In the latter case the observed redshifts of extragalactic objects are thought to be Doppler shifts caused by an expansion triggered by the initial "Big Bang" and augmented by Einstein's "cosmological constant." The Einstein Universe is static and the redshifts are due to loss of energy by the photons while propagating along the circular geodesics of the space-time ("tired light"). The lost energy goes into the cosmic microwave background, and Segal was able to use its temperature ($\sim 3^o K$) to estimate the "radius of the universe." The blue regression line is a least squares fit to the data. It seems to favor Segal's theory over the expanding universe. This is important because without a theory along the lines of Segal's, the astronomical community has had to posit "dark matter" and "dark energy"" to keep expansion theory consistent with new observations.

[1] B. W. Rust, The Use of Supernovae Light Curves for Testing the Expansion Hypothesis and Other Cosmological Relations, ORNL-4953, Oak Ridge, TN, 1974.

[2] G. de Vaucouleurs and W. D. Pence, Type I Supernovae as Cosmological Clocks, *The Astrophysical Journal* **2**:9 (1976), 687-692.

[3] Y. P. Pskovskii, Photometric Classification and Basic Parameters of Type I Supernovae, *Soviet Astronomy* **28** (1984), 658-664.

[4] I. E. Segal, *Mathematical Cosmology and Extragalactic Astronomy*, Academic Press, New York, 1976.

Advanced Materials

Delivering technical support to the nation's manufacturing industries as they strive to out-innovate and outperform the international competition has always been a top priority at NIST. Mathematical modeling, computational simulation, and data analytics are key enablers of emerging manufacturing technologies. This is most clearly evident in the Materials Genome Initiative, an interagency program with the goal of significantly reducing the time from discovery to commercial deployment of new materials through the use of modeling, simulation, and informatics. ACMD's role in advanced manufacturing centers on the development and assessment of modeling and simulation tools, with emphasis on uncertainty quantification, as well as support of NIST Laboratory efforts in such areas as materials modeling and smart manufacturing.

Micromagnetic Modeling

Michael Donahue
Donald Porter
Robert McMichael (NIST CNST)
June Lau (NIST MML)

http://math.nist.gov/oommf/

Advances in magnetic devices such as recording heads, field sensors, spin torque oscillators, and magnetic nonvolatile memory (MRAM) are dependent on an understanding of magnetization processes in magnetic materials at the nanometer level. Micromagnetics, a mathematical model used to simulate magnetic behavior, is needed to interpret measurements at this scale. ACMD is working with industrial and academic partners, as well as with colleagues in the NIST CNST, MML, and PML, to improve the state-of-the-art in micromagnetic modeling.

We have developed a public domain computer code for performing computational micromagnetics. The Object-Oriented Micromagnetic Modeling Framework (OOMMF) serves as an open, well-documented environment in which algorithms can be evaluated on benchmark problems. OOMMF has a modular structure that allows independent developers to contribute extensions that add to its basic functionality. OOMMF also provides a fully functional micromagnetic modeling system, handling three-dimensional problems, with extensible input and output mechanisms. In FY 2016 alone, the software was downloaded more than 6 500 times, and use of OOMMF was acknowledged in more than 170 peer-reviewed journal articles. OOMMF was also cited in US patents awarded to Hitachi, IBM, and Intel. OOMMF has become an invaluable tool in the magnetics research community.

Key developments over the last year include the following.

- Established online availability of OOMMF at the nanoHUB project of Purdue University [1]. This allows researchers to easily experiment with OOMMF without the inconvenience of installing and maintaining OOMMF on their own system.
- Developed an extended precision ("double-double") numerics library and incorporated it into OOMMF so that full double-precision accuracy of the demagnetization tensor can be computed.
- Continued simulation work at extremely high spatial resolutions using parallel calculations on the high memory bandwidth available in modern commodity computer hardware. These simulations, which manage a billion degrees of freedom, are key to developing quantitative measures of error in micromagnetic calculations.
- Released OOMMF version 1.2b0 in Sept. 2016 [2].

OOMMF is part of a larger activity, the Micromagnetic Modeling Activity Group (muMAG), formed to address fundamental issues in micromagnetic modeling through two activities: the development of public domain reference software, and the definition and dissemination of standard problems for testing modeling software. ACMD staff members are involved in development of the standard problem suite as well. Solutions to Standard Problem 5 [3] were computed and submitted. [4] The high resolution OOMMF simulations also make use of the standard problems as calculations of interest, and sample inputs files for computing standard problem solutions are included in OOMMF releases.

In addition to the continuing development of OOMMF, the project also does collaborative research using OOMMF. Collaboration with the University of California, San Diego has produced a port of OOMMF for computing on massively parallel graphical processing units (GPUs) [5]. Collaboration with the Technological Educational Institute of Eastern Macedonia and Thrace examined the computational challenge of stiff modes encountered in the simulation of spin-valves, a design important in spintronic devices [6].

In total, the ACMD micromagnetic project produced one invited talk [7], one conference presentation [8], and two manuscripts published [5, 6] during this past year.

[1] http://nanohub.org/
[2] http://math.nist.gov/oommf/software-12.html
[3] http://www.ctcms.nist.gov/~rdm/std5/spec5.xhtml

[4] http://www.ctcms.nist.gov/~rdm/std5/results.html

[5] S. Fu, W. Cui, M. Hu, R. Chang, M.J. Donahue and V. Lomakin, Finite Difference Micromagnetic Solvers with Object Oriented Micromagnetic Framework on Graphics Processing Units, *IEEE Transactions on Magnetics* **52** (2016), 7100109.

[6] S. Mitropoulos, V. Tsiantos, K. Ovaliadis, D. Kechrakos and M. J. Donahue, Stiff modes in Spinvalve Simulations with OOMMF, *Physica B - Condensed Matter* **486** (2016), 169-172.

[7] M. J. Donahue, "Quantitative Effect of Cell Size on Precision of Micromagnetic Energy Calculation," Micromagnetics: Analysis, Numerics, Applications (MANA) 2016, Vienna, Austria, February 18, 2016.

[8] M. J. Donahue and D. G. Porter, "Quantitative Effect of Cell Size on Precision of Micromagnetic Energy Calculations," 13th Joint MMM-Intermag Conference, San Diego, CA, January 12, 2016.

OOF: Finite Element Analysis of Material Microstructures

Stephen A. Langer
Andrew C.E. Reid (NIST MML)
Günay Doğan (Theiss Research)
Shahriyar Keshavarz (Theiss Research)
Lizhong Zhang (ISIMA)
David Feraud (ISIMA)

http://www.ctcms.nist.gov/oof/

The OOF Project, a collaboration between ACMD and MML, is developing software tools for analyzing real material microstructure. The microstructure of a material is the (usually) complex ensemble of polycrystalline grains, second phases, cracks, pores, and other features occurring on length scales large compared to atomic sizes. The goal of OOF is to use data from a micrograph of a real or simulated material to compute the macroscopic behavior of the material via finite element analysis.

The OOF user loads images into the program, assigns material properties to the features of the image, generates a finite element mesh that matches the geometry of the features, chooses which physical properties to solve for, and performs virtual experiments to determine the effect of the microstructural geometry on the material. OOF is intended to be a general tool, applicable to a wide variety of microstructures in a wide variety of physical situations. It is currently used by academic, industrial, and government researches world-wide.

There are two versions of OOF, OOF2 and OOF3D, freely available on the OOF website. OOF2 starts with two dimensional images of microstructures and solves associated two dimensional differential equations, assuming that the material being simulated is either a thin freely suspended film or a slice from a larger volume that is unvarying in the third dimension (generalizations of plane stress and plane strain, respectively). OOF3D starts with three dimensional images and solves equations in three dimensions.

A. Reid and S. Keshavarz have completed the implementation of a large-deformation elasticity property in a prototype code which mimics the OOF API, in preparation for implementing plasticity within OOF. As part of this processes, they learned that the initial prototype code had abstracted away more of the OOF features than was desirable, and so adapted it to be more faithful to the OOF process. They are now implementing large-deformation elasticity in this new code. It seems likely that this will motivate the addition of some architectural features in OOF that are specific to mechanics problems, in particular the ability to do integrals and derivatives with respect to the deformed system. The precise contours of the trade-off between full generality on the one hand, and a plasticity capability which is recognizable to the intended audience (i.e., users familiar with conventional plasticity models), and can be executed efficiently on the other, remain a topic of investigation.

G. Doğan has been developing algorithms to automate segmentation and meshing of microstructure images. His segmentation algorithms build on a shape optimization framework, which is used to detect optimal region boundaries in microstructure images. This is done by minimizing specially-designed image segmentation energies in this framework. He has previously implemented edge-based and region-based segmentation energies, and he developed a new anisotropic boundary energy in the last year. The isotropic edge-based boundary energy has a curve-shortening bias, and this sometimes causes it to miss concavities of the regions to be detected. The anisotropic energy, however, tries to align the normal of the curve with the extended image gradient, and in this way, it can detect region concavities better by bending the curve towards them.

A typical OOF user usually does not have much image analysis experience, and thus can be overwhelmed by the decisions, e.g. multiple parameters to set and algorithm initialization, to achieve acceptable results with a given segmentation algorithm. To simplify the process of tuning the segmentation parameters, Doğan implemented heuristic decisions to automate the definition of the edge-based segmentation energies. He has also been working on interfacing his segmentation package with OOF. Currently, his image-based meshing algorithm can be invoked by pressing a button on the OOF GUI. This algorithm takes a segmented microstructure image as input, and automatically creates a triangulation that matches the regions and their boundaries very well. Moreover, the triangles are guaranteed to be high quality as needed by the finite element simulations. An important advantage of this algorithm is that it does not require the user to set any parameters.

L. Zhang, a French graduate student interning at NIST, worked on optimizing OOF2. D. Feraud, from the same institute, took over from Zhang and worked on the general infrastructure of OOF, making recommendations for how it could be modernized.

S. Langer continued rewriting the core part of OOF3D that computes the volume of the intersection of an agglomeration of voxels (3D pixels) and a tetrahedral finite element. This calculation is central to the computation of element homogeneity, which is used to quantify how well a finite element mesh matches the geometry of a microstructure. The calculation is difficult because small round-off errors in computing the relative location of two points can lead to large errors in the final intersection volume. Work this year concentrated on methods that preserve topological information. Instead of storing points by their coordinates in *XYZ* space, all planes that meet at each point are recorded. These planes are either pixel planes (which form the boundaries of the voxel set and are perpendicular to the *X*, *Y*, or *Z* directions) or are element face planes (which may or may not be congruent to pixel planes). During the calculation, it may be determined that the computed *XYZ* positions of two nearby points are inconsistent with the existing topological knowledge of the planes that meet at those points, unless the two points coincide. This type of argument, in several specific geometrical circumstances, allows ambiguities induced by round-off error to be resolved in many cases. It is not known yet whether it will work in all cases, but it currently works in far more circumstances than it did at the beginning of the year.

Determination of Diffusion Coefficients in Alloys

Geoffrey McFadden
Paul Patrone
William Boettinger (NIST MML)
Carelyn Campbell (NIST MML)
Kil-Won Moon (NIST MML)
John Perepezko (University of Wisconsin)
Robert Sekerka (NIST MML, Carnegie Mellon U.)

Fick's law relates the flux of solute to the instantaneous composition gradients at each point; the constants of proportionality are known as diffusion coefficients, which are generally functions of the local composition at each point. The experimental determination of diffusion coefficients is the goal of the project.

Understanding alloy diffusion is critical in a variety of engineering applications. For example, turbine blades in jet engines are subject to extreme forces and temperature. Such conditions enhance bulk diffusion of the constituent metals, which may thereby lead to creep deformation and, ultimately, catastrophic failure of the engine. Thus, engineers require reliable estimates of diffusion rates (for example as a function of temperature and alloy composition) to ensure that engine operating conditions remain within safe limits.

A common technique for the measurement of alloy diffusion coefficients is through the analysis of diffusion couples. A diffusion couple consists of two long homogeneous solid samples, each of differing alloy compositions, which are joined together to form a single sample with discontinuous concentration profiles. At high enough temperatures, significant inter-diffusion may occur, allowing the concentrations profiles to relax in time. After a long enough time, this diffusion process would eventually lead to a homogeneous sample. At intermediate times the sample may be quenched to low temperatures, halting the diffusion process, and the spatial distribution of the resulting concentration profiles can be measured in detail. Ideally, the time of measurement is chosen so that the diffusion process is confined to the vicinity of the initial junction, leaving the far ends of the sample undisturbed at their initial concentrations. An example is shown in Figure 35.

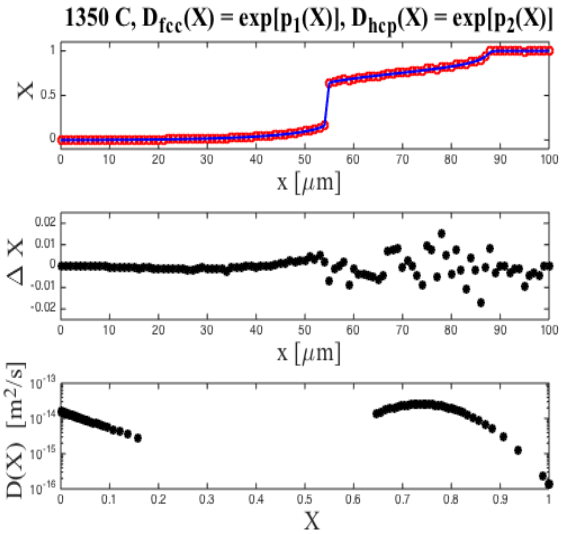

Figure 35. *Top: The composition X (mole fraction of rhenium in a binary nickel-rhenium alloy) versus distance x (in meters) in a diffusion couple. The red symbols are experimental data, and the solid blue curve is a numerical solution to the ODE using a diffusion coefficient with two or three degrees of freedom that is chosen to fit the data. Middle: The difference between the ODE solution and the experimental data versus distance. Bottom: The diffusion coefficient D(X) versus composition X resulting from the analysis. At this temperature, T=1350 C, the binary alloy exhibits both a face-centered-cubic phase (Ni-rich left hand side in upper plot) and a hexagonal-close-packed phase (Re-rich right hand side), resulting in a discontinuous composition profile at the interface between the two phases.*

Under the right conditions the diffusion couple can be modeled as a one-dimensional sample of infinite extent in each direction. The diffusion process is then modeled as a diffusion equation for the composition. For the idealized initial conditions, there is a similarity solution due to Boltzmann in which the composition depends on the single independent coordinate $(x - x_0)/t^{1/2}$, where x_0 is the position of the initial discontinuity, and t is the elapsed time. Under this change of variables, the diffusion equation reduces to second order nonlinear ordinary differential equations (ODEs) with far-field boundary conditions given by the initial compositions in each sample. An inverse approach to the determination of diffusion coefficients is then to compare numerical solutions of the ODEs with the experimentally measured profiles, iterating on the diffusion coefficients to minimize the difference. Typically, we assume a low-order power series for the composition dependence of the logarithm of the diffusion coefficients, using the polynomial coefficients as the unknowns in minimizing the error. An example of the resulting fit is shown in Figure 35. A large part of the project is devoted to an analysis of the uncertainty in the computed diffusion coefficient, which is a novel feature of the work [1].

In some cases, an analytical approach can be used to obtain direct relations between the diffusion coefficients and the concentration profiles. For example, an appropriate integration of the ODEs produces a direct relation between the solute flux at a point and specific integrals of the concentration profiles. We have recently extended analyses of this type that pertain to single phase binary alloy systems to the more general case of multiphase, multicomponent systems [2].

[1] W. J. Boettinger, M. E. Williams, K.-W. Moon, G. B. McFadden, P. N. Patrone and J. H. Perepezko, Interdiffusion in the Ni-Re System: Evaluation of Uncertainties, in review.

[2] R. F. Sekerka, G. B. McFadden and W. J. Boettinger, Analytical Derivation of the Sauer-Freise Flux Equation for Multicomponent Multiphase Diffusion Couples with Variable Molar Volume, *Journal of Phase Equilibria and Diffusion* **37**:6 (2016) 640-650.

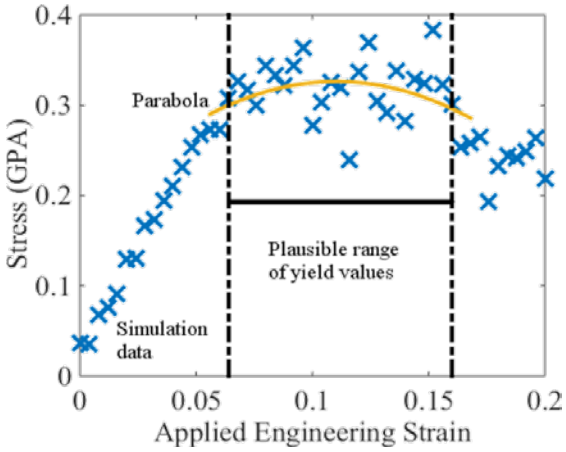

Figure 36. *Uncertainty in the yield strain is too large to be of practical use.*

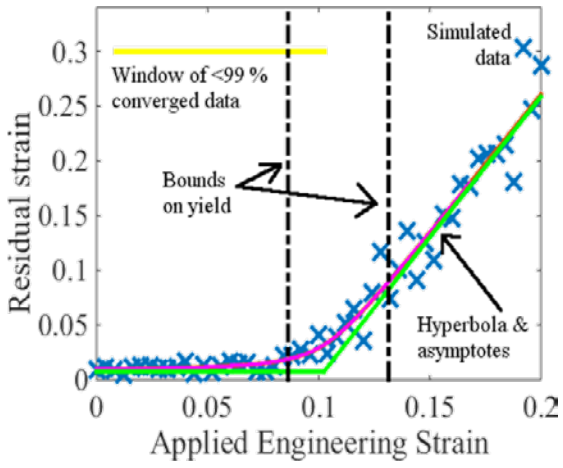

Figure 37. *The residual strain based analysis leads to smaller uncertainty windows.*

Simulations and Uncertainty Quantification of Materials Modeling for Aerospace Applications

Paul Patrone
Andrew Dienstfrey
Sam Tucker (Boeing)

In the aerospace industry, engineers must be able to predict when a wing will break under load so that they can design aircraft to safely handle the service conditions it will encounter. To that end, standard practice within the community is to "make it and break it." Dramatically, this often culminates in a full-scale test wherein a production-quality air-frame is stressed (e.g., the wings are bent) to the point of catastrophic failure [1]. Preceding this, however, are numerous component and coupon-scale experiments that assess the mechanical properties of various sub-assemblies in an effort to ensure that larger-scale tests will be successful. For aircraft made of next-generation composites (such as the Boeing 787), total costs are often hundreds of millions, if not billions of dollars [2]. Given the capital required to develop such aircraft, manufacturers are increasingly looking for alternative ways to design materials and test their properties [2].

Motivated by these observations, P. N. Patrone and A. Dienstfrey have continued collaborative efforts with research scientists at Boeing to develop simulation and uncertainty quantification (UQ) methods for modeling

of composite materials. Recent work has focused on developing new methods for estimating the yield strain, which is directly related to the amount of bending required to break a wing. In the past, this quantity has been estimated by simulating stress-strain curves of a given material and identifying yield as the first local maximum. However, high-throughput molecular dynamics simulations – a favorite tool in industry – suffer from extreme noise due to limited ability to model large systems [3]. In many cases, this gives rise to unacceptably large uncertainties that all but render predictions useless [4]; see Figure 36.

To address this, the ACMD-Boeing collaboration developed a simulation technique that directly identifies yield as the onset of irrecoverable deformation [4, 5]. In particular, the system is incrementally deformed and allowed to relax, each time checking to see if it returns to its original dimensions. The deviation-from-original-dimensions as a function of applied strain is defined as the residual strain; see Figure 37. Importantly, this approach provides a sharper signal for yield in the form of a transition from (approximately) zero residual to a linear trend with applied strain. Moreover, this bilinear behavior admits simple UQ techniques that were developed previously for simulated estimates of the glass-transition temperature. Using these, it is possible to show that the residual-strain method reduces uncertainty in the simulated predictions, thereby increasing their potential impact for industry.

Results have been presented at the Composites and Advanced Materials Expo [4] and written in a publication that is currently under review. Moreover, collaborators at Boeing, Solvay, and Schrodinger are currently using these tools or are developing them into their workflows. Future work aims to develop independent UQ tools to better assess and possibly reduce uncertainties in more traditional analyses of stress-strain curves.

[1] J. Paur, Boeing 787 Passes Incredible Wing Flex Test, *Wired*, March 29, 2010. Web: December 13, 2016.

[2] S. Christensen, Using Computation for Composite Matrix Development, in *Proceedings of the Composites and Advanced Materials Expo* (CAMX), Anaheim CA, September 28, 2016.

[3] V. Sundararaghavan and A. Kumar, Molecular Dynamics Simulations of Compressive Yielding in Cross-Linked Epoxies in the Context of Argon Theory, *International Journal of Plasticity* **47** (2013) 111-125.

[4] P. N. Patrone, S. Tucker and A. Dienstfrey, Estimating Yield-Strain Via Deformation-Recovery Simulations, submitted.

[5] P. N. Patrone, Estimation and Uncertainty Quantification of Yield Via Strain Recovery Simulations, in *Proceedings of the Composites and Advanced Materials Expo* (CAMX), Anaheim CA, September 27 2016.

A Spectral Approach to Coarse-Graining and the Radial Distribution Function

Paul Patrone
Thomas Rosch (NIST MML)[10]

In condensed matter physics, the radial distribution function (RDF) $g(r)$ is fundamental quantity that characterizes correlations between particle positions in atomically resolved systems. As a result, $g(r)$ is used to (i) link thermodynamic (or bulk) properties to microscopic details [1]; (ii) compute structure factors for comparison with X-ray diffraction experiments [2]; and more recently, (iii) calibrate interparticle forces for coarse-grained molecular dynamics (MD) simulations [3]. Given its importance, the RDF is therefore a central focus of many computational studies. However, $g(r)$ is an expensive and sometimes difficult quantity to compute, since it requires averaging over combinatorially many simulated pair-separations. Given these observations, it is therefore surprising that state-of-the-art approaches still reconstruct $g(r)$ from a histogram of pair-separations, with little thought to developing more efficient mathematical algorithms.

To address this problem, P. Patrone, in collaboration with T. Rosch, developed a spectral Monte Carlo (SMC) method that efficiently reconstructs RDFs in terms of smooth functions. The key idea of this analysis is to represent $g(r)$ via an expansion of the form

$$g(r) \approx g_M(r) = \sum_{j=0}^{M} a_j \varphi_j(r)$$

where $\varphi_j(r)$ are orthogonal functions on a domain $[0, r_{max}]$, a_j are the spectral coefficients, and M is a mode cutoff that determines (in part) the accuracy of the reconstruction. Combining the orthogonality relationship with Monte Carlo quadrature, it is possible to approximate the a_j via

$$a_j \approx \frac{2}{n_{pairs}} \sum_{k=1}^{n_{pairs}} \frac{\varphi_j(r_k)}{4\pi r_k^2 \varrho}$$

where r_k is the k^{th} pair separation output by a simulation such as MD, and ϱ is the number density. In contrast to histogram-based approaches, this method leads to dramatically smoother RDFs that converge more quickly; see Figure 38.

Moreover, analysis of the spectral coefficients allows one to estimate uncertainty in the RDF in terms of the omitted modes. Thus, SMC also provides reconstructions that are more objective than histogram-based approaches, which rely on subjective choices of bin widths and smoothing methods.

[10] Currently at JHU Applied Physics Laboratory

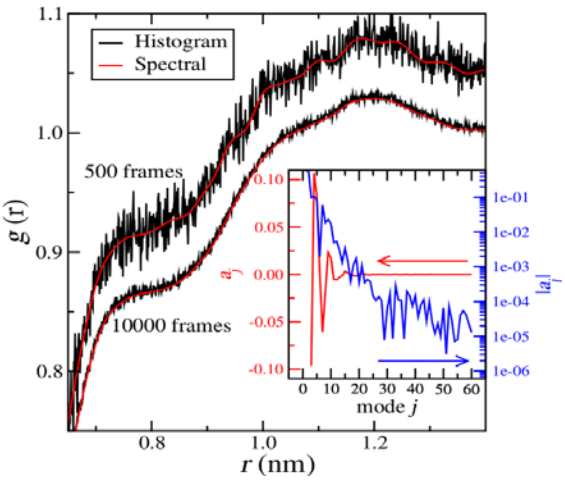

Figure 38. *Two RDFs computed for polystyrene using SMC and a histogram-based approach. SMC yields dramatically smoother reconstructions. The inset shows the SMC spectral coefficients as a function of the mode index j for the 10 000-frame RDF.*

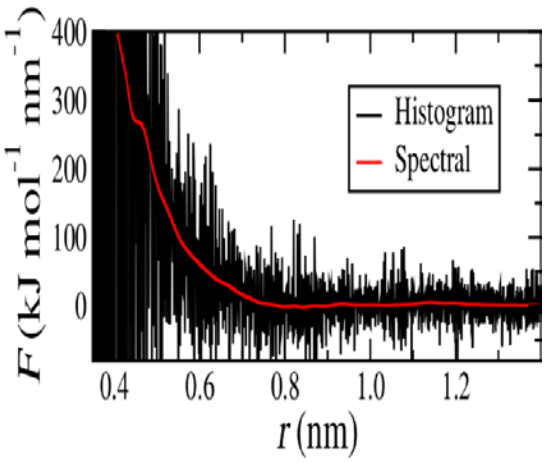

Figure 39. *Typical forces that might be computed during iterative Boltzmann inversion, a coarse-graining technique that calibrates interparticle forces using RDFs. The SMC force is dramatically smoother than its histogram counterpart.*

Results of this work have been described in a publication that is currently under review [4]. In this manuscript, the authors showed that SMC can be used to more efficiently perform coarse-graining tasks (e.g. iterative Boltzmann inversion) that calibrate interparticle forces against the RDF. In terms of CPU-hours, computational savings may be as large as two orders of magnitude. Moreover, the resulting forces are more physically reasonable, as shown in Figure 39.

Future work aims to combine this method with a Bayesian calibration technique developed by the authors in 2015.

[1] M. Allen and D. Tildesley, *Computer Simulation of Liquids*, Oxford Science Publications, Clarendon Press, 1987.

[2] N. Ashcroft and N. Mermin, *Solid State Physics*, HRW International Editions, Holt, Rinehart and Winston, 1976.

[3] C.-C. Fu, P. M. Kulkarni, M. Scott Shell and L. Gary Leal, A Test of Systematic Coarse-Graining of Molecular Dynamics Simulations: Thermodynamic Properties, *The Journal of Chemical Physics* **137** (2012) 164106.

[4] T. W. Rosch and P. N. Patrone, Beyond Histograms: Efficiently Estimating Radial Distribution Functions via Spectral Monte Carlo, submitted.

Analysis of a Generalized Planar Ginzburg-Landau Equation

Sean Colbert-Kelly
Geoffrey McFadden
Daniel Phillips (Purdue University)
Jie Shen (Purdue University)

A planar Ginzburg-Landau equation can be used to describe elastic energy for the molecular orientation of a thin film ferroelectric liquid crystal [1, 2]. If a particle is introduced in the thin film, then a singularity in the spontaneous polarization field will occur. This will cause an island to nucleate around the defect, with an island several layers thicker than the film's thickness [1]. On the island's boundary, the alignment of the molecules is tangential and is initially tangential in the interior of the disk, producing a degree 1 vector field. Distinct textural transformations in the director field could occur due to the increase in the island's size or to external forces causing a simple spiral pattern, tangential on the boundary and approximately radial at the smoke particle boundary [1].

The elastic energy of this system in the island can be described by

$$E_\varepsilon(u) = \frac{1}{2}\int_{B_1} k_s\,(\nabla\cdot u)^2 + k_b(\nabla\times u)^2 + \tfrac{1}{2\varepsilon^2}(1-|u|^2)^2\,dx$$

where k_s, k_b are the splay and bend constants for the liquid crystal, and $\varepsilon > 0$ is the radius of the defect core; in this model u is not restricted to having unit length. The director field u is given boundary conditions, i.e. $u = g$, where $|u| = 1$ and g has degree $d > 0$. Previous work has shown that for each ε, a minimizing vector field u_ε exists and as $\varepsilon \to 0$, $u_\varepsilon \to u_*$. The asymptotic field u_* is degree one on the boundary and near the singularity in the island a, the field behaves locally as

$$u_* = \alpha_a \frac{x-a}{|x-a|},$$

where $\alpha_a = \pm 1$ for $k_s < k_b$ for and $\alpha_a = \pm i$ for $k_s > k_b$ [3].

Building upon work from [3], we developed a spectral-Galerkin numerical method to solve the Euler-

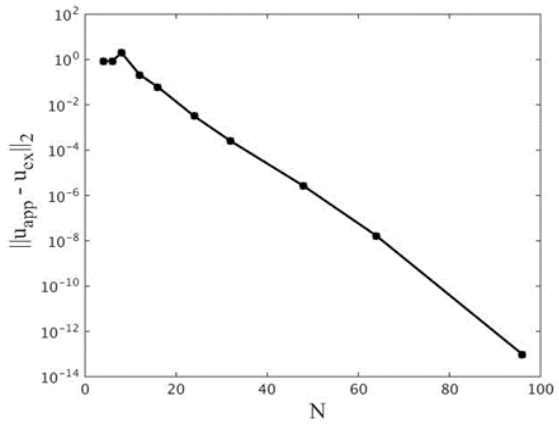

Figure 40. *Linear-log plot of the error as a function of the number of radial grid points.*

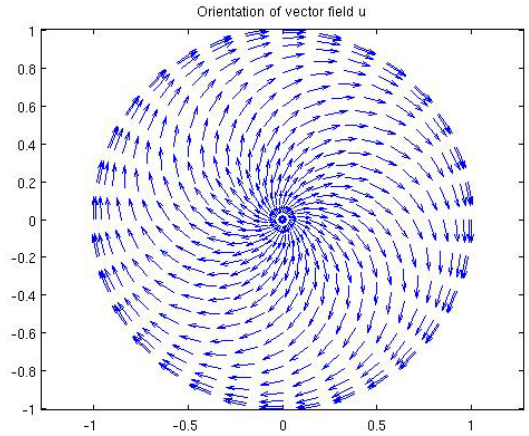

Figure 41. *Stable vector field, tangential boundary condition.*

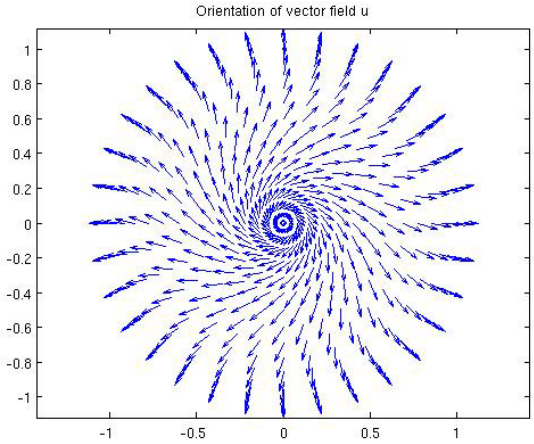

Figure 42. *Stable vector field, radial boundary condition*

Lagrange equations for E_ε, when ε is small, so as to capture the experimental observations and analytical results described above. This numerical method is advantageous in observing the nature of the defects computationally and results not currently proven. Various numerical methods deal with the simpler case $k_s = k_b$, resulting in a vector version of the Allen-Cahn equation. Our method will also simulate the case $k_s \neq k_b$ [4, 5]. A gradient flow stabilized scheme for the Euler-Lagrange equations was utilized and the solutions stabilized to an equilibrium state. The Euler-Lagrange equation was discretized via a first order semi-implicit stabilized scheme. The equation is then converted into a polar geometry representation. With this representation, we can approximate the solution with a Fourier expansion in the angle variable using an FFT and then approximate the Fourier coefficients using Chebyshev polynomials in the radius variable. We tested the scheme with boundary conditions of the form $g = e^{di\theta}$, for any positive integer d.

The spectral accuracy of the scheme in space was tested for the degree two case by increasing the mesh size by various factors. Figure 40 shows a plot of the error between the approximate solutions for various grid sizes and the solution with the largest tested grid size. After $N = 12$, the linear-log plot exhibits a linear behavior with a negative slope, which is indicative of spectral convergence of the solution.

For degree one solutions where the singularity is located at the origin, the vector field exhibits either a splay orientation, if $k_s < k_b$, or a bend orientation, if $k_s > k_b$, locally near the origin, as depicted in Figure 41 and Figure 42, respectively. Figure 41 is the stable solution for the energy with values $k_s = 0.5$, $k_b = 1.5$ and $g = e^{i(\theta-\pi/2)}$ while Figure 42 is the stable solution for the energy with values $k_s = 1.5$, $k_b = 0.5$ and $g = e^{i\theta}$. These results coincide with results shown both experimentally and analytically.

Lee, Konovalov, and Meyer [1] note that the size of the island also affects the transformation of the vector field: if the island radius is small the pure bend patterns rarely transform to a simple spiral. Related computational results are shown in Figure 43.

The equilibrium configuration of the degree one solutions in Figure 43 can be represented in the form

$$u(r,\theta) = v(r)\,\hat{r}(\theta) + w(r)\,\hat{\theta}(\theta) = [v(r) + iw(r)]\,e^{i\theta},$$

where the scalar functions $v(r)$ and $w(r)$ represent the splay and bend components of u in the radial and angular direction respectively. The left plot is a plot of the maximum value of the bend component w as a function of ε, which describes a bifurication from the splay solution, $w = 0$, at $\varepsilon_b \approx 0.244$. The right plot is the energy of the spiral solution (black curve) and the splay solution (red curve) versus ε, which shows that the spiral solution is stable for $\varepsilon = \varepsilon_b$.

Further simulations have been conducted of both the lowest energy solution and higher energy solutions with a variety of boundary conditions of various degrees d, which is further detailed in an accepted publication

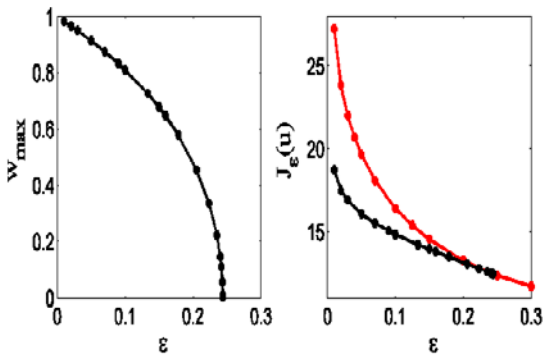

Figure 43. *The behavior of steady-state spiral solutions as a function of epsilon*

[6]. When $d = 2$, the minimal vector field has two degree one singularities that are located symmetrically about the origin. The vector field locally near both vortices either has a splay pattern or a bend pattern, just as in the degree one case. The vortices tend to be unique, where the vortices lie along the real axis for $k_s < k_b$ and the imaginary axis for $k_b < k_s$. For higher degrees, stable and metastable solutions exists. The higher energy solutions are generally degenerate, with several possible locations of the defects that depend on the values of k_s and k_b.

[1] J.-B. Lee, D. Konovalov, and R. B. Meyer, Textural Transformations in Islands on Free Standing Smectic-C* Liquid Crystal Films, *Physical Review E* **73** (2006), 051705 (7 pages).

[2] P.-G. de Gennes and J. Prost, *The Physics of Liquid Crystals*, Oxford University Press, New York, 1993.

[3] S. Colbert-Kelly and D. Phillips, Analysis of a Ginzburg-Landau Type Energy Model for Smectic C* Liquid Crystals with Defects, *Annales de l'Institut Henri Poincare (C) Non Linear Analysis* **30**:6 (2013), 1009-1026.

[4] J. Shen, Efficient Spectral-Galerkin Methods III: Polar and Cylindrical Geometries, *SIAM Journal on Scientific Computing* **18**:6 (1997), 1583-1604.

[5] J. Shen and X. Yang, Numerical Approximations of Allen-Cahn and Cahn-Hilliard Equations, *Discrete and Continuous Dynamical Systems. Series A* **28**:4 (2010), 1669-1691.

[6] S. Colbert-Kelly, G.B. McFadden, D. Phillips and J. Shen, Numerical Analysis and Simulation for a Generalized Planar Ginzburg-Landau Equation in a Circular Geometry, *Communications in Mathematical Sciences*, to appear.

Emulsion Stability Modeled with a Surfactant Phase and Interfacial Viscosity

Sean Colbert-Kelly
Trevor Keller (NIST MML)
Geoffrey McFadden
Frederick Phelan, Jr. (NIST MML)

Surfactants have important applications in detergents, droplet break-up, reducing the risk from bubbles formed in blood due to rapid decompression and prevention of lung collapse at the end of expiration [1, 3]. While surfactants are very low in overall composition, their dominant effect at the interface makes accounting for them in modeling a very important and challenging problem. Current models do not accurately model the dramatic effects of surfactants on emulsion properties and dynamics.

Modeling of binary emulsions stabilized by surfactants is an unresolved problem in the science of emulsions. Surfactants migrate to the fluid interface in a binary mixture due to the amphiphilic nature of these molecules [1]. This alters the interfacial tension and interfacial viscosity between the two phases leading to greater emulsion stability. They further play a profound role on the drop size distribution that emerges from processing. To first order, drop size is controlled by the surface tension between the two phases, but the rise of gradients in the surfactant concentration on the drop surface introduces Marangoni stresses that alter drop shape, breakup and coalescence dynamics, and lead to flow induced migration [2].

In this study we formulate diffuse interface models to investigate binary emulsions with a ternary surfactant component. We have extended previous models for the free energy of two-phase systems to include a third stabilizing surfactant phase, resulting, for example, in a modified three-phase Ginzburg-Landau formulation. Many of these models represent the two-phase fluid in terms of a conserved order parameter φ, with $\varphi \in [-1,1]$, where $\varphi = -1$ represents one phase and $\varphi = 1$ represents the second. The surfactant phase is added by introducing a second conserved order parameter ψ, with $\psi \in (0,1)$, where $\psi = 0$ represents the surfactant-free system. A representative free energy density is given by

$$G(\varphi,\psi) = \tfrac{1}{4}(\varphi^2-1)^2 + \left[\tfrac{1}{4} + \left(\psi - \tfrac{1}{2}\right)^2\right]^2 + \frac{W}{2}\psi\varphi^2 - 1 \qquad (1)$$

where W is an interaction parameter that measures the coupling between the surfactant and fluid phases. To aid in the physical interpretation of the model, the order parameters can be re-expressed in terms of an equivalent ternary alloy system, letting X_1 and X_2 represent mole

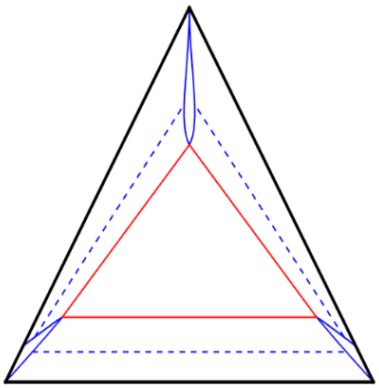

Figure 44. *A Gibbs triangle (solid black lines) depicting the concentrations of equilibrium phases of the ternary system for the free energy given in Eqn. (1) with W=1.75. Mole fractions are represented along the sides of the Gibbs triangle. The blue solid curves in each corner of the Gibbs triangle delimit the extent of single phases, with a surfactant phase near the top corner and the two fluid phases at the bottom two corners. Tie lines (dashed blue lines) that connect edges of the blue regions represent two-phase equilibria. A region of three-phase equilibria (red triangle) is delimited by the three vertices of the blue single-phase regions.*

fractions of the majority species composing the two fluid phases and X_3 representing the mole fraction of the surfactant, with $X_1 + X_2 + X_3 = 1$ at each point in the system. The relation between the order parameters and the mole fractions are given by [1]

$$X_1 = \frac{(1-\varphi)(1-\psi)}{2}, X_2 = \frac{(1+\varphi)(1-\psi)}{2}, X_3 = \psi$$

The equilibrium properties of the various models are depicted by means of ternary phase diagrams that represent the phases supported by each model. An example of a phase diagram that includes regions of single-phase equilibria, two-phase equilibria, and three phase equilibria for the free energy density in Eqn. (1) is shown in Figure 44.

We are currently using these models to incorporate concentration-dependent interfacial viscosity in flow calculations to study emulsion stability and droplet growth rates. A mixing rule for the interfacial viscosity in the surfactant-free case [4] is being generalized to include viscosity changes in the interfacial layer due to the decreased entanglement of polymers. Once an accurate description of the interfacial viscosity is obtained, droplet dynamics in some simple flow fields will be considered, including the predictions of the models for droplet size distributions.

[1] S. Engblom, M. Do-Quang, G. Amberg and A.-K. Tornberg, On Diffuse Interface Modeling and Simulation of Surfactants in Two-Phase Fluid Flow, *Communications in Computational Physics* **14**:4 (2013), 879-915.

[2] J. T. Schwalbe, F. R. Phelan, Jr., P. M. Vlahovska and S. D. Hudson, Interfacial Effects on Droplet Dynamics in Poiseuille Flow, *Soft Matter* **7** (2011) 7797–7804.

[3] C.-H. Teng, I.-L. Chern and M.-C. Lai, Simulating Binary Fluid-Surfactant Dynamics by a Phase Field Model, *Discrete and Continuous Dynamical Systems Series B* **17**:4 (2012), 1289–1307.

[4] W. Yu and C. Zhou, The Effect of Interfacial Viscosity on the Droplet Dynamics Under Flow Field, *Journal of Polymer Science Part B: Polymer Physics* 46:14 (2008), 1505-1514.

Deconvolution and Unfolding of the Abel Equation by the Truncated Singular Components Method

Timothy J. Burns
Bert W. Rust

We have been developing a new approach to the problem of estimating the shear flow stress in machining based on an inverse method. Most material constitutive response models for high-speed machining simulations have been based on direct methods, which fit compression test data of small samples of the material of interest to a given highly nonlinear constitutive response model. The main problem with this approach has been that the conditions under which compression tests can be performed are not nearly as extreme as the actual conditions that are present in a typical high-speed machining operation [1], so that a finite-element machining process simulation using the nonlinear material response model necessarily requires huge extrapolations to simulate actual cutting conditions. Thus, such simulations typically do a poor job of predicting important cutting conditions, such as the temperature distribution on the cutting face of the tool [2], which has a big influence on tool wear and tool breakage.

Our new approach is based on recent progress in obtaining good experimental measurements of the temperature distribution on the tool-material interface during a high-speed machining test [3, 4]. By finding an asymptotic solution of a convection-diffusion problem that models the flux of heat into the chip and the tool during a cutting experiment, the temperature distribution along the tool face can be shown to satisfy Abel's equation, a Volterra integral equation of the first kind with a weakly singular kernel, which is convolved with the material flow stress [2]. Thus, given good steady-state temperature measurements on the tool face obtained during an instrumented high-speed machining test, inversion of this Abel equation provides an estimate of the distribution of flow stress in the chip material near the tool-chip interface. It is well-known that this inverse problem is ill-posed; see, e.g., [5].

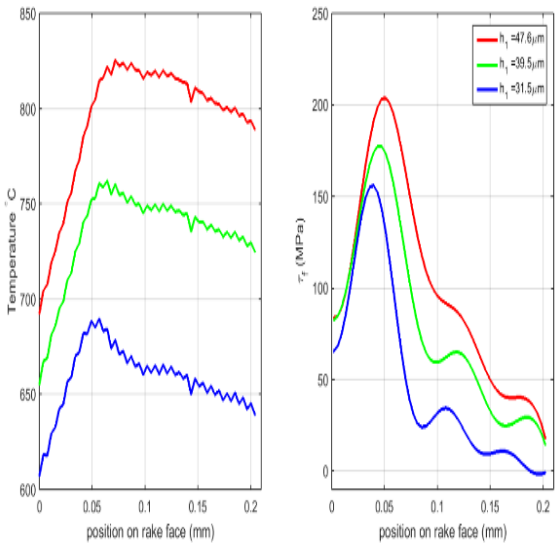

Figure 45. *We have applied our method to three sets of temperature data on the tool-chip interface that were obrained in a series of orthogonal cutting experiments on AISI 1045 steel by Davies, et al. [3]. In these tests, the cutting speed was held fixed at 3.7 m/s, and the temperature distribution along the rake face of the tool was determined for three different uncut chip thickness* $\boldsymbol{h_1}$*; the temperature results are plotted on the left. The corresponding estimates of the shear flow stress* $\boldsymbol{\tau_f}$ *using our method, without correcting for the heat flow into the tool, are plotted on the right.*

The Abel equation, which is often referred to as the Abel transform, also occurs in several other important applications, including astronomy, interferometry, seismology, and tomography. We have developed a numerical method for the stable inversion of the Abel transform, that is based on Rust's Truncated Singular Components Method for Fredholm integral equations of the first kind [6, 7]. Using the fact that the Abel transform can be formulated as a compact linear operator acting on and into weighted L_2 spaces, and a little-known result that the corresponding operator equation has a singular value decomposition that can be expressed as an infinite sum of singular functions which are closely related to Jacobi polynomials, Rust's method in this case can be shown to separate signal from noise in experimental data that have been contaminated by random perturbations. It does this by filtering out higher-frequency components that can be identified as noise, using methods from the statistical analysis of time series, prior to performing a numerical inversion of the discretized problem. Without this filtering, the computed inverse would be corrupted by large amplitude oscillatory components resulting from amplification of noise in the data.

Results from this work were presented at the SIAM Annual Meeting (AN16) in Boston, and the 24th International Congress of Theoretical and Applied Mechanics (ICTAM2016) in Montreal; see Figure 45.

[1] S. P. Mates, R. L. Rhorer, E. P. Whitenton, T. J. Burns and D. Basak, A Pulse-Heated Kolsky Bar Technique for Measuring Flow Stress of Metals Subjected to High Loading and Heating Rates, *Experimental Mechanics* **48** (2008), 799–807.

[2] T. J. Burns, S. P. Mates, R. L. Rhorer, E. P. Whitenton and D. Basak, Inverse Method for Estimating Shear Stress in Machining. *Journal of Mechanics and Physics of Solids* **86** (2016), 220–236.

[3] M. A. Davies, H. Yoon, T. L. Schmitz, T. J. Burns and M. D. Kennedy, Calibrated Thermal Microscopy of the Tool–Chip Interface in Machining, *Machining Science and Technology* **7** (2003), 167–190.

[4] T. Menon and V. Madhavan, Infrared Thermography of the Chip-Tool Interface through Transparent Cutting Tools, in *Proceedings of the North American Manufacturing Research Institution/SME*, Ann Arbor, MI, June 2014.

[5] I. J. D. Craig and J. C. Brown, *Inverse Problems in Astronomy*, Adam Hilger Ltd., Bristol and Boston, 1986.

[6] B. W. Rust, Truncating the Singular Value Decomposition for Ill-Posed Problems, NIST IR 6131, July 1998.

[7] B. W. Rust and D. P. O'Leary, Residual Periodograms for Choosing Regularization Parameters for Ill-Posed Problems, *Inverse Problems* **24** (2008), 034005 (30 pages).

High Performance Computing and Visualization

Computational capability is advancing rapidly, with the result that modeling and simulation can be done with greatly increased fidelity (e.g., higher resolution, more complex physics). However, developing the requisite large-scale parallel applications remains highly challenging, requiring expertise that scientists rarely have. In addition, the hardware landscape is changing rapidly, so new algorithmic techniques must constantly be developed. We are developing and applying such expertise for application to NIST problems. In addition, computations and laboratory experiments often produce large volumes of scientific data, which cannot be readily comprehended without some form of visual analysis. We are developing the infrastructure necessary for advanced visualization of scientific data, including the use of 3D immersive environments and applying this to NIST problems. One of our goals is to develop the 3D immersive environment into a true interactive measurement laboratory.

Rheology of Dense Suspensions

William George
Judith Terrill
Steven Satterfield
Nicos Martys (NIST EL)
Chiara Ferraris (NIST EL)
Pascal Hebraud (CNRS/IPCMS, Strasbourg, France)

Understanding the mechanisms of dispersion or agglomeration of particulate matter in complex fluids, such as suspensions, is of technological importance in many industries such as pharmaceuticals, coatings, and construction. These fluids are disordered systems consisting of a variety of components with disparate properties that can interact in many ways. Modeling and predicting the flow of such systems represents a great scientific and computational challenge requiring large-scale simulations. In collaboration with scientists in NIST's Engineering Laboratory (EL), we have developed an application, called QDPD (Quaternion-based Dissipative Particle Dynamics) [1], which can perform large-scale simulations of dense suspensions. This simulator uses a modified version of the DPD technique [2] for the simulation of Newtonian fluids, and the Smoothed Particle Hydrodynamics technique (SPH) [3] for non-Newtonian fluids.

QDPD is highly parallel and has been shown to efficiently scale up to at least 2^{17} processors (131 072 processors) when running on the DOE supercomputer Mira, an IBM Blue Gene/Q, at the Argonne National Laboratory Leadership Computing Facility. Our goal in this project is to advance our understanding of the flow properties of a specific material, fresh concrete, a dense suspension composed of cement, water, sand, and rocks.

We are currently using this computational approach in the development of standard reference materials (SRMs) for the calibration of vane rheometers used to measure the flow properties of fresh concrete [4]. Figure 46 shows a snapshot of a simulation of the proposed mortar SRM in a 6-blade vane rheometer. While concrete flow measurements, using different concrete rheometers, can be found to correlate, they usually do not provide results in fundamental units. This is a consequence of the complex flow patterns that develop in the rheometer, combined with the non-Newtonian behavior of the mortar or concrete. This results in complex local stress and strain/strain rate fields which make it difficult to express measurement data in terms of fundamental rheological parameters. By modeling the flow of an SRM in a vane rheometer we are able to predict what should be measured by an experimentalist, and further, our simulations are designed to enable us to map out many details of the local flow, such as stress/strain fields

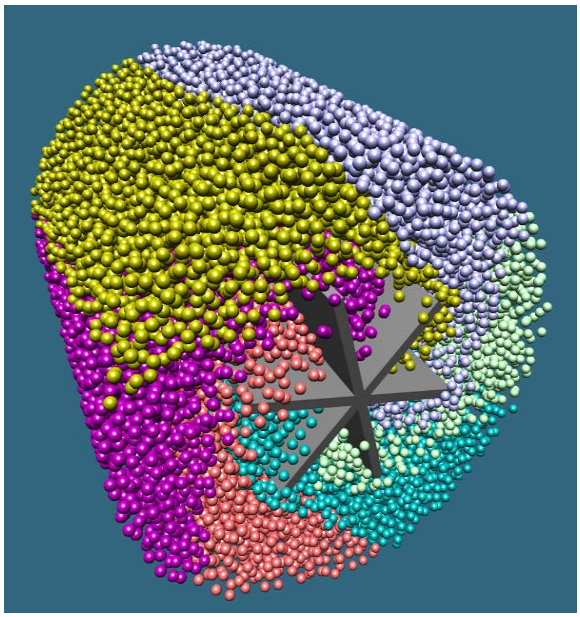

Figure 46. *A snapshot from a QDPD simulation of a proposed mortar SRM in a 6-blade rheometer viewed from the bottom of the rheometer. From this view, the blades are rotating clockwise. The suspended spheres are color-coded by their starting section.*

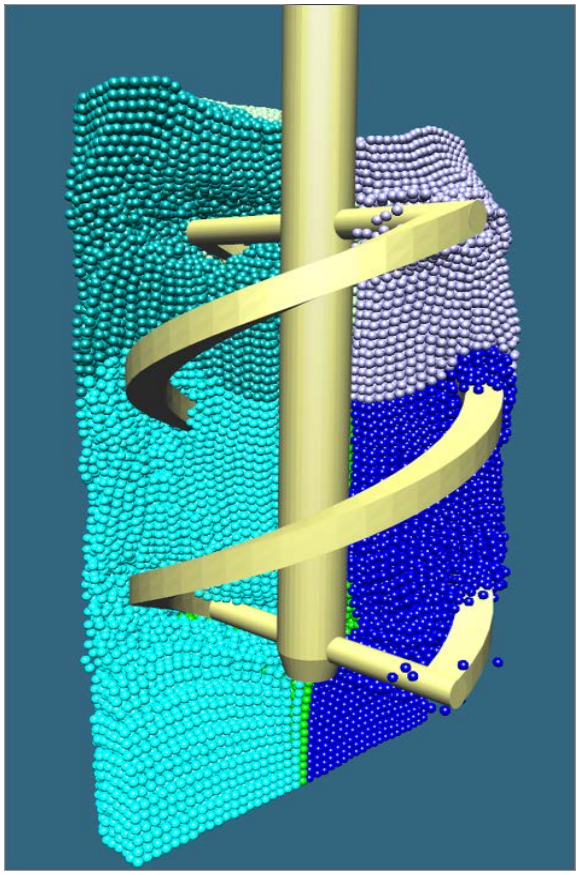

Figure 47. *A snapshot from a QDPD simulation of a proposed mortar SRM in a double-helix rheometer viewed from the side of the rheometer. Half of the suspended spheres have been omitted from the image in order to show the blade geometry. If viewed from above, the blades are rotating clockwise. The suspended spheres are color-coded by their starting section.*

in 3D, and bring insight into the vane rheometer measurement process.

Most research on suspensions has made the simplifying assumption that the matrix fluid, that is, the fluid supporting the suspended particle, is Newtonian. With the use of high-performance computing, we have been able to extend this research to include the simulation of suspensions with non-Newtonian fluid matrices, which includes most suspensions of interest to industry. One result of our studies has been to show that the viscosity versus shear rate curves for suspensions having various volume fractions can be collapsed onto a single universal curve parameterized by the properties of the underlying non-Newtonian matrix fluid [5]. This, along with other results from our studies, has advanced our basic understanding of the flow of dense suspensions.

Building on this research, we have begun using simulation in the design process for new standard reference materials (SRMs), as described earlier, which will be used for calibrating mortar and concrete rheometers. The first such SRM to be developed will be a mortar SRM, followed by a concrete SRM. The mortar SRM should be ready for release in 2017, with the concrete SRM in the following year.

Along with the development of these SRMs, in 2016 we also investigated another flow geometry of interest to industry, the flow of suspensions through a pipe. Many experiments were required to develop a model of the forces between the wall of the pipe and the suspended inclusions, as well as the forces between the matrix fluid and the pipe. Although, as of December 2016, these simulations are still underway, initial results of this study have been presented [6, 7]. A more complete report will be published once all our pipe-flow simulations have been completed.

Our simulations in 2017 will continue to focus on the design of blades within the rheometers. The current typical design, with 4 or 6 flat blades, has been shown to be sub-optimal, and other blade designs are under consideration. We have modified our simulator to study one of the newly proposed blade designs, a “double-helix” blade. A snapshot from an early simulation of the proposed mortar in such a rheometer is shown in Figure 47. We also intend to begin the simulation of these rheometers with random-shaped rocks suspended instead of the spherical beads of the proposed SRMs.

An award of computer time to support this effort was provided by the Department of Energy (DOE) Innovative and Novel Computational Impact on Theory and Experiment (INCITE) program. This research used resources of the Argonne Leadership Computing Facility, which is a DOE Office of Science User Facility supported under Contract DE-AC02-06CH11357.

[1] N. Martys, Study of a Dissipative Particle Dynamics Based Approach for Modeling Suspensions, *Journal of Rheology* **49**:2 (2005), 401-424.

[2] P. J. Hoogerbrugge and J. M. V. A. Koelman, Simulating Microscopic Hydrodynamic Phenomena with Dissipative Particle Dynamics, *Europhysics Letters* **19** (1992), 155-160.

[3] J. J. Monaghan, Smoothed Particle Hydrodynamics, *Reports on Progress in Physics* **68** (2005), 1703-1759.

[4] C. Ferraris, N. Martys, W. George, E. Garboczi and A. Olivas, “Calibration of Rheometers for Cementitious Materials,” International Concrete Sustainability Conference (2016).

[5] M. Liard, N. S. Martys, W. L. George, D. Lootens and P. Hebraud, Scaling Laws for the Flow of Generalized Newtonian Suspensions, *Journal of Rheology* **58**:6 (2014), 1993-2015.

[6] N. S. Martys, C. F. Ferraris and W. L. George, “Modeling of Suspension Flow in a Pipe Geometry and Rheometers,” International Concrete Sustainability Conference, 2016.

[7] N. S. Martys, C. F. Ferraris and W. L. George, “Computational Modeling of Suspension Flow in Pipes with Generalized Newtonian Matrix Fluids,” 87th Annual Meeting of the Society of Rheology, Baltimore, MD, October 11-15, 2015.

HydratiCA: A Parallelized Numeric Model of Cement Hydration

John Hagedorn
Afzal Godil
Wesley Griffin
Judith Terrill
Jeffrey Bullard (NIST EL)

HydratiCA is a stochastic reaction-diffusion model of cement hydration. The hydration that occurs when cement powder is mixed with water that subsequently transforms the paste from a fluid suspension into a hardened solid. This process involves complex chemical and microstructural changes. Understanding and predicting the rates of these changes is a longstanding goal.

Computational modeling of the hydration of cement is challenging because it involves many coupled nonlinear rate equations that must be solved in a highly irregular three-dimensional spatial domain. HydratiCA addresses these challenges with a computational model that has several advantages over other models of cement hydration. Parallelization of the model and the visualization of the output data are important components of this project. With parallelization, we can simulate systems that are large enough to be realistic, avoiding finite size effects, and still can complete the simulations in a reasonable amount of time. Visualization of the data volumes produced by HydratiCA is important both for validation and for understanding of the results.

This year we continued work on HydratiCA with significant improvements to the algorithm, the parallel implementation, and visualization. Large-scale runs have enabled us to make direct comparisons between simulations and experiments. We have an on-going series of runs that focus on calculating the time-dependent rate of heat release and development of the percolating solid network responsible for the hardening of concrete. We are also investigating the effect of the size and spacing of the computational lattice.

Visualization. We have pursued two avenues of development for the visualization of HydratiCA results. First, we developed a new 3D visualization using an isosurface extraction algorithm that provides a more realistic and useful view of the simulation data. As part of this effort, we also streamlined the 2D quantitative visualization to better meet end-user needs and requirements. As shown in Figure 48 and Figure 49, the visualization remains a hybrid immersive 3D and quantitative 2D tool. These are used by the scientist to examine the latest simulation runs and are also used to generate a time-lapse movie of the simulation.

A second avenue of visualization development was a prototype in situ visualization tool. This tool visualizes the varying time step at each iteration of a running simulation. The prototype was designed to aid the simulation programmer in understanding the time step variation while the simulation was executing. Figure 50 shows the time-step after 22 000 iterations. The geometric progression used in the modification of the time step after critical events can be clearly seen.

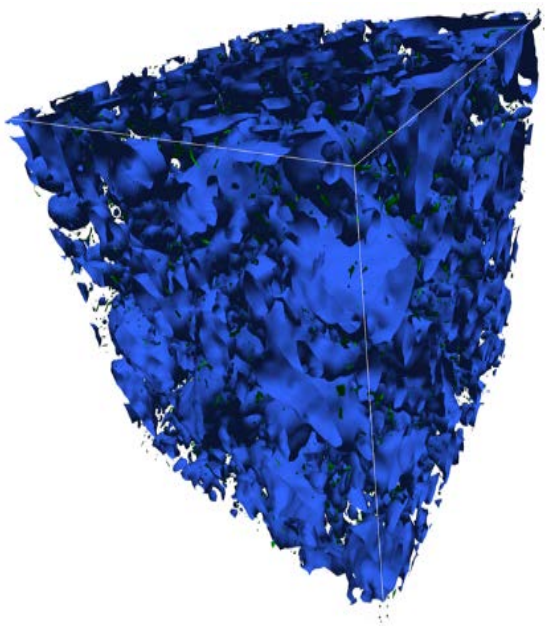

Figure 48. *The full simulation output volume of $Ca(OH)_2$ concentration (green) where the surface represents a concentration of 0.50229, Ca_3SiO_5 concentration (blue) where the surface represents a concentration of 0.49448, and CSH(I) concentration (yellow) where the surface represents a concentration of 0.10479.*

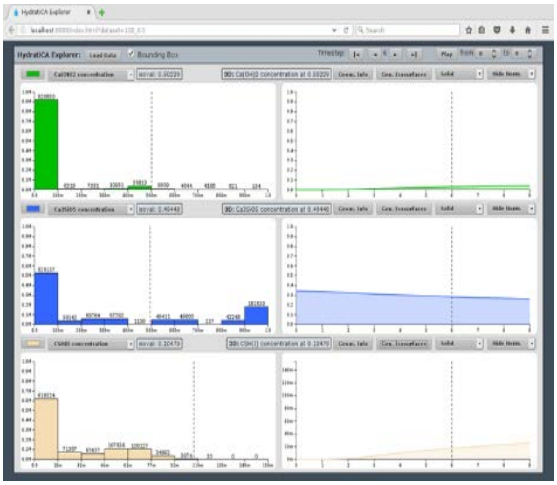

Figure 49: *Web 2D quantitiative visualization of the concentrations of three different compounds. The left plots show the concentration histogram across all time-steps, while the right plots show a time-series of the concentration.*

Results. We have continued our large-scale runs on Stampede, a system at the Texas Advanced Computing Center, under a grant from NSF's XSEDE program [6].

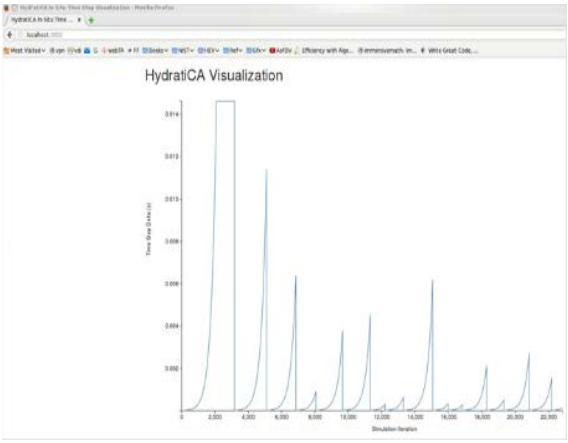

Figure 50. *A snapshot of the time step delta in seconds after 22 000 iterations of the simulation. The web page is a live view into the running simulation and provides an in situ visualization of the variable time step.*

These runs have enabled us to continue our direct comparisons between experiments and HydratiCA simulations of the hydration of tricalcium silicate. In comparing experiment and simulation, some results are consistent but there are other points at which the experiment and simulation diverge. For example, the simulated and observed amounts of Ca_3SiO_5 dissolution agree to within the measurement uncertainty. At the same time, the number of moles, and especially the apparent volume of hydration product phases, observed are greater than either the simulations predict or the observed amount of Ca_3SiO_5 dissolution can produce. This and other discrepancies between experiment and simulation are a subject of ongoing investigation. These results are being reported in detail in a paper that is currently in preparation.

Using an additional XSEDE grant of time on Stampede, we are focusing on calculating the time-dependent rate of heat release and development of the percolating solid network responsible for the hardening of concrete. We are also investigating the effect of the size and spacing of the computational lattice. These runs are currently in progress.

Continuing Work. We are continuing our development of the HydratiCA code. This involves improvements to the algorithm, its implementation, and data visualization. We are currently enhancing the algorithm by adding new boundary conditions and we are investigating improvements to our handling of adaptive time steps. Our efforts in improving the implementation are focusing on efficiency, communications, parallelization, and vectorization techniques. The visualization work will largely concentrate on *in situ* visualization, in which we will visualize results as the simulation is running. This will enable us to more effectively gain insights and make decisions about the running simulation. We will also be looking at integrating the *in situ* visualization with our immersive visualization capabilities.

We are proceeding with our investigation of rate of heat release and the evolution of the percolating network in concrete. These runs are continuing to produce data which we are analyzing as it becomes available. In addition, we are developing a series of simulations to characterize the sulfate-silicate interplay in concrete. We will model the full range of complexity found in real cementitious materials validated by experimental measurements on materials that approximate those being simulated as closely as possible. We are submitting another application to XSEDE for time on Stampede to pursue these runs.

Acknowledgement. This work used the Extreme Science and Engineering Discovery Environment (XSEDE), which is supported by National Science Foundation grant number ACI-1053575.

[1] J. Bullard, J. Hagedorn, M. T. Ley, Q. Huc, W. Griffin and J. Terrill, A Critical Comparison of 3D Experiments and Simulations of Tricalcium Silicate Hydration, in review.

[2] J. Bullard, E. Garboczi, P. Stutzman, P. Feng, A. Brand, P. LaKesha, J. Hagedorn, W. Griffin and J. Terrill, Measurement and Modeling Needs for Next-Generation Concrete Binders, in preparation.

[3] J. Bullard, T. Ley, J. Hagedorn, R. Desaymons, W. Griffin, J. Terrill, Q. Hu, S. Satterfield and P. Gough, "Direct Comparisons of 3D Hydration Experiments and Simulations," 6th Advances in Cement-Based Materials Conference, Manhattan, KS, July 2015.

[4] J. W. Bullard, E. Enjolras, W. L. George, S. G. Satterfield and J. E. Terrill, A Parallel Reaction-Transport Model Applied to Cement Hydration and Microstructure Development, *Modeling and Simulation in Materials Science and Engineering* **18** (2010), 025007.

[5] W. Griffin, D. Catacora, S. Satterfield, J. Bullard and J. Terrill, Incorporating D3.js Information Visualization into Immersive Virtual Environments, in *Proceedings of IEEE Virtual Reality (VR2015)*, March 2015, 187-188.

[6] J. Towns, T. Cockerill, M. Dahan, I. Foster, K. Gaither, A. Grimshaw, V. Hazlewood, S. Lathrop, D. Lifka, G. D. Peterson, R. Roskies, J. R. Scott and N. Wilkins-Diehr, XSEDE: Accelerating Scientific Discovery, *Computing in Science & Engineering* **16**:5 (Sept.-Oct. 2014), 62-74.

Nano-Structures, Nano-Optics, and Controlling Exciton Fine Structure with Electric and Magnetic Fields

James S. Sims
Wesley Griffin
Garnett W. Bryant (NIST PL)
Jian Chen (UMBC)
Henan Zhao (UMBC)

Research and development of nanotechnology, with applications ranging from smart materials to quantum computation to biolabs on a chip, is a national priority. Semiconductor nanoparticles, also known as nanocrystals and quantum dots (QDs), are one of the most intensely studied nanotechnology paradigms. Nanoparticles are typically 1 nm to 10 nm in size, with a thousand to a million atoms. Precise control of particle size, shape and composition allows one to tailor charge distributions and control quantum effects to tailor properties completely different from the bulk and from small clusters. Because of enhanced quantum confinement effects, nanoparticles can act as artificial, man-made atoms with discrete electronic spectra exploitable as light sources for novel enhanced lasers, discrete components in nanoelectronics, qubits for quantum information processing, and enhanced ultrastable fluorescent labels for biosensors to detect, for example, cancers, malaria or other pathogens, and to do cell biology.

We are developing computationally efficient large scale simulations of such nanostructures, and developing immersive visualization techniques and tools to enable analysis of highly complex computational results of this type. The electrical, mechanical, and optical properties of semiconductor nanocrystals and quantum dots are studied. In the most complex structures this entails modeling structures with on the order of a million atoms. Highly parallel computational and visualization platforms are critical for obtaining the computational speeds necessary for a systematic, comprehensive study.

Our current code analyzes wave functions, obtaining the one with maximum spin up, the one with maximum spin down, and two intermediate ones. The addition of a magnetic field provides a probe to split excitonic states, providing a more complete spectroscopy of quantum dot (QD) optics. This allows us to isolate contributions from spin-orbit coupling, Zeeman and spatial motion.

The intrinsic spins of the electrons lead to different effects in a magnetic field depending on the QD size and shape, and, as a result, it is necessary to be able to see the effect of spin in different QD arrangements. Without visualization, it becomes very difficult to understand what this distribution is and how it changes for different magnetic fields, electric fields or strain. This distribution

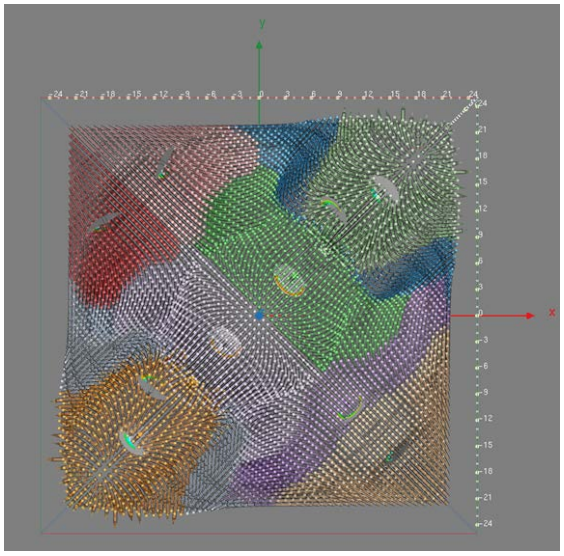

Figure 51. *Expectation-Maximization clustering of spin magnitude.*

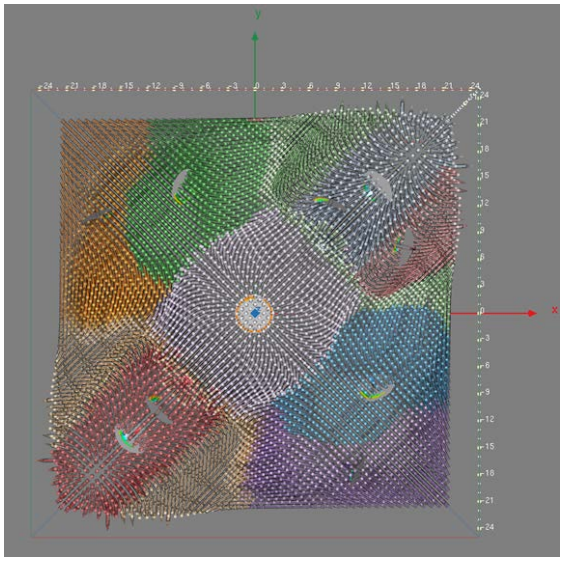

Figure 52: *K-Means clustering of spin magnitude.*

is critical for understanding exchange interactions or electron/nucleus interactions in quantum devices. These properties are intimately connected with the performance of these structures in quantum information processing. This can entail modeling structures with on the order of a million atoms.

As the device size in Si electronics continues to decrease, the devices are rapidly approaching the atomic scale where a change in only a few atoms can make a significant change in device performance. At the same time, the ability to make Si nanodevices with only a few deterministically placed dopant atoms opens the possibility to create quantum information processing devices with these structures. We currently have a program to

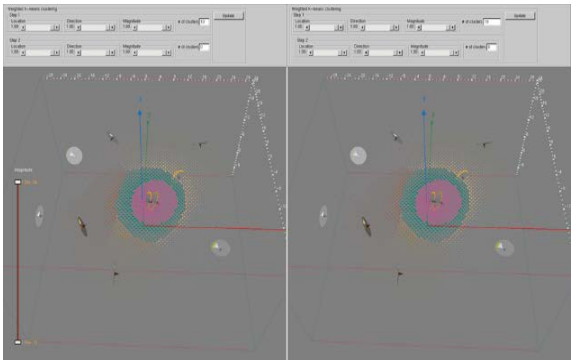

Figure 53. *Random initialization (left) and initialization via hierarchical clustering output (right) approaches for K-Means clustering.*

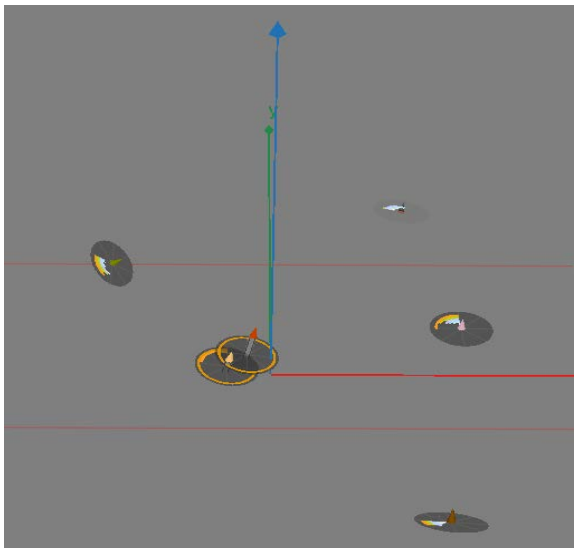

Figure 54: *Several overview glyphs showing average orientation and magnitude for each cluster.*

make, characterize and model both traditional and quantum Si devices at this few-dopant atom limit.

During the last year, the computational nanodevices project has been working to extend the atomistic tight-binding simulation tool to study systems made with random alloys. The use of random alloys allows for greater flexibility in engineering the electronic, optical and quantum properties of nanodevices. In particular, a random alloy has been modeled by replacing randomly chosen atoms in specified regions of the nanodevice with different atoms with different properties. Tools were developed to place atoms at randomly chosen sites in and around the nanodevice. The current simulation tools were enhanced to treat this added complexity. Extensive effort has to be made to compile these new codes given the changes that were recently made in the computational resources at NIST. Significant support from ITL made this possible.

At the same time, ongoing analysis of results from the simulations of various nanodevices has been supported by a new visualization tool. The significant speedup of this visualization tool makes it practical to use on data from million-atom device simulations both for visualization at the desktop and for immersive 3D visualization. This will greatly facilitate analysis of these systems with large amounts of data. The visualization tool employs a novel visualization technique [1, 2], which continues to undergo iteration as we apply the tool to datasets.

Given the amount of data being visualized, we spent significant time this year working on visualization methods to aid in gaining coarse-grained understanding of the data. Since clustering can provide a sense of the overall trends in the data, we implemented and evaluated two different clustering approaches for the three spin attributes location, orientation, and magnitude and also designed an overview glyph to summarize the average orientation and magnitude distribution. These two results were refined via iteration of the visualization tool.

The two clustering approaches we implemented were: Expectation-Maximization (EM) and K-Means. EM clustering works by estimating the parameters to an analytical data model using the log-likelihood of the observed data. A key underlying assumption we made in our application of the EM algorithm is that the data are described by a Gaussian distribution. K-Means clustering operates by partitioning the observed data into k clusters by minimizing the distance of each data point to the cluster mean. After implementing both algorithms, we found the K-Means clustering provided results that better fit with scientific expectations and didn't require the assumption of a Gaussian distribution of data. Figure 51 and Figure 52 show the EM clustering and K-Means clustering approaches respectively.

After deciding on K-Means clustering, we evaluated two initialization techniques for the clustering algorithm: random initialization and hierarchical clustering output initialization. As Figure 53 shows, there is no discernible difference between the two approaches, therefore we chose to use the faster approach of random initialization.

Figure 53 also shows the overview glyph we designed to summarize the average orientation and magnitude distribution. Figure 54 shows several overview glyphs with the average orientation and magnitude for each cluster. Finally, Figure 55 and Figure 56 are the visualization tool with the clustering and overview glyphs incorporated. The figures show the same dataset with two different clusterings.

[1] J. Chen, H. Zhao, W. Griffin, J. Terrill and G. Bryant, "Validation of Split Vector Encoding and Stereoscopy for Quantitative Visualization of Quantum Physics Data in Virtual Environment," poster, IEEE Virtual Reality (VR2015), Arles France, March 23-27, 2015.

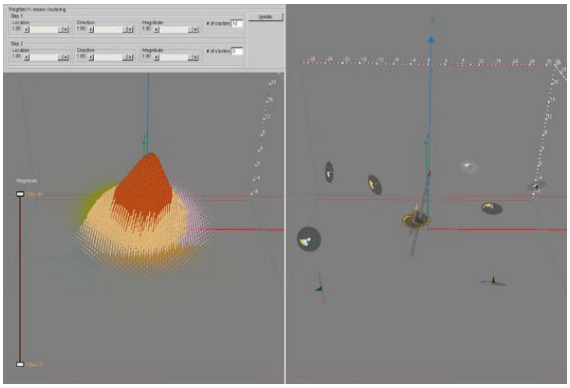

Figure 55. *Clustering of a dataset in the current visualization tool.*

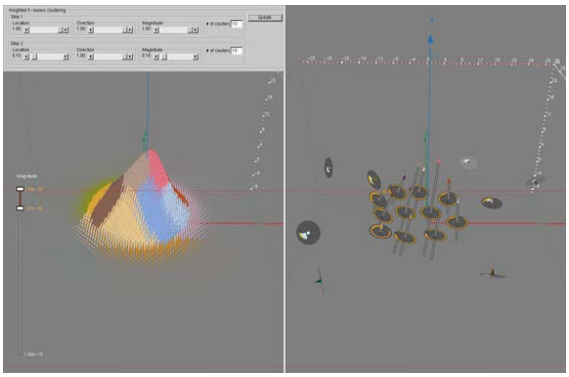

Figure 56. *Clustering of a dataset in the current visualization tool.*

[2] H. Zhao, G. Bryant, W. Griffin, J. Terrill and J. Chen, Validation of Split Vector Encoding and Stereoscopy for Quantitative Visualization of Quantum Physics Data, to appear.

High Precision Calculations of Fundamental Properties of Few-Electron Atomic Systems

James Sims
Stanley Hagstrom (Indiana University)
M. B. Ruiz (University of Erlangen, Germany)
Bholanath Padhy (Khallikote College, India)

NIST has long been involved in supplying critically evaluated data on atomic and molecular properties such as the atomic properties of elements in the Periodic Table and the vibrational and electronic energy level data for neutral and ionic molecules contained in the NIST Chemistry WebBook. Fundamental to this endeavor is the ability to predict, theoretically, a property more accurately than even the most accurate experiments. It is our goal to be able to accomplish this for few-electron atomic systems.

While impressive advances have been made throughout the years in the study of atomic structure, at both the experimental and theoretical levels, the scarcity of information on atomic energy levels is acute, especially for highly ionized atoms. The availability of high precision results tails off as the state of ionization increases, not to mention higher angular momentum states. In addition, atomic anions have more diffuse electronic distributions, and therefore represent more challenging computational targets than the corresponding ground states.

In the past two decades, there have been breathtaking improvements in computer hardware and innovations in formulations and algorithms, leading to "virtual experiments" becoming a more and more cost-effective and reliable way to investigate chemical and physical phenomena. Our contribution in this arena has been the theoretical development of our hybrid Hylleraas-CI (Hy-CI) wave function method to bring sub-chemical accuracy to atomic systems with more than two electrons. This method has been employed over the past few years to explore its utility for both three electron lithium systems and four electron beryllium systems. In the case of lithium, we have computed four excited states of the lithium atom to two orders of magnitude greater precision than has been done before [1].

At the four-electron level, to get truly accurate chemical properties, like familiar chemical electron affinities and ionization energies, it is important to get close to the nanohartree level we achieved for the three-election atom, a significantly more difficult problem for four electrons than for three. By investigating more flexible atomic orbital basis sets and better configuration state function filtering techniques to control expansion lengths, we have been able to successfully tackle the four-electron case. Progress to date has included computing the non-relativistic ground state energy of not only beryllium, but also many members of its isoelectronic sequence to eight significant digit accuracy. With the results from our calculations and a least squares fit of the calculated energies, we have been able to compute the entire beryllium ground state isoelectronic sequence for Z = 4 through Z = 113 [2].

The next step to enabling the calculation not just for the ground singlet S symmetry of the beryllium atom and other members of its isoelectronic sequence, but higher angular momentum states as well, is to complete the process of making the four electron integrals, the real bottleneck at the four and more electron level, as efficient as possible, as well as to modify the codes to be able to compute the energy levels of the Be atom for states of spin, angular momentum and N quantum number different than the ground state. The first part of this code revision has been completed and a paper on the math and computational science issues involved in doing Hy-CI four electron integrals has been published [3].

Progress this past year has been to calculate the first excited Be 3 S state 20 nanohartrees better than the previous best result for this state. Armed with this result, it should be possible to improve the higher, more diffuse Rydberg states to something approaching this level of accuracy. Work is in progress to accomplish this for the Be 4 S through 7 S excited states. The first member of the Be isoelectronic ground state sequence, the negative Li- ion, is also a four-electron system in which correlation plays a very important part in the binding. However, due to the reduced nuclear charge, it is a more diffuse system in which one of its outer two L shell electrons moves at a greater distance from the nucleus than the other and hence its nodal structure is different from that of a coupled L shell identical pair of electrons. We have also undertaken a study of this system and have proeduced results better than all previous calculations but one (we are within 50 nanohartrees of that result). Current plans are to finish the Li- calculation to the point of publishing, modify our parallel quadruple precision generalized eigenvalue problem solver to include pivoting, and then complete the calculation of the Be 4 S through 7 S excited states.

[1] J. S. Sims and S. A. Hagstrom, Hy-CI Study of the 2 Doublet S Ground State of Neutral Lithium and the First Five Excited Doublet S States, *Physical Review A* **80** (2009), 052507.

[2] J. S. Sims and S. A. Hagstrom, Hylleraas-Configuration-Interaction Nonrelativistic Energies for the Singlet S Ground States of the Beryllium Isoelectronic Series Up Through Z = 113, *Journal of Chemical Physics* **140** (2014), 224312.

[3] J. S. Sims and S. A. Hagstrom, Mathematical and Computational Science Issues in High Precision Hylleraas-Configuration Interaction Variational Calculations: III. Four-electron Integrals, *Journal of Physics B: Atomic Molecular and Optical Physics* **48** (2015), 175003.

WebVR Graphics

Sandy Ressler
Eric Dougherty (SURF student)

Graphics presented in web pages has become enhanced with the arrival and support of WebGL, a web based version of the time-tested GL specification. Simply put, if you go to a page with WebGL 3D graphics it will be displayed correctly in your web browser without the need of any browser plug-ins. This means that complex 3D graphics can be placed into web pages and the rich capabilities of these graphics can be used directly within a web page.

WebVR is virtual reality (VR) displayed in a web page. Scientific 3D content formerly displayed via VR with expensive hardware can often be displayed using WebVR directly in a web browser using inexpensive hardware. Nearly everyone has access to a web browser. As web browsers become more capable we can place interactive 3D content inside of web pages and use these web pages with immersive hardware (head mounted displays). NIST as a public institution is well served to utilize 3D WebVR content to present content viewable by as much of the public as possible.

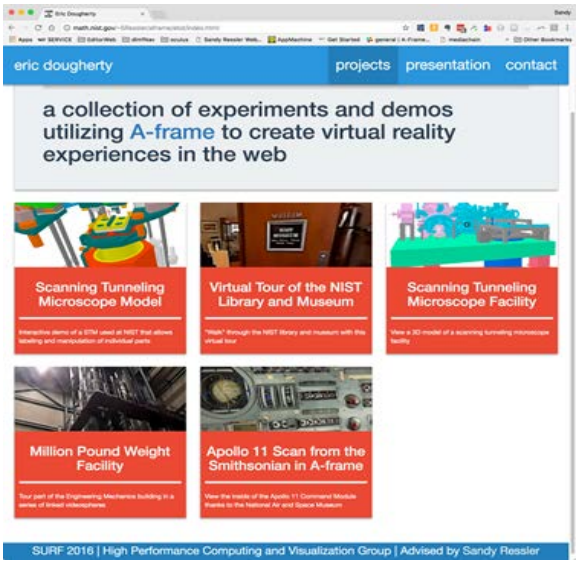

Figure 57. *WebVR Content Home Page.*

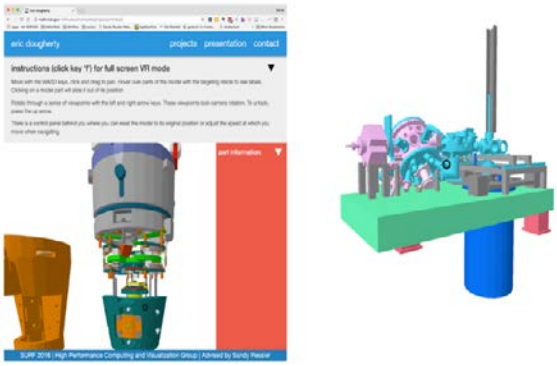

Figure 58. *Scanning Tunneling Microscope Head (left) microscope facility (right).*

We will illustrate four types of WebVR content we are developing. These are 1) pure geometric computer graphics, 2) pure image based video, 3) hybrid computer graphics with image based video, and 4) pure computer graphics from image based (CAVE content) video.

Pure Geometric Computer Graphics. This type of WebVR content is good for demonstrations of lab equipment and facilities, for example. A scanning tunneling microscope and the facility in which it is housed is illustrated in Figure 58. These computer graphics are also displayed using true stereo when viewed with a head-mounted display.

Figure 59. *Descriptive 3D text in 360-degree video.*

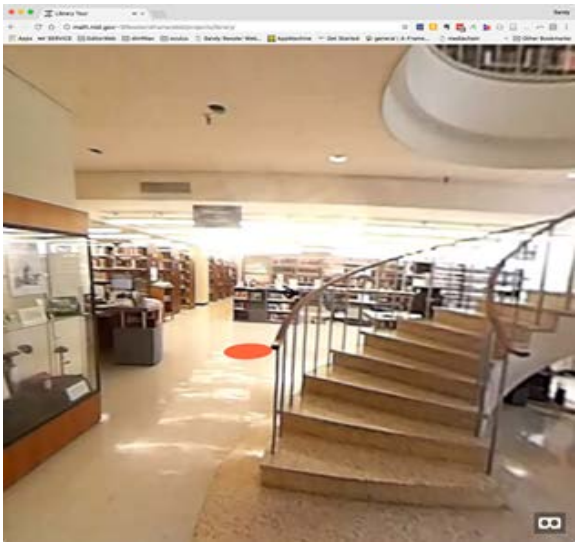

Figure 60. *Virtual tour of NIST Library.*

Pure Image Based Video. This type of content is ideal for creating so called "virtual lab tours." We shoot a series of video spheres using any of the many available 180 degree or 360 degree cameras. If necessary, the images are stitched together to produce a complete sphere. The spherical video is projected onto the flat screen of the display, either a desktop window, or inside of a head mounted display (HMD). Note that we are currently only shooting and displaying mono, not stereo views of video. When displayed in an HMD the same image is displayed to both eyes. Stereo video requires additional equipment and processing and we expect to accomplish that in subsequent versions of this content production process.

Hybrid video with graphics. Hybrid video is simply the same "pure" 360-degree video images with the addition of 3D textual and interactive elements. Currently we have a small tour of a few locations in the NIST Engineering Mechanics Building. One location is standing in front of the million-pound weight facility. There are computer graphic labels that pop on when in the correct view. We also have a tour of the NIST Library. Here the interactive elements, which are circles on the floor, allow the user to move from one 360 video sphere to another. These are crude initial experiments with interactivity, which will be made more visually satisfying in future versions.

We are just at the beginning of devising a well-defined process for creating virtual lab tours. We anticipate working with staff of the NIST library to make this type of capability to all of NIST staff. There are many locations at NIST (and many other institutions) that would be useful to show the public, but for scientific or security reasons actual visits are problematic. For example, walking through a clean-room is not possible due to contamination. Commercial software exists for certain domains, such as real-estate, that allows visitors to take part in virtual tours. Our requirements however go further than existing software capabilities allow, and our desire to host publically available sites inside of web browsers also motivate our software development. Image-based VR using 360 degree videos which can offer video-based demonstrations combined with computer graphic overlays will allow for richer possibilities.

This can be extended much further by, for example, placing a computer graphic representation of a facility within the context of a video environment. We could virtually place electron microscope equipment on the floor of the Engineering Mechanics Building. These types of arrangements could be useful for learning environments and to illustrate complex pieces of equipment in the context of their environments.

Image based computer graphics (from the CAVE). We have a CAVE facility to enable interaction with scientific data in an immersive environment. The CAVE is a room sized facility that projects stereo imagery which one views with stereo glasses. There are times, however, when we would like to illustrate the graphics possible in the CAVE in a more portable manner. We can export the images displayed on the walls of the cave into a 360-stereo video that can be viewed with portable HMDs using WebVR. This CAVE and 360 video integration is the subject of another project.

Our goal is to create a production path, along with the necessary tools, to allow people to author 360-degree image based environments with interactive features. Given appropriately authored "hot-spots" users will be able to obtain additional information about objects in the scene, all within a web page. The end user will simply go to a URL and (while wearing appropriate VR headset) look around the environment selecting points of interest. For example, the environment of a clean room for semiconductor manufacturing, (a place with restricted access) can be explored with the user clicking

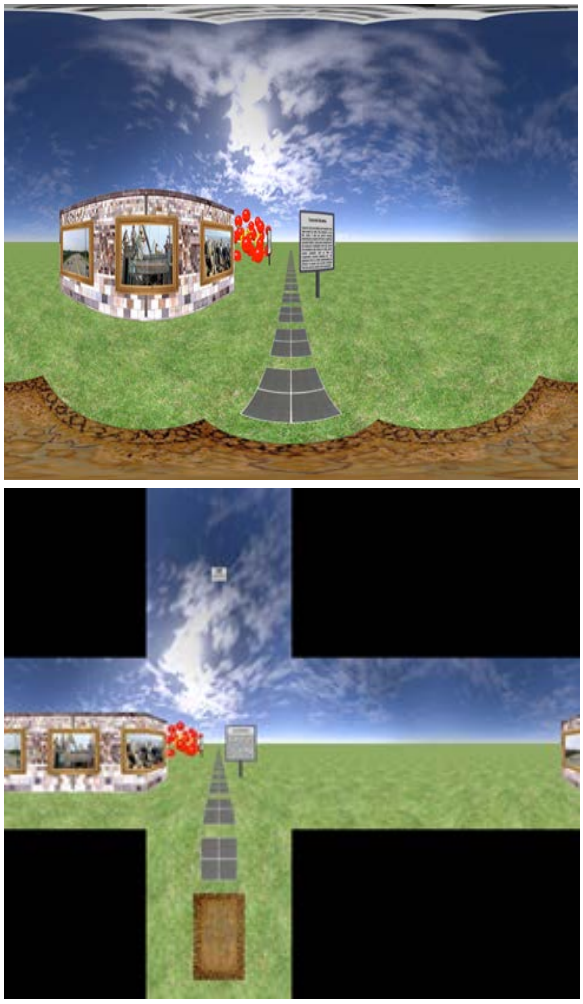

Figure 61. *Imagery from CAVE mapped to 360-degree video.*

on pieces of equipment getting additional information. WebVR is a powerful tool for the distribution of 3D scientific information and for visualizing real world environments.

[1] S. Ressler, "WebVR: Virtual Reality On the Web," Visualization, Big Data, Art + Science 2016," QUT, Brisbane Australia, February 18, 2016. http://slides.com/sressler/visartsci2016 - /

Texture Compression Evaluation and Optimization

Wesley Griffin
Marc Olano

http://www.nist.gov/itl/math/texture_compression

Texture compression is widely used in real-time rendering to reduce storage and bandwidth requirements. Hardware-based texture compression has not fundamentally changed since its introduction in 1999. Recently, however, interest has grown in improving hardware-based texture compression.

Our research has explored new techniques for reducing the number of bits that need to be stored or transmitted for current fixed bit rate algorithms, as well as new variable bit rate algorithms that can be efficiently decoded in graphics hardware. This work benefits the rendering and visualization communities by providing a methodology for evaluating and optimizing texture compression. It also can be directly applied to existing applications to improve the quality of compressed textures.

In evaluating texture compression, the most common approach is to use some combination of the mean square error (MSE), peak signal-to-noise ratio (PSNR), or visual image inspection of the compressed texture. Last year we introduced a new evaluation methodology that accounts for the two ways in which textures are used in rendering for which the MSE and PSNR measures cannot account. Our evaluation approach combines final image rendering with objective image comparison metrics.

This year we published our results in the form of Wesley Griffin's Ph.D. dissertation [1]. These results include a new database of images with chrominance-only distortions and the associated subjective image quality ratings [2]. The results also recommend using final rendered images to evaluate texture compression artifacts and also show a proof-of-concept framework for guiding texture compression based on the new evaluation methodology.

[1] W. Griffin, *Quality Guided Variable Bit Rate Texture Compression*, Ph.D. Dissertation, University of Maryland, Baltimore County, (2016).

[2] https://bitbucket.org/wgriffin/cdid

Quantum Information

An emerging discipline at the intersection of physics and computer science, quantum information science is likely to revolutionize science and technology in the same way that lasers, electronics, and computers did in the 20th century. By encoding information into quantum states of matter, one can, in theory, exploit the seemingly strange behavior of quantum systems to enable phenomenal increases in information storage and processing capability, as well as communication channels with high levels of security. Although many of the necessary physical manipulations of quantum states have been demonstrated experimentally, scaling these up to enable fully capable quantum computers remains a grand challenge. We engage in (a) theoretical studies to understand the power of quantum computing, (b) collaborative efforts with the multi-laboratory experimental quantum science program at NIST to characterize and benchmark specific physical implementations of quantum information processing, and (c) the demonstration and assessment of technologies for quantum communication.

Quantum Information Science

Scott Glancy
Emanuel Knill
Peter Bierhorst (University of Colorado)
Adam Keith (University of Colorado)
Karl Mayer (University of Colorado)
Jim van Meter (University of Colorado)
Kevin Coakley (NIST ITL)
Sae Woo Nam (NIST PL)
Dietrich Leibfried (NIST PL)
David Wineland (NIST PL)
David Pappas (NIST PL)
Cindy Regal (JILA and University of Colorado)
Ana Maria Rey (JILA and University of Colorado)
Konrad Lehnert (JILA and University of Colorado)
Gerardo Ortiz (Indiana University)
Yanbao Zhang (University of Waterloo, Canada)
Carlton Caves (University of New Mexico)

Recent years have seen rapid progress in the development of quantum technologies suitable for quantum information processing, with multiple qubits being readily available in ion traps, atom traps, superconducting qubits and photonics. For communication, several systems have demonstrated entanglement over distances from meters to kilometers. ACMD researchers are collaborating with experimental groups to characterize and take advantage of available quantum information processing systems, and investigating how this growing technology can contribute to future advances in quantum measurement science. To that end, they propose benchmark experiments, assist with their implementation and analysis, and determine the ultimate limits to quantum measurement precision at the statistical and fundamental levels.

In several systems, the types of quantum control that are available without complications are restricted. For example, in ion traps, it is often easiest to apply equal rotations to every qubit and enact couplings that are symmetric under permutation of the qubits. One of the most useful quantum circuit elements (gate) is the controlled-controlled-not. A variant of this element, the controlled-controlled-signflip (CCS) is symmetric under permutations and is in principle implementable with the mentioned restricted operations. We investigated the minimum number of symmetric coupling steps, interleaved with rotations, required to implement it. By a numerical search, a solution with six such couplings was found. ACMD researchers are now investigating whether this is optimal. A promising approach involves the use of Gröbner basis to show that fewer couplings do not suffice.

NIST ion quantum information technology has advanced tremendously, with gates between identical and different ions now having high fidelity. Soon it will be possible to routinely manipulate three or more ions. With this in mind, ACMD researchers are proposing to demonstrate the advantages of the three-qubit noiseless subsystem. This is a subsystem that is immune to noise acting equally on three ions. It is the smallest non-trivial error-protecting system. It also allows for protected encoded operations without decoding. The first experiment will establish the fidelity of stored information after long storage times. The second will use benchmarking techniques to establish the fidelity of universal control. It was established that the latter requires a special choice of multi-species ion “crystal” and careful design of a sequence of pulses with nested couplings. Whether these crystals are sufficiently controllable is being investigated experimentally in the PML Ion Storage Group.

Looking forward, ACMD researchers are considering the application of quantum measurement methods to determine properties of space-time such as the amplitude of gravitational waves. As a first step, they participated in work that uses the locally covariant formalism for quantum fields on space-time to establish parameter uncertainty principles for the properties of interest [1]. The formalism was applied to the problem of determining the sensitivity of interferometers such as LIGO to changes in proper distance, with results agreeing with the shot noise limit if coherent light is used.

Extensions to using so-called squeezed light give the expected improvements.

An interesting question is whether it is possible to harvest entanglement from the vacuum of free quantum fields. Many papers suggest that this is possible; see for example [2]. These harvesting methods generally require special detectors sensitive to particular modes of the quantum field. One way to confirm the needed entanglement is to use homodyne detection methods from quantum optics. ACMD researchers are investigating whether such methods can be adapted to verify the presence of entanglement with realistic devices.

A key feature of the relevant modes is that they are extremely broad band. Since NIST has world-leading high-efficiency calorimetric photon detectors based on transition edge sensors, ACMD researchers generalized the standard theory of homodyne detection to the problem of broad-band detection with calorimeters. Whether NIST detectors can be used to demonstrate this technique is under investigation.

[1] T. G. Downes, J. R. van Meter, E. Knill, G. J. Milburn and C. M. Caves, Quantum Estimation of Parameters of Classical Spacetimes, arXiv:1611.05449 (2016).

[2] T. Ralph and N. Walk, Quantum Key Distribution Without Sending a Quantum Signal, arXiv:1409.2061 (2014).

Quantum Estimation Theory and Applications

Charles Baldwin
Peter Bierhorst (University of Colorado)
Scott Glancy
Adam Keith (University of Colorado)
Emanuel Knill
Karl Mayer (University of Colorado)
Kevin Coakley (NIST ITL)
Ryan Bowler (NIST PML)
John Gaebler (NIST PML)
Dietrich Leibfried (NIST PML)
Yiheng Lin (NIST PML)
Konrad Lehnert (JILA)
Adam Reed (JILA)
Ting Rei Tan (NIST PML)
John Teufel (NIST PML)
Yong Wan (NIST PML)
David Wineland (NIST PML)
L. Burkhart (Yale University)
W. Pfaff (Yale University)
M. Reagor (Yale University)
F. Reiter (University of Copenhagen)
R. J. Schoelkopf (Yale University)
A. S. Sørensen (University of Copenhagen)

Many emerging technologies will exploit quantum mechanical effects to enhance metrology, computation, and communication. Developing these technologies requires improved methods to measure the states of quantum systems. Quantum estimation is a statistical problem of estimating an underlying quantum state, measurement, or process by using a collection of measurements made on independently prepared copies of the state or applications of the measurement or process. Accurate quantum estimation allows experimentalists to answer the question "What is happening in my quantum experiment?" and to characterize uncertainty in that answer.

NIST's Ion Storage Group has pioneered one of the world's most successful quantum computer development projects. To keep pace with their recent advances in qubit preparation, logical operation, and measurement fidelities, ACMD researchers have developed more advanced statistical techniques to characterize the trapped ion quantum computers. In collaboration with the Ion Storage Group, ACMD researchers developed tools to estimate properties of quantum states for experiments with extremely high fidelity. These tools include a single procedure for both calibrating measurements (using data from qubits with known states) and estimating the quantum state (of qubits in an unknown state) [1]. Because both the measurements and the unknown state are estimated together, uncertainty is reduced and higher fidelity states can be analyzed reliably. These algorithms were used to analyze data from two new trapped ion experiment, one of which demonstrated a novel method for preparing an entangled state [2] and the other reporting an entangling logic gate error of only 8×10^{-4} [3]. See Figure 62.

In many quantum experiments, the state can be only partially inferred from the available measurements. However, the available measurements may be able to place useful bounds on parameters of interest, even if they cannot be inferred exactly. Tools for finding these bounds in particular cases have been present in the literature, but they have usually used ad-hoc techniques tailored for particular experiments. ACMD researchers have developed a framework based on semi-definite programming for finding bounds on linear parameters from any data set [1]. These tools for measurement and state estimation and bounding parameters using incomplete measurements have been implemented in software that is now used routinely in the Ion Storage Group.

ACMD researchers are also helping to analyze experiments involving superconducting qubits. One such experiment at JILA involves transferring quantum information originally stored in a superconducting qubit into a mechanical oscillator and then into a traveling microwave photon [4]. The mechanical oscillator acts as both a short-term memory and an amplifier. ACMD researchers estimated that fidelity of the transfer process is 83^{+3}_{-6} %. Characterizing the fidelity of the last transfer required maximum likelihood methods previously used for tomography of optical modes.

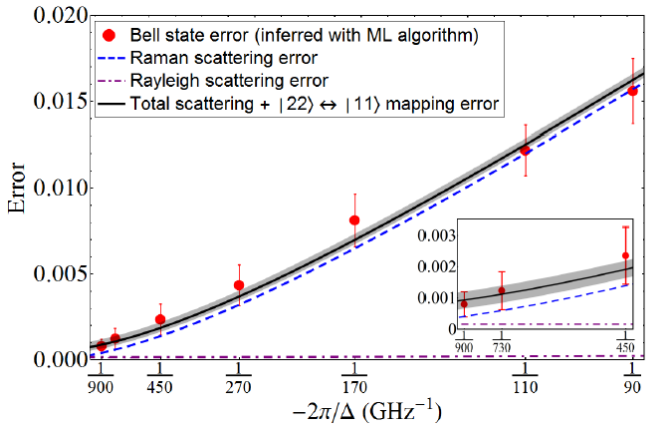

Figure 62. *Error in the preparation of an entangled Bell state as a function of control laser detuning from [3]. The measured states' error, inferred from ACMD's maximum likelihood alogirthm, (red dots) closely matches the physical model of the dominant error sources. Error bars for the measured Bell state fidelity are determined from parametric bootstrap resampling of the data and represent a 1σ statistical confidence interval.*

These statistical tools developed by the ACMD can improve the characterization of a wide range of quantum information experiments in different physical systems, such as trapped ions, neutral atoms, photons, superconducting qubits. In the next year ACMD researchers plan to prepare the software for public release.

[1] A. C. Keith, C. H. Baldwin, S. Glancy and E. Knill, Partial Quantum Tomography Using Maximum Likelihood Estimation, in preparation.

[2] Y. Lin, J. P. Gaebler, F. Reiter, T. R. Tan, R. Bowler, Y. Wan, A. Keith, E. Knill, S. Glancy, K. Coakley, A. S. Sørensen, D. Leibfried and D. J. Wineland, Preparation of Entangled States by Hilbert Space Engineering, *Physical Review Letters* **117** (2016), 140502.

[3] J. P. Gaebler, T. R. Tan, Y. Lin, Y. Wan, R. Bowler, A. C. Keith, S. Glancy, K. Coakley, E. Knill, D. Leibfried and D. J. Wineland, High-Fidelity Universal Gate Set for 9Be+ Ion Qubits, *Physical Review Letters* **117** (2016), 060505.

[4] A. P. Reed, K. H. Mayer, J. D. Teufel, M. Reagor, L. Burkhart, W. Pfa, R. J. Schoelkopf and K. W. Lehnert, Faithful Conversion of Propagating Quantum Bits to Mechanical Motion, in review.

Phase Retrieval and Quantum Tomography

Yi-Kai Liu
Shelby Kimmel (University of Maryland)
Felix Krahmer (Technical University of Munich)

Phase retrieval is the task of learning an unknown n-dimensional vector $\boldsymbol{x}$ from measurements of the form

$$y_i = |\langle a_i, x\rangle|^2 \quad i = 1, 2, \ldots, m,$$

where the vectors a_i are chosen by the observer. Such measurements arise in a variety of applications, including optical imaging (where one measures the intensity of the light field, but not the phase), and quantum tomography (where one measures the probability, but not the complex amplitude, of the wave function).

We have studied the performance of PhaseLift, a well-known algorithm for phase retrieval that is based on convex relaxation, using different kinds of structured measurements, i.e., different choices for the vectors a_i. In particular, we studied two kinds of measurements: so-called Bernoulli random vectors sampled from the hypercube $\{1, -1\}^n$, and random vectors sampled from spherical and unitary 2-designs.

In both cases, there exist vectors x that cannot be recovered uniquely, given these measurements. However, we showed that these failures are rare, and there exist large classes of vectors that can be recovered successfully using PhaseLift [1, 2].

Measurements using spherical and unitary 2-designs are of interest for quantum tomography, as they can be implemented easily in many experimental setups by using stabilizer states and Clifford operations. Using this connection, we showed a method for quantum process tomography that combines ideas from randomized benchmarking and compressed sensing [2]. This method is robust to state preparation and measurement errors, and it is quadratically faster than conventional tomography for processes that are generic (Haar-random) unitaries. We are currently trying to give a more precise theoretical analysis of this method, by making use of recent results that show that random stabilizer states and Clifford operations are "almost" 4-designs.

Finally, in collaboration with the superconducting qubits group at Yale, we investigated the optimal design of tomographic measurements for continuous-variable quantum systems using photon-number-resolving detectors [3].

[1] F. Krahmer and Y.-K. Liu, Phase Retrieval Without Small-Ball Probability Assumptions, arXiv:1604.07281, April 2016.

[2] S. Kimmel and Y.-K. Liu, Quantum Compressed Sensing Using 2-Designs, arXiv:1510.08887, October 2015.

[3] C. Shen, R. W. Heeres, P. Reinhold, L. Jiang, Y.-K. Liu, R. J. Schoelkopf and L. Jiang, Optimized Tomography of Continuous Variable Systems Using Excitation Counting, *Physical Review A* **94**, 052327.

Device Independently Secure Randomness from Loophole-Free Bell Tests

Peter Bierhorst (University of Colorado)
Scott Glancy
Stephen Jordan
Emanuel Knill
Paulina Kuo
Yi-Kai Liu
Alan Mink (Theiss Research)
Xiao Tang
Michael S. Allman (NIST PML)
Lawrence Bassham (NIST ITL)
Joshua C. Bienfang (NIST PML)
Harold Booth (NIST ITL)
Kevin J. Coakley (NIST ITL)
Shellee D. Dyer (NIST PML)
Thomas Gerrits (NIST PML)
Michaela Iorga (NIST ITL)
John Kelsey (NIST ITL)
Dietrich Leibfried (NIST PML)
Yiheng Lin (NIST PML)
Adriana E. Lita (NIST PML)
Alan L. Migdall (NIST PML)
Richard P. Mirin (NIST PML)
Murugiah Souppaya (NIST ITL)
Sae Woo Nam (NIST PML)
René Peralta (NIST ITL)
Andrew Rukhin (NIST ITL)
Lynden K. Shalm (NIST PML)
Martin J. Stevens (NIST PML)
Ting Rei Tan (NIST PML)
Varun B. Verma (NIST PML)
Yong Wan (NIST PML)
Michael A. Wayne (NIST PML)
David Wineland (NIST PML)
Bradley G. Christensen (University of Illinois)
Yanbao Zhang (University of Waterloo, Canada)

Before the invention of quantum theory, theories of physics obeyed the principle of local realism. In theories that obey realism, all possible measurement results are determined and fixed before the measurement occurs, though that result might be random and hidden. In local realistic theories, the hidden measurement results cannot be communicated between entities faster than the speed of light. The principle of local realism constrains the probability distributions that can be produced by local realistic systems. In 1964, John S. Bell described those constraints with a system of inequalities involving probabilities of measurement outcomes. Bell also showed that quantum physics can violate local realism. Last year, ACMD researchers participated in a NIST-led team that achieved a loophole-free test of local realism [1], demonstrating that local realism is violated with strong statistical significance.

In 2006 it was discovered that tests of local realism could be used to generate random bits for cryptographic applications in a device-independently secure manner [2]. This means that, given a secure random seed, trust in the unpredictability of the secure string of bits can be derived solely from the outcomes of the Bell experiment, without needing to trust the internal workings of the hardware, even under the most pessimistic assumption that the hardware was provided by an untrustworthy adversary.

This year ACMD researchers used the data from the loophole-free Bell test to produce such a string of uniformly random bits. Production happens in two steps: (1) entropy estimation and (2) randomness extraction. During entropy estimation, one quantifies the amount of secure randomness available in the data from the test of local realism. ACMD researchers developed a new entropy estimation algorithm that, unlike previous algorithms, is sensitive to the low level of randomness per trial that was present in the experiment. During randomness extraction, one converts the data from the test of local realism, which is highly biased and whose distribution drifts in time, into a string of uniformly distributed random bits. ACMD researchers customized an implementation of the Trevisan extractor [3] and used it to extract the bits. The extractor customization includes a streaming feature that provides continuous operation, which will be required by applications like the NIST Randomness Beacon [4]. These tools allowed ACMD researchers to extract 256 random bits that are uniform to within 0.001 and cannot be predicted within any physical theory that allows one to make independent measurement choices and limits all signals to travel no faster than the speed of light.

A long-term goal for this project is integration of the test of local realism with the NIST Randomness Beacon, a cryptographic service being run by the Computer Security Division. The NIST Randomness Beacon provides a public source of cryptographically signed random bits currently produced by conventional hardware random bit generators. Current work at NIST includes engineering to develop the technology used in the test of local realism into a reliable device that can be operated continuously for long periods without human oversight. Such a device could be integrated as an entropy source for the NIST Randomness Beacon. ACMD researchers are improving algorithms to reduce the amount of seed randomness required for randomness generation and to make the algorithms adaptive in order to extract greater randomness in spite of changing experimental conditions.

Integrating the test of local realism with the NIST Randomness Beacon will provide greater assurance both to NIST and the public that the output of the Beacon is

truly unpredictable, which will increase its utility for applications such as unpredictable sampling, new authentication mechanisms, and secure multi-party computation.

Last year's photonic loophole-free test of local realism demonstrated violation of local realism, but it was not designed to quantify the amount of violation. This year, ACMD researchers collaborated with NIST's Ion Storage Group to perform an experiment to quantify the violation of local realism with trapped ions [5]. One can model a series of measurements on entangled particles as if they were produced by a system that, during each measurement, obeys local realism with probability P_{local} or maximally violates local realism with probability $1 - P_{\text{local}}$. Smaller values of P_{local} indicate greater departure from local realism. The trapped ion experiment used a chained Bell inequality (a generalization of the usual Bell inequality) to show $P_{\text{local}} \leq 0.327$ at the 95 % confidence level, which is the lowest value yet demonstrated for any deterministically prepared entangled state. ACMD researchers developed the statistical protocol for bounding P_{local} without making assumptions that previous protocols have required. In addition to its relevance to fundamental physics, this experiment demonstrated many essential components of a quantum computer in a single system, so these results can be regarded as a useful benchmark towards the goal of a general-purpose quantum computer.

[1] L. K. Shalm, E. Meyer-Scott, B. G. Christensen, P. Bierhorst, M. A. Wayne, M. J. Stevens, T. Gerrits, S. Glancy, D. R. Hamel, M. S. Allman, K. J. Coakley, S. D. Dyer, C. Hodge, A. E. Lita, V. B. Verma, C. Lambrocco, E. Tortorici, A. L. Migdall, Y. Zhang, D. R. Kumor, W. H. Farr, F. Marsili, M. D. Shaw, J. A. Stern, C. Abellán, W. Amaya, V. Pruneri, T. Jennewein, M. W. Mitchell, P. G. Kwiat, J. C. Bienfang, R. P. Mirin, E. Knill and S. W. Nam, A Strong Loophole-Free Test of Local Realism, *Physical Review Letters* **115** (2015), 250402.

[2] R. Colbeck, *Quantum and Relativistic Protocols for Secure Multiparty Computation*, Ph.D. Thesis, University of Cambridge (2006), arXiv:0911.3814.

[3] L. Trevisan, Extractors and Pseudorandom Generators, *Journal of the ACM* **48** (2001), 860.

[4] NIST Randomness Beacon, https://www.nist.gov/programs-projects/nist-randomness-beacon.

[5] T. R. Tan, Y. Wan, S. Erickson, P. Bierhorst, D. Kienzler, S. Glancy, E. Knill, D. Leibfried, and D. J. Wineland, Chained Bell Inequality Experiment with High-Efficiency Measurements, arXiv:1612.01618, in review.

Computational Complexity of Quantum Field Theory

Stephen Jordan
Keith Lee (University of Toronto)
John Preskill (Caltech)
Hari Krovi (Raytheon/BBN)
Ali Moosavian (University of Maryland)
Troy Sewell (University of Maryland)

Quantum field theory is central to both high energy physics and condensed-matter physics. In particular, the Standard Model of particle physics, which describes all known forces other than gravity, is a quantum field theory. In many circumstances, particularly when the interactions between particles are strong, quantum field theories are intractable to simulate even on the most powerful supercomputers. In this project, we seek to find out whether quantum computers will be able to simulate quantum field theories using exponentially fewer computational steps and (qu)bits of memory than are required by classical computers. Our results so far suggest that quantum computers do provide such an advantage. Specifically, in 2013 and 2014 we published polynomial-time quantum algorithms to solve certain quantum field theory simulation problems which do not have any known classical polynomial-time algorithms.

Our recent and ongoing work builds upon these earlier results in several ways. Currently, this research program has three primary thrusts:

1. Improve upon our earlier quantum simulation algorithms both by increasing their efficiency and extending their applicability to a broader class of quantum field theory simulation problems.

The most problematic step in quantum algorithms for simulating quantum field theories is state preparation. That is, at the beginning of the simulation, a model of the vacuum state in the quantum field theory with a small number of well-characterized particles must be constructed and stored in the quantum computer's memory. At present, this step is the slowest part of the quantum algorithm, which therefore determines the scaling of the runtime as a function of the parameters of the problem, such as energy scale and precision. Furthermore, the state preparation methods in our quantum algorithms from 2013 and 2014 can only prepare the initial state for quantum field theories that are in the same quantum phase as a non-interacting quantum field theory. Presently, we are working on alternative quantum algorithms for state preparation which should be applicable to a wider variety of quantum phases, and which may also be faster.

2. Amass formal complexity-theoretic evidence about the intrinsic computational difficulty of quantum field theory simulation problems.

Currently, no classical algorithm is known to compute scattering probabilities in a quantum field theory in polynomial time. But how do we know that one won't be discovered in the future? Unconditionally proving the non-existence of any polynomial time algorithm for a given computational problem is generally beyond the reach of present-day mathematical techniques. However, in the field of computational complexity, there are now standard methods for obtaining evidence of intractability. Specifically, if a large class of problems thought to be intractable are all reducible to instances of a given problem, then this constitutes evidence that the given problem is genuinely hard. Along these lines, we are currently in the process of completing a reduction of the problem of simulating an arbitrary quantum circuit to the problem of approximating a certain scattering probability in a quantum field theory. Such a reduction would show that classical computers cannot efficiently approximate these scattering probabilities unless they can also efficiently simulate all quantum computation, which is generally considered very unlikely.

3. Investigate what high energy physics has to say about the ultimate limits to computational power.

The foundational question in computational complexity theory asks what are the ultimate capabilities and limitations of computers. Prior to the 1980s it was widely believed that the class of problems in-principle solvable with polynomial resources in our universe is equal to P, defined as the set of problems solvable in polynomially many steps on a Turing machine. However, the discovery of quantum computing changed this, and led to a new conjecture that the class of problems in-principle solvable with polynomial resources in our universe is BQP, defined as the set of problems solvable by quantum circuits of polynomially many elementary gates. Polynomial-time quantum algorithms have been developed to simulate essentially all non-relativistic quantum systems. Thus, it is unlikely that any low energy physical system could pose a challenge to this conjecture. But what about high energy physics? Our quantum algorithms for simulating quantum field theory suggest that even special relativity does not fundamentally increase the power of quantum computation. Thus, the main remaining question is whether general relativity, i.e., gravity, affects computational power.

A complete quantum theory of gravity is not known. However, by extrapolating well-understood physics it is possible to make some nontrivial predictions about quantum gravitational systems, in particular, that black holes should gradually evaporate through the emission of Hawking radiation. Several competing proposals have been made regarding the general features that a complete quantum description of black hole evaporation may be expected to have. Several these proposals involve modifications to the axioms of quantum mechanics. In recent work [1], we have found that some of these models, in certain parameter regimes, imply computational power well beyond that of standard quantum computation (BQP). However, in each case, we found that in the parameter regime in which computational power extends beyond BQP, the proposals also imply the ability to transmit information instantaneously across arbitrary distances, in conflict with the principle of causality. We conclude that it is unlikely that the dynamics of black holes can be used to solve problems exponentially faster than standard quantum computers, and that limitations on computational power may be derivable directly from foundational principles such as causality rather than depending upon the full details of quantum dynamics.

Instead of developing sophisticated quantum algorithms to solve problems with fewer computational steps than are needed classically, there is also a much simpler way to speed up computation: simply run the computer at extremely high clock speed. What are the ultimate limits to this? Several papers have argued that the energy-time uncertainty principle of quantum mechanics fundamentally limits the clock speed of classical and quantum computers. Essentially, the argument states that for a system with energy uncertainty less than ΔE, the uncertainty in the timing of each computational step must be greater than $h\Delta E$ where h is Planck's constant. If the time between logical operations is shorter than $h\Delta E$ then these uncertainties overlap and the ordering of operations becomes uncertain, thereby spoiling the computation. In [2] we show that these arguments, though plausible and widely repeated, do not represent a genuine limit to computational clock speed. We exhibit an explicit architecture that can in principle maintain constant computational clock speed for either classical or quantum computation as both absolute energy E and energy uncertainty ΔE are taken to zero. We conclude that energy alone does not impose a limit on computational speed, and to obtain such a limit one must consider more detailed geometrical constraints such as the time needed for signals to propagate between memory elements.

[1] A. Bouland, N. Bao and S. Jordan. Grover Search and the No-signaling Principle, *Physical Review Letters* **117** (2016), 120501.

[2] S. Jordan. Fast Quantum Computation at Arbitrarily Low Energy, to appear.

Quantum and Stochastic Optimization Algorithms

Stephen Jordan
Alan Mink (Theiss Research)
Aniruddha Bapat (University of Maryland)
Jake Bringewatt (University of Maryland)
Bill Dorland (University of Maryland)
Michael Jarret (Perimeter Institute)
Brad Lackey (University of Maryland)

Discrete optimization is one of the most widely applicable and heavily researched problems in computer science. Many discrete optimization problems are NP-hard. Therefore, it is expected that neither classical nor quantum computers can find exact solutions to worst case instances of these problems in polynomial time. Nevertheless, much current research focuses on developing classical and quantum algorithms to rapidly find exact or approximate solutions to discrete optimization problems in various special cases.

In 2000 Farhi et al. proposed a method for solving discrete optimization problems called quantum adiabatic optimization. Since then adiabatic optimization has been a subject of intense theoretical and experimental research. A company called D-wave is working to commercialize the technology. However, most adiabatic optimization uses quantum states that involve only positive amplitudes. In these systems, interference effects are not manifest. This raises a question whether these quantum systems can be efficiently simulated by classical randomized algorithms. If so, this would mean that these positive-amplitude adiabatic quantum computers are incapable of exponential speedup over classical computation.

Path Integral Monte Carlo (PIMC) is one of the most effective and widely used classical randomized algorithms for simulating quantum systems. Conventional wisdom among PIMC practitioners suggests that it should converge efficiently when used to simulate quantum systems without negative amplitudes. However, in 2013 Hastings constructed counterexamples which do not contain any negative amplitudes but for which PIMC simulations provably require exponential time to converge due to topological obstructions.

Aside from PIMC, the other main classical algorithm for simulating quantum systems is diffusion Monte Carlo (DMC). Unlike PIMC, DMC is unaffected by topological obstructions. In recent work [1], we investigated whether DMC can be used to efficiently simulate adiabatic optimization. Despite the absence of both negative amplitudes and topological obstructions, we were able to find counterexamples in which DMC fails to efficiently simulate adiabatic optimization. On the other hand, when we implemented a variant of DMC and tried it on standard benchmarking instances of a discrete optimization problem called MAXSAT, we found that it worked very well. In fact, our DMC simulation of adiabatic optimization turned out to be a powerful MAXSAT solver in its own right, competitive with top discrete optimization software [2]. Presently we are attempting to better understand the performance of DMC, particularly relative to adiabatic optimization.

In 2016, Yang et al. introduced a control-theoretic framework for analyzing quantum adiabatic optimization and other related quantum optimization algorithms. They proved that the fastest optimization is achieved not by varying parameters smoothly in time, as is done in the original adiabatic optimization algorithm of Farhi et al., but rather by switching them according to step functions. (In control theory language this is known as bang-bang control.) In recent work, we have been adapting this framework to the analysis of classical stochastic optimization algorithms such as simulated annealing.

Our results so far show that the bang-bang version of simulated annealing can in some cases exponentially outperform standard quasi-equilibrium simulated annealing. In particular, two example problems have been proposed in which adiabatic optimization provably exponentially outperforms standard quasi-equilibrium simulated annealing. These two problems are called the "Hamming ramp" and the "bush of implications." It is now known that PIMC matches the asymptotic performance of adiabatic optimization for the Hamming ramp. We have discovered that the bang-bang version of simulated annealing, in which the simulated temperature transitions sharply from infinite temperature to zero temperature, solves the bush of implications problem in polynomial time. This eliminates the main remaining known example of exponential speedup by quantum adiabatic optimization.

[1] M. Jarret, S. P. Jordan and B. Lackey, Adiabatic Optimization versus Diffusion Monte Carlo, *Physical Review A* **94** (2016), 042318.

[2] http://brad-lackey.github.io/substochastic-sat/

One-Time Programs Using Isolated Qubits

Yi-Kai Liu

A one-time program is a type of trusted computing hardware that performs a pre-programmed computation exactly once, and then self-destructs. One-time programs can be used to perform actions that should not be repeated, such as spending a set amount of money, or casting a vote in an election. They can also be used to protect mobile devices, such as smartphones or autonomous drones, from being stolen and reverse-engineered by an adversary.

We are continuing to develop constructions for one-time programs based on isolated qubits. These are qubits

that can be accessed individually, but cannot be entangled. Solid-state quantum systems, such as nuclear spins, are one possible approach to the experimental realization of isolated qubits.

On the theoretical side, we are investigating ways of proving that these one-time programs can be composed securely. In particular, we are trying to show that these devices will remain secure when they are accessed sequentially or in parallel, as part of a larger system. We are investigating how techniques involving program obfuscation can be applied here. In addition, we are studying quantum protocols for password-based identification, which might also be achievable in the isolated qubits model.

On the experimental side, we are studying possible implementations of isolated qubits, using solid-state nuclear spins, quantum dots, and trapped ions. While a full-scale implementation of a one-time program would be quite challenging, in the near term it may be possible to do a more limited demonstration. For instance, one may be able to observe a quantum effect called "nonlocality without entanglement," or "quantum data hiding," using a system of 5-10 trapped ions, with individual control of each ion.

Post-Quantum Cryptography

Stephen Jordan
Yi-Kai Liu
Jacob Alperin-Sheriff (NIST ITL)
Larry Bassham (NIST ITL)
Lily Chen (NIST ITL)
Carl Miller (NIST ITL)
Dustin Moody (NIST ITL)
Rene Peralta (NIST ITL)
Ray Perlner (NIST ITL)
Daniel Smith-Tone (NIST ITL)

Public-key cryptosystems are a crucial tool for electronic commerce. They enable the transmission of sensitive information over the Internet by providing functionalities such as digital signatures, encryption, and key exchange. However, many of today's public-key cryptosystems are vulnerable to attack using quantum computers. While large quantum computers have not yet been built, they are believed to be a potential future threat to information security. For this reason, NIST is taking steps to standardize new cryptosystems that are secure against quantum attacks; these are often called *post-quantum cryptosystems*. In addition, NIST is carrying out research on the security and performance of these cryptosystems, and on related topics such as quantum algorithms.

In 2016 we published a short report summarizing the status of post-quantum cryptography [1]. We discussed our plans for standardizing post-quantum cryptosystems at the PQCrypto conference in February [2], and we had a formal public comment period in August and September [3]. Finally, in December we published a formal call for proposals, to be considered for future NIST standards for post-quantum cryptography [4]. Proposals are due in November of 2017, and will be made public to encourage analysis and evaluation by researchers and stakeholders in academia, industry and government.

Developing standards for post-quantum cryptography poses both scientific and practical challenges. The techniques used to design post-quantum public-key cryptosystems are based on high-dimensional lattices, error-correcting codes, and systems of multivariate quadratic equations over finite fields. These topics are the subject of ongoing research. Compared to symmetric cryptography (e.g., block ciphers and hash functions), public-key cryptography is less completely understood. In addition, the security of these cryptosystems against quantum computers has received only a limited amount of theoretical and experimental investigation.

From a practical perspective, post-quantum cryptography is challenging because it involves complex functionalities, such as key exchange, which are tightly integrated into higher-level protocols, such as Transport Layer Security (TLS) and Internet Protocol Security (IPSec). In addition, many of the proposed post-quantum cryptosystems suffer from a performance penalty, compared to current quantum-vulnerable cryptosystems, such as elliptic curve cryptography.

NIST is working on several of these problems. First, in its call for proposals, NIST has identified a set of core requirements for post-quantum cryptosystems, including digital signatures, and various forms of key encapsulation, key exchange and key transport. This was done to focus attention on those functionalities that are the most useful for providing long-term security for commonly used Internet applications. In addition, NIST has proposed a technical approach for measuring the security of these schemes against quantum attacks.

NIST researchers have also published several papers on post-quantum cryptography [5-7], and have continued to track the development of quantum algorithms and quantum cryptography [8, 9]. Finally, NIST has continued to engage with other standards organizations involved in post-quantum cryptography, such as the European Telecommunications Standards Institute (ETSI) [10].

[1] L. Chen, S. Jordan, Y.-K. Liu, D. Moody, R. Peralta, R. Perlner and D. Smith-Tone, *Report on Post-Quantum Cryptography*, NISTIR 8105, April 2016.

[2] D. Moody, "Post-Quantum Cryptography: NIST's Plan for the Future," *International Conference on Post-Quantum Cryptography (PQCrypto)*, Fukuoka, Japan, February 24-26, 2016.

[3] Request for Comments on Post-Quantum Cryptography Requirements and Evaluation Criteria, *Federal Register*, 81 FR 50686, Aug. 2, 2016.

[4] Announcing Request for Nominations for Public-Key Post-Quantum Cryptographic Algorithms, *Federal Register*, 81 FR 92787, Dec. 20, 2016.

[5] D. Moody and R. Perlner, Vulnerabilities of 'McEliece in the World of Escher,' in *Proceedings of PQCrypto 2016*, Fukuoka, Japan, February 2016, 104-117.

[6] R. Cartor, R. Gipson, D. Smith-Tone and J. Vates, On the Differential Security of the HFEv- Signature Primitive, in *Proceedings of PQCrypto 2016*, Fukuoka, Japan, February 2016, 162-181.

[7] R. Perlner and D. Smith-Tone, Security Analysis and Key Modification for ZHFE, in *Proceedings of PQCrypto 2016*, Fukuoka, Japan, February 2016, 197-212.

[8] S. Jordan, Quantum Algorithm Zoo, http://math.nist.gov/quantum/zoo/

[9] Y.-K. Liu, Chair, Steering Committee, International Conference on Quantum Cryptography (QCrypt), Washington, DC, Sept. 12-16, 2016.

[10] L. Chen, "Towards Post-Quantum Cryptography Standardization," 4th ETSI/IQC Workshop on Quantum-Safe Cryptography, Toronto, Canada, Sept. 19-21, 2016.

Quantum Repeater R & D

Lijun Ma
Oliver Slattery
Barry Hershman
Xiao Tang

A July 2016 report by the National Science and Technology Council referred to quantum communications as a key "National Challenges and Opportunity." Quantum repeaters are a vital element in quantum communication and future quantum computing systems. In a quantum key distribution (QKD) system, for example, single photons serve as information carriers but are subject to losses which limit its transmission distance. Quantum repeaters can be used to extend the working distance for point-to-point QKD systems, and can also be used to distribute quantum entanglement states to future quantum computers and form quantum networks. Our current research focuses on the development of the essential elements necessary for practical quantum repeaters including quantum memories, narrow linewidth photon sources and quantum interfaces.

Quantum memory is a key component in the implementation of quantum repeaters for quantum communications and quantum networks. In FY 2015, we demonstrated an electromagnetically-induced transparency (EIT) quantum memory in a warm cesium (Cs) atomic vapor cell. An EIT quantum memory with Cs atomic vapor provides an inexpensive and scalable scheme for quantum repeaters. Preliminary results were reported at the 2015 SPIE conference [1].

In order to provide higher fidelity of the quantum system, we focused our 2016 research on reducing noise for the EIT quantum memory. In our EIT quantum memory system, a high intensity control beam is combined with the single-photon-level signal with only a small frequency difference separating them. While preserving the single-photon-level signal, the residual control beam must be filtered and reduced by more than twelve orders of magnitude (120 dB) to satisfy the noise requirements of the quantum memory system, which is very challenging. To accomplish this, we have developed two types of atomic filters. By combining the atomic filters with a custom designed Fabry Perot etalon filter and a high extinction ratio polarization filter, we successfully reduced the residual control beam by 125 dB, resulting in greatly improved performance. The related results were reported at the 2016 SPIE Conference.

In addition, we were invited to write a topical review article [2] by the editor of the *Journal of Optics*. In this paper, following a brief overview of the main approaches to quantum memory, we provide details of the physical principle and theory of quantum memory based specifically on EIT. We discuss the key technologies for implementing quantum memory based on EIT and review important milestones, from the first experimental demonstration to current applications in quantum information systems. With 190 reference articles, this review provided a broad vision of EIT-based quantum memory to readers in this scientific research field.

Entangled photon pair sources are also essential for a quantum repeater. The frequency of one photon in the pair must be in a telecommunication band for long distance transmission while the frequency and bandwidth of the other photon must be matched to the atomic transition line of atoms (Cs in our case) for quantum memory. Atomic transitions usually occur in the visible or near-visible bands, far away from the telecommunication bands. It is relatively difficult to generate photon pairs with large frequency separation (so called greatly non-degenerate photon pairs). In FY 2015, we demonstrated such a photon pair source [3]. Here, one photon is at 1310 nm (telecommunication wavelength) and the other is at 894.6 nm (matching the Cs atomic D1 line). A narrow linewidth of 28 MHz was achieved, suitable for so-called cold atomic quantum memory. For warm atomic quantum memory based on cesium, a linewidth of a few MHz is more desirable. The linewidth is determined by the quality factor (q-factor) of the cavity or resonator used. The higher the q-factor, the narrower the linewidth will be. In FY 2016, we demonstrated photon pair generation based on Four Wave Mixing (FWM) in

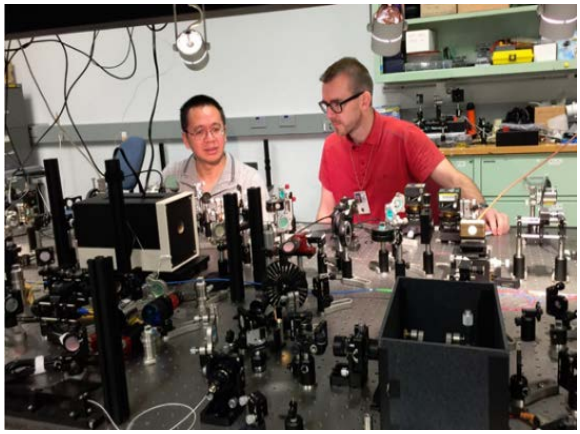

Figure 63. *Oliver Slattery (right) and Lijun Ma were the first authors of the Best Posters awarded at ITL Science Day 2015 and 2016, respectively. The photo shows them as they are performing a quantum memory experiment.*

a micro-toroid device developed at Washington University, St Louis. Since micro-toroid devices are made of silica with a very high optical q-factor and small mode volume, we expect to generate photon pairs with MHz linewidth. Unpackaged micro-toroid devices are very fragile and require near clean-room conditions to avoid dust contamination. To overcome this challenge, we have started to work on a commercial packaged micro-resonator made of calcium fluoride with even higher q-factor. We have obtained initial results and expect to generate some good results in FY 2017.

Photon pairs generated based on four wave mixing are not greatly non-degenerate. In our case, both photons are close to the atomic transition we are targeting. In this case, a quantum interface is needed to convert the frequency of one of the photons to the telecommunication band for long distance transmission. We have been developing frequency conversion technology and applications for many years [4]. Some techniques have been adopted for commercialization through the SBIR programs of NIST and DARPA. In 2017 we will develop a quantum interface to convert the wavelength of single photons from near 895 nm to the telecommunication wavelengths.

[1] L. Ma, O. Slattery, P. Kuo and X. Tang, EIT Quantum Memory with Cs Atomic Vapor for Quantum Communication, Proceedings of SPIE 9615 (2015), 96150D–1.

[2] L. Ma, O. Slattery and X. Tang, Optical Quantum Memory Based on Electromagnetically Induced Transparency, *Journal of Optics*, to appear.

[3] O. Slattery, L. Ma, P. Kuo and X. Tang, Narrow-linewidth Source of Greatly Non-Degenerate Photon Pairs for Quantum Repeaters from a Short Singly Resonant Cavity, *Applied Physics B* **121** (2015), 413-419.

[4] L. Ma, O. Slattery and X. Tang, Single Photon Frequency Up-Conversion and Its Applications, *Physics Reports* **521** (2012), 69-94.

Joint Center for Quantum Information and Computer Science

Dianne P. O'Leary
Stephen Jordan
Yi-Kai Liu
Jacob Taylor (NIST PML)
Carl Williams (NIST PML)
Andrew Childs (University of Maryland)

https://quics.umd.edu/

The Joint Center for Quantum Information and Computer Science (QuICS) is a cooperative venture of NIST and the University of Maryland (UMD) to promote basic research in understanding how quantum systems can be effectively used to store, transport and process information. QuICS brings together researchers from the University of Maryland Institute for Advanced Computer Studies (UMIACS) and the UMD Departments of Physics and Computer Science with NIST's Information Technology and Physical Measurement Laboratories, together with postdocs, students and a host of visiting scientists.

Dianne O'Leary, a Professor of Computer Science at UMD and a long-time faculty appointee in ACMD, served as a founding Co-Director of QuICS until her retirement. Jacob Taylor of the NIST PML, is the current NIST Co-Director, along with Andrew Childs of UMD. Stephen Jordan and Yi-Kai Liu of ACMD are QuICS Fellows.

QuICS has quickly established itself as a substantial research presence in quantum information science, with 13 Fellows, 15 postdocs and 21 students currently associated with the center. In CY 2016 some 60 research papers were completed and 41 seminars were held. 46 visiting scientists spent periods of from one day to one year working at the Center. Carl Miller of the ITL Computer Security Division became the latest QuICS Fellow this year. Miller's research is on security proofs for quantum cryptography, especially in the context of untrusted devices.

This year QuICS hosted the 6th International Conference on Quantum Cryptography (QCrypt), which is the premier annual event on this topic. Held in Washington, DC on September 12-16, 2016, this was the first time that QCrypt was held in the US, and, with more than 250 participants, it was the largest such gathering to date. QuICS Fellow and ACMD researcher Yi-Kai Liu was the lead local organizer of the event and Chair of its International Steering Committee.

Foundations of Measurement Science for Information Systems

Modern information systems are astounding in their complexity. Software applications are built from thousands of interacting components. Computer networks interconnect millions of independently operating nodes. Large-scale networked applications provide the basis for services of national scope, such as financial transactions and power distribution. In spite of our increasing reliance on such systems, our ability to build far outpaces our ability to secure. Protocols controlling the behavior of individual nodes lead to unexpected macroscopic behavior. Local power anomalies propagate in unexpected ways leading to large-scale outages. Computer system vulnerabilities are exploited in viral attacks resulting in widespread loss of data and system availability. The actual resilience of our critical infrastructure is simply unknown. Measurement science has long provided a basis for the understanding and control of physical systems. Such deep understanding and insight is lacking for complex information systems. We seek to develop the mathematical foundations needed for a true measurement science for complex networked information systems.

Quantifying Information Exposure in the Global Internet

Peter Mell (NIST ITL)
Assane Gueye (University of Maryland)
Richard Harang (Army Research Laboratory)
Chris Schanzle

Data sent over the Internet can be manipulated and monitored by the entities that transmit that data from the original source to the final destination. For unencrypted communications (and some encrypted communications with known weaknesses), eavesdropping and man-in-the-middle attacks are possible. For encrypted communication, the identification of the communicating endpoints can still be revealed. In addition, encrypted communications may be stored until such time as newly discovered weaknesses in the encryption algorithm or advances in computer hardware render them readable by attackers.

Every router used to transmit information over the Internet resides within a unique national boundary. These routers are required to operate according to the laws of the nations in which they reside, and are vulnerable to physical interference and attack. In addition, every router is part of an autonomous system (AS), and every AS has a country of registration. ASs are required to follow the laws of their registered country. Certain countries have stronger laws and more rigorous enforcement to guarantee the privacy of the transmitted information. Thus, from a privacy point of view, certain routes through the Internet may be preferable to other routes. In addition, some countries may not trust other countries to safeguard their data in transit.

In this work, we will evaluate both advertised and observed routes through the Internet to measure this form of privacy and to provide statistics to show the degree to which this problem exists. We will also develop the capability to detect non-preferred routes (given user input of a set of legally non-compliant or untrusted countries) and prevent the transmission of data over routes managed by those countries. In addition, we will explore the capability to dynamically reroute traffic through preferred routes without making changes to standard Internet protocols.

To do our analysis, we will use two sets of connectivity data: (1) the public Border Gateway Protocol (BGP) data provided voluntarily by network operators who establish BGP sessions with route collectors that record this data, and (2) the IP level path information gleaned from the Center for Advanced Internet Data Analysis (CAIDA) global network of Ark monitors.

Our study will enable a better understanding of Internet communications with respect to national boundaries. The developed capabilities will be important to any organization with globally distributed satellite offices (or personnel) where an enhancement in communication privacy is desired without resorting to the costs and extremes of using out-of-band communications or the low throughput and high latency of using anonymization systems such as Tor. We expect this to be of especial use for governments (e.g., embassies, classified facilities, and for classified intergovernmental relationships).

We have gathered the two sets of data and have built suitable data structures for exploitation. Analysis of the data is currently under way.

A New Metric for Externalities in Interdependent Security of Complex Systems

Richard J. La (University of Maryland)

Understanding the security of large, complex systems with many interdependent components has emerged as one of key challenges information system engineers face today. Examining the system-level security of complex

networks or systems is hindered by the fact that security measures adopted by various agents or organizations or lack thereof produce either positive or negative network externalities on others, leading to so-called interdependent security (IDS).

Many, if not most, of existing studies on IDS fail to consider the fact that agents can adapt and employ security measures that are best suited for their risks. Our efforts aimed at examining the scenarios where the nodes are strategic entities interested in optimizing their own objectives. The goal of this project is to understand how the underlying network structure and properties affect the choices made by strategic agents and influence the network-level security.

It is well documented that many natural and engineered networks exhibit non-negligible correlations in the degrees of end nodes. Furthermore, these degree correlations (also known as networking mixing or assortativity) have significant impact on the robustness of network and the effectiveness of botnet takedown strategies. In the past year, we investigated how network mixing affects the network-level security with strategic agents.

There are two key findings from our study: First, when nodes with larger degrees see more risks (per neighbor) than those with smaller degrees, the overall network-level security degrades in that the total number of attacks or infections that spread through the network (from nodes to their neighbors) rises. Secondly, the overall effects of assortativity on network security depend very much on the (cost) effectiveness of security measures available to agents/nodes; when the security measures are ineffective in protecting the agents against attacks, increasing assortativity (resp. decreasing assortativity) leads to deteriorating network security (resp. improving network security). On the other hand, when the security measures are effective, assortativity has the opposite effects. In other words, as a network becomes more assortative (resp. disassortative), network security improves (resp. degrades) instead.

[1] R. J. La, Interdependent Security with Strategic Agents and Global Cascades, *IEEE/ACM Transactions on Networking* **24**:3 (June 2016), 1378-1391.

[2] R. J. La, Influence of Network Mixing on Interdependent Security: Local Analysis, in *Proceedings of IEEE Globecom*, Washington D.C., December 2016.

[3] R. J. La, Internalization of Externalities in Interdependent Security: Large Network Cases, in review.

[4] R. J. La, Network Mixing in Interdependent Security: Friend or Foe, in review.

Defining Resilience and Centrality Metrics for Interdependent Systems

Assane Gueye (University of Maryland)
Brian Cloteaux
Richard J. La (University of Maryland)

Modern society is increasingly dependent on large-scale networked systems (e.g., power grid, communication, water distribution, financial) that are often designed, operated and managed independently by different entities, but must work together to enable critical services. These constituent systems are interdependent, interacting with each other at different levels and multiple points. Due to this interconnectivity and interdependence, failures of nodes/links in one system can potentially have devastating consequences in other systems and in the global system. Furthermore, malicious agents can use nodes/links in constituent systems as a stepping stone to launch attacks on nodes/links in other systems. As a consequence, the resilience of a given constituent system depends not only upon its own nodes and links, but also on those in other constituent systems. Moreover, the importance of nodes/links in a constituent system cannot be judged solely based on the interconnectivity of the constituent system, but instead the overall connectivity of the global system needs to be considered.

The goal of this project is to develop a new methodology to assess the robustness of complex systems consisting of multiple interdependent systems and to identify "critical" constituent systems that are more vulnerable or play a more prominent role in the resilience of the overall system. To quantify the importance of a node/link, the concept of centrality has been developed and many centrality measures have been proposed for homogenous systems, each being more or less relevant for a given context. In this project, we plan to develop similar notion of "importance" of a constituent system in the context of measuring the resilience (of both the global system and constituent systems).

To guide our study, we plan to use real-world interdependent network data. We have acquired data for a major power grid and communication network, and are expecting to receive additional data sets. Using these data sets, we plan to first derive and validate a model for capturing interdependency among the nodes/links. Based on this model, we will propose metrics for the resilience of the global and constituent systems. Once resilience metrics are defined, we can quantify the importance of nodes/links by (for example) measuring how much each node/link contributes to the resilience (or, equivalently, fragility) of the global system as well as that of each constituent system. The expected outcomes from our efforts will naturally lead to a new method/tool for assessing the improvement of the resilience of existing complex systems and guide the design of new ones.

A New Metric for Robustness of System of Systems and Effects of Dependence Structure

Richard J. La (University of Maryland)

Many critical systems (e.g., smart grids, manufacturing systems, transportation systems) are made up of multiple heterogeneous systems whose agents depend on other agents belonging to different constituent or component systems (CSes). For instance, a modern power system not only includes an electrical grid/network, but also relies on an information and communication network (ICN) to monitor the state of the electrical network and to take appropriate actions based on the observed state.

Intricate (inter-)dependence among agents in CSes makes the analysis of these complex systems challenging. Moreover, in some cases, a (random or targeted) failure of a small number of agents in one CS has potential to cause unexpected widespread failures of many agents in multiple CSes. In the previous example of a modern power system, a failure in the ICN can hamper gathering crucial sensor measurements regarding the state of the electrical network (e.g., phase or voltage measurements) in a timely manner. This failure to collect critical information can in turn lead to an outage in parts of the electrical network.

Due to increasing reliance of modern societies on such complex systems and greater inter-dependence among CSes, there is a growing interest in modeling and understanding the interaction between (agents in) interdependent CSes and the robustness of the overall systems. The goal of this project is three-fold: (i) develop a new model for capturing the interdependence among the agents in CSes; (ii) compute the likelihood of experiencing widespread, cascading failures across the system, starting with a limited or localized failure in one CS; and (iii) identify more vulnerable systems that will serve as the "weak" links in complex systems.

In order to achieve these goals, borrowing tools from random graph theory and multi-type branching process theory, we developed a novel model that allows us to estimate the probability that the system will experience an epidemic of failures, beginning with a single (random) failure in a CS. We call this the Probability of Cascading Failures (PoCF). The PoCF depends on the CS in which the initial failure originates, and hence helps us identify the CSes that are more vulnerable in that localized failures in these CSes are more likely to result in a widespread outage throughout the entire system spanning multiple CSes. Moreover, using the same model, we investigated how the underlying structure of (inter-)dependence among the agents in the CSes shapes the PoCF. To be more precise, our analytical findings revealed that (i) the higher variability of (inter-)dependence among the agents leads to smaller PoCF and, hence, more robust systems; and (ii) positive correlations in the (inter-)dependence of agents across different CSes reduce the PoCF and improve the resilience of the system.

Our findings are somewhat surprising in the view of a common belief that more widespread degree distributions, such as power laws that allow the existence of large-degree hubs in the systems, are good for disseminating failures, information or rumors. They instead suggest that more concentrated degree distributions, such as Poisson distributions, are in fact more conducive to disseminating failures or information in complex systems, starting with randomly chosen nodes. Furthermore, given two distinct systems with similar levels of (inter-)dependence among the agents, having positive correlations in their degrees across different CSes hampers the spread of failures.

[1] R. J. La, Effects of Degree Variability and Dependence: Case Study of Two Interdependent Systems, in review.

[2] R. J. La, Cascading Failures in Interdependent Networks: Study of Degree Variability and Dependence, in preparation.

Critical Infrastructures: Resiliency by Controlling Systemic Risks

Vladimir Marbukh

The trend towards interconnectivity in large-scale infrastructures is driven by economic incentives, including the incentive to mitigate both unavoidable variability in exogenous demand and failures of the system components. Interconnectivity enables dynamic resource sharing, which allows systems to accommodate "small" local demand/capacity imbalances by dynamically redirecting load to underutilized network resources. However, these benefits come at a cost of possible misuse of the allowed flexibility in dynamic resource sharing. Numerous recent systemic failures of various networked infrastructures suggest that a market economy has difficulty in estimating and mitigating this cost.

Our investigation indicates that economic pressures may contribute to the risk of systemic failures in networked infrastructures. Indeed, the same economic pressures, which drive the system towards interconnectivity, also drive it towards the boundary of the system capacity/operational region, where all system resources are fully utilized. Matching of the expected demand with available resources is typically achieved through a combination of demand pricing and resource provisioning. Our investigation suggests that growing system interconnectivity may transform system instability from gradual/continuous to abrupt/discontinuous as the

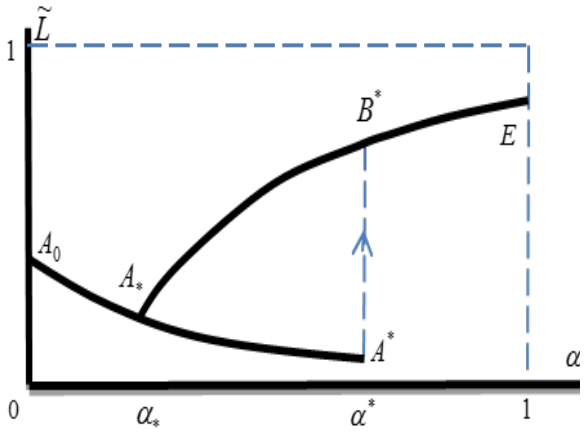

Figure 64. *Persistent revenue loss vs. level of resource sharing.*

boundary of the capacity/operational region is breached due to unavoidable exogenous demand variability or breakdowns in the system components.

Abrupt/discontinuous instabilities are often associated with metastability and manifest themselves as cascading failures. These cascades may even occur within the capacity/operational region as the system transitions to an undesirable metastable regime due to some random event. Motivated by higher performance losses and lower predictability of abrupt/discontinuous vs. gradual/continuous systemic instabilities, we associate abrupt/discontinuous instability with fragility while gradual/continuous instability with resilience. This allows us to frame the problem as managing system performance measured by the size of the capacity/operational region subject to controlling risk of abrupt/discontinuous instability. In effect, the problem is managing a "robust yet fragile" phenomenon, where robustness to small demand/capacity imbalances coexists with fragility to sufficiently large demand/capacity imbalances.

At the micro-level, we model contagion as a Markov process with locally interacting components, where system topology is encoded as a directed graph with nodes representing system components, and links representing the contagion flow [1]. In applications, some internal node states represent component failure, overload, etc., and thus can be deemed vulnerable/undesirable. This motivates the definition of the individual node risk as the probability of this node being in such a state, and systemic risk as the individual risk averaged over all the nodes in the system. We assume that an increase in the node risk exposure immediately drives downstream adjacent nodes towards higher risk exposure creating a possibility of contagion and undesirable cascades. Since a systemic event is an inherently macroscopic phenomenon, we employ "complex systems" methodology, and associate instabilities with phase transitions.

Some of our results [2-5] are illustrated in Figure 64, which sketches the persistent portion of lost revenue as a function of slowly changing level of resource sharing α. The figure illustrates a combination of positive and negative effects of dynamic resource sharing on persistent system performance. As resource sharing α slowly increases (decreases), the persistent loss rate $\tilde{L}$ follows the curve $A_0A_*A^*B^*E$ ($EB^*A_*A_0$), and thus $[0, \alpha^*)$ and $[0, \alpha_*)$ represent the "feasible region" and the "safe region" for α. The hysteresis loop $A_*A^*B^*A_*$ is indicative of discontinuous phase transitions and metastability.

Figure 64 illustrates that performance oriented networks are driven towards resource sharing level $\alpha = \alpha^*$ from below. However, since α^* depends on uncontrollable variable parameters, including the exogenous utilization ρ, the system is likely to transition to undesirable operating point B^*. Lowering the level of resource sharing to $\alpha = \alpha_*$ eliminates the possibility of abrupt/discontinuous overload at the cost of a corresponding reduction in the expected performance. The expected performance vs. overload risk tradeoff can be managed by controlling the resource sharing level.

The goal of our research is to develop quantitative resiliency metrics for realistic large-scale networked infrastructures, and then use these metrics to evaluate various strategies for managing system performance/resiliency tradeoffs. Our initial results suggest the following macroscopic description of networked systems under a fluid approximation at the onset of systemic instability of operational equilibrium L=0:

$$L = [\gamma L + bL^2 + cL^3]^+$$

where L is the lost revenue, $[x]^+ := \max(0, x)$, γ is the Perron-Frobenius eigenvalue of the linearized macro-evolutionary operator, and b and $c < 0$ some constants. The operational equilibrium $L = 0$ is asymptotically stable if $\gamma < 1$, and is unstable if $\gamma > 1$. The condition $b < 0$ ensures gradual/continuous stability loss on the boundary $\gamma = 1$. Since macro-parameters and γ and b depend on uncertain exogenous and endogenous micro-parameters, the probabilistic characterization of this uncertainty naturally leads to the following quantification of the system resiliency: $R = \Pr(\gamma<0, b<0)$. Numerous questions deserve further investigation. Of particular interest is the potential ability of online measurements of macro-parameters to provide early warning signals of the system approaching the instability/breaking point for the purpose of initiating appropriate control actions.

[1] V. Marbukh, Towards Unified Perron-Frobenius Framework for Managing Systemic Risk in Networked Systems, in *Proceedings of the annual European Safety and Reliability Conference*, Zurich, Switzer-land, September 7-10, 2015.

[2] V. Marbukh, Towards Systemic Risk Aware Engineering of Large-Scale Networks: Complex Systems Perspective, in *Proceedings of IEEE Computer Society's Modeling, Analysis, and Simulation of Computer and Telecommunication Systems*, London, England, September 19-21, 2016.

[3] V. Marbukh, Systemic Risks in the Cloud Computing Model: Complex Systems Perspective, in *Proceedings of The 9th IEEE International Conference on Cloud Computing*, San Francisco, USA, June 27 – July 2, 2016.

[4] V. Marbukh, Effect of Bounded Rationality on Tradeoff between Systemic Risks & Economic Efficiency in Networks, in *Proceedings of the Eighth International Conference on Ubiquitous and Future Networks*, Vienna, Austria, July 5-8, 2016.

[5] V. Marbukh, "Towards Classification, Evaluation, and Quantification of Systemic Risks of Dynamic Resource Sharing in Networked Systems," International Conference on Network Science 2017, Tel Aviv, Israel, January 15-18, 2017.

Scalable Network Anomaly Detection in SDNs and a New Metric for Relevance of Features

Richard J. La (University of Maryland)
Yang Guo (NIST ITL)

Timely detection of network anomalies (e.g., network intrusion and security breaches) is becoming increasingly important as critical systems (e.g., power grids, IoT, and financial systems) become more and more connected and dependent on a distributed information and communication infrastructure. A key step to ensuring proper operation and preventing catastrophic failures of critical networked information systems is to discover anomalies and suspicious activities in the systems before they can cause damages.

Most of existing network intrusion detection solutions today rely on collecting many low-level features of network traffic and analyzing the data to extract useful information on which actions can be taken. Unfortunately, they suffer from a major drawback; ubiquitous collection of fine-grained traffic measurements imposes significant burden on the network in terms of both communication and computational overheads, and does not scale to a large network. Several possible solutions, such as packet sampling and probabilistic based statistics collection, have been developed to address the scalability issue. However, studies have shown that these can negatively affect the performance of anomaly detection.

An emerging network technology, namely Software Defined Networks (SDNs), offers a promising solution to overcome the scalability issue by offering the flexibility to dynamically adjust the network features to be monitored based on the current network state. A key challenge to taking advantage of this new capability is to efficiently identify a small subset of features to monitor and analyze to detect and act on any sign that suggests anomalous activities.

To address this challenge, we investigated the possibility of employing machine learning techniques to (i) systematically aggregate network features based on a new metric for the "relevance" of network features for network monitoring. This new metric in turn allows us to aggregate many features into a much smaller number in an iterative manner. This is done in such a way that we can significantly reduce the number of features to monitor and report, thereby curtailing communication and computational overheads, without degrading the ability to detect unusual activities which might be indicative of malicious actions. When potential threats are identified, new threat and topology specific measurements will be enabled on specific switches to dynamically "drill down" and provide the fine-grained data necessary to isolate the problem.

Our experimental studies so far have focused on analyzing NIST network traces collected over several months (June through September, 2016). By utilizing the k-means clustering algorithm, our initial experimental studies suggest that, even after aggregating the network features using our method, the clustering algorithm allows us to identify the same set of potentially anomalous traffic measurements that we identified before the aggregation.

We are currently working to obtain additional traces with labels so that we can test the effectiveness of our method on additional data. Furthermore, we plan to design a new method for identifying new threat- and topology-specific features to monitor in case of potential threat detected by our network classification algorithms.

An Algebraic Formulation for the Analysis and Visualization of Network Graphs

Roldan Pozo

Characterizing the topological structure of large graphs remains an important problem in network science. While it is straightforward to visualize small networks of hundreds or a few thousands of vertices and edges using conventional graph visualization packages, attempting to render large real networks is nearly impossible. This is particularly true for information networks and social networks, where the graph sizes number into the millions and billions of nodes. And with the amount of data being generated and gathered from large social media sites ever increasing, characterizing larger and larger networks is only becoming more challenging. Conventional algorithms for graph visualization result in a rendering of very large networks as a solid blot of color from which it is difficult to obtain meaningful information. This difficulty is strongly influenced by the sheer volume of nodes and edges

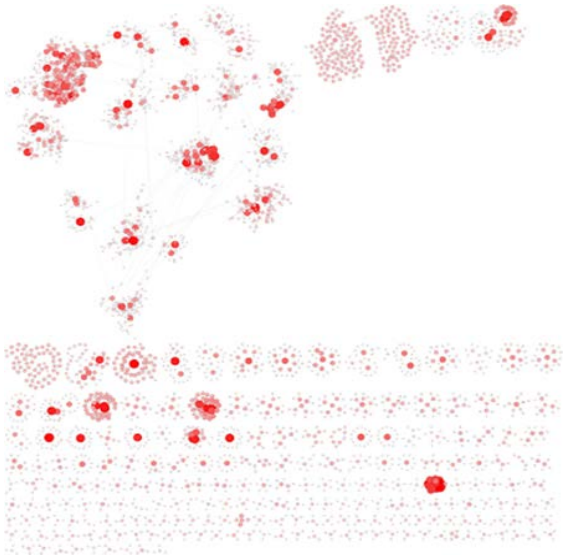

Figure 65. *Non-trivial components of math.nist.gov web graph, restricted to nodes with combined degree less than or equal to 25.*

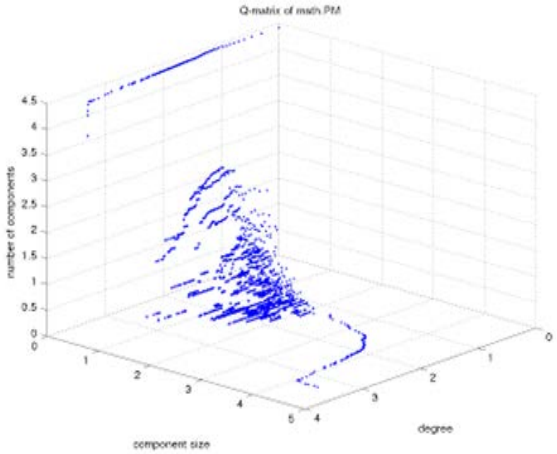

Figure 66. *Q-matrix plot of math.nist.gov web graph (29K vertices, 62K edges) showing the component size distribution of degree-limited subgraphs.*

which makes rendering into a reasonable image size for viewing and printing impractical. It is exacerbated by the presence of high-degree nodes (hubs) which entangle many parts of the graph with itself.

An alternate approach is to visualize important network properties, rather than the actual network itself. Such network portraits attempt to capture interesting attributes of a large graph, such as degree distribution, or its connective properties. In this research, we focus on a particular type of information: the distribution of "fringe" communities, i.e., connected components of a graph in the absence of high-degree hubs. In a social science context, for example, they represent independent or rogue groups, highly connected amongst themselves, but which are often lost with the inclusion of more popular nodes.

Our approach, the *Q*-matrix of a network, in its fundamental form, is a connected component size distribution matrix for a series of degree-limited subgraphs of the original network (or weakly-connected component for directed networks.) Thus, $Q(i,j)$ is the number of connected components of size j in a subgraph where the maximum degree is equal to or less than i. Consider, for example, a Web graph, where nodes are individual pages, and edges are directed hyperlinks between two web pages. Figure 65, for example, illustrates connected components of the math.nist.gov Web graph, where nodes of degree greater than 25 have been removed. The result is a collection of non-trivial components of the math.nist.gov web graph, restricted to nodes with combined degree less than or equal to 25. The image reveals various structures, such as ladder, star, and cluster patterns, representing tightly coupled web pages. These form the nucleus of fringe communities of web pages, and by varying the degree parameter we can direct the size and granularity of groups revealed.

As the degree threshold is increased from one to the largest degree in the original graph, we can form a connected component size distribution, which can be encoded as a row of a matrix. This sparse matrix may still be too large to view directly, but can be compactly rendered by projecting its nonzero values onto the z-axis and displaying it as a three-dimensional plot, as shown in Figure 66. This *Q*-matrix plot of the math.nist.gov webgraph (29K vertices, 62K edges) shows the component size distribution of degree-limited subgraphs.

The *Q*-matrix of a graph can be considered to be a generalization of its degree-distribution. However, it encodes other properties, such as the formation and growth of its giant component, its connected subparts, as well as its size parameters. In fact, common network metrics (e.g., degree distribution, number of connected components, number of vertices and edges) can be extracted from the *Q*-matrix using simple linear algebra operations.

Among the interesting characteristics of the *Q*-matrix formulation is that network graphs from similar application areas (e.g., social networks, email networks, web graphs, peer-to-peer networks, road networks, citation graphs) share similar visual characteristics, creating a potential framework for network identification and classification. Indeed, we have used the *Q*-matrix formulation to generate meaningful thumbnail images for network data collections. The computation of the *Q*-matrix is relatively efficient; graphs with millions of vertices and edges can be processed in less than one minute.

We have extended this framework by developing a measure that compares *Q*-matrices of networks in varying sizes and scale. This is critical in developing the theory as it allows one to compare vastly different

networks and provide a numerical similarity between them, and establish a taxonomy based on these characteristics. We have also provided an extended measure formulated on second and third-generation degree distributions, which provides a refined fingerprint of network graphs. To each vertex we assign not just its degree (d), but the average degree of all its neighbors (d_1), average degree of all its neighbor's neighbors (d_2), and so on. This replaces a single vertex value with a finite vector (d, d_1, d_2, …, d_k). Such vectors can be arranged in lexicographical order along one dimension, creating a much richer profile than the conventional degree distribution.

Currently, the Q-matrix decomposition is being used to aid the study of communication and information spreading through graph topologies. Identifying critical nodes in the network structure is an important, but computationally expensive problem. New heuristics are being developed using the Q-matrix decomposition to find natural fracture points in the graph, which could help identify nodes as effective spreaders.

[1] R. Pozo, Q-matrix: An Algebraic Formulation for the Analysis and Visual Characterization of Network Graphs, *Journal of Research of NIST* **121**:1, 16 pages.

Algorithms for Identifying Important Network Nodes for Communication and Spread

Fern Y. Hunt
Roldan Pozo

The identification of nodes in a network that enable the fastest spread of information is an important if not fundamental problem in network control and design. It is applicable to the optimal placement of sensors, the design of secure networks, and the problem of control when network resources are limited. In our work, the mode of communication among nodes is described by simple models of random or deterministic propagation of information from a node to its neighbors.

We take two approaches to the problem of finding sets of effective spreaders. Let graph $G = (V, E)$, represents a network with a set of nodes V, and corresponding edges E. Borkar et al. [1] consider a discrete time model of information spread (represented by a variable assigned to each node) where a subset A of K nodes is initially assigned a single value. Propagation occurs by iterated averaging or diffusion defined by a stochastic matrix P. All node values will eventually converge to the single value at a speed determined by the sub-stochastic matrix P_A determined by A.

An effective spreader in this situation is then a set of K nodes for which convergence to this single value is fastest, i.e., the set A for which the Perron-Frobenius eigenvector of P_A is largest. Using a classical result of Markov chain theory, the problem is recast in terms of finding the set A of cardinality K that minimizes the hitting time, i.e., the average expected time a random walker starting outside A, reaches A for the first time. The random walk is related to actual information spread only through the common use of the matrix P. As stated, solution of this minimization problem requires an examination of all subsets of cardinality K. The essence of our approximation method is to reduce the search space of the problem to a much smaller class of optimal and "nearly" optimal subsets of cardinality K [2].

During this year the algorithm we recently developed was used to solve the problem on larger and more realistic graphs, building on the theoretical and empirical results reported in [2]. There the method was compared to the greedy algorithm for constructing approximate solutions and it was rigorously proved to perform at least as well. When additional information about the hitting function is available, the improvement our method offers can be quantified. If N is the number of vertices in the graph G then the complexity of the method is $O(N^{m+3})$ where $m \leq 2$. For very large graphs in typical complex network applications (thousands to millions of nodes) this is still not practical.

We are currently experimenting with a method that combines Monte Carlo simulation and graph heuristics. It is very fast on large graphs and its results compare favorably with exact calculations and the results of the algorithm in [2]. Developing a method that combines these two approaches looks like a promising next step.

[1] V.S. Borkar, J. Nair and N. Sanketh, Manufacturing Consent, in *Proceedings of the 48th Annual Allerton Conference*, University of Illinois at Urbana-Champaign, September 2010, 1550-1555

[2] F. Hunt, An Algorithm for Identifying Optimal Spreaders in a Random Walk Model of Network Communication, Journal *of Research of the NIST* **121** (2016).

Treewidth for Network Reliability Measurement

Isabel Beichl

We are investigating the use of treewidth as a metric to estimate reliability of networks. Treewidth is a number associated with an undirected graph $G = (V, E)$. It is the minimum size of the largest vertex set in a tree decomposition, minimized over all tree decompositions. A tree decomposition of G is a tree where the vertices are subsets of the vertices of G, called bags, and edges that connect these bags. Finding the treewidth is NP hard. However, given a k, there is a linear time algorithm by

Bodlaender [1] for determining if there exists a tree decomposition of size at most k, and if there is, it returns the decomposition.

Research on this topic has assumed that k is small. For reliability of large-scale networks, however, one cannot assume small tree width. A network that is a tree (which has treewidth 1) is unreliable because each edge is a "bridge", i.e. its removal disconnects the network. So for reliability, we want large tree width. Thus we would select a k that would be acceptable for reliability and apply Bodlaender, asking whether there is there a tree decomposition of size k. We want a "no" answer. Such an approach would be computationally feasible, and hence this provides a possible research direction for a fast and straightforward method for determining reliability. There would be applications to designs for networks of interconnections of processors in massively parallel machines. This idea still needs to be tested.

[1] H. L. Bodlaender, A Linear-Time Algorithm for Finding Tree-Decompositions of Small Treewidth, *SIAM Journal of Computing* **25**:6 (1996), 1305-1317.

Random Graph Creation and Forced Edges

Brian Cloteaux

An important task in investigating many networks is creating a random model having a given degree sequence. Generating such random instances is challenging because of the limitations of current methods. The most common algorithm used is to create a non-random instance and then modifying it using a Monte Carlo Markov chain approach. Besides open questions about the mixing time of this approach, a more serious problem is that it requires holding an entire graph in memory. Sequential importance sampling methods have also been developed, but suffer from a severe penalty in speed. This past year, we introduced a new algorithm for creating random instances [2], which overcomes the space and speed limitations of earlier methods.

We have also been looking at approaches to improving existing algorithms. An investigation of these algorithms reveals that they often have difficulty with forced or forbidden edges in a degree sequence. A *forced edge* for a degree sequence is a labeled edge that appears in every realization of sequence, while a *forbidden edge* appears in no realization. Figure 67 shows that there is a strong correlation between being able to successfully select random edges and the majorization gap of a sequence. In general, the smaller the majorization gap, the greater the number of forced and forbidden edges.

Part of this investigation into improving the graph sampling algorithms involves looking how these forced and forbidden edge affect the structure of realizations.

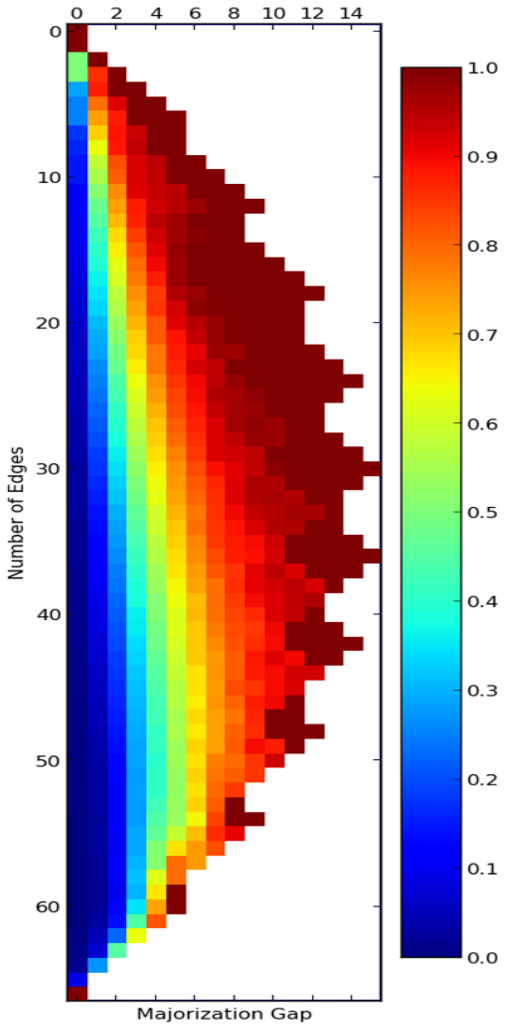

Figure 67. *Probabilities that a uniformly selected random reduction will be graphic across all sequences of length 12 and less.*

We have made several discoveries [4], including (a) if a sequence has either forced or forbidden edges, then every realization of that sequence has a maximum diameter of three, and (b) every realization is maximally edge connected, meaning that there is no easier way to disconnect a graph than removing all the edges adjacent to the smallest node.

This investigation has also led to a new result for establishing when a degree sequence is *graphic* [3], i.e., it has a realization in some graph. For a degree sequence d where n is the length of the sequence and s is the sum of the sequence, then if

$$(d_1 - d_n)\left[\frac{n - d_1 - 1}{nd_1 - s} + \frac{d_n}{s - nd_n}\right] \geq 1$$

the sequence d is graphic. This result is useful when coupled with the usual Erdos-Gallai conditions for checking if a sequence is graphic [1]. Before a sequence can be tested using the Erdos-Gallai conditions, it must

first be sorted. During this sorting step, the values for largest and smallest indices, sequence length, and sequence sum can be easily extracted. Thus, this new condition can save several steps in graphic testing for certain sequences.

The next steps for this project will be to publish a series of improvements to existing algorithms using this enhanced understanding of forced and forbidden edges. Also, new software that take advantage of these refinements will be published. Finally, we are looking to see if we can extend these results to other definitions such as the joint degree sequence.

[1] B. Cloteaux, Is This for Real? Fast Graphicality Testing, *Computing in Science & Engineering* **17**:6 (2015), 91-95.

[2] B. Cloteaux, Fast Sequential Creation of Random Realizations of Degree Sequences, *Internet Mathematics* **12**:3 (2016), 205-219.

[3] B. Cloteaux, A Sufficient Condition for Graphic Lists with Given Largest and Smallest Entries, Length and Sum, in review.

[4] B. Cloteaux, Forced Edges and Graph Structure, in review.

Counting the Number of Linear Extensions of a Partially Ordered Set

Isabel Beichl
Alathea Jensen (George Mason University)
Francis Sullivan (IDA Center for Computing Sciences)

Given a partially ordered set (P,lt) a linear extension is a linear ordering (P,<) of the elements of P that is consistent with (P,lt), i.e. if p_1 .lt. p_2 then $p_1 < p_2$. The ability to count the number of linear extensions is central to the theory of sorting which in turn is extremely important in the design of algorithms for advanced computers. A count of linear extensions is also important in ranking alternatives in scheduling problems where one might want to keep options open as long as possible, and in applications that arise in the social sciences where one wants to rank products or job candidates from a given partial order. It also appears in big data applications where one might need to set priorities while keeping as many options open as possible. The number of linear extensions is also a measure of the entropy of a graph.

While it is computationally easy to generate a single linear extension of (P,lt) it is known that counting the number of linear extensions is #P-complete and so one must resort to approximation. One Monte Carlo technique, called Monte Carlo Markov Chain (MCMC), has been devised and investigated extensively in the literature of theoretical computer science [1]. It has been proved that the method does give an accurate approximation for this problem. However, the method is not helpful for practical computation because it still requires work (n^5) for an n-element partially ordered set.

Because the aim of our work is practical computational methods, we decided to investigate an alternative Monte Carlo method that has been used with success in other #P-hard counting problems. The alternate method, called sequential importance sampling (SIS), is based on non-uniform sampling based on an importance function. In this case, the importance function is derived from the famous Möbius inversion formula. A second importance function has been invented that changes dynamically as the problem is run. Because the number of extensions is the same if the direction of all the inequalities is reversed we were led to improvements in efficiency by flipping from one direction to another within the problem. A recursive version was also developed which also lowers variance. This SIS-based algorithm has been found to work extremely well in test cases.

[1] G. Brightwell and P. Winkler, Counting Linear Extensions, *Order* **8** (1991), 225-242.

A Low-Cost Network and Applications for Underserved Areas: A Deployment in Rural Senegal

Assane Gueye (University of Maryland)
Charif Mahmoudi (NIST ITL)

Information and communication technologies (ICTs) have always been an enabler for innovation and economic growth, giving to those with access to connectivity the opportunity to develop innovative services across key sectors such as health, education and agriculture. Unfortunately, however, people in rural and underserved areas have hardly benefited from such new opportunities mostly due of the lack of connectivity infrastructure. The goal of this project is to study sustainable connectivity solutions that will permit to people in rural and underserved areas to enjoy the opportunities brought by ICTs.

The solution we propose is based on a simple opportunistic principle: given any situation, use the best connectivity solution available; and when no solution is available at the moment, use delay-tolerant networking (DTN) to offer offline services. This network will be backboned using point-to-point long-distance Wifi links. On the access links, it will use data services wherever available. If none of the data services is available, we will use (compressed) SMS service as a support for data communication. In areas with no network coverage, we will use DTN solutions. For the seamless integration of all these technologies, we use the newly proposed *Named Data Networking* Internet architecture, which is

found to be naturally suitable to environments where connectivity is intermittent.

The focus in this project will be on building a "local" Internet that interconnects rural communities among themselves (which we term as "in-out approach"). This is complementary to the most known ("out-in approach") that aims at bringing the Internet to rural communities. However, this task is harder to achieve, requiring a huge preliminary investment (mostly from government to build infrastructures and lay fiber), which is slow to materialize. In the meantime, rural communities have been waiting, and hence missing opportunities that would be possible by being "locally" connected. This is what motivated our in-out approach to building a "local Internetwork" for rural communities. Bearing in mind that the ultimate end will be to connect communities to the global Internet, we plan to build a system that is "easily pluggable to the Internet".

In our first deployment, we are targeting two main applications:

1. *Organization of rural flea markets.* Preliminary studies have revealed a lot of inefficiencies in the weekly flea markets in the villages surrounding Bambey, Senegal. Often a product is brought in a market while it was needed in another one, and it is often obtained in a given market while it was available at a better price in a different market. We aim to use our rural network to build an information system (a rural "craigslist") that will enable people to push/pull information about needed/offered products prior to the day of the markets.
2. *Collection of environmental data*. Due to the increasing usage of products (fertilizers) that are hostile to the environment, monitoring of the environment is becoming more and more vital. Unfortunately, the data that can enable such monitoring is almost non-existent for most parts of the developing world. This lack of data is mostly due to the lack of proper infrastructure to collect, store and disseminate the data. As a solution to this problem, we plan to use our rural network as a data collection, storage and dissemination system.

Other services that we are planning to build include content building, knowledge sharing, e-government, remote health and e-agriculture.

Combinatorial Methods in Software and System Testing

Raghu N. Kacker
D. Richard Kuhn (NIST ITL)
Yu Lei (University of Texas at Arlington)
James F. Lawrence
Dimitris Simos (SBA-Research, Austria)
Itzel Dominguez-Mendoza (CENAM, Mexico)

Many critical system failures have been traced to interaction faults in the underlying software. For example, the 1997 Mars Pathfinder mission began experiencing system resets at seemingly unpredictable times soon after it landed and began collecting data. Fortunately, engineers were able to deduce and correct the problem, which occurred only when (1) a particular type of data was being collected and (2) intermediate priority tasks exceeded a certain load, allowing a blocking condition that eventually triggered a reset.

Combinatorial testing (CT) is based on an empirical conclusion, referred to as the interaction rule, that while the behavior of a software system may be affected by a large number of factors, only a few factors are involved in a given failure-inducing fault. Actual faults show that most involved one or two factors; however, some may involve three, four or more factors (a fault involving more than six factors has not been reported yet).

NIST has taken the lead to advance CT technology from pair-wise to higher strength testing, to make research tools and techniques available for US industry, and to help promote their effective use. CT has become a versatile and broadly applicable methodology that is helping to reduce testing costs in software based systems for science, commerce, defense and security, and electronic medical systems. CT is useful for hardware testing as well. CT is now included in software engineering courses taught in over fifteen U.S. universities. A NIST special publication on CT [1] has been downloaded more than 30 000 times.

ACTS (Automated Combinatorial Testing for Software) is a research tool developed by NIST and the University of Texas at Arlington to generate high strength test suites for CT. More than 2 600 users have downloaded an executable version of the ACTS tool from a NIST website[11] for combinatorial testing. We allow further distribution of the ACTS tool by its recipients. We are now distributing version 3.0 of the ACTS tool. The ACTS tool is optimized to support constraints among test settings, i.e., efficiently avoiding forbidden combinations of test settings.

CCM (for Combinatorial Coverage Measurement) is a new research tool developed jointly by NIST and guest researcher Itzel Dominguez-Mendoza to determine the combinatorial coverage of a test suite that may

[11] http://csrc.nist.gov/groups/SNS/acts/index.html

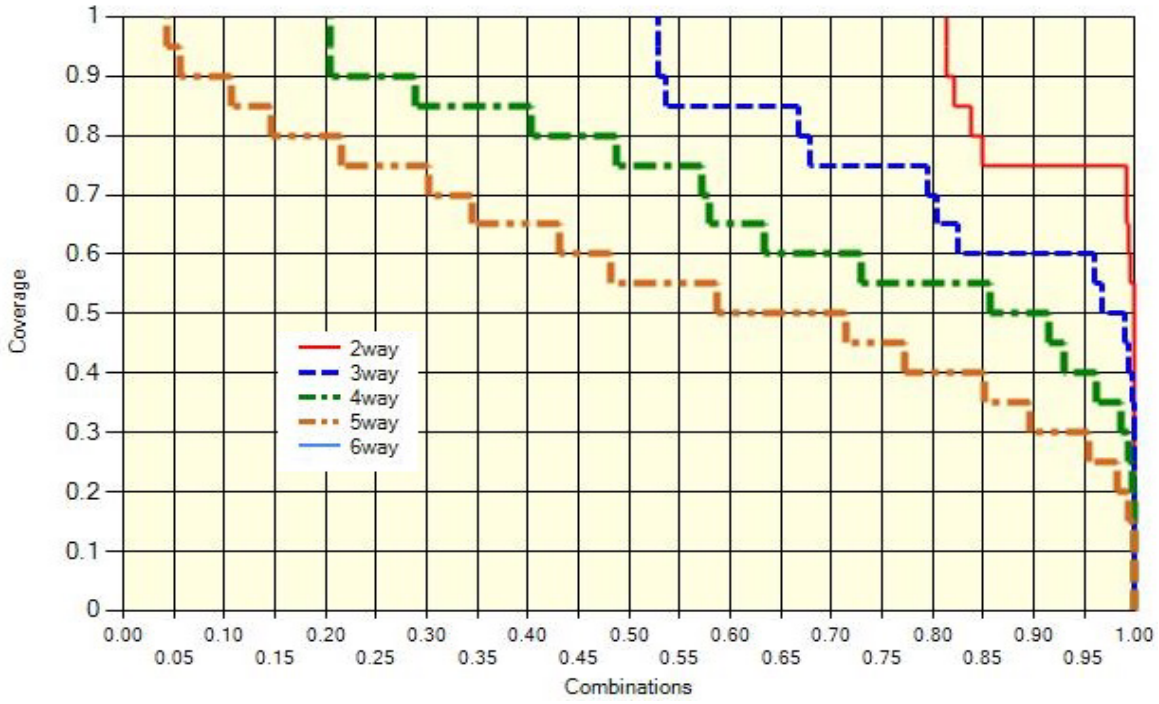

Figure 68. *Combinatorial t-way coverage of a test suite of 7489 tests of 82 variables for t=2, 3, 4, and 5.*

not have been developed from a CT viewpoint. The latest version of CCM supports constraints. A parallel processing version of CCM is also available. The most important use of CCM is to assess the coverage of the input space by a test suite. Combinatorial deficiency of a test suite can be remedied by additional tests so CCM can help expand a test suite to satisfy stated combinatorial requirements. A graph of combinatorial coverage depicts the percentage (ordinate) of the fraction (abscissa) of all *t*-way combinations that are covered by the test suite. Figure 68 shows combinatorial *t*-way coverage of a test suite of 7489 tests of 82 factors for $t = 2, 3, 4$, and 5. The area under a curve represents the proportion of combinations that are covered by the test suite; thus, the area above the curve represents input parameter combinations for which correct operation has not been verified.

The 5th International Workshop on Combinatorial Testing (IWCT) was held in conjunction with the 9th IEEE International Conference of Software Testing, Verification and Validation (ICST) in Chicago Illinois (April 10 - 15, 2015) to bring together researchers, developers, users, and practitioners to exchange ideas and experiences with CT methods and tools. Four of us (Kuhn, Kacker, Lei and Simos) were co-organizers. IWCT-2016 received 18 submissions of which 10 papers were selected by the Program Committee.

A consortium of universities and industry, SBA-Research is a leading Austrian research center for information security. We are jointly investigating research issues in using combinatorial test methods for cybersecurity applications. SBA-Research used the NIST CCM tool to analyze the combinatorial coverage of test inputs of some open-source cryptographic suites. In most cases combinatorial coverage was low; suggesting that standard test sets for these widely used cryptographic packages may provide insufficient testing.

We also developed an oracle-free software testing method for which NIST filed a patent application. In software testing, the oracle problem refers to determining the expected output for a given set of inputs. Determination of the expected output requires expert knowledge and normally cannot be automated without a mathematical model of the specified software. The test settings for an input factor may represent ranges of values (called equivalence classes) for which the output is expected to remain unchanged. For example, a shipping program may charge the same rate for any package under one pound, a second rate for packages one pound to 10 pounds, and a third rate for packages over 10 pounds. Values within each of these ranges are equivalent with respect to the cost calculation. Thus, any value within an equivalence class may be substituted for any other and the program output should be unchanged. Similarly, equivalent values for any combination of input variables should also produce the same output.

The test method works by generating two test arrays: a primary array and a secondary array. The entries of primary array represent names of equivalence classes of input factors. For each test row of the primary array, a second array is computed. The settings in second array

are the values from equivalence classes corresponding to the names of equivalence classes in the primary array. If the outputs corresponding to one row of the primary array differ then either the equivalence classes were defined incorrectly or the code is faulty in some way. This method can detect certain software faults without a conventional test oracle automatically after the equivalence classes have been defined.

[1] D. R. Kuhn, R. N. Kacker, Y. Lei, *Practical Combinatorial Testing*, NIST Special Publication 800-142, October 2010, 76 pages.

[2] W. Wang, S. Sampath, Y. Lei, R. N. Kacker, D. R. Kuhn and J. F. Lawrence, Using Combinatorial Testing to Build Navigation Graphs for Dynamic Web Applications, *Journal of Software Testing, Verification and Reliability* **26** (2016), 318-346.

[3] D. R. Kuhn, R. N. Kacker and Y. Lei, Measuring and Specifying Combinatorial Coverage of Test Input Configurations, *Innovations in Systems and Software Engineering – A NASA Journal* **12**:4 (2015), 249-261.

[4] J. Chandrasekaran, L. Ghandehari, Y. Lei, R. N. Kacker and D. R. Kuhn, Evaluating the Effectiveness of BEN in Localizing Different Types of Software Fault, in *Proceedings of the Ninth IEEE International Conference on Software Testing, Verification and Validation Workshops (ICSTW)*, Chicago, IL, April 10-15, 2016, 26-34.

[5] D. R. Kuhn, V. Hu, D. F. Ferraiolo, R. N. Kacker and Y. Lei, Pseudo-Exhaustive Testing of Attribute Based Access Control Rules, in *Proceedings of the Ninth IEEE International Conference on Software Testing, Verification and Validation Workshops (ICSTW)*, Chicago, IL, April 10-15, 2016, 51-58.

[6] D. Simos, K. Kleine, A. Voyiatzis, D. Kuhn and R. Kacker, TLS Cipher Suites Recommendations: A Combinatorial Coverage Measurement Approach, in *Proceedings of the 2016 IEEE International Conference on Software Quality, Reliability and Security* (QRS), Vienna, Austria, August 1-3, 2016, 69-73.

[7] D. E. Simos, D. R. Kuhn, A. G. Voyiatzis and R. N. Kacker, Combinatorial Methods in Security Testing, *IEEE Computer* **49** (2016), 80-83.

[8] Z. Ratliff, D. Kuhn, R. Kacker, Y. Lei and K. Trivedi, The Relationship Between Software Bug Type and Number of Factors Involved in Failures, in *Proceedings of the IEEE International Symposium on Software Reliability Engineering Workshops* (ISSREW), Ottawa, Canada, October 23-27, 2016, 119-124.

[9] V. Hu, D. F. Ferraiolo, D. R. Kuhn, R. N. Kacker and Yu Lei, Implementing and Managing Policy Rules in Attribute Based Access Control, in *Proceedings of Sixteenth IEEE International Conference on Information Reuse and Integration (IRI)*, San Francisco. CA, August 13-15, 2015, 518-525.

Mathematical Knowledge Management

We work with researchers in academia and industry to develop technologies, tools, and standards for representation, exchange, and use of mathematical data. Of particular concern are semantic-based representations which can provide the basis for interoperability of mathematical information processing systems. We apply this to the development and dissemination of reference data for applied mathematics. The centerpiece of this effort is the Digital Library of Mathematical Functions, a freely available interactive and richly linked online resource, providing essential information on the properties of the special functions of applied mathematics, the foundation of mathematical modeling in all of science and engineering.

Digital Library of Mathematical Functions

Barry I. Schneider
Daniel W. Lozier
Adri B. Olde Daalhuis (University of Edinburgh)
Bruce R. Miller
Bonita V. Saunders
Howard S. Cohl
Marjorie A. McClain
Ronald F. Boisvert
Brian Antonishek (NIST ITL)
Charles W. Clark (NIST PML)
Amanda Hu (Poolesville High School)
Grace Tang (Poolesville High School)
Nina Tang (Poolesville High School)

http://dlmf.nist.gov/

Progress in science has often been catalyzed by advances in mathematics, while cutting-edge science has been a major driver of mathematical research. This symbiotic relationship has been extremely beneficial to both fields. Often the mathematical objects at the intersection of mathematics and physical science are mathematical functions. Effective use of these tools requires ready access to their many properties, a need that was capably satisfied for more than 50 years by the 1964 National Bureau of Standards (NBS) *Handbook of Mathematical Functions with Formulas, Graphs, and Mathematical Tables* [1].

The 21st century successor to the NBS Handbook, the Digital Library of Mathematical Functions (DLMF) together with the accompanying book, *NIST Handbook of Mathematical Functions* [2], published by Cambridge University Press in 2010, are collectively referred to as the DLMF. The DLMF continues as the gold standard reference for the properties of what are termed the special functions of mathematical physics. The DLMF has considerably extended the scope of the original handbook, as well as improved accessibility to the worldwide community of scientists and mathematicians. For example, the new handbook contains more than twice as many formulas as the old one, coverage of more functions, in more detail, and an up-to-date list of references. The website covers everything in the printed handbook and much more: additional formulas and graphics, interactive search, zooming and rotation of 3D graphs, internal links to symbol definitions and cross-references, and external links to online references and sources of software.

In order to help assess the impact of the DLMF project, the NIST library has undertaken a project to track citations to the DLMF, as well as to the original NBS Handbook. While the original Handbook still receives an enormous number of citations, citations to the DLMF are steadily growing. As of this writing, Google Scholar identifies more than 2 900 citations to the DLMF.

Today's DLMF is the product of many years of effort by more than 50 expert contributors. Its appearance in 2010, however, was not the end of the project. To assure the continued vitality of the DLMF deep into the 21st century, corrections to errors, clarifications, bibliographic updates, and addition of important new material all continually need to be made, and new chapters covering emerging subject areas need to be added.

During the past year, the DLMF project has seen continued progress on several fronts. In FY 2016, there were four releases of the DLMF: 1.0.11, 1.0.12, 1.0.13 and 1.0.14. This is now meeting the target of four updates a year.

One of the design goals for the DLMF was that each formula would be connected to a proof in the literature. The "Notes" to relevant chapter, sections, and subsections would give either a short proof for the formulas or a reference to a proof in the literature. Unfortunately, this information has not been provided in all cases. In FY 2015 we began an effort to systematically verify the completeness and traceability to published proofs for DLMF formulae. This audit is first being undertaken for Chapter 25 (Zeta and Related Functions) and Chapter 27 (Functions of Number Theory). In addition, work has begun to make proof-related information visible in metadata at the equation level. Improvements in markup to more accurately identify the nature of the added material have been developed and is being deployed.

Work has also begun on the first major update and expansion of the DLMF. Topics include updates to the Orthogonal Polynomials and Painlevé Transcendents chapters, as well as a new treatment of Orthogonal Polynomials of Several Variables. Contracts have been set in place with four authors to carry out this work. Submitted chapter outlines were recently accepted, and the actual writing of the chapters is about to begin. The DLMF LaTeX Guide for Authors has been extensively updated in preparation for this, and a new LaTeX package will enable authors to more easily integrate their contributions with the existing DLMF.

Two related projects described elsewhere in this report continue to evolve, and remain important parts of the overall NIST goal to present useful mathematical information to the community in a trustworthy manner: DLMF Tables, an on-demand table generation web service for special functions (see page 96), and the Digital Repository of Mathematical Formulae, a community-based compendium of mathematical formulas and associated mathematical data (see page 100).

[1] M. Abramowitz and I. Stegun, eds., *Handbook of Mathematical Functions with Formulas, Graphs and Mathematical Tables*, Applied Mathematics Series 55, National Bureau of Standards, Washington, DC 1964.

[2] F. Olver, D. Lozier, R. Boisvert and C. Clark, eds., *NIST Handbook of Mathematical Functions*, Cambridge University Press, 2010.

Visualization of Complex Functions Data

Bonita Saunders
Brian Antonishek (NIST EL)
Qiming Wang
Bruce Miller
Sandy Ressler

Although this project originated from a desire to create informative graphs to help scientists understand the properties of mathematical functions featured in the NIST Digital Library of Mathematical Functions (DLMF), it has evolved alongside new technologies for viewing and manipulating 3D graphics on the web. From our first visualizations using a web 3D format called Virtual Reality Modeling Language (VRML), we moved to an XML based format, X3D, and finally to X3DOM/WebGL. X3DOM, a framework for creating graphics applications on the Web, was developed by Johannes Behr et al. at Fraunhofer IGD [1], and WebGL, developed by the Khronos Group [2], is a JavaScript application programming interface (API) for rendering 3D graphics in a web browser without a plugin.

Basing our WebGL code on X3DOM allowed us to quickly build our WebGL applications around our X3D codes. Using these technologies, we have created cutting edge visualizations that have been praised by DLMF users and 3D graphics web designers alike. At Web3D 2015, Behr said that he was so impressed with our implementation of cutting planes that he would incorporate a clipping plane feature in the specifications for X3D. Figure 69 shows a cutting plane intersecting the modulus of the hyperbolic umbilic canonical integral function $\Psi^{(H)}(x, y, 3)$. Figure 70 shows a density plot for the phase, or argument, of the complex function.

While the DLMF visualizations might be viewed as a "mature" component, the digital nature of the DLMF opens the door to numerous possibilities for enhancements. Current work is focused on improving the visualizations by adding new features and increasing the quality of the underlying meshes, or grids, used to compute the function data. However, this is not trivial work.

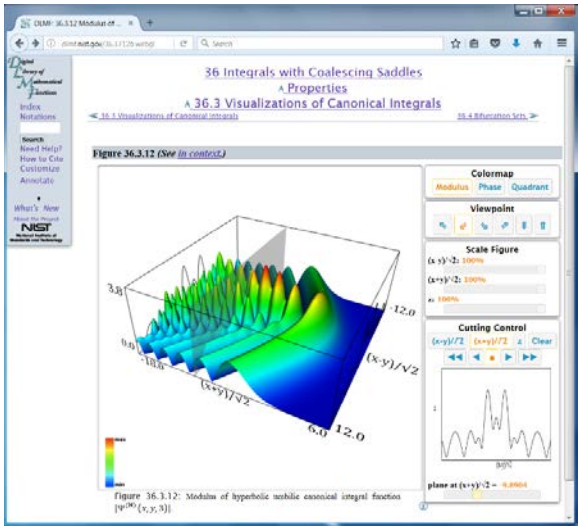

Figure 69. *DLMF webpage with embedded visualization of hyperbolic umbilic canonical integral function* $\Psi^{(H)}(x, y, 3)$.

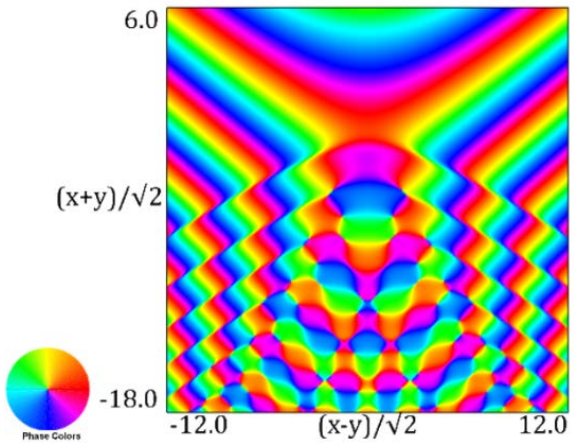

Figure 70. *DLMF image of phase density plot for hyperbolic umbilic canonical integral function* $\Psi^{(H)}(x, y, 3)$.

For example, progress was made in the development of a continuous surface spin option. This feature would permit a user to create a continuous spin in any direction by touching and flicking the surface. The speed of the spin would vary according to how fast the surface is flicked. This would be an effective tool for drawing interest during a talk or for creating an instant animation in an exhibit. The feature was available in the early CosmoPlayer VRML plugin designed by Silicon Graphics, but it was implemented in only a few VRML or X3D plugins developed subsequently. Sandy Ressler completed preliminary work, first implementing the feature directly in WebGL and then successfully creating a rough X3DOM version by modifying codes pieced together from software freely shared by a designer at Shapeways, a 3D printing firm [13]. However, since a substantial effort is needed to streamline, restructure, and integrate the code into our current X3DOM/WebGL visualizations and the implementation of the spin feature directly in WebGL appears to be a much simpler task, we have suspended this work until the feasibility of converting our visualizations directly into WebGL is studied.

We are also working on the reduction of graphics file sizes using adaptive grid generation. We have successfully adapted several grids for trigonometric and simple algebraic functions using mean curvature or gradient information. Since most DLMF function data was computed in Mathematica, our next task, already in progress, is to develop code that exports data from Mathematica and inputs it into the grid generation code.

Another area for future development is an accurate zoom feature, which would require real time computation of the function data. One possibility is to use hierarchical grid generation techniques for this. Tor Dokken of SINTEF (Norway) suggested that it might be better to compute the functions on a very fine grid initially rather than try to compute grids with different levels of concentration in real time. This was illustrated very clearly when we used our laptops to compare WebGL visualizations. His visualization, which computed the data on a server in Norway and then sent it to the screen, was extremely slow. Still, there is probably a way to do it that might make creating such a zoom more feasible, but more thought is needed.

The motivation for our current work comes both from internal observations by the DLMF team and feedback from users. Part of our effort is to get more user feedback by improving the visibility of the visualizations. To accomplish this, a List of Figures entry was added in DLMF Update 1.0.10 to provide users quicker access to nearly 600 graphs and visualizations. We are also looking at other options, including the use of animations in selective locations of the DLMF, and a stronger Wikipedia presence. Of course, we continue to generate publications, and present talks and displays at a variety of venues to publicize our work [3-12].

[1] J. Behr, P. Eschler, Y. Jung and M. Zollner, X3DOM: a DOM-based HTML5/X3D Integration Model, in *Proceedings of the 14th International Conference on 3D Web Technology (Web3D '09)*, S. N. Spencer, Ed., Darmstadt, Germany, June 16-17, 2009, 127–135.

[2] https://www.khronos.org/webgl/

[3] C. Clark and B. Saunders, DLMF gamma, digamma phase plot display, MICRO/MACRO: Big Images of Small Things from NIST Labs, Johns Hopkins University Montgomery County Campus, Rockville, MD, September 6 – November 11, 2016.

[4] B. Saunders, B. Antonishek, B. Miller and Q. Wang, "Adaptive Curvature-Based Composite Grid Generation Techniques Applied to 3D Visualizations," 9th International Conference on Mathematical Methods for Curves and Surfaces, Tonsberg, Norway, June 23, 2016.

[5] B. Saunders, "Slices of 3D Surfaces on the Web Using Tensor Product B-Spline Grids," SIAM Conference on Geometric and Physical Modeling (GD/SPM15), Salt Lake City, UT, October 12, 2015.

[6] B. Saunders, "Cutting Edge Information Technology Applied to the NIST Digital Library of Mathematical Functions," MAA MathFest 2015, Washington, D.C., August 8, 2015.

[7] B. Saunders, "X3DOM/WebGL Visualizations in the NIST DLMF, Web3D Showcase," 20th International Conference on 3D Web Technology (Web3D 2015), Heraklion, Crete, Greece, June 20, 2015.

[8] B. Saunders, B. Antonishek, Q. Wang and B. Miller, "State of the Art Visualizations of Complex Function Data," International Conference on Orthogonal Polynomials, Special Functions and Applications, NIST, June 4, 2015.

[9] B. Saunders, B. Antonishek, Q. Wang and B. Miller, Dynamic 3D Visualizations of Complex Function Surfaces Using X3DOM and WebGL, in *Proceedings of the 20th International Conference on 3D Web Technology (Web3D 2015)*, Crete, Greece, June 18-21, 2015, 219-225.

[10] B. Saunders, Q. Wang and B. Antonishek, Adaptive Composite B-Spline Grid Generation for Interactive 3D Visualizations, in *Proceedings of MASCOT/ISGG 2012*, Las Palmas de Gran Canaria, Spain, October 22-26, 2012, IMACS Series in Computational and Applied Mathematics **18** (2014), 241-250.

[11] S. Ressler and B. Antonishek, "New WebGL Graphics in the NIST DLMF, Web3D Emerging Technology Showcase," Virginia Tech Research Center, Arlington, VA, March 25, 2014.

[12] B. Saunders, "Adaptive Grid Generation, 3D Graphics on the Web, and a Digital Library," Infinite Possibilities Conference, Oregon State University, Corvallis, Oregon, March 2, 2015.

[13] http://www.shapeways.com/

DLMF Standard Reference Tables on Demand

Bonita Saunders
Bruce Miller
Marjorie McClain
Daniel Lozier
Andrew Dienstfrey
Annie Cuyt (U. Antwerp)
Stefan Becuwe (U. Antwerp)
Franky Backeljauw (U. Antwerp)
Chris Schanzle

http://dlmftables.uantwerpen.be/

The original NBS Handbook of Mathematical Functions [1] was a product of the age of hand computation. Its main purpose was to be a compendium of tables of function values. Today manual interpolation in tables has been superseded by software for evaluating special functions at any argument. Thus, exhaustive tables of function values were not included in the follow-on NIST Digital Library of Mathematical Functions (DLMF) [2].

Nevertheless, there is still a need for a reliable source of function values that are certifiably accurate. This was made even more clear by recent DLMF feedback. An email from Tim Nielsen at Boeing Research & Technology, expressed his desire for a system where he could test a table of function values against reference values. Another DLMF user made the following comment:

> *"It is no longer useful to include large tables of function values for the purpose of interpolation. But a set of test values for each function with various decimal precisions would be useful for developers as they try to test implementations of special functions. This could be the beginning of a benchmark for numeric software."* [9]

Comments like these make it clear that there remains a need for tables, though the size of the potential user base is hard to ascertain.

The DLMF Standard Reference Tables on Demand Project (DLMF Tables) is designed to address this need. The goal is to develop an online service where users can generate tables of special function values with an error certification. The project is a collaboration between the ACMD and the University of Antwerp Computational Mathematics Research Group (CMA).

ACMD is working on the front-end interface while CMA, under the direction of Professor Annie Cuyt, is developing the system's computational engine based on their MpIeee library. MpIeee is an IEEE 754/854 compliant C++ library for mixed precision floating point arithmetic in base 2^n or 10^m. IEEE compliance implies, among other things, that basic arithmetic operations, as well as remainder and square root operations, are rounded correctly, that is, the result of the operation is

Figure 71. *Table of contents for DLMF Tables website.*

Computed values of $J_\nu(x)$

Computed using MpIeee+R(on odd lines), compared to ν, x, $J_\nu(x)$ (on even lines), for ν, x, $J_\nu(x)$ from file Jv_user_valus.txt; output to 12 digits, using interval mode; computation and output in base 10 .

ν	x	$J_\nu(x)$	Relative Error
0	1	7.65197 68655 7 96655±5×10⁻¹	
		7.65197 68655 7 ×10⁻¹	1.3 ×10⁻¹²
5	2	7.03962 97558 7 16855±5×10⁻⁹	
		7.03962 97558 7 ×10⁻⁹	2.4 ×10⁻¹³
10	5	1.46780 26473 1 04745±5×10⁻⁹	
		1.46780 26473 3 ×10⁻⁹	1.4 ×10⁻¹¹
20	50	-1.16704 35275 9 57975±5×10⁻¹	
		-1.16704 35276 0 ×10⁻¹	3.7 ×10⁻¹²

Figure 72. *Output for comparison of DLMF Tables computations with table of function values submitted by user.*

the floating-point value that would be obtained by first computing the exact mathematical value and then rounding it to its floating point representation. IEEE compliance provides a solid foundation for building reliable software [4-8].

A challenging, but critical, part of creating a system such as DLMF Tables is determining the likely users and assessing their needs. To help us address this problem, we have built and publicly released a beta version that includes design features we feel are crucial. By publicizing this fully operational site, we hope to obtain feedback that can be considered as we expand and enhance the service. Currently, users may request a table of values displayed in interval mode with a strict enclosure (upper and lower bounds) or displayed exactly in one of the following rounding modes: round-to-nearest (even), round toward ∞, round toward $-\infty$, round toward 0, round away from 0. Alternatively, the user may upload a data file and request a comparison. The output table will show the reference values displayed in the user-specified mode alternated with the values provided by the user. The approximate relative error is also

shown. Differences between reference values and uploaded values are highlighted in either yellow (warning) or red (error) as shown in Figure 72.

The release of the site has been announced in several places, including the DLMF (as a news item); OP-SF NET, the electronic newsletter of the SIAM Activity Group on Orthogonal Polynomials and Special Functions; and NA-Digest. But, the sparsity of feedback suggests that a more aggressive campaign, including talks at conferences, and announcements and articles in more widely read publications is needed. Also, visibility of DLMF Tables from the DLMF site is crucial.

Our current work is focused in parallel directions designed to increase the site's visibility, enhance its features, and increase the number of functions offered. Some specific activities include working on modifications to a DLMF Tables paper to address feedback from the SIAM Liaison on Orthogonal and Special Functions [10], presenting talks at conferences and workshops [11, 12], making the code changes necessary to view new functions completed by the Antwerp group, and examining recent work on the development of high precision codes that might be relevant to our project [13, 14].

[1] M. Abramowitz and I. Stegun, eds., *Handbook of Mathematical Functions*, Applied Mathematics Series **55**, National Bureau of Standards, Washington, DC, 1964.

[2] NIST Digital Library of Mathematical Functions (DLMF)[12], Release 1.0.10 of 2015-08-07. Online companion to [3].

[3] F. W. J. Olver, D. W. Lozier, R. F. Boisvert and C. W. Clark, eds., *NIST Handbook of Mathematical Functions*, Cambridge University Press, New York, NY. Print companion to [2].

[4] F. Backeljauw, S. Becuwe, A. Cuyt, J. Van Deun and D. Lozier, Validated Evaluation of Special Mathematical Functions, *Science of Computer Programming* **10** (2013), 1016.

[5] M. Colman, A. Cuyt and J. Van Deun, Validated Computation of Certain Hypergeometric Functions, *ACM Transactions on Mathematical Software* **38**:2 (January 2012), Article 11.

[6] F. Backeljauw, A Library for Radix-independent Multiprecision IEEE-compliant Floating-point Arithmetic, Technical Report 2009-01, Department of Mathematics and Computer Science, Universiteit Antwerpen, 2009.

[7] A. Cuyt, V. B. Petersen, B. Verdonk, H. Waadeland and W. B. Jones, *Handbook of Continued Fractions for Special Functions*, Springer, New York, 2008.

[8] A. Cuyt, B. Verdonk and H. Waadeland, Efficient and Reliable Multiprecision Implementation of Elementary and Special Functions, *SIAM Journal of Scientific Computing* **28** (2006), 1437-1462.

[9] E. Smith-Rowland, Personal communication, DLMF Feedback, September 20, 2016.

[10] B. Saunders, B. Miller, F. Backeljauw, S. Becuwe, M. McClain, D. Lozier, A. Cuyt and A. Dienstfrey, DLMF Tables: A Computational Resource Inspired by the NIST Digital Library of Mathematical Functions, in review.

[11] B. Saunders, B. Miller, M. McClain, D. Lozier, A. Dienstfrey, A. Cuyt, S. Becuwe and F. Backeljauw, "DLMF Standard Reference Tables on Demand (DLMF Tables), Minisymposium on Orthogonal Polynomials and Special Functions: Computational Aspects," 2015 International Conference on Orthogonal Polynomials, Special Functions and Applications, NIST, Gaithersburg, MD, June 1, 2015.

[12] B. Saunders, "NIST Projects: Graphics in the Digital Library of Mathematical Functions (DLMF) and DLMF Standard Reference Tables on Demand (DLMF Tables)," Careers in Mathematical Sciences Workshop for Underrepresented Groups, Institute for Mathematics and Its Applications, University of Minnesota, Minneapolis, MN, March 29, 2015.

[13] J. Le Maire, N. Brunie, F. de Dinechin and J. Muller, Computing Floating-point Logarithms with Fixed-point Operations, in *Proceedings of the IEEE 23nd Symposium on Computer Arithmetic (ARITH)*, 2016, 156-163.

[14] N. Brunie, F. de Dinechin, O. Kupriianova and C. Lauter, Code Generators for Mathematical Functions, in *Proceedings of the IEEE 22nd Symposium on Computer Arithmetic (ARITH)*, 2015, 66-67.

Mathematical Knowledge Management

Bruce Miller
Steffen Maas (Jacobs University, Germany)

The general theme of our mathematical knowledge management (MKM) work this year has been the infrastructure supporting the machine representation of semantic content of scientific documents. Both the mathematical semantics as well metadata about the mathematics, such as its source, are of interest here. The primary target of our attention is the Digital Library of Mathematical Functions (DLMF), but also the trove of LaTeX formatted articles in the arXiv[13] (see [1]).

Let us first contrast the two categories of MathML, the W3C standard for representing mathematics. Presentation MathML is used for encoding the layout and appearance of the formula such as viewing in a web browser, while Content MathML is focused on the meaning and hence is potentially useful for computation. The needs and structures of the two are necessarily different, but both forms are desirable. Parallel markup provides the best of both by combining them side-by-side, ideally with the corresponding symbols within each sub-tree cross referenced to each other. With such a system, the symbols within a displayed user-interface

[12] http://dlmf.nist.gov/

[13] http://arxiv.org

can be associated with the underlying semantics, providing a much richer set of queries and operations.

In the DLMF, for example, symbols representing special functions are hyperlinked to their definitions. Recent developments in LaTeXML (our LaTeX to XML converter) generate fully parallel markup from both "semantic" macros and from the result of parsing of the mathematical formula. A tedious set of tree traversals [2] establish which nodes in the presentation and content trees correspond to each other, allowing the cross-referencing to be implemented. As we thus progress towards better content representation of the formula, we must ask what, after all, do those symbols represent?

The DLMF discusses the properties of several hundred special functions of varying degrees of importance and standardization. Even with the most important functions, there can be different argument conventions, definitions or branch cuts used by different communities. For automatic usage, it is critical to be communicate exactly which variant of each function is being discussed. This is the role that OpenMath Content Dictionaries can play in providing a vocabulary of mathematical entities associated with their definitions; different flavors of elliptic function, $\mathrm{sn}(u,k)$ vs. $\mathrm{sn}(u,m)$ for example, would be represented as symbols from different dictionaries; these specific symbols are then embedded in the Content MathML. Thus we set out to refine our collection of semantic macros that we accumulated during the development of the DLMF with an eye to several goals: to round out the feature set; to rationalize the naming scheme based on common usage; and to localize the definition of each symbol within the DLMF. The ulterior goals are publication of the macros so that others may use them and the publication of a set of Content Dictionaries representing the special functions as they are used in the DLMF.

The latter goal takes on an increased significance with the launching of the Special Function Concordance activity and the International Mathematical Knowledge Trust (IMKT) established by the Global Digital Mathematical Library (GDML) working group of the International Mathematical Union. We are participating in this effort to establish a "concordance" between the various special functions, in all their flavors, as used within various handbooks, such as the DLMF, and software systems, such as Mathematica, Maple and NAG, to assure interoperability. Finally, at the broader level of the documents themselves, we are monitoring such efforts as Scholarly HTML[14] and schema.org[15]. Ontologies and vocabularies are being developed by which scientific documents can be enriched with machine-readable metadata representing the roles and relationships between parts of the document and other documents. This data is expected to greatly improve information discovery and search. Towards this end, with summer student Steffen Maas, we have begun to develop markup to encode the sources of information within the DLMF, and found appropriate vocabularies for encoding it. We will thus be able to encode the provenance of (eventually) all the formula in the DLMF.

[1] H. Stammerjohanns, M. Kohlhase, D. Ginev, C. David and B. Miller, Transforming Large Collections of Scientific Publications to XML, *Mathematics in Computer Science* **3**:3 (2010), 299-307.

[2] B. R. Miller, Strategies for Parallel Markup, *Lecture Notes in Artificial Intelligence* **9150** (2015), 203-210.

Part-of-Math Tagging

Abdou Youssef

A part-of-math (POM) tagger, simply stated, determines the mathematical category/role (called tag) of every math symbol in a given math expression or equation. Also, the POM tagger should often be able to determine the mathematical meaning of a symbol by using the symbol's expression-level context and manuscript-level context, as well as broad domain-level and sub-domain-level knowledge. To that end, a tagset for math terms and expressions has been created and will be evolved further as the project advances, and a knowledge base of over 3 000 math symbols has been developed.

The tagger will work in several scans and interact with other mathematical language processing (MLP) algorithms that will be developed in this project. In the first scan of an input math document, each math term and some sub-expressions will be tagged with two kinds of tags. The first consists of definite tags (such as operation, relation, numerator, etc.) that the tagger is certain of. The second kind consists of alternative, tentative features (including alternative roles and meanings) drawn from the knowledge base. The second and third scan will select the right features from among the alternative features computed in the first scan, disambiguate the terms, group subsequences of terms into unambiguous sub-expressions and tag them, and thus derive definite unambiguous semantics of math terms and expressions.

The first scan is done and already being used at NIST for preliminary presentation-to-computation conversion at NIST; see page 99. The next step will be to develop techniques and algorithms for scans two and three.

Math-sense disambiguation is a critical component of POM tagging and of any serious application thereof. We have identified the following ambiguities (described very briefly), for which we will develop disambiguation algorithms:

[14] https://www.w3.org/community/scholarlyhtml/

[15] http://schema.org/

- *Superscript ambiguity*: Is a superscript an exponent, a notation index, or differentiation?
- *Missing-operator ambiguity:* Is a missing operator intended to be multiplication, function application, or something else?
- *Scope ambiguity (or missing-delimiters ambiguity)*: Delimiters (around certain function arguments or around numerators and denominators) are sometimes left out. The intended locations of implicit delimiters are a major math ambiguity to resolve.
- *Definition-overload ambiguity*: Many math symbols have well-known meanings, and yet are sometimes used to stand for something else (e.g., π is used to denote a particular irrational number, but this symbol is often used as something else; i can be $\sqrt{(-1)}$, or a generic index, but is often redefined). Nearly all the letters of the Latin and Greek alphabets are plagued (or blessed!) with the same polysemy problem, and need to be disambiguated.
- *Role ambiguities*: There are function vs. variable vs. parameter ambiguities, and operation vs. relation ambiguities.
- *Punctuation mark ambiguities*: Commas and semicolons can serve as normal punctuation, or as separators between arguments of a function or elements of a sequence, or as connectors between different components of a formula or definition.
- *Fence ambiguities*: A fence (e.g., braces and brackets) can play different roles: (i) as a delimiter, (ii) as a math-object constructor (e.g., such as braces, brackets and parentheses for defining sets and intervals), (iii) as a part of a multi-glyph operator (e.g., "| . |", "< .|", "< . , .> ", etc.), or (iv) even as a relation (as in the case of "<" and ">").
- *Accent ambiguities*: Primes ($'$), over-line(s), over-dot(s), hats, and other accents placed next to, above (or sometimes below) individual symbols, can be an integral accent (a morphological part of the name), or an operator applied on the symbol (e.g., y' and $v\dot{}$ can designate derivatives or simply entity names, $\bar{z}$ can designate the complement of z or the conjugate of complex number z, $\hat{\theta}$ can denote an estimator of parameter θ, etc.).
- *Datatype resolution*: Variables, parameters, operations and relations have data types that would be desirable to determine for more specific semantics.
- *Arity resolution*: Operations and relations have arities (e.g., unary, binary, etc.), and must be determined for full semantics.
- *Signature resolution*: Math functions have signatures, i.e., number and data types of arguments, and number and data types of "returned" values. Function signature need to be determined since they form a key component of function semantics.

[1] M. Schubotz, A. Grigorev, M. Leich, H. S. Cohl, N. Meuschke, B. Gippx, A. Youssef and V. Markl, Semantification of Identifiers in Mathematics for Better Math Information Retrieval, in *Proceedings of the 39th International ACM SIGIR Conference on Research and Development in Information Retrieval*, July 17-21, 2016, Pisa, Italy, 135-144.

[2] Moritz Schubotz, Abdou Youssef, Volker Markl and Howard S. Cohl, Challenges of Mathematical Information Retrieval in the NTCIR-11 Math Wikipedia Task, in *Proceedings of the 38th International ACM SIGIR Conference on Research and Development in Information Retrieval*, August 9-13, 2015, Santiago, Chile, 951-954.

[3] Q. Zhang and A. Youssef, Performance Evaluation and Optimization of Math-Similarity Search, *Lecture Notes in Computer Science* **9150** (2015), Proceedings of the Conference on Intelligent Computer Mathematics (CICM 2015), July 2015, Washington, DC, 243-257.

Automated Presentation-to-Computation Conversion

Abdou Youssef
Howard S. Cohl
Moritz Schubotz (University of Konstanz, Germany)
André Greiner-Petter (Technische Universität Berlin)

For increased efficiency and productivity, and maximum convenience, it is desirable to have computer systems algorithmically convert math expressions and equations into procedures for computing math functions and equations. To make that possible (at least in some situations), it is imperative to determine procedurally and unambiguously the definite mathematical sense of every term in a given mathematical expression, much as the POM tagger will provide. The presentation to computation (P2C) conversion will push the POM tagger to its extreme, uncover issues and subtle ambiguities as yet unknown, and open up new possibilities for mathematical computing.

Howard Cohl and his team have already started to use the first scan of the POM tagger to convert a fairly large set of mathematical expressions (written in LaTeX and some pre-defined macros) to Maple expressions, with considerable success. The preliminary results of this P2C conversion are quite encouraging, and prompt us to pursue this application of POM tagging more fully once the whole POM tagger (especially its disambiguation modules) have been completed.

NIST Digital Repository of Mathematical Formulae

Howard S. Cohl
Marjorie A. McClain
Bonita V. Saunders
Abdou Youssef
Moritz Schubotz (University of Konstanz, Germany)
André Greiner-Petter (Technische Universität Berlin)
Alan P. Sexton (University of Birmingham, UK)
Yash Kapoor (Clarksburg High School)
Rahul Shah (Clarksburg High School)
Sourabh Vellala (Poolesville High School)
Seong Joon Yoo (Poolesville High School)
Oksana Tkach (Poolesville High School)
Claude Zou (Poolesville High School)
Joon Bang (Poolesville High School)
Kevin Chen (Poolesville High School)
Edward Bian (Poolesville High School)
Jagan Prem (Poolesville High School)
Kevin Shen (Poolesville High School)
Philip Wang (Poolesville High School)
Parth Oza (Poolesville High School)

http://drmf.wmflabs.org/wiki/Main_Page

The NIST Digital Repository of Mathematical Formulae (DRMF) is a Wiki-based compendia of formulae for orthogonal polynomials and special functions (OPSF) designed to (1) facilitate interaction among a community of mathematicians and scientists interested in OPSF; (2) be expandable, allowing the input of new formulae from the literature; (3) provide information for related linked open data projects; (4) represent the context-free full semantic information concerning individual formulas; (5) have a user friendly, consistent, and hyperlinkable viewpoint and authoring perspective; (6) contain easily searchable mathematics; and (7) take advantage of modern MathML tools for easy-to-read, scalably rendered content-driven mathematics. Our DRMF implementation is built using MediaWiki, the wiki software used by Wikipedia. See Figure 74 for a sample DRMF formula home page. The DRMF has been described in a series of publications and talks [1-6].

A key asset in the development of DRMF context-free semantic content is the utilization of a set of LaTeX macros originally created by Bruce Miller (ACMD) to achieve the encapsulation of semantic information within the NIST Digital Library of Mathematical Functions (DLMF) [7]. These macros give us the capability to tie LaTeX commands in a mostly unambiguous way to mathematical functions defined in an OPSF context. There are currently 533 DLMF LaTeX macros, as well as an additional 156 which have been created specifically for the DRMF. All DLMF macros have at least one DLMF web page associated with them, and the goal is to have definition pages for all additional DRMF macros. The use of DLMF and DRMF macros guarantees mathematical and structural consistency throughout the DRMF. We refer to LaTeX source with incorporated DLMF and DRMF macros as semantic LaTeX.

DRMF formula seeding is currently focused on

(1) DLMF chapters 5 (Gamma Functions), 15 (Hypergeometric Function), 16 (Generalized Hypergeometric Functions and Meijer G-Function), 17 (q-Hypergeometric and Related Functions), 18 (Orthogonal Polynomials), and 25 (Zeta and Related Functions);

(2) Koekoek, Lesky, and Swarttouw (KLS) chapters 1 (Definitions and Miscellaneous Formulas), 9 (Hypergeometric Orthogonal Polynomials), and 14 (Basic Hypergeometric Orthogonal Polynomials) [8];

(3) Koornwinder KLS addendum LaTeX data [9];

(4) Bateman Manuscript Project (BMP) books [10];

(5) Wolfram Computational Knowledge of Continued Fractions Project (eCF);

(6) Continued Fractions for Special Function (CFSF) Maple dataset hosted by the University of Antwerp [11].

In August, 2014, the DRMF Project obtained permission and license to use BMP material as seed content for the DRMF from Adam Cochran, Associate General Counsel of Caltech. Caltech has loaned us copies of the BMP. We have forwarded these copies to Alan Sexton, Scientific Document Analysis Group, School of Computer Science, University of Birmingham, UK. Sexton has scanned the BMP and is developing software to perform mathematical optical character recognition to obtain LaTeX source. To enhance the development process of the OCR software, we have developed an automated testing framework that uses visual diffs of the original scanned source and the rendering of the generated LaTeX source.

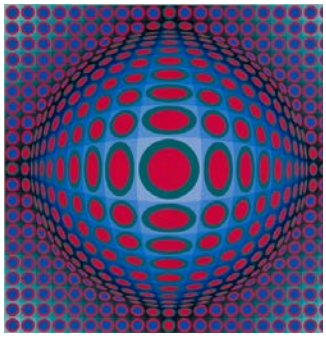

Figure 73. *DRMF Logo*

With regard to the seed project (1), the DLMF source already has DLMF macros inserted. However, for seed projects (2-6), we are developing Python and Java software to incorporate DLMF and DRMF macros into the corresponding LaTeX source. Our coding efforts have also focused on extracting formula data from LaTeX source as well as generating DRMF Wikitext. We are developing Python software for the seeding of the eCF and CFSF projects which involve conversion

from Mathematica and Maple format to DLMF and DRMF macro incorporated LaTeX.

Current and future DRMF MediaWiki development projects include the production of formula output representations (such as semantic LaTeX, MathML, Mathematica, Maple, and Sage); incorporation of sophisticated DLMF and DRMF macro related formula search; and the development of capabilities for user community formula input. In this vein, Abdou Youssef has written a grammar-based mathematical language processor (MLP) that uses JavaCC to parse mathematical LaTeX expressions. Based on the MLP, André Greiner-Petter has developed a Java tool to convert mathematical LaTeX expressions, which contains DLMF and DRMF macros, to a given computer algebra system source format. This Java tool provides further information of the conversion about possible ambiguities and differences in definitions, domains and branch cuts between the semantic LaTeX source and the CAS source. Furthermore, it is designed to be easily extendable to other computer algebra systems and currently supports Maple and Mathematica input sources.

Our current DRMF server, both public and development instances, have been deployed using the Wikitech server of the Wikimedia Foundation in San Francisco. We use the vagrant virtualization service and configure our machines using puppet roles, which fully automates the installation of new testing or deployment instances. For an efficient data import, we rely on the standard MediaWiki XML Dump format.

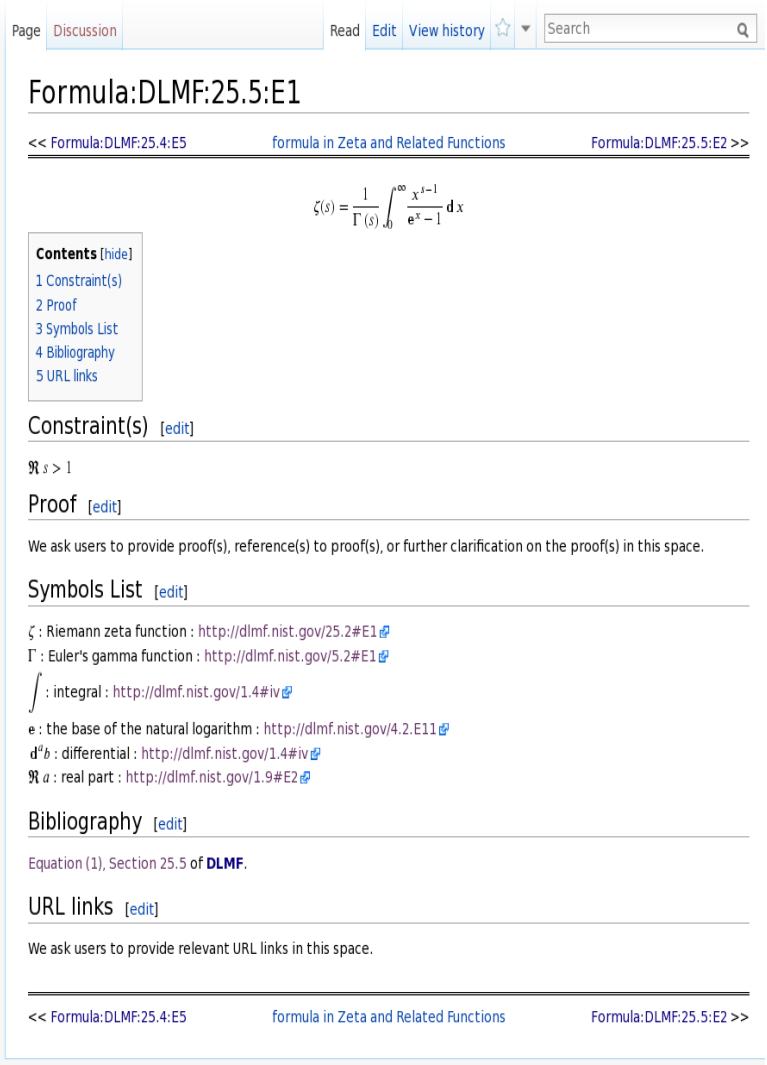

Figure 74. *Sample DRMF formula home page.*

The DLMF Chapter 25 source has been uploaded to the Wikitech instances as well as the KLS and KLSadd datasets, which have been uploaded for a total of 1842 Wikitext pages [3]. This includes 1 Main page, 1 Bibliography page, 1 Common.css page, 1 DRMF Requirements page, 2 Table of Contents Pages, 76 Lists of Formulas Pages, 124 Definition Pages, and 1636 Formula Home Pages.

By working with Andrea Fisher-Scherer, Rights Administrator, Artists Rights Society, New York, NY, we have received permission from Foundation Vasarely, to use an image of one of Victor Vasarely's paintings as a DRMF logo; see Figure 73.

[1] H. S. Cohl, M. A. McClain, B. V. Saunders, M. Schubotz and J. C. Williams, Digital Repository of Mathematical Formulae, *Lecture Notes in Artificial Intelligence* **8543** (2014), Proceedings of the Conferences on Intelligent Computer Mathematics 2014, Coimbra, Portugal, July 7-11, 2014, (S. M. Watt, J. H. Davenport, A. P. Sexton, P. Sojka and J. Urban, eds.), Springer, 419-422.

[2] H.S. Cohl, M. Schubotz, M.A. McClain, B. V. Saunders, Cherry Y. Zou, Azeem S. Mohammed and Alex A. Danoff, *Lecture Notes in Artificial Intelligence* **9150** (2015), Proceedings of the Conference on Intelligent Computer Mathematics 2015, Washington DC, USA, July 13-17, 2015, (M. Kerber, J. Carette, C. Kaliszyk, F. Rabe and V. Sorge, eds.), Springer, 280-287.

[3] H. S. Cohl, M. A. McClain, B. V. Saunders and M. Schubotz, "Outgrowths of the Digital Library of Mathematical Functions Project, Part II: NIST Digital Repository of Mathematical Formulae," Workshop on Challenges in 21st Century Experimental Mathematical Computation, Institute for Computational and Experimental Research in Mathematics, Providence, Rhode Island, July, 2014.

[4] H. S. Cohl, M. A. McClain, B. V. Saunders, M. Schubotz, A. Danoff, J. Li, J. Migdall, A. Liu, C. Zou, A. Mohammed and S. Madhu, "XSEDE and the NIST Digital Repository of Mathematical Formulae" XSEDE Science Gateways Community Series, August 2014.

[5] M. Schubotz, "Implicit Content Dictionaries in the NIST Digital Repository of Mathematical Formulae," OpenMath Workshop, 9th Conference on Intelligent Computer Mathematics, CICM 2016, Bialystok, Poland.

[6] M. Schubotz, "The NIST Digital Repository of Mathematical Formulae and Scalable Math Search," ACMD Seminar Series, NIST, Gaithersburg, MD, July 24, 2015.

[7] B. Miller, "Drafting DLMF Content Dictionaries," OpenMath Workshop, 9th Conference on Intelligent Computer Mathematics, CICM 2016, Bialystok, Poland.

[8] R. Koekoek, P. A. Lesky and R. F. Swarttouw, *Hypergeometric Orthogonal Polynomials and their q-Analogues*, Springer Monographs in Mathematics, Springer-Verlag, Berlin, 2010.

[9] T. H. Koornwinder, Additions to the Formula Lists in *Hypergeometric Orthogonal Polynomials and their q-analogues by Koekoek, Lesky and Swarttouw*, arXiv:1401.0815, June 2015.

[10] A. Erdelyi, W. Magnus, F. Oberhettinger and F. G. Tricomi, *Higher Transcendental Functions*, Vols. I, II, III, Robert E. Krieger Publishing Co., Melbourne, FL, 1981.

[11] M. Cuyt, V. Petersen, H. Waadeland, W. B. Jones, F. Backeljauw, C. Bonan-Hamada and S. Becuwe, *Handbook of Continued Fractions for Special Functions*, Springer, New York, 2008.

Fundamental Solutions and Expansions for Special Functions and Orthogonal Polynomials

Howard S. Cohl
Roberto S. Costas-Santos (University of Alcalá, Spain)
Hans Volkmer (University of Wisconsin-Milwaukee)
Gestur Olafsson (Louisiana State University)
Michael A. Baeder (Citigroup Inc.)
Rebekah M. Palmer (Temple University)
Jessica E. Hirtenstein (University of California Davis)
Philbert R. Hwang (University of Maryland)
Wenqing Xu (Caltech)
Justin Park (Poolesville High School)
Tanay Wakhare (University of Maryland)
Thinh H. Dang (George Washington University)
Sean J. Nair (Montgomery Blair High School)

The concept of a function expresses the idea that one quantity (the input) completely determines another quantity (the output). Our research concerns special functions and orthogonal polynomials. A *special function* is a function that has appeared in the mathematical sciences so often that it has been given a name. Green's functions (named after the British mathematician George Green, who first developed the concept in the 1830s) describe the influence of linear natural phenomena such as electromagnetism, gravity, heat and waves. For example, in electrostatics, a Green's function describes the influence of a point charge, called the source, over all of space. The inputs for Green's functions are all of space (except for a singular region), and the output is the "force" exerted from the point throughout space. Green's functions are fundamental to the study of inhomogeneous partial differential equations and are powerful in that they provide a mechanism for obtaining their solutions.

We investigate fundamental solutions (Green's functions) of linear partial differential equations on highly symmetric Riemannian manifolds (harmonic, rank-one symmetric spaces) such as real, complex, quaternionic, and octonionic Euclidean, hyperbolic, and projective spaces. Our recent focus has been on applications of fundamental solutions for linear elliptic partial differential operators on spaces of constant curvature. For instance, we have an accepted paper [1] which derives fundamental solution expansions (azimuthal Fourier and Gegenbauer) with applications to Newtonian potential theory on d-dimensional spaces of constant positive curvature, namely hyperspherical geometry. We have also recently constructed closed-form expressions of a fundamental solution for the Helmholtz equation in d-dimensional spaces of constant negative curvature, namely the hyperboloid model of hyperbolic geometry, in terms of associated Legendre and Ferrers functions. We also continue our ongoing harmonic analysis of fundamental solutions for Laplace's equation on rank one symmetric spaces of compact and noncompact type.

In the following sequence of efforts, we derive specializations and generalizations of generalized and basic hypergeometric orthogonal polynomial generating functions as well as corresponding definite integrals using orthogonality.

- In Baeder, Cohl, Costas-Santos, and Xu [2], we present the power collection method for hypergeometric orthogonal polynomials, and summarize for which orthogonal polynomials in the Askey and q-Askey schemes, it can be applied. We apply the power collection method to Meixner polynomials and compute a series of connection and connection-type relations for these orthogonal polynomials. We also apply these connection and connection-type relations to generating functions for Meixner and Krawtchouk polynomials.
- In Cohl, Costas-Santos, and Xu [3], we present contour integral orthogonality relations for the Al-Salam-Carlitz polynomials which are valid for arguments in the complex plane and complex-valued parameters. We also compute generalized generating functions for

the Al-Salam-Carlitz polynomials using connection relations for these polynomials.

- In Cohl, Nair, and Palmer [4], we derive definite integrals for Bessel functions of the first kind by applying the method of integral transforms (Hankel transform) to know definite integrals which are found in famous compendia of definite integrals.
- In Cohl, Hirtenstein and Volkmer [5], we derive explicit bounds of convergence for an integral addition theorem due to Magnus which expresses a Kummer confluent hypergeometric function of the second kind $U(x+y)$ as an integral over a product of U with argument x and U with argument y. We also show how this integral addition theorem can also be expressed in terms of modified parabolic cylinder functions, Hankel, Macdonald, and Bessel functions of the first and second kind with order zero and one.
- In Cohl, Costas-Santos, Hwang, Wakhare [6], we derive generalizations of generating functions for basic hypergeometric orthogonal polynomials, namely Askey-Wilson, continuous q-Jacobi, continuous q-ultraspherical/Rogers, q-Laguerre, and little q-Laguerre. We also derive a new quadratic transformation for basic hypergeometric functions using a result of Ismail and Simeonov.

There are several connections with conferences for this project. For instance, Cohl served on both the scientific and local organizing committees for the 13th International Symposium on Orthogonal Polynomials, Special Functions and Applications which was held on June 1-5, 2015 at NIST, and is now serving as guest editor for the proceedings of that conference in the journal *Symmetry, Integrability and Geometry: Methods and Applications* [7]. Cohl also served on the Scientific and Local Organizing committees for the Orthogonal Polynomials and Special Functions Summer School 6 (OPSF-S6) workshop held on June 17-23, 2016 at the Norbert Wiener Center for Harmonic Analysis and Applications at the University of Maryland, and is now acting as editor for the lecture notes which will most likely be published with Cambridge University Press. This OPSF-S6 summer school was co-organized with Daniel Lozier, Mourad Ismail, and Kaso Okoudjou.

[1] H. S. Cohl and R. M. Palmer, Fourier and Gegenbauer Expansions for a Fundamental Solution of Laplace's Equation in Hyperspherical Geometry, *Symmetry, Integrability and Geometry: Methods and Applications* **11** (2015), 15.

[2] M. A. Baeder, H. S. Cohl, R. S. Costas-Santos and W. Xu, The Power Collection Method for Connection Relations: Meixner Polynomials, in review.

[3] H. S. Cohl, R. S. Costas-Santos and W. Xu, The Orthogonality of Al-Salam-Carlitz Polynomials for Complex Parameters, in *Frontiers in Orthogonal Polynomials and q-Series*, (Z. Nashed and X. Li, eds.), World Scientific Publishing (2017), to appear.

[4] H. S. Cohl, S. J. Nair and R. M. Palmer, Some Dual Definite Integrals for Bessel Functions, *Scientia, Series A, Mathematical Sciences* **27** (2016).

[5] H. S. Cohl, J. E. Hirtenstein and H. Volkmer, Convergence of Magnus Integral Addition Theorems for Confluent Hypergeometric Functions, *Integral Transforms and Special Functions* **27**:10 (2016).

[6] H. S. Cohl, R. S. Costas-Santos, P. R. Hwang and T. Wakhare, Generalizations of Generating Functions for Basic Hypergeometric Orthogonal Polynomials, in review.

[7] H. S. Cohl, ed., Report from the Open Problems session at OPSFA13, with Richard A. Askey, Rick K. Beatson, Ted S. Chihara, Charles F. Dunkl, Christoph Koutschan, Sheehan Olver, Yuan Xu, Wolfgang zu Castell, Wadim Zudilin, *Symmetry, Integrability and Geometry: Methods and Applications* **12** (2016), 71.

Part IV

Activity Data

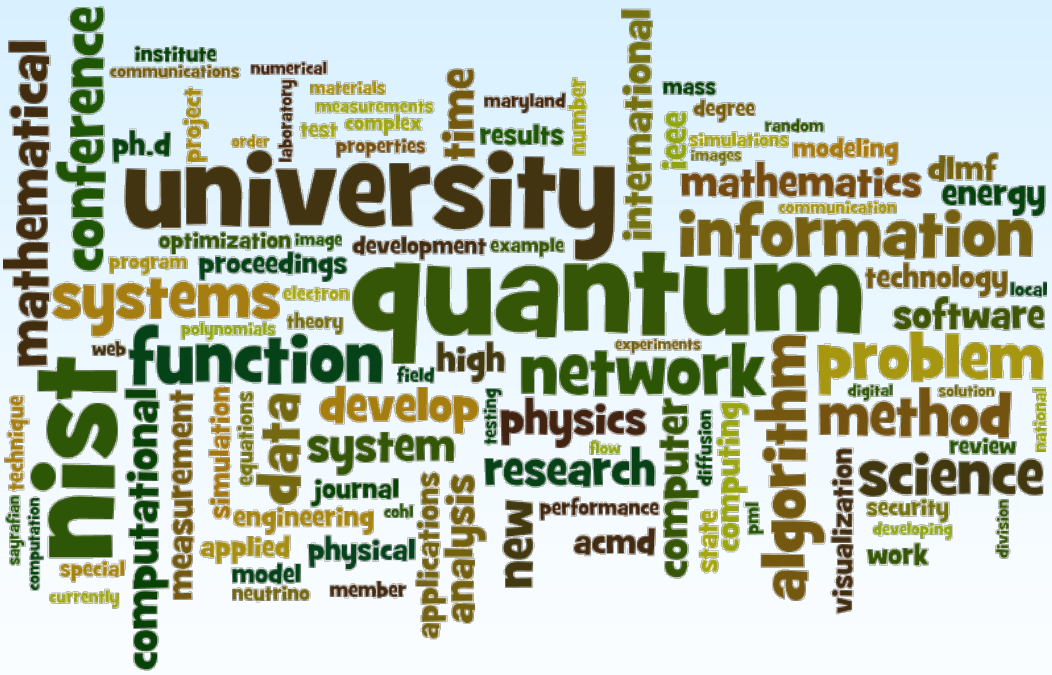

Publications

Note: Names of (co-)authors with a Division affiliation during this reporting period are underlined.

Appeared

Refereed Journals

1. G. Alagic, M. Jarret and S. Jordan, Yang-Baxter Operators Need Quantum Entanglement to Distinguish Knots, *Journal of Physics A* **49** (2016), 075203. DOI: 10.1088/1751-8113/49/7/075203
2. B. Alpert, E. Ferri, D. Bennett, M. Faverzani, J. Fowler, A. Giachero, J. Hays-Wehle, M. Maino, A. Nucciotti, A. Puiu, D. Swetz and J. Ullom, Algorithms for Identification of Nearly-Coincident Events in Calorimetric Sensors, *Journal of Low Temperature Physics* **184** (2016), 263-273. DOI: 10.1007/s10909-015-1402-y
3. R. Askey, R. Beatson, T. Chihara, H. Cohl, C. Dunkl, C. Koutschan, S. Olver, Y. Xu, W. Zu Castell and W. Zudilin, Report from the Open Problems Session at OPSFA13, *Symmetry, Integrability and Geometry: Methods and Applications* **12** (2016), 071. DOI: 10.3842/SIGMA.2016.071
4. N. Bao, A. Bouland and S. Jordan, Grover Search and the No-Signaling Principle, *Physical Review Letters* **117** (2016), 120501. DOI: 10.1103/PhysRevLett.117.120501
5. P. Bierhorst, Geometric Decompositions of Bell Polytopes with Practical Applications, *Journal of Physics A: Mathematical and Theoretical* **49** (2016), 215301. DOI: 10.1088/1751-8113/49/21/215301
6. T. Burns, S. Mates, R. Rhorer, E. Whitenton and D. Basak, Inverse Method for Estimating Shear Stress in Machining, *Journal of the Mechanics and Physics of Solids* **86** (2016), 220-236. DOI: 10.1016/j.jmps.2015.10.008
7. A. Carasso, Stable Explicit Time Marching in Well-Posed or Ill-Posed Nonlinear Parabolic Equations. *Inverse Problems in Science and Engineering* **24** (2016), 1364-1384. DOI: 10.1080/17415977.2015.1110150
8. A. Carasso, Stable Explicit Stepwise Marching Scheme in Ill-Posed Time-Reversed Viscous Wave Equations. *Inverse Problems in Science and Engineering* **24** (2016), 1454-1474. DOI: 10.1080/17415977.2015.1124429.
9. C. Cho, J. Lee, P. Hale, J. Jargon, P. Jeavons, J. Schlager and A. Dienstfrey, Calibration of Time-Interleaved Errors in Digital Real-Time Oscilloscopes, *IEEE Transactions on Microwave Theory and Techniques* **64**:11, (2016), 4071-4079. DOI: 10.1109/TMTT.2016.2614928
10. B. Cloteaux, Is This for Real? Fast Graphicality Testing, *Computing in Science & Engineering* **17**:6 (2015), 91-95. DOI: 10.1109/MCSE.2015.125
11. B. Cloteaux, Fast Sequential Creation of Random Realizations of Degree Sequences, *Internet Mathematics*, **12**:3 (2016), 205-219. DOI: 10.1080/15427951.2016.1164768.
12. H. Cohl, J. Hirtenstein and H. Volkmer, Convergence of Magnus Integral Addition Theorems for Confluent Hypergeometric Functions, *Integral Transforms and Special Functions* **27**:10 (2016), 767-774. DOI: 10.1080/10652469.2016.1198792
13. H. Cohl, S. Nair and R. Palmer, Some Dual Definite Integrals for Bessel Functions, *Scientia, Series A, Mathematical Sciences*, **27** (2016), 15-30. URL: http://www.mat.utfsm.cl/scientia/archivos/vol27/Articulo-2.pdf
14. S. Eichstadt, V. Wilkens, A. Dienstfrey, P. Hale, B. Hughes and C. Jarvis, On Challenges in the Uncertainty Evaluation for Time-Dependent Measurements, *Metrologia* **53**:4 (2016), S125-S135. DOI: 10.1088/0026-1394/53/4/S125
15. J. Fong, J. Filliben, N. Heckert, P. Marcal, R. Rainsberger and L. Ma, Uncertainty Quantification of Stresses in a Cracked Pipe Elbow Weldment Using a Logistic Function Fit, a Nonlinear Least Squares Algorithm, and a Super-Parametric Method, *Procedia Engineering* **130** (2015), 135-149. DOI: 10.1016/j.proeng.2015.12.183
16. J. W. Fowler, B. Alpert, W.B. Doriese, Y. I. Joe, G. O'Neil, J. Ullom and D. Swetz, The Practice of Pulse Processing, *Journal of Low Temperature Physics* **184** (2016), 374-381. DOI: 10.1007/s10909-015-1380-0
17. S. Fu, W. Cui, M. Hu, R. Chang, M. Donahue and V. Lomakin, Finite Difference Micromagnetic Solvers with the Object Oriented Micromagnetic Framework on Graphics Processing Units, *IEEE Transactions on Magnetics* **52** (2016), 7100109. DOI: 10.1109/TMAG.2015.2503262
18. J. Gaebler, T. Tan, Y. Lin, Y. Wan, R. Bowler, A. Keith, S. Glancy, K. Coakley, E. Knill, D. Leibfried and D. Wineland, High-Fidelity Universal Gate Set for $^{9}Be^{+}$ Ion Qubits, *Physical Review Letters* **117** (2016), 060505. DOI: 10.1103/PhysRevLett.117.060505
19. A. Garcia, N. Warner, N. D'Souza, E. Tuncer, L. Nguyen, M. Denison and J. Fong, Reliability of High-Voltage Molding Compounds: Particle Size, Curing Time, Sample Thickness, and Voltage Impact on Polarization, *IEEE Transactions on Industrial Electronics* **63**:111 (2016), 7104-711. DOI: 10.1109/TIE2016.2585467.

20. M. Jarret, S. Jordan and B. Lackey, Adiabatic Optimization versus Diffusion Monte Carlo, *Physical Review A* **94** (2016), 042318. DOI: 10.1103/PhysRevA.94.042318

21. R. Kacker, R. Kessel and J. Lawrence, Removing Divergence of JCGM Documents from the GUM (1993) and Repairing Other Defects, *Measurement*, **88** (2016), 194-201. DOI: 10.1016/j.measurement.2016.03.057

22. Y. Kemper and I. Beichl, Approximating the Chromatic Polynomial, *Congressus Numerantium* **125** (2015), 127-152. Preprint: https://arxiv.org/abs/1608.04883

23. D. R. Kuhn, R. Kacker and Y. Lei, Measuring and Specifying Combinatorial Coverage of Test Input Configurations, *Innovations in Systems and Software Engineering – A NASA Journal* **12**:4 (2015), 249-261. DOI: 10.1007/s11334-015-0266-2

24. R. La, Interdependent Security with Strategic Agents and Global Cascades, *IEEE/ACM Transactions on Networking* **24**:3 (2016), 1378-1391. DOI: 10.1109/TNET.2015.2408598

25. Y. Lin, J. Gaebler, F. Reiter, T. Tan, R. Bowler, Y. Wan, A. Keith, E. Knill, S. Glancy, K. Coakley, A. Sørensen, D. Leibfried and D. Wineland, Preparation of Entangled States Through Hilbert Space Engineering, *Physical Review Letters* **117** (2016), 14052. DOI: 10.1103/PhysRevLett.117.140502

26. H. Mahboubi, W. Masoudimansour, A. Aghdam and K. Sayrafian, Maximum Lifetime Strategy for Target Monitoring with Controlled Node Mobility in Sensor Networks with Obstacles, *IEEE Transactions on Automatic Control* **61**:11 (2016), 3493-3508. DOI: 10.1109/TAC.2016.2536800

27. H. Mahboubi, A. Aghdam and K. Sayrafian, Toward Autonomous Mobile Sensor Networks Technology, *IEEE Transactions on Industrial Informatics* **12**:2 (2016), 576-586. DOI: 10.1109/TII.2016.2521710

28. P. Marcal, J. Fong, R. Rainsberger and L. Ma, Finite Element Analysis of a Pipe Elbow Weldment Creep-Fracture Problem Using an Extremely Accurate 27-Node Tri-Quadratic Shell and Solid Element Formulation, *Procedia Engineering* **130** (2015), 1110-1120. DOI: 10.1016/j.proeng.2015.12.275

29. L. Miaja-Avila, G. C. O'Neil, Y. I. Joe, B. Alpert, N. H. Damrauer, W. B. Doriese, S. M. Fatur, J. W. Fowler, G. C. Hilton, R. Jimenez, C. D. Reintsema, D. R. Schmidt, K. L. Silverman, D. S. Swetz, H. Tatsuno and J. Ullom, Ultrafast Time-Resolved Hard X-Ray Emission Spectroscopy on a Tabletop, *Physical Review X* **6** (2016), 031047. DOI: 10.1103/PhysRevX.6.031047

30. S. Mitropoulos, V. Tsiantos, K. Ovaliadis, D. Kechrakos and M. Donahue, Stiff Modes in Spinvalve Simulations with OOMMF, *Physica B-Condensed Matter* **486** (2016), 169–172. DOI: 10.1016/j.physb.2015.10.010

31. K. M. Morgan, B. Alpert, D. A. Bennett, E. V. Denison, W. B. Doriese, J. W. Fowler, J. D. Gard, G. C. Hilton, K. D. Irwin, Y. I. Joe, G. C. O'Neil, C. D. Reintsema, D. R. Schmidt, J. Ullom, D. Swetz, Code-Division-Multiplexed Readout of Large Arrays of TES Microcalorimeters, *Applied Physics Letters* **109** (2016), 112604. DOI: 10.1063/1.4962636

32. P. Patrone, A. Dienstfrey, A. Browning, S. Tucker and S. Christensen, Uncertainty Quantification in Molecular Dynamics Studies of the Glass Transition Temperature, *Polymer* **87**:22 (2016), 246-259. DOI: 10.1016/j.polymer.2016.01.074

33. P. Patrone, T. Rosch and F. Phelan Jr., Bayesian Calibration of Coarse-Grained Forces: Efficiently Addressing Transferability, *Journal of Chemical Physics* **144** (2016), 154101. DOI: 10.1063/1.4945380.

34. J. Penczek, S. Satterfield, E. Kelley, T. Scheitlin, J. Terrill and P. Boynton, Evaluating the Visual Performance of Stereoscopic Immersive Display Systems, *Presence: Teleoperators and Virtual Environments*, **24**:4 (2015), 279-297. DOI: 10.1162/PRES_a_00235

35. F. Potra, Sufficient Weighted Complementarity Problems, *Computational Optimization and Applications* **64**:2 (2016), 467-488. DOI: 10.1007/s10589-015-9811-z

36. S. Pourarian, A. Kearsley, J. Wen and A. Pertzborn, Efficient and Robust Optimization for Building Energy Simulation, *Energy and Buildings* **122** (2016), 53-62. DOI: 10.1016/j.enbuild.2016.04.019

37. K. Sayrafian and K. Y. Yazdandoost, Toward 5G Emerging Technologies: Selected Papers from IEEE PIMRC 2014, *International Journal of Wireless Information Networks* **22**:4 (2015), 295-297. DOI: 10.1007/s10776-015-0289-5

38. R. Sekerka, G. McFadden and W. Boettinger, Analytical Derivation of the Sauer Freise Flux Equation for Multicomponent Multiphase Diffusion Couples with Variable Partial Molar Volumes, *Journal of Phase Equilibria and Diffusion* **37**:6 (2016), 640-650. DOI: 10.1007/s11669-016-0500-0

39. L. Shalm, E. Meyer-Scott, B. Christensen, P. Bierhorst, M. Wayne, M. Stevens, T. Gerrits, S. Glancy, D. Hamel, M. Allman, K. Coakley, S. Dyer, C. Hodge, A. Lita, V. Verma, C. Lambrocco, E. Tortorici, A. Migdall, Y. Zhang, D. Kumor, W. Farr, F. Marsili, M. Shaw, J. Stern, C. Abellan, W. Amaya, V. Pruneri, T. Jennewein, M. Mitchell, P. Kwiat, J.

Bienfang, R. Mirin, E. Knill and S. Nam, A Strong Loophole-Free Test of Local Realism, *Physical Review Letters* **115** (2015), 250402. DOI: 10.1103/PhysRevLett.115.250402

40. C. Shen, R. Heeres, P. Reinhold, L. Jiang, Y.-K. Liu, R. Schoelkopf and L. Jiang, Optimized Tomography of Continuous Variable Systems Using Excitation Counting, *Physical Review A* **94**:5 (2016), 052327. DOI: 10.1103/PhysRevA.94.052327

41. D. E. Simos, D. R. Kuhn, A. G. Voyiatzis and R. N. Kacker, Combinatorial Methods in Security Testing, *IEEE Computer* **49** (2016), 80-83. DOI: 10.1109/MC.2016.314

42. O. Slattery, L. Ma, P. Kuo and X. Tang, Narrow-Linewidth Source of Greatly Non-Degenerate Photon Pairs for Quantum Repeaters from a Short Singly Resonant Cavity, *Applied Physics B* **121** (2015), 413-419. DOI: 10.1007/s00340-015-6198-6

43. J. Torres-Jimenez, N. Rangel-Valdez, R. Kacker and J. Lawrence, Combinatorial Analysis of Diagonal, Box, and Greater-Than Polynomials as Parking Functions, *Applied Mathematics and Information Sciences* **9**:6 (2015), 2757-2766. DOI: 10.12785/amis/090601

44. W. Wang, S. Sampath, Y. Lei, R. Kacker, D. Kuhn and J. Lawrence, Using Combinatorial Testing to Build Navigation Graphs for Dynamic Web Applications, *Journal of Software Testing, Verification and Reliability* **26** (2016), 318-346. DOI: 10.1002/stvr.1599

45. J. Wu, A. Martin and R. Kacker, Validation of Nonparametric Two-sample Bootstrap in ROC Analysis on Large Datasets, *Communications in Statistics – Simulation and Computation* **45**:5 (2016), 1689-1700. DOI: 10.1080/03610918.2015.1065327

Journal of Research of NIST

1. F. Hunt, An Algorithm for Identifying Optimal Spreaders in a Random Walk Model of Network Communication, *Journal of Research of the NIST*, **121** (2016), 180-195. DOI: 10.6028/jres.121.008

2. R. Pozo, Q-matrix: An Algebraic Formulation for the Analysis and Visual Characterization of Network Graphs, *Journal of Research of the NIST* **121** (2016), 1-16. DOI: 10.6028/jres.121.001

Books

1. M. Kohlhase, M. Johansson, B. R. Miller and L. de Moura, F. Tompa (Editors), *Proceedings of Conference on Intelligent Computer Mathematics*, Bialystok, Poland, July 25-29, 2016, Lecture Notes in Artificial Intelligence **9791**, Springer. DOI: 10.1007/978-3-319-42547-4

Book Chapters

1. K. Sayrafian (Section Editor), Wireless Body Area Communications, Chapter 5 of *Cooperative Radio Communications for Green Smart Environments*, (N. Cardona, Ed.), River Publishers, June 2016. URL: http://www.riverpublishers.com/book_details.php?book_id=318

2. B. Schneider, X. Guan and K. Bartschat, Time Propagation of Partial Differential Equations Using the Short Iterative Lanczos Method and Finite-Element Discrete Variable Representation, Chapter 5 of *Concepts of Mathematical Physics in Chemistry: A Tribute to Frank E. Harris – Part B*, Advances in Quantum Chemistry **72**, Elsevier, 2016. DOI: 10.1016/bs.aiq.2015.12.002

In Conference Proceedings

1. M. Barbi, K. Sayrafian and M. Alasti, Impact of the Energy Detection Threshold on Performance of the IEEE 802.15.6 CSMA/CA, in *Proceedings of the 2015 IEEE Conference on Standards for Communications & Networking* (CSCN'15), Tokyo, Japan, Oct. 28-30, 2015. DOI: 10.1109/CSCN.2015.7390448

2. M. Barbi, K. Sayrafian and M. Alasti, Using RTS/CTS to Enhance the Performance of IEEE 802.15.6 CSMA/CA, in *Proceedings of the IEEE 27th Annual International Symposium on Personal, Indoor and Mobile Radio Communications* (PIMRC), Valencia, Spain, Sept 4-7, 2016. DOI: 10.1109/PIMRC.2016.7794841

3. J. Bernal, G. Doğan and C. Hagwood, Fast Dynamic Programming for Elastic Registration of Curves, in *Proceedings of IEEE Conference on Computer Vision and Pattern Recognition Workshops*, Las Vegas, NV, June 26 - July 1, 2016, 1066-1073. DOI: 10.1109/CVPRW.2016.137

4. D. Budic, D. Simunic and K. Sayrafian, Kinetic-Based Micro Energy-Harvesting for Wearable Sensors, in *Proceedings of the 6th IEEE International Conference on Cognitive Infocommunications* (IEEE Coginfocom 2015), Gyor, Hungary, Oct. 19-21, 2015. DOI: 10.1109/CogInfoCom.2015.7390645

5. J. Chandrasekaran, L. Ghandehari, Y. Lei, R. Kacker and D. Kuhn, Evaluating the Effectiveness of BEN in Localizing Different Types of Software Fault, in *Proceedings of the Ninth IEEE International Conference on Software Testing, Verification and Validation Workshops* (ICSTW), 26-34, Chicago, IL, April 10-15, 2016. DOI: 10.1109/ICSTW.2016.44

6. H. Cohl, M. Schubotz, M. McClain, B. Saunders, C. Zou, A. S. Mohammed and A. A. Danoff, Growing the Digital Repository of Mathematical

Formulae with Generic LaTeX Sources, in *Proceedings of the Conference on Intelligent Computer Mathematics, Lecture Notes in Artificial Intelligence* **9150** (2015)**,** 280-287. DOI: 10.1007/978-3-319-20615-8_18

7. M. Schubotz, D. Veenhuis and H. S. Cohl, Getting the Units Right, in *Joint Proceedings of the FM4M, MathUI, and ThEdu Workshops, Doctoral Program, and Work in Progress at the Conference on Intelligent Computer Mathematics 2016*, December 22, 2016. URL: http://www.cicm-conference.org/2016/ceur-ws/CICM2016-WIP.pdf

8. C. Ferraris, N. Martys, W. George, E. Garboczi and A. Olivas, Calibration of Rheometers for Cementitious Materials, in *Proceedings of the 8th International RILEM Symposium on Self-Compacting Concrete*, Washington DC, May 2016.

9. J. Fong, N. Heckert, J. Filliben, P. Marcal and R. Rainsberger, Uncertainty of FEM Solutions Using a Nonlinear Least Squares Fit Method and a Design of Experiments Approach, in *Proceedings of the 2015 International COMSOL Users' Conference*, Boston, MA, October 7-9, 2015.

10. J. Fong, J. Filliben, N. Heckert, P. Marcal and M. Cohn, A Statistical Approach to Estimating a 95 % Confidence Lower Limit for the Design Creep Rupture Time vs. Stress Curve when the Stress Estimate Has an Error Up to 2 %, in *Proceedings of the ASME* **50367**, Volume 1B: Codes and Standards, PVP2016-63350, 12 pages, Pressure Vessels and Piping Division Conference, Vancouver, British Columbia, Canada, July 17-21, 2016. DOI: 10.1115/PVP2016-63350

11. W. Griffin, W. George, T. Griffin, J. Hagedorn, M. Olano, S. Satterfield J. Sims and J. Terrill, Application Creation for an Immersive Virtual Measurement and Analysis Laboratory, in *Proceedings of the 9th IEEE Workshop on Software Engineering and Architectures for Realtime Interactive Systems* (SEARIS), March 20, 2016. DOI: 10.1109/SEARIS.2016.7551580

12. D. Kuhn, V. Hu, D. Ferraiolo, R. Kacker and Y. Lei, Pseudo-Exhaustive Testing of Attribute Based Access Control Rules, in *Proceedings of the Ninth IEEE International Conference on Software Testing, Verification and Validation Workshops* (ICSTW), Chicago, IL, April 10-15, 2016, 51-58. DOI: 10.1109/ICSTW.2016.35

13. V. Marbukh, Towards Systemic Risk Aware Engineering of Large-Scale Networks: Complex Systems Perspective, in *Proceedings of IEEE 24th International Symposium on Modeling, Analysis and Simulation of Computer and Telecommunication Systems* (MASCOTS), London, England, September 19-21, 2016, 391-393. DOI: 10.1109/MASCOTS.2016.20

14. V. Marbukh, Effect of Bounded Rationality on Tradeoff Between Systemic Risks & Economic Efficiency in Networks, in *Proceedings of the Eighth International Conference on Ubiquitous and Future Networks* (ICUFN), Vienna, Austria, July 5-8, 2016, 353-355. DOI: 10.1109/ICUFN.2016.7537047

15. V. Marbukh, Towards Cross-Layer Design of Communication Network for Smart Grid with Real-Time Pricing, in *Proceedings of the 8th IEEE International Conference on Smart Grid Communications* (SmartGridComm), Sydney, Australia, November 6-9, 2016, 411-416. DOI: 10.1109/SmartGridComm.2016.7778796

16. V. Marbukh, M. Barbi, K. Sayrafian and M. Alasti, A Queue-Size & Channel Quality Based Adaptation of the Energy Detection Threshold in IEEE802.15.6 CSMA/CA, in *Proceedings of the IEEE 18th International Conference on e-Health Networking, Applications and Services* (HealthCom), Munich, Germany, September 14-16, 2016, 1-6. DOI: 10.1109/HealthCom.2016.7749526

17. V. Marbukh, M. Barbi, K. Sayrafian and M. Alasti, A Regret Matching Strategy Framework for Inter-BAN Interference Mitigation, in *Proceedings of the 8th IFIP Wireless and Mobile Networking Conference*, Munich, Germany, October 5-7, 2015, 231-234. DOI: 10.1109/WMNC.2015.15

18. P. Marcal, J. Fong, R. Rainsberger and Li Ma, A High-Accuracy Approach to Finite Element Analysis Using the Hexa 27-node Element, in *Proceedings of the ASME* **50367**, Volume 1B: Codes and Standards, PVP2016-63715, 12 pages, Pressure Vessels and Piping Division Conference, Vancouver, British Columbia, Canada, July 17-21, 2016. DOI:.10.1115/PVP2016-63715

19. N. Martys, C. Ferraris and W. George, Modeling of Suspension Flow in Pipes and Rheometers, in *Proceedings of the 8th International RILEM Symposium on Self-Compacting Concrete*, Washington DC, May 2016.

20. B. R. Miller, Strategies for Parallel Markup, in *Proceedings of the Conference on Intelligent Computer Mathematics, Lecture Notes in Artificial Intelligence* **9150** (2015)**,** 203-210. DOI: 10.1007/978-3-319-20615-8_13

21. P. Patrone, Estimation and Uncertainty Quantification of Yield via Strain Recovery Simulations, in *Proceedings of the Composites and Advanced Materials Expo* (CAMX), Anaheim CA, September 27 2016. URL: https://www.nist.gov/node/1090826

22. R. Rainsberger, J. Fong and P. Marcal, A Super-Parametric Approach to Estimating Accuracy and Uncertainty of the Finite Element Method, in *Proceedings of the ASME* **50367**, Volume 1B: Codes and Standards, PVP2016-63890, 12 pages, Pressure Vessels and Piping Division Conference, Vancouver, British Columbia, Canada, July 17-21, 2016. DOI:.10.1115/PVP2016-63890

23. Z. Ratliff, D. Kuhn, R. Kacker, Y. Lei and K. Trivedi, The Relationship Between Software Bug Type and Number of Factors Involved in Failures, in *Proceedings of the IEEE International Symposium on Software Reliability Engineering Workshops* (ISSREW), Ottawa, Canada, October 23-27, 2016, 119-124. DOI: 10.1109/ISSREW.2016.26

24. B. Schneider, How Novel Algorithms and Access to High Performance Computing Platforms Are Enabling Scientific Progress in Atomic and Molecular Physics, *Journal of Physics Conference Series* **759**:1 (2016), 012002. XXVII IUPAP Conference on Computational Physics (CCP2015). DOI: 10.1088/1742-6596/759/1/012002

25. B. Schneider, X. Guan and K. Bartschat, Time Propagation of Partial Differential Equations Using the Short Iterative Lanczos Method and Finite-Element Discrete Variable Representation: An Experiment Using the Intel Phi Coprocessors, in *Proceedings of the Conference on Diversity, Big Data and Science at Scale* (XSEDE16), Miami, FL, July 17-21, 2016, Article 4. DOI: 10.1145/2949550.2949565

26. M. Schubotz, A. Grigoriev, M. Leich, H. Cohl, N. Meuschke, B. Gipp, A. Youssef and V. Markl, Semantification of Identifiers in Mathematics for Better Math Information Retrieval, in *Proceedings of the 39th Annual ACM SIGIR Conference on Research and Development in Information Retrieval*, Pisa, Tuscany, Italy, July 17-21, 2016, 135-144. DOI: 10.1145/2911451.2911503

27. M. Schubotz, A. Youssef, V. Markl and H. Cohl, Challenges of Mathematical Information Retrieval in the NTCIR-11 Math Wikipedia Task, in *Proceedings of the 38th International ACM SIGIR Conference on Research and Development in Information Retrieval*, Santiago, Chile, August 9-13, 2015, 951-954. DOI: 10.1145/2766462.2767787

28. D. Simos, K. Kleine, A. Voyiatzis, D. R. Kuhn and R. Kacker, TLS Cipher Suites Recommendations: A Combinatorial Coverage Measurement Approach, in *Proceedings of the 2016 IEEE International Conference on Software Quality, Reliability and Security* (QRS), Vienna, Austria, August 1-3, 2016, 69-73. DOI: 10.1109/QRS.2016.18.

Technical Magazine Articles

1. S. Jordan, Black Holes, Quantum Mechanics, and the Limits of Polynomial-time Computability, *ACM XRDS* **23:**1 (Fall 2016), 30–33. DOI: 10.1145/2983539

2. D. Simos, D. R. Kuhn, A. Voyiatzis and R. Kacker, Combinatorial Methods in Security Testing, *IEEE Computer* **49**:10 (2016), 80-83. DOI: 10.11-9/MC.2016.314

Technical Reports

1. R. F. Boisvert (Editor), Applied and Computational Mathematics Division, Summary of Activities for Fiscal Year 2015, *NISTIR 8132*, May 2016, 133 pages. DOI: 10.6028/NIST.IR.8132

2. L. Chen, S. Jordan, Y.-K. Liu, D. Moody, R. Peralta, R. Perlner and D. Smith-Tone, Report on Post-Quantum Cryptography, *NISTIR 8105*, April 2016. DOI: 10.6028/NIST.IR.8105

3. A. Fein, W. Mitchell, J. Senseney and J. Sims, The OISM Guide to the NIST Scientific Computing Linux Cluster, September 13, 2016.

4. S. Kimmel and Y.-K. Liu, Quantum Compressed Sensing Using 2-Designs, October 2015. Preprint: https://arxiv.org/abs/1510.08887

5. F. Krahmer and Y.-K. Liu, Phase Retrieval Without Small-Ball Probability Assumptions, April 2016. Preprint: https://arxiv.org/abs/1604.07281

6. A. Olivas, M. A. Helsel, N. Martys, C. F. Ferrais, W. L. George and R. Ferron, Rheological Measurement of Suspensions without Slippage: Experiment and Model, NIST TN 1946, December 13, 2016. DOI: 10.6028/NIST.TN.1946

NIST Blog Posts

1. S. Ressler, A Slice of Math Functions for Pi Day, *Taking Measure*, NIST, March 14, 2016. URL: http://nist-takingmeasure.blogs.govdelivery.com/slice-math-functions-pi-day/

Accepted

1. M. Barbi, K. Sayrafian and M. Alasti, Low Complexity Adaptive Schemes for Energy Detection Threshold in the IEEE802.15.6 CSMA/CA, 2016 IEEE Conference on Standards for Communications & Networking (CSCN'16), Berlin, Germany, October 31 - November 2, 2016.

2. J. W. Bullard, E. J. Garboczi, P. E. Stutzman, P. Feng, A. S. Brand, L. Perry, J. Hagedorn, W. Griffin and J. E. Terrill, Measurement and Modeling Needs for Next-Generation Concrete Binders, *Cement and Concrete Composites* (invited).

3. A. Carasso, Stabilized Richardson Leapfrog Scheme in Explicit Stepwise Computation of Forward or Backward Nonlinear Parabolic Equations, *Inverse Problems in Science and Engineering*. DOI: 10.1080/17415977.2017.1281270
4. H. Cohl, R. Costas-Santos and W. Xu, The Orthogonality of Al-Salam-Carlitz Polynomials for Complex Parameters, in *Frontiers in Orthogonal Polynomials and q-Series*, World Scientific Publishing.
5. S. Colbert-Kelly, G. B. McFadden, D. Phillips and J. Shen, Numerical Analysis and Simulation for a Generalized Planar Ginzburg-Landau Equation in a Circular Geometry, *Communications in Mathematical Sciences.*
6. J. W. Fowler, B. Alpert, W. B. Doriese, J. Hays-Wehle, Y. I. Joe, K. M. Morgan, G. C. O'Neil, C. D. Reintsema, D. R. Schmidt, J. Ullom and D. Swetz, When Optimal Filtering Isn't, *IEEE Transactions on Applied Superconductivity.*
7. L. Ma, O. Slattery and X. Tang, Optical Quantum Memory Based on Electromagnetically Induced Transparency, *Journal of Optics*.
8. F. Maggioni, F. Potra and M. Bertocchi, A Scenario-Based Framework for Supply Planning Under Uncertainty: Stochastic Programming Versus Robust Optimization Approaches, *Computational Management Science.*
9. H. Mahboubi, W. Masoudimansour, A. Aghdam and K. Sayrafian, An Energy-Efficient Target Tracking Strategy for Mobile Sensor Networks, *IEEE Transactions on Cybernetics*. DOI: 10.1109/TCYB.2016.2519939
10. L. Rabieekenari, K. Sayrafian and J. S. Baras, Autonomous Relocation Strategies for Cells on Wheels in Public Safety Networks, 14th Annual IEEE Consumer Communications & Networking Conference (IEEE CCNC 2017), Las Vegas, USA, January 8-11, 2017
11. H. Zhao, G. Bryant, W. Griffin, J. Terrill and J. Chen, Validation of SplitVector Encoding and Stereoscopy for Quantitative Visualization of Quantum Physics Data, *IEEE Transactions on Visualization and Computer Graphics.*

In Review

1. D. Anderson, J. Benson and A. Kearsley, Foundations of Modeling in Cryobiology II: Heat Mass Transport in Bulk and at Cell Membrane and Ice-Liquid Interfaces.
2. J. W. Bullard, J. Hagedorn, M. T. Ley, Q. Huc, W. Griffin and J. E. Terrill, A Critical Comparison of 3D Experiments and Simulations of Tricalcium Silicate Hydration.
3. B. Cloteaux, A Sufficient Condition for Graphic Lists with Given Largest and Smallest Entries, Length and Sum.
4. B. Cloteaux, Forced Edges and Graph Structure.
5. H. Cohl, R. Costas-Santos, P. Hwang and T. Wakhare, Generalizations of Generating Functions for Basic Hypergeometric Orthogonal Polynomials.
6. M. Baeder, H. Cohl, R. Costas-Santos and W. Xu, The Power Collection Method for Connection Relations: Meixner Polynomials.
7. R. Denlinger, L. Greengard, Z. Gimbutas and V. Rokhlin, A Fast Summation Method for Oscillatory Lattice Sums.
8. G. Doğan, J. Bernal and C. Hagwood, Efficient Computation of the Elastic Tangent-Based Shape Distances Between Closed Curves.
9. J. Fong, N. Heckert, J. Filliben, P. Marcal and S. Freiman, A Model-Screening Tool Using a Composite Goodness-of-Fit Index Approach.
10. J. W. Fowler, B. Alpert, W. B. Doriese, G. C. Hilton, L. T. Hudson, T. Jach, Y. I. Joe, K. M. Morgan, G. C. O'Neil, C. D. Reintsema, D. R. Schmidt, D. Swetz, C. Szabo-Foster and J. Ullom, A Reassessment of Absolute X-Ray Line Energies for Lanthanide Metals.
11. P. Guba and D. Anderson, Pattern Selection in Ternary Mushy Layers.
12. C. Hagwood, G. Doğan and J. Bernal, Optimality of a Class of Variations Problems Occurring in Shape Analysis.
13. T. Hoft and B. Alpert, Fast Updating Multipole Coulombic Potential Calculation.
14. F. Hunt, Optimal Seeds for Network Consensus.
15. Y. Kemper and J. Lawrence, The Odd-Even Invariant and Hamiltonian Circuits in Tope Graphs.
16. S. Keshavarz, Z. Molaeinia, A. Reid and S. Langer, Morphology Dependent Flow Stress in Nickel-Based Superalloys in the Multi-Scale Crystal Plasticity Framework.
17. M. Kovarek, L. Amatucci, K. Gillis, F. Potra, J. Ratino, M. Levitan and D. Yeo, Calibration of Dynamic Pressure in a Tubing System and Optimized Design of Tube Configuration: A Numerical and Experimental Study.
18. P. Kuo, T. Gerrits, V. Verma and S. Nam, Spectral Correlation and Interference in Non-Degenerate Photon Pairs at Telecom Wavelengths.

19. R. La, Internalization of Externalities in Interdependent Security: Large Network Cases.
20. R. La, Network Mixing in Interdependent Security: Friend or Foe?
21. J. Lawrence and R. Kacker, The Pair of Distributions that Brackets a Trapezoidal Distribution.
22. W. Mitchell, 30 years of Newest Vertex Bisection.
23. W. Mitchell, Performance of *hp*-Adaptive Strategies for 3D Elliptic Problems.
24. G. C. O'Neil, L. Miaja-Avila, Y. I. Joe, B. Alpert, M. Balasubramanian, S. Dodd, W. B. Doriese, J. W. Fowler, W. K. Fullagar, G. C. Hilton, R. Jimenez, B. Ravel, C. D. Reintsema, D. R. Schmidt, K. L. Silverman, D. Swetz, J. Uhlig and J. Ullom, Ultrafast Time-Resolved X-Ray Absorption Spectroscopy of Ferrioxalate Photolysis with a Laser Plasma X-Ray Source and Microcalorimeter Array.
25. P. Patrone, S. Tucker and A. Dienstfrey, Estimating Yield-Strain via Deformation-Recovery Simulations.
26. F. Potra, An Iterative Method of Order 1+√(2) Requiring the Same Work per Iteration as Newton's Method.
27. L. Rabieekenari, K. Sayrafian and J. S. Baras, Autonomous Relocation Strategies for Cells on Wheels in Environments with Prohibited Areas.
28. T. Rosch and P. Patrone, Beyond Histograms: Efficiently Estimating Radial Distribution Functions via Spectral Monte Carlo.
29. B. Saunders, B. Miller, F. Backeljauw, S. Becuwe, M. McClain, D. Lozier, A. Cuyt and A. Dienstfrey, DLMF Tables: A Computational Resource Inspired by the NIST Digital Library of Mathematical Functions.
30. J. Schneider, P. Patrone and D. Margetis, Towards a High-Supersaturation Theory of Crystal Growth: nonlinear one-step flow model in 1+1 dimensions.
31. G. B. Silva, S. Glancy and H. M. Vasconcelos, Investigating Bias in Maximum Likelihood Quantum State Tomography.
32. F. Sullivan and I. Beichl, Merging Data Science and Large Scale Computational Modeling.
33. T. R. Tan, Y. Wan, S. Erickson, P. Bierhorst, D. Kienzler, S. Glancy, E. Knill, D. Leibfried and D. J. Wineland, Chained Bell Inequality Experiment with High-Efficiency Measurements. Preprint: 1612.01618

Presentations

Note: When multiple presenters are listed, names of co-presenters with a Division affiliation during this reporting period are underlined.

Invited Talks

1. B. Alpert, "Algorithms for Identification of Nearly-Coincident Events in Calorimetric Sensors," Determination of Electron (Anti-)Neutrino Mass Workshop, Trento, Italy, April 7, 2016.
2. I. Beichl, "Sequential Importance Sampling for Counting Linear Extensions," University of Maryland, College Park, November 9, 2016.
3. R. F. Boisvert, Panelist, Federal Panel on CSE Software Investments, Computational Science and Engineering Software Sustainability and Productivity Challenges (CSESSP) Workshop, Rockville, MD, October 15, 2016.
4. R. F. Boisvert, "Reproducibility in Computing: The Role of Professional Societies," *Rethinking Experimental Methods in Computing*, Schloss Dagstuhl, Germany, March 14, 2016.
5. R. F. Boisvert, "Reproducibility in Computing: The Role of Professional Societies," Reproducibility Seminar Series, NIST MML, March 24, 2016.
6. R. F. Boisvert, "Elias Houstis: One of Many Threads in a Multi-Faceted Career," Computational and Informational Science and Engineering Conference, Portaria, Greece, June 23, 2016.
7. R. F. Boisvert, "Reproducibility in Computing: The Role of Professional Societies," *IFIP Working Group 2.5 Meeting*, Oxford, UK, August 1, 2016.
8. A. Carasso, "Stabilized Richardson Leapfrog Scheme in Explicit Stepwise Computation of Forward or Backward Nonlinear Parabolic Equations," Inverse Problems Symposium, Virginia Military Institute, Lexington, VA, June 5-7 2016.
9. B. Cloteaux, "Graph Generation for Fun and Profit," Computer Science Seminar, New Mexico State University, April 29, 2016.
10. B. Cloteaux, "Graph Generation for Fun and Profit," Computer Science Seminar, The University of Texas at El Paso, October 28, 2016.
11. H. Cohl, "Generalizations of the Generating Function for Gegenbauer Polynomials," Analysis Seminar, Department of Mathematical Sciences, University of Wisconsin–Milwaukee, Milwaukee, WI, November 11, 2016.

12. A. Dienstfrey and P. Patrone, "Uncertainty Quantification, Molecular Dynamics, and the Glass-Transition Temperature of Aerospace Polymers," Mathematics of Metrology, Physikalisch-Technische Bundesanstalt, Berlin, Germany, November 7, 2016.
13. M. Donahue, "Quantitative Effect of Cell Size on Precision of Micromagnetic Energy Calculation," Micromagnetics: Analysis, Numerics, Applications (MANA) Workshop, Technische Universität Wien, Vienna, Austria, February 18, 2016.
14. J. Fong, "A New Approach to Verification and Validation (V&V) of the Finite Element Method," Department of Civil and Environmental Engineering Seminar, University of South Carolina, Columbia, SC, April 29, 2016.
15. J. Fong, "A Finite Element Analysis, with Uncertainty Quantification, for Finding the First Resonance Frequency of a NIST Magnetic Resonance Imaging (MRI) Birdcage Coil," Electromagnetics Division Seminar, Physical Measurement Laboratory, NIST, Boulder, CO, June 3, 2016.
16. J. Fong, "A Finite Element Analysis, with Uncertainty Quantification, of the Resonance of a Prototype MRI Low-Pass RF Coil," Electromagnetics Division Seminar, Physical Measurement Laboratory, NIST, Boulder, CO, June 3, 2016.
17. J. Fong, "A New Approach to Real-Time-NDE-Based and Fatigue-Model-Assisted Maintenance Decision Making," IEEE Far East Non-Destructive Testing (FENDT) Forum, Nanchang, China, June 22-24, 2016.
18. J. Fong, "NDE Uncertainty Quantification Software Tools for Component and System Reliability + Integrity Management," ASME Boiler & Pressure Vessel Code Committee Section XI Special Working Group (SWG) on Reliability + Integrity Management (RIM), Washington, DC, Aug. 21-26, 2016.
19. C. Hagwood, G. Doğan and J. Bernal, "An Analytical Approach for Computing Shape Geodesics," ICSA Applied Statistics Symposium, Atlanta, GA, June 12-15, 2016.
20. C. Hagwood, G. Doğan and J. Bernal, "Some Analytical Results for Shape Space Computations", IMS Meetings and World Congress in Probability and Statistics, Toronto, Canada, July 11-15, 2016.
21. F. Hunt, "An Algorithm for Identifying Optimal Spreaders in a Random Walk Model of Network Communication", Probability Seminar at the Mathematics Department, University of Delaware, November 2, 2015.
22. F. Hunt, "An Algorithm for Identifying Optimal Spreaders in a Random Walk Model," Mathematics Department, Indiana University of Pennsylvania, February 2016.
23. F. Hunt, "A Mathematician Looks at Paint, Hollywood and DNA", Indiana University of Pennsylvania, February 2016.
24. S. Jordan, "Computational Complexity of Quantum Field Theory," Joint Quantum Institute Seminar, College Park, MD, October 5, 2015.
25. S. Jordan, "Permutational Quantum Computation," Workshop Around BQP, Tokyo, December 7, 2015.
26. S. Jordan, "Adiabatic Optimization vs. Monte Carlo," Center for Quantum Information and Control Seminar, University of New Mexico, March 24, 2016.
27. S. Jordan, "Adiabatic Optimization vs. Monte Carlo," Workshop on Quantum Algorithms and Devices, Microsoft Faculty Summit, Redmond, WA, July 15, 2016.
28. S. Jordan, "Adiabatic Optimization vs. Monte Carlo," Canadian Institute for Advanced Research Program Meeting, College Park, MD, April 3, 2016.
29. S. Jordan, "Topological Quantum Field Theory and Quantum Computing," Workshop on Quantum Stochastic Differential Equations for the Quantum Simulation of Physical Systems, Army Research Laboratory, Adelphi, MD, August 22, 2016.
30. Y.-K. Liu, "Phase Retrieval Using Structured Measurements," Mathematical Sciences Colloquium, George Mason University, March 4, 2016.
31. Y.-K. Liu, "Phase Retrieval Using Structured Measurements," Norbert Wiener Seminar, University of Maryland, March 8, 2016.
32. Y.-K. Liu, "Quantum Compressed Sensing Using 2-Designs," CIFAR Quantum Information Science Program Meeting, College Park, MD, April 6, 2016.
33. Y.-K. Liu, "QCRYPT Conference Summary," 4th ETSI/IQC Workshop on Quantum-Safe Cryptography, Toronto, Canada, September 20, 2016.
34. L. Ma, Z. Hu, O. Slattery and X. Tang, "Atomic Filters for Noise Reduction in EIT Quantum Memory Based on Warm Cs Atomic Ensembles," SPIE: Optics and Photonics, Quantum Communications and Quantum Imaging XIV, San Diego, CA, August 28, 2016.

35. V. Marbukh, "Towards Unified Perron-Frobenius Framework for Managing Systemic Risk in Networked Systems," Department of Mathematics of Macquarie University, Sydney, Australia, November 10, 2016.
36. P. Patrone, "Energy Drift in Molecular Dynamics Simulations: what causes it, can we quantify its effects, and should we even do so?" Research Collaboration Workshop: Optimization and Uncertainty Quantification in Energy and Industrial Applications, University of Minnesota, Minneapolis, MN, February 24, 2016.
37. P. Patrone, "Why Your Molecular Dynamics Needs Uncertainty Quantification," Webinar, Schrödinger LLC, August 17, 2016.
38. S. Ressler, "WebVR: Virtual Reality On the Web," Visualization, Big Data, Art + Science 2016, Queensland University of Technology, Brisbane, Australia, February 18, 2016.
39. K. Sayrafian, "Smart Watches for Medicine: Hype or Revolution," Panelist, IEEE Wireless Health Conference, National Institute of Health, Bethesda, Maryland, October 14, 2015.
40. K. Sayrafian, "Low Complexity Adaptive Schemes for Energy Detection Threshold in the IEEE 802.15.6 CSMA/CA", IEEE CSCN 2016 Conference on Standards for Communications & Networking (CSCN'16), Berlin, Germany, October 31 – November 2, 2016.
41. B. Schneider, "45 Years of Computational Atomic and Molecular Physics: What Have We Learned?" George Mason University Computational and Data Sciences, September 2016.
42. B. Schneider, "CyberScience and CyberInfrastructure: A New Approach to Discovery in Science and Engineering," NIST National Strategic Computing Initiative Seminar Series, October 2016.
43. J. Van Meter, "Locally Covariant Approach to Relativistic Quantum Metrology," Center for Quantum Information and Control Seminar, University of New Mexico, February 4, 2016.

Conference Presentations

1. B. Alpert, "Toward Retaining Energy Resolution with Detector Nonlinearity at High Event Rates," Applied Superconductivity 2016 Conference, Denver, CO, September 5, 2016.
2. D. Anderson, J. Benson and A. Kearsley, "Investigating Assumptions in Single Cell Cryobiological Modeling," 53rd Annual Meeting of the Society for Cryobiology, Ottawa, Canada, July 24, 2016.
3. I. Beichl, "Merging Data Science and Large Scale Computational Modeling," High Performance Computing 2016, Cetraro, Italy, June 30, 2016
4. J. Bernal, G. Doğan and C. Hagwood, "Fast Dynamic Programming for Elastic Registration of Curves," International Workshop on Differential Geometry in Computer Vision and Machine Learning (DIFF-CVML) 2016, Las Vegas, NV, June 26-July 1, 2016.
5. P. Bierhorst, "A Strong Loophole Free Test of Local Realism," American Physical Society March Meeting, Baltimore, MD, March 17, 2016.
6. P. Bierhorst, "A Strong Loophole Free Test of Local Realism," Workshop on Information and Processes, Fontainebleau, France, April 27, 2016.
7. P. Bierhorst, "Quantum Randomness Certified by the Impossibility of Superluminal Signaling," International Conference on Quantum Cryptography (QCrypt), Washington, DC, September 16, 2016.
8. J. Bullard, P. Stutzman, P. Feng, J. Hagedorn, W. Griffin and J. Terrill, "Measurement and Modeling Needs for Next-Generation Construction Materials," International Conference on Grand Challenges in Construction Materials, Los Angeles, CA, March 17-18, 2016.
9. J. Bullard, M. Ley, Q. Hu, J. Hagedorn, W. Griffin and J. Terrill, "Direct Comparison of Measurements and Simulation of Cement Hydration," 7th Annual Advances in Cement-Based Materials, Evanston, IL, July 10-13, 2016.
10. J. Bullard, P. Stutzman, P. Feng, J. Hagedorn, W. Griffin, J. Terrill, M. Ley and Q. Hu, "Toward a Virtual Microprobe of Cement Hydration and Deterioration," 3rd RILEM International Conference on Microstructure Related Durability, Nanjing, China, October, 24-26, 2016.
11. T. Burns and B. Rust, "Estimation of Shear Stress in Machining by Inversion of Abel Transform," SIAM Annual Meeting, Boston, MA, July 11-15, 2016.
12. T. Burns and B. Rust, "Estimation of Shear Stress in Machining Using the Temperature Distribution on the Tool Face," 24th International Congress of Theoretical and Applied Mechanics (ICTAM 2016), Montreal, Canada, August 21-26, 2016.
13. H. Cohl, "Orthogonal Polynomial Seeding for the Digital Repository of Mathematical Formulae", Joint Mathematics Meetings, Special Session on Mathematical Information in the Digital Age of Science, Seattle, WA, January 7, 2016.

14. G. Doğan, J. Bernal and C. Hagwood, "A Fast Iterative Algorithm to Compute Elastic Shape Distance Between Curves", SIAM Conference on Imaging Science, Albuquerque, NM, May 23-26, 2016.

15. C. Ferraris, N. Martys, W. George, E. Garboczi, A. Olivas, "Calibration of Rheometers for Cementitious Materials," 8th International RILEM Symposium on Self-Compacting Concrete, Washington DC, May 2016.

16. J. Fong, "Uncertainty of FEM Solutions Using a Nonlinear Least Squares Fit Method and a Design of Experiments Approach," International COMSOL Users' Conference, Boston, MA, October 7-9, 2015.

17. J. Fong, "A New Approach to Finite Element Method Error Estimation Using a Nonlinear Least Squares Logistic Fit of Candidate Solutions," ASME Verification and Validation Symposium, Las Vegas, NV, May 15-20, 2016.

18. J. Fong, "A Statistical Approach to Estimating a 95 % Confidence Lower Limit for the Design Creep Rupture Time vs. Stress Curve when the Stress Estimate has an Error Up to 2 %," ASME Pressure Vessels and Piping Division Conference, Vancouver, British Columbia, Canada, July 17-21, 2016.

19. S. Glancy, "Data Analysis for a Strong Loophole-Free Test of Local Realism," Southwest Quantum Information and Technology (SQUINT) Workshop, Albuquerque, NM, February 18, 2016.

20. S. Glancy, "Data Analysis for a Strong Loophole-Free Test of Local Realism," Quantum and Beyond, Linnaeus University, Sweden, June 16, 2016.

21. W. Griffin, W. George, T. Griffin, J. Hagedorn, M. Olano, S. Satterfield, J. Sims and J. Terrill, "Application Creation for an Immersive Virtual Measurement and Analysis Laboratory," 9th IEEE Workshop on Software Engineering and Architectures for Realtime Interactive Systems, Greenville, SC, March 19 – 23, 2016.

22. W. Griffin, Steven Satterfield, Sandy Ressler and Judith Terrill, "360 Video from a Virtual Six-Sided Cave," Immersive Visualization for Science and Research, SIGGRAPH Birds of a Feather Session, Anaheim CA, July 25, 2016.

23. S. Ressler, "WebVR using A-Frame for Scientific Visualization", Immersive Visualization for Science and Research, SIGGRAPH Birds of a Feather 2016, Anaheim CA, July 25, 2016.

24. P. Kuo, "Spectral Correlation and Interference in CW Non-Degenerate Photon Pairs at Telecom Wavelengths," Conference on Lasers and Electro-optics (CLEO), San Jose, CA, June 5-10, 2016.

25. R. La, "Influence of Network Mixing on Interdependent Security: Local Analysis," IEEE Global Communications (GLOBECOM), Washington DC, December 2016.

26. Y.-K. Liu, "Quantum Compressed Sensing Using 2-Designs," American Physical Society March Meeting, Baltimore, MD, March 14, 2016.

27. V. Marbukh, "Towards Systemic Risk Aware Engineering of Large-Scale Networks: Complex Systems Perspective," IEEE Conference on Modeling, Analysis, and Simulation of Computer and Telecommunication Systems (IEEE MASCOTS 2016), London, England, September 19-21, 2016.

28. V. Marbukh, "Systemic Risks in the Cloud Computing Model: Complex Systems Perspective," 9th IEEE International Conference on Cloud Computing (IEEE CLOUD 2016), San Francisco, USA, June 27 – July 2, 2016.

29. V. Marbukh, "Effect of Bounded Rationality on Tradeoff Between Systemic Risks & Economic Efficiency in Networks," 8th International Conference on Ubiquitous and Future Networks (IEEE ICUFN 2016), Vienna, Austria, July 5-8, 2016.

30. V. Marbukh, "Towards Cross-Layer Design of Communication Network for Smart Grid with Real-Time Pricing," IEEE International Conference on Smart Grid Communications (IEEE SmartGridComm 2016), Sydney, Australia, November 6-9, 2016.

31. V. Marbukh, "Towards Classification, Evaluation, and Quantification of Systemic Risks of Dynamic Resource Sharing in Networked Systems," InterNational Conference on Network Science (NetSci X), Tel Aviv, Israel, January 15-18, 2017.

32. N. Martys, C. Ferraris and W. George, "Computational Modeling of Suspension Flow in Pipes with Generalized Newtonian Matrix Fluids," 87th Annual Meeting of the Society of Rheology, Baltimore, MD October 11-15, 2015.

33. N. Martys, C. Ferraris and W. George, "Modeling of Suspension Flow in Pipes and Rheometers," 8th International RILEM Symposium in Self-Compacting Concrete, Washington DC, May 2016.

34. B. Miller, "Drafting DLMF Content Dictionaries," Conference on Intelligent Computer Mathematics, Bialystok, Poland, July 22, 2016.

35. W. Mitchell, "Performance of Some *hp*-Adaptive Strategies for 3D Elliptic Problems," Computation and Information Science and Engineering Conference, Portaria, Greece, June 21-24, 2016.

36. W. Mitchell, "Performance of Some *hp*-Adaptive Strategies for 3D Elliptic Problems," International Conference on Spectral and High Order Methods, Rio de Janeiro, Brazil, June 27-July 1, 2016.
37. S. Pal and R. La, "Simple Learning in Weakly Acyclic Games," Annual Allerton Conference, Monticello, IL, October 2016.
38. P. Patrone, "Estimation and Uncertainty Quantification (UQ) of Yield via Strain Recovery Simulations," Composites and Advanced Materials Expo, Anaheim, CA, September 29, 2016.
39. D. Porter, "Tcl Values – Past, Present and Tales from the Future," 23rd Annual Tcl/Tk Conference, Houston, TX, November 16, 2016.
40. F. Potra, "Weighted Complementarity Problems and Applications," 28th European Conference on Operational Research (EURO 2016), Poznan, Poland, July 3-6, 2016.
41. F. Potra, "Interior Point Methods," 16th International Conference on Operational Research (KOI 2016), Osijek, Croatia, September 27-29, 2016.
42. B. Saunders, B. Antonishek, B. Miller and Q. Wang, "Adaptive Curvature-Based Composite Grid Generation Techniques Applied to 3D Visualizations," 9th International Conference on Mathematical Methods for Curves and Surfaces, Tonsberg, Norway, June 23, 2016.
43. B. Saunders, B. Miller, M. McClain, D. Lozier, A. Dienstfrey, F. Backeljauw, S. Becuwe and A. Cuyt, "DLMF Live! Tables: NIST/Antwerp Collaboration for Standard Reference Tables on Demand," Joint Mathematics Meetings, Seattle, Washington, January 8, 2016.
44. B. Saunders, "Slices of 3D Surfaces on the Web Using Tensor Product B-Spline Grids," SIAM Conference on Geometric and Physical Modeling (GD/SPM15), Salt Lake City, Utah, October 12, 2015.
45. K. Sayrafian, "Kinetic-Based Micro Energy-Harvesting for Wearable Sensors," 6th IEEE International Conference on Cognitive Infocommunications (IEEE CogInfocom, Gyor, Hungary, October 20, 2015.
46. K. Sayrafian, "Impact of the Energy Detection Threshold on Performance of the IEEE 802.15.6 CSMA/CA," IEEE 2015 Conference on Standards for Communications & Networking (CSCN'15), Tokyo, Japan, October 30, 2015.
47. K. Sayrafian, "Medical Internet of Things", COST 15104 (IRACON) 1st Technical Meeting, Lille, France, May 30 - June 1, 2016.
48. K. Sayrafian, "Using RTS/CTS to Enhance the Performance of IEEE 802.15.6 CSMA/CA," IEEE 2016 Conference on Personal Indoor Mobile Radio Communication (PIMRC), Valencia, Spain, September 5, 2016.
49. K. Sayrafian, "A Study of the Energy Detection Threshold in the IEEE802.15.6 CSMA/CA," COST 15104 (IRACON) 2nd Technical Meeting, Durham, UK, October 3-6, 2016.
50. K. Sayrafian, "Low Complexity Adaptive Schemes for Energy Detection Threshold in the IEEE 802.15.6 CSMA/CA," IEEE 2016 Conference on Standards for Communications & Networking (CSCN'16), Berlin, Germany, November 2, 2016.
51. M. Schubotz, A. Grigorev, M. Leich, H. Cohl, N. Meuschke, B. Gippx, A. Youssef and V. Markl, "Semantification of Identifiers in Mathematics for Better Math Information Retrieval," 39th Annual ACM SIGIR Conference on Research and Development in Information Retrieval, Pisa, Italy, July 17-21, 2016.
52. M. Schubotz, D. Veenhuis and H. Cohl, "Getting the Units Right," 9th Conference on Intelligent Computer Mathematics, Bialystok, Poland, July 25-29 2016.
53. D. Simos, R. Kacker and Y. Lei, "Workshop on Combinatorial Security Testing, IEEE International Conference on Software Quality, Reliability and Security (QRS)," Vienna, Austria, August 1-3, 2016.

Poster Presentations

1. D. Anderson, J. Benson and A. Kearsley, "Simulation of Single Cell Cryobiological Freezing," 1st IIR International Conference of Cryogenics and Refrigeration Technology, Bucharest, Romania, June 23 2016.
2. J. Bernal, G. Doğan and C. Hagwood, "Fast Dynamic Programming for Elastic Registration of Curves," 2nd International Workshop on Differential Geometry in Computer Vision and Machine Learning (DIFF-CVML) 2016, Las Vegas, NV, June 26-July 1, 2016.
3. P. Bierhorst, "Geometric Decompositions of Bell Polytopes with Practical Applications," American Physical Society March Meeting, Baltimore, MD, March 15, 2016.
4. G. Doğan, "A Python Toolbox for Shape Optimization in Imaging and Data Analysis," SIAM Conference on Computational Science and Engineering, Salt Lake City, UT, March 14, 2015

5. G. Doğan, J. Bernal and C. Hagwood, 'Fast Computation of Elastic Shape Distance between 2d Objects," BioImage Informatics Conference, Gaithersburg, MD, October 15, 2015.

6. G. Doğan, "A Python Toolbox for Shape Detection and Analysis in Images," BioImage Informatics Conference, Gaithersburg, MD, October 15, 2015.

7. G. Doğan, "Measuring Shape Dissimilarity of Acquired Characteristics in Footwear Impressions," National Commission on Forensic Science Meeting, Gaithersburg, MD, September 12, 2016.

8. A. Keith, "Partial Quantum Tomography Using Maximum Likelihood Estimation," Southwest Quantum Information and Technology (SQUINT) Workshop, Albuquerque, NM, February 18-20, 2016.

9. P. Kuo, "Characterization of Type-II Spontaneous Parametric Down-Conversion in Domain-Engineered PPLN," SPIE Photonics West, San Francisco, CA, February 14-18, 2016.

10. Y.-K. Liu, "Quantum Compressed Sensing Using 2-Designs," 19th Conference on Quantum Information Processing, Banff, Canada, January 14, 2016.

11. K. Mayer, "Optimizing Control Parameters for Three-Qubit Gates, Southwest Quantum Information and Technology (SQUINT) Workshop, Albuquerque, NM, February 18-20, 2016.

12. D. Porter and M. Donahue, "Quantitative Effect of Cell Size on Precision of Micromagnetic Energy Calculations," 13th Joint MMM-Intermag Conference, San Diego, CA, January 12, 2016.

13. A. Reid and S. Langer, "OOF3D: A Materials Science Focused Finite Element System", 3rd International Congress on 3D Materials Science, St. Charles, IL, July 11, 2016.

14. A. Reid and S. Langer, "OOF: Flexible Finite Element Modeling for Materials Science", 2nd International Workshop on Software Solutions for Integrated Computational Materials Engineering, Barcelona, Spain, April 13, 2016.

15. X. Tang, B. Hershman, P. Kuo, A. Mink, L. Ma and O. Slattery, "An Overview of Quantum Communication Research at NIST," QCrypt 2016, Washington DC, September 12-16, 2016.

Web Services

Note: ACMD provides a variety of information and services on its website[16]. Below is a list of major services provided that are currently under active maintenance.

1. *Digital Library of Mathematical Functions*: a repository of information on the special functions of applied mathematics.
2. *Digital Repository of Mathematical Formulae*: a repository of information on special function and orthogonal polynomial formulae.
3. *DLMF Standard Reference Tables on Demand*: an online service providing tables of values for special functions, with guaranteed accuracy to high precision.
4. *muMAG*: a collection of micromagnetic reference problems and submitted solutions.
5. *NIST Adaptive Mesh Refinement Benchmark Problems*: a collection of benchmark partial differential equations for testing and comparing adaptive mesh refinement algorithms.
6. *Quantum Algorithm Zoo*: A repository of quantum algorithms.

Software Released

Note: ACMD distributes a large number of software packages that have been developed in the course of its work[17]. Listed below are particular packages which have seen new releases during the reporting period.

1. *ACTS Combinatorial Test Suite*: generation with support of constraints, Version 3.0: Y. Lei, R. Kacker, D. R. Kuhn.
2. *CCM Combinatorial Coverage Measurement:* GUI Java version with support of constraints, Version 1.0, D. R. Kuhn, R. Kacker.
3. *CCMCL Combinatorial Coverage Measurement:* Command line version with support of constraints, Version 1.0, D. R. Kuhn, R. Kacker.
4. *Itcl*: C++ inspired Object Oriented commands for Tcl. Versions 3.4.3, 4.0.4, 4.0.5. D. Porter.
5. *LaTeXML*: A LaTeX to XML Converter, Version 0.8.2 released; continuous access from svn/git repository. B. Miller.
6. *Mpexpr*: Tcl package for arbitrary precision calculations. Version 1.2. D. Porter.

[16] http://www.nist.gov/itl/math/

[17] http://www.nist.gov/itl/math/software

7. *OOMMF*: Micromagnetics software suite. Versions 1.2a6, 1.2b0. M. Donahue and D. Porter.
8. *PHAML*: solution of elliptic boundary value and eigenvalue problems, using finite elements, *hp*-adaptive refinement, and multigrid, on distributed memory and shared memory parallel computers. Version 1.16.0, March 14, 2016. Version 1.17.0, November 22, 2016. W. F. Mitchell.
9. *Substochastic-SAT*: Substochastoc Monte Carlo solver for MAX-SAT optimization problems. Version 1.0. B. Lackey, S. Jordan and M. Jarret.
10. *Tcl/Tk*: extensible scripting language and GUI toolkit. Versions 8.5.19, 8.6.5, 8.6.6. D. Porter.
11. *TDBC*: database connection commands for Tcl. Versions 1.0.4. D. Porter.
12. *Thread:* thread management commands for Tcl. Version 2.7.3, 2.8.0. D. Porter.
13. *Trofs*: read-only archive system for Tcl virtual filesystems. Version 0.4.9. D. Porter.
14. *Sqlite3*: bindings to the SQLite database engine for Tcl. Versions 3.9.1, 3.9.2, 3.10.0, 3.11.0, 3.13.0, 3.14.1, 3.14.2. D. Porter.

Conferences, Minisymposia, Lecture Series, Courses

ACMD Seminar Series

Brian Cloteaux served as Chair of the ACMD Seminar Series. There were 17 talks presented during this period; all talks are listed chronologically.

1. P. Krajcevski, University of North Carolina, "GPU Focused Image Compression Techniques," October 19, 2015.
2. A. Carasso, NIST ACMD, "Taming Explosive Computational Instability: Compensated Explicit Time-Marching Schemes in Multidimensional, Nonlinear, Well-Posed or Ill-Posed Initial Value Problems for Partial Differential Equations," October 29, 2015.
3. R. Evans, University of Delaware, "Multiple-Component Reactions in Optical Biosensors," November 17, 2015.
4. K. Mills, NIST Advanced Network Technologies Division, "The Influence of Realism on Congestion in Network Simulations," December 1, 2015.
5. P. Patrone, NIST ACMD, "Uncertainty Quantification of Molecular Dynamics Simulations for Crosslinked Polymers," February 16, 2016.
6. S. Sheetlin, NIST Biomolecular Measurement Division, "Constructing High Resolution Consensus Spectra for a Peptide Library," May 2, 2016.
7. W. Yu, Tsinghua University, "Utilizing Macromodels in Floating Random Walk Based Capacitance Extraction for Nanometer Integrated Circuits," May 23, 2016.
8. S. Tucker, The Boeing Company, "Using Simulation for Materials Development and Troubleshooting at Boeing," May 24, 2016.
9. I. Kozine, Technical University of Denmark, "Risk Research for Safety Critical Systems at the Technical University of Denmark," July 12, 2016.
10. A. Godil, NIST Information Access Division, "Apache Hadoop and Spark: Introduction and Use Cases for Data Analysis," July 21, 2016.
11. A. Gargantini, University of Bergamo, Italy, "Validation of Constraints among Configuration Parameters using Search-based Combinatorial Interaction Testing," August 31, 2016.
12. S. D. Casey, American University, "Sampling in Euclidean and Non-Euclidean Domains: A Unified Approach," September 13, 2016.
13. S. Glancy, NIST ACMD, "A Strong Loophole-free Test of Local Realism," September 26, 2016.
14. G. S. Pogosyan, University of Guadalajara, Mexico, "Lie Algebra Contractions and Separation of Variables in Two-dimensional Hyperboloids, Basis Functions and Interbasis Expansions, September 29, 2016.
15. T. Goldstein, University of Maryland, "Large-scale, Highly Parallel Methods for Machine Learning and Sparse Signal Recovery," October 19, 2016.
16. E. W. Bethel, Lawrence Berkeley National Laboratory, "Management, Analysis and Visualization of Experimental and Observational Data – the Convergence of Data and Computing," October 24, 2016.
17. I. Beichl, "Sequential Importance Sampling for Counting Linear Extensions," November 8, 2016.

Shortcourses

1. J. Fong, Application of a Nonlinear Least Squares Fit Algorithm Coded in DATAPLOT for Uncertainty Quantification and Verification of an FEM Solution, Department of Civil and Environmental Engineering, University of South Carolina, Columbia, SC, April 29, 2016.
2. J. Fong, Uncertainty Quantification in Finite Element Method, Structures Division, Engineering Laboratory, NIST, December 7, 2016.

3. S. Jordan, Simulating Physics on Quantum Computers, Qubit Summer School, Perimeter Institute, Waterloo, Canada. July 23-25, 2016.

Conference Organization

Leadership

1. I. Beichl, Organizer, NIST/CSCAMM Day, College Park, MD, February 24, 2017.
2. H. Cohl and D. Lozier, Co-Organizers, Orthogonal Polynomials and Special Functions Summer School 6 (OPSF-S6), Norbert Wiener Centers for Harmonic Analysis and Applications, University of Maryland, July 11-15, 2016.
3. W. Griffin, Organizer, Software Engineering and Architectures for Realtime Interactive Systems (SEARIS) Working Group.
4. S. Jordan, Co-Coordinator, Program on Quantum Physics of Information, Kavli Institute for Theoretical Physics, University of California at Santa Barbara.
5. R. Kacker, Co-Organizer and Member, Program Committee, Fifth International Workshop on Combinatorial Testing (IWCT 2016) in Conjunction with ICST 2016, Chicago, IL, April 10-15, 2016.
6. B. Miller, Program Chair, Mathematical Knowledge Management, Conferences on Intelligent Computer Mathematics, Bialystok, Poland, July 25-29, 2016.
7. Y.-K. Liu, Chair, Steering Committee, International Conference on Quantum Cryptography, Washington, DC, September 12-16, 2016.
8. K. Sayrafian, Industrial Seminar Chair, IEEE Global Communications Conference, Washington, DC, December 4-8, 2016.
9. K. Sayrafian, Tutorial Chair, IEEE 27th Annual Symposium on Personal, Indoor and Mobile Radio Communications, Valencia, Spain, September 4-8, 2016.

Committee Membership

1. R. Kacker, Member, Program Committee, Tenth IEEE International Conference on Software Testing, Verification and Validation, (ICST 2017), Tokyo, Japan, March 13-18, 2017.
2. R. La, Member, Technical Program Committee, SIGMETRIC/Performance 2016, Antibes, France, June 14-18, 2016.
3. R. La, Member, Technical Program Committee, IEEE International Conference on Computer Communications (IEEE INFOCOM 2016), San Francisco, CA, April 10-16, 2016.
4. Y.-K. Liu, Member, Program Committee, International Conference on Post-Quantum Cryptography (PQCrypto), Fukuoka, Japan, February 24-26, 2016.
5. Y.-K. Liu, Member, Program Committee, Asian Quantum Information Science (AQIS) Conference, Taipei, Taiwan, August 28 – September 2, 2016.
6. W. Mitchell, Member, Scientific Committee, 14th International Conference of Numerical Analysis and Applied Mathematics, (ICNAAM), Rhodes, Greece, September 19-25, 2016.
7. R. Pozo, Member, Steering Committee, Computational Science and Engineering Software Sustainability and Productivity Challenges (CSESSP) Workshop Report, Washington DC, October 15-16, 2016.
8. S. Ressler, Tutorial Committee Web3D 2017, Brisbane, Australia, June 5-7, 2017.
9. O. Slattery, Member, Program Committee, Single Photon Workshop, Boulder, CO, August 1-4, 2017.

Session Organization

1. G. Doğan, Co-Organizer, Theoretical and Computational Aspects of Geometric Shape Analysis, SIAM Conference on Imaging Science, Albuquerque, NM, May 25, 2016.
2. Y. Parker and J. Terrill, Co-Organizers, NIST Booth, International Conference for High Performance Computing, Networking, Storage and Analysis (SC15), Austin, TX, November 15- 20, 2015.
3. Y. Parker and J. Terrill, Co-Organizers, NIST Booth, International Conference for High Performance Computing, Networking, Storage and Analysis (SC16), Salt Lake City, Utah, November 13 - 18, 2016.
4. F. Potra, Stream Co-Organizer, Mathematical Programming, 28th European Conference on Operational Research, (EURO 2016) Poznan, Poland, July 3-6, 2016.
5. F. Potra, Organizer, Special Section on Interior Point Methods and Related Topics in Honor of Goran Lešaja, 16th International Conference of Operational Research (KOI 2016) Osijek, Croatia, September 27-29, 2016

6. B. Saunders, Chair, Session on Spline Surfaces, SIAM Conference on Geometric and Physical Modeling (GD/SPM15), Salt Lake City, Utah, October 12, 2015.
7. K. Sayrafian, Member, Technical Program Committee, 5th International Conference on the Internet of Things, Seoul, South Korea, October 26-28, 2015.
8. K. Sayrafian, Member, Technical Program Committee, International Symposium of Information and Internet Technology (SYMINTECH 2016), Melaka, Malaysia, January 26-28, 2016
9. K. Sayrafian, Member, Technical Program Committee, 10th International Symposium on Medical Information and Communication Technology (ISMICT 2016), Worcester, Massachusetts, March 20-23, 2016.
10. K. Sayrafian, Member, Technical Program Committee, IEEE 83rd Vehicular Technology Conference (VTC2016-Spring), Nanjing, China, May 15-18, 2016.
11. K. Sayrafian, Member, Technical Program Committee, 23rd International Conference on Telecommunications (ICT 2016), Thessaloniki, Greece, May 16-18, 2016.
12. K. Sayrafian, Member, Technical Program Committee, IoT for Healthcare Workshop, St. Louis, MO, May 18-20, 2016.
13. B. Schneider, Organizer, Petascale and Beyond Computational Methods in Physics Focus Session, American Physical Society March Meeting, Baltimore, MD, March 14-18, 2016
14. J. Terrill, Co-Organizer, Birds of a Feather (BOF), Immersive Visualization for Science and Research, 43nd International Conference and Exhibition on Computer Graphics and Interactive Technologies (SIGGRAPH 2016), Anaheim, CA, July 24-28, 2016,

Other Professional Activities

Internal

1. R. Boisvert and S. Glancy, Members, ITL Diversity Committee.
2. B. Cloteaux and W. Griffin, Chairs, ACMD Seminar Series.
3. B. Cloteaux, Member, NIST Editorial Review Board.
4. H. Cohl, Co-Director, ITL Summer Undergraduate Research Fellowship (SURF) Program.
5. B. Hershman, ACMD Division Safety Officer.
6. A. Kearsley, Chair, ITL Awards Committee.
7. C. Schanzle, NIST Scientific Computing Steering Group.
8. B. Schneider, Co-Organizer, NIST National Strategic Computing Initiative Seminar Series.

External

Editorial

1. I. Beichl, Member, Editorial Board, *IEEE/AIP Computing in Science & Engineering.*
2. R. F. Boisvert, Associate Editor, *ACM Transactions on Mathematical Software*.
3. H. Cohl, Co-Editor, *OP-SF NET*.
4. H. Cohl, Guest Editor, Special Issue on Orthogonal Polynomials, Special Functions and Applications, *Symmetry, Integrability and Geometry: Methods and Applications.*
5. A. Dienstfrey, Member, Editorial Board, *International Journal of Uncertainty Quantification.*
6. Z. Gimbutas, Member, Editorial Board, *Advances in Computational Mathematics.*
7. R. La, Associate Editor, *IEEE Transactions on Mobile Computing.*
8. R. La, Associate Editor, *IEEE Transactions of Information Theory.*
9. R. La, Editor, *IEEE Communications Surveys and Tutorials.*
10. W. Mitchell, Associate Editor, *Journal of Numerical Analysis, Industrial and Applied Mathematics.*
11. F. Potra, Regional Editor, Americas, *Optimization Methods and Software*.
12. F. Potra, Associate Editor, *Journal of Optimization Theory and Applications*.
13. F. Potra, Associate Editor, *Numerical Functional Analysis and Optimization*.
14. F. Potra, Associate Editor, *Optimization and Engineering.*
15. K. Sayrafian, Associate Editor, *International Journal on Wireless Information Networks*.
16. K. Sayrafian, Member, Editorial Board, *IEEE Wireless Communications.*
17. B. Schneider, Associate Editor-in-Chief, *IEEE Computing in Science & Engineering*.

Boards and Committees

1. R. F. Boisvert, Member, Publications Board, Association for Computing Machinery (ACM).
2. R. F. Boisvert, External Advisory Council, Department of Computer Science, George Washington University.
3. R. F. Boisvert, Member, Working Group 2.5 (Numerical Software), International Federation for Information Processing (IFIP).
4. B. Cloteaux, Member, Advisory Board, Department of Computer Science, New Mexico State University.
5. A. Dienstfrey, Member, Working Group 2.5 (Numerical Software), International Federation for Information Processing (IFIP).
6. A. Dienstfrey, Member, Participating Institutions Council, Institute for Mathematics and its Applications, University of Minnesota.
7. J. Fong, Member, Verification and Validation Committee V&V50 on Advanced Manufacturing, American Society for Mechanical Engineering (ASME).
8. J. Fong, Member, Boiler & Pressure Vessel Code Committee, Section XI Special Working Group on Reliability and Integrity Management Program, American Society for Mechanical Engineering (ASME).
9. W. George, Member, Leadership Computing Facility User Advisory Committee, Argonne National Laboratory.
10. F. Hunt, Member, Committee of Visitors, National Science Foundation.
11. S. Jordan, Member, Interagency Working Group on Quantum Information Science, National Science and Technology Council.
12. G. B. McFadden, Member, Council, Society for Industrial and Applied Mathematics (SIAM).
13. B. Miller, Member, OpenMath Society.
14. D. Porter, Member, Tcl Core Team.
15. S. Ressler, Member, WebVR Community Group, World Wide Web Consortium (W3C).
16. S. Ressler, Member, Declarative 3D for the Web Architecture Community Group, World Wide Web Consortium (W3C).
17. B. Saunders, Secretary-Elect, Activity Group on Geometric Design, Society for Industrial and Applied Mathematics (SIAM).
18. B. Saunders, Member, Business, Industry, and Government (BIG) Committee, Mathematics Association of America (MAA).
19. B. Saunders, Webmaster, Activity Group on Orthogonal Polynomials and Special Functions, Society for Industrial and Applied Mathematics (SIAM).
20. B. Saunders, Moderator, OP-SF Talk listserv, SIAM Activity Group on Orthogonal Polynomials and Special Functions.
21. K. Sayrafian, Member, International Advisory Board, International Symposium on Medical Information and Communication Technology (ISMICT).
22. K. Sayrafian, Member, External Advisory Committee, Quantum Medical Device Interoperability Project, National Institute of Health.
23. B. Schneider, Chair, Fellowship Committee, Division of Computational Physics, American Physical Society.
24. B. Schneider, NIST Representative, High End Computing Interagency Coordination Group, Networking and Information Technology R&D (NITRD) Program.
25. J. Terrill, NIST Alternate Representative, High End Computing Interagency Coordination Group, Networking and Information Technology R&D (NITRD) Program.

Adjunct Academic Appointments

1. S. Jordan, Institute for Advanced Computer Studies (UMIACS), University of Maryland.
2. E. Knill, Department of Physics, University of Colorado.
3. Y.-K. Liu, Institute for Advanced Computer Studies (UMIACS), University of Maryland.
4. X. Tang, Department of Physics and Energy, University of Limerick, Ireland.

Thesis Direction

1. I. Beichl, Member, Ph.D. Thesis Committee: Alathea Jensen, George Mason University.
2. B. Miller, Member, Ph.D. Thesis Committee: Deyan Ginev, Computer Science, Jacobs University, Bremen. Title: *Designing Definition Discovery: Read, Recognize, Reflect, Repeat*.
3. F. Potra, Advisor, Ph.D. Thesis Committee: H. Park, University of Maryland.

4. K. Sayrafian, Member, Thesis Committee: Yishuang Geng, Worcester Polytechnic Institute. Title: *Radio Propagation for Localization and Motion Tracking in Three Body Area Network Applications.*
5. K. Sayrafian, Co-Advisor: Ladan Rabiee, University of Maryland, College Park. Title: *Coverage and Routing in Dynamic Networks*.
6. X. Tang, Advisor, Ph.D. Thesis Committee: Oliver Slattery, University of Limerick, Ireland. Title: *Development of Single-Photon Sources, Detectors, Spectrometers and Interfaces for Quantum Communication Systems.*
7. J. Terrill, Member, Member, Ph.D. Thesis Committee: Henan Zhao, University of Maryland, Baltimore County.

Community Outreach

1. ACMD Staff, NIST Site Visit, Math SPIRAL Program participants, Morgan State University, July 13, 2016.
2. F. Hunt, Participant, Career Day, Westland Middle School, September 2016.
3. A. Kearsley and R. Evans, Hosts, NIST Site Visit, Partial Differential Equations class, Mathematics Department, Shippensburg University (PA), November 7, 2016.
4. B. Saunders, Judge (Mathematics), Siemens Competition in Math, Science and Technology, Discovery Communications, Silver Spring, MD October 7-9, 2016.
5. B. Saunders, Organizer, Virginia Standards of Learning Tutoring Program, Northern Virginia Chapter, Delta Sigma Theta Sorority, Inc. and the Dunbar Alexandria-Olympic Branch of the Boys and Girls Clubs of Greater Washington, January-May, 2016.

Awards and Recognition

1. NIST Information Technology Laboratory, Gold Medal (Institutional Award), US Department of Commerce, 2016. ACMD Participants: P. Bierhorst, S. Glancy and E. Knill.
2. P. Bierhorst, Associate of the Year, NIST Information Technology Laboratory, 2016.
3. R. F. Boisvert, Fellow, American Association for the Advancement of Science, 2016.
4. B. Cloteaux, Gold Nugget Award, College of Engineering, The University of Texas at El Paso, 2016
5. G. Doğan and J. Bernal, ITL Outstanding Conference Proceeding Award, NIST Information Technology Laboratory, 2016.
6. B. Hershman, Outstanding Technical Support Award, NIST Information Technology Laboratory, 2016.
7. S. Jordan, NIST Sigma Xi Katharine Gebbie Young Investigator Award, 2016.
8. E. Knill, NIST Samuel Wesley Stratton Award, 2015.
9. B. Saunders, 2016 Community Service Award, Northern Virginia Alumnae Chapter, Delta Sigma Theta Sorority, Inc.
10. B. Saunders, exhibit, DLMF gamma phase density plots, in MICRO/MACRO: Big Images of Small Things from NIST Labs, Johns Hopkins University Montgomery County Campus, September 6 - November 11, 2016.
11. B. Saunders, featured in display, Recognizing African American Female Scientists at NIST, National African American History Month 2016, NIST Civil Rights and Diversity Office.
12. K. Sayrafian, NIST Bronze Medal Award, 2015.
13. K. Sayrafian, Certificate of Appreciation, IEEE International Symposium on Personal, Indoor and Mobile Radio Communications, 2016.
14. X. Tang, O. Slattery, P. Kuo and B. Hershman, NIST Bronze Medal Award, 2015.
15. X. Tang, Fellow, American Physical Society (APS), 2016.

Grants Received

1. W. George, N. Martys (EL), J. Terrill, M. Olano and P. Hebraud (Institute of Physics and Chemistry of Materials, Strasbourg, France), 50M million CPU-hours on the IBM Blue Gene/Q machine “Mira” at the Argonne Leadership Computing Facility, DOE ASCR Leadership Computing Challenge (ALCC) program., Project: *Computational Design of Novel Multiscale Concrete Rheometers*.
2. B. Schneider, 3.5M service units of computer time on Texas Advanced Computer Center (TACC) Stampede and Louisiana State University SuperMiC supercomputers, NSF XSEDE Program. Project: *Numerical Solution of the Time-Independent and Time-Dependent Schrödinger Equation*.
3. J. Terrill, J. Bullard (EL) and John Hagedorn, 743K service units of computer time on Texas Advanced

Computer Center (TACC) Stampede supercomputer, NSF XSEDE Program. Project: *Rate Controlling Mechanism for Early-Age Cement Hydration.*

Grants Awarded

ACMD awards a small amount of funding through the NIST Measurement Science Grants Program for projects that make direct contributions to its research programs. Often such grants support direct cooperation between an external awardee and ACMD. This year the following new cooperative agreements were initiated.

1. Theiss Research: *Algorithms for Image and Shape Analysis in 3D*, $577,377 (3 years). PI: Gunay Doğan.
2. Theiss Research: *Classical Processing for Quantum Information*, $254,341 (3 years). PI: Alan Mink
3. University of Maryland: *In-situ Visualization for Immersive Environments*, $500,000 (5 years). PI: Amitabh Varshney
4. University of Maryland: *New Theory and Resilience Metrics for Systems-of-Systems*, $457,288 (3 years). PI: Richard La

External Contacts

Note: ACMD staff members interact with a wide variety of organizations in the course of their work. Examples of these follow.

Industrial Labs

Avaya
The Boeing Company
Center for Integration of Medicine and Innovative Technology
Centre Suisse d'Electronique et Microtechnique (Switzerland)
Exxon Mobil
Ford Motor Company
Fraunhoffer
Frequentis
General Electric Global Research Center
Mechdyne
Mentor Graphics
Microsoft
SIKA Technology (Switzerland)
Qcode (UK)
SINTEF (Norway)
Schrodinger LLC
Solvay SA (Belgium)

Government/Non-profit Organizations

Air Force Institute of Technology
Air Force Office of Scientific Research
American Institute of Physics
Argonne National Laboratory
Army Research Laboratory
Association for Computing Machinery
Bureau of the Census
Canadian Institute for Advanced Research
Defense Advanced Research Projects Agency
Department of Defense
Department of Energy
Eglin Air Force Base
Electric Power Research Institute
European Telecommunications Standards Institute
Food and Drug Administration
Gentoo Linux
IDA Center for Computing Sciences
IDA Center for Communications Research
IEEE Computer Society
Institute of Physics and Chemistry of Materials (France)
International Federation for Information Processing
Jet Propulsion Laboratory
Johns Hopkins University Applied Physics Laboratory
Livermore National Laboratory
Montgomery County
NASA Glenn Research Center
NASA Jet Propulsion Laboratory
National Center for Scientific Research (France)
National Institute of Biomedical Imaging and Bioengineering
National Institutes of Health
National Physical Laboratory (UK)
National Science Foundation
Naval Facilities Engineering Command
Nuclear Regulatory Commission
Oak Ridge National Laboratory
Open Math Society
Pacific Northwest National Laboratory
Perimeter Institute (Canada)
Physikalisch-Technische Bundesanstalt (Germany)
Princeton Plasma Physics Laboratory
Sandia National Laboratories
SBA-Research (Austria)
Commonwealth Scientific and Industrial Research Organization (Australia)
Smithsonian Institution
Social Security Administration
Society for Industrial and Applied Mathematics
Southwest Research Institute
Special Equipment Inspection and Research Institute (China)
Web3D Consortium
World Wide Web Consortium

Universities

Arizona State University
Beijing Institute of Technology (China)
University of Petroleum (China)
Carnegie Mellon University
City University of Hong Kong (China)
Colorado State University
Columbia University
Concordia University (Canada)
Courant Institute of Mathematical Sciences
Dalian University of Technology (China)
Dartmouth College
Duke University
East Carolina University
East China University of Science and Tech. (China)
Federal University of Rio Grande do Norte (Brazil)
George Mason University
Georgetown University
George Washington University
Howard University
Imperial College London (UK)
Indiana University
Iowa State University
Jacobs University Bremen (Germany)
Karlsruhe Institute of Technology (Germany)
Khallikote College (India)
Kings College London (UK)
Lanzhou University of Technology (China)
Lund University (Sweden)
Nanyang University (Singapore)
National University of Singapore
Naval Postgraduate School
New York University
Ningbo University (China)
Northwestern University
Oslo University (Norway)
Polytechnic University of Valencia (Spain)
Purdue University
Queensland University of Technology (Australia)
Rice University
Rochester Institute of Technology
Russian Academy of Sciences
Shandong University (China)
Stanford University
Tel-Aviv University (Israel)
Texas Tech University
Three Gorges University (China)
Tokyo Institute of Technology (Japan)
Tsinghua University (China)
Tulane University
Universidad de Castilla (Spain)
University of Antwerp (Belgium)
University of Bergamo (Italy)
University of Bologna (Italy)
University of Bordeaux (France)
University of British Columbia (Canada)
University of California, Berkeley
University of California, San Diego
University of Campinas (Brazil)
University of Colorado, Boulder
University of Erlangen-Nuremberg (Germany)
University of Hong Kong (China)
University of Houston
University of Illinois, Urbana-Champaign
University of Indiana, Bloomington
University of Innsbruck (Austria)
University of Limerick (Ireland)
University of Lisbon (Portugal)
University of Maryland, Baltimore County
University of Maryland, College Park
University of Maryland, University College
University of Miami
University of Michigan
University of Minnesota
University of North Texas
University of Oslo (Norway)
University of Oulu (Finland)
University of South Carolina
University of Southampton (UK)
University of Surrey (UK)
University of Texas, Arlington
University of Waterloo (Canada)
University of Windsor (Canada)
University of Wisconsin
University of Zagreb (Croatia)
Vanderbilt University
Virginia Polytechnic Institute
Virginia State University
Washington University, St. Louis
Worcester Polytechnic University
Yale University
Yokohama National University (Japan)

Part V

Appendix

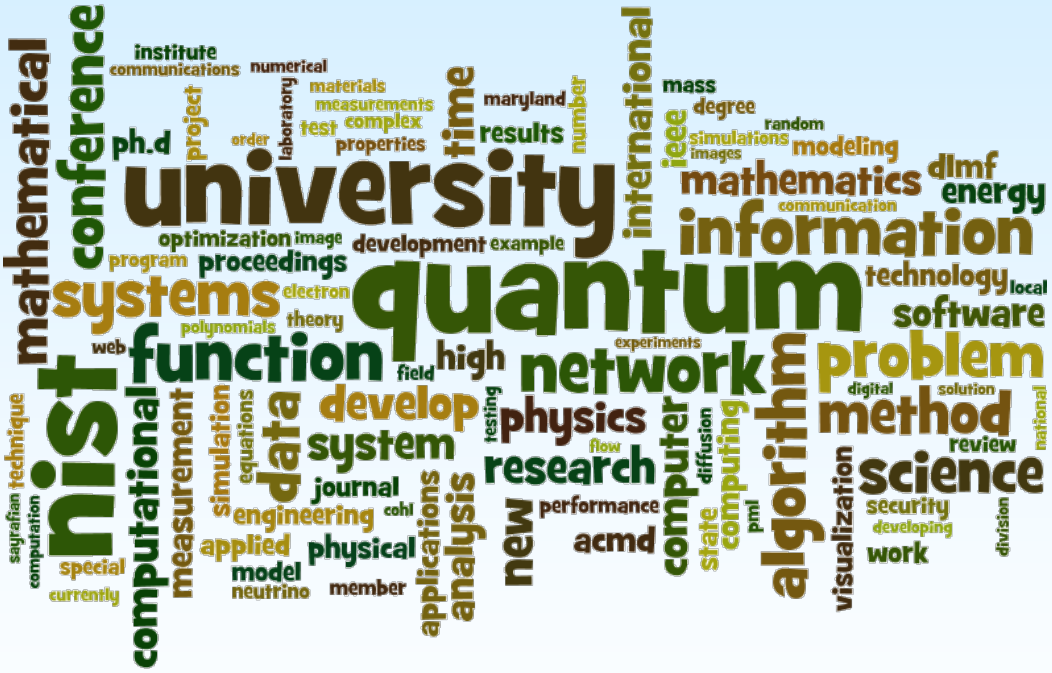

Staff

ACMD consists of full time permanent staff located at NIST laboratories in Gaithersburg, MD and Boulder, CO. This is supplemented with a variety of special appointments. The following list reflects all non-student appointments held during any portion of the reporting period (October 2015 – December 2016). Students and interns, are listed in Table 1 and Table 2 below. * Denotes staff at NIST Boulder.

Division Staff

Ronald Boisvert, *Chief*, Ph.D. (Computer Science), Purdue University, 1979
Catherine Graham, *Secretary*
Lochi Orr, *Administrative Assistant*, A.A. (Criminal Justice), Grantham University, 2009
Alfred Carasso, Ph.D. (Mathematics), University of Wisconsin, 1968
Roldan Pozo, Ph.D. (Computer Science), University of Colorado at Boulder, 1991
Kamran Sayrafian-Pour, Ph.D. (Electrical and Computer Engineering), University of Maryland, 1999
Christopher Schanzle, B.S. (Computer Science), University of Maryland Baltimore County, 1989

Mathematical Analysis and Modeling Group

Timothy Burns, *Leader*, Ph.D. (Mathematics), University of New Mexico, 1977
*Bradley Alpert, Ph.D. (Computer Science), Yale University, 1990
Sean Colbert-Kelly, Ph.D. (Mathematics), Purdue University, 2012
*Andrew Dienstfrey, Ph.D. (Mathematics), New York University, 1998
Jeffrey Fong, Ph. D. (Applied Mechanics and Mathematics), Stanford University, 1966
*Zydrunas Gimbutas, Ph.D. (Applied Mathematics), Yale University, 1999
Fern Hunt, Ph.D. (Mathematics), New York University, 1978
Raghu Kacker, Ph.D. (Statistics), Iowa State University, 1979
Anthony Kearsley, Ph.D. (Computational and Applied Mathematics), Rice University, 1996
Geoffrey McFadden, *NIST Fellow*, Ph.D. (Mathematics), New York University, 1979
Paul Patrone, Ph.D. (Physics), University of Maryland, 2013
Bert Rust, Ph.D. (Astronomy), University of Illinois at Urbana-Champaign, 1974

NRC Postdoctoral Associates
Ryan Evans, Ph.D. (Applied Mathematics), University of Delaware, 2016

Faculty Appointee (Name, Degree / Home Institution)
Daniel Anderson, Ph.D. / George Mason University
Dianne O'Leary, Ph.D. / University of Maryland College Park
Michael Mascagni, Ph.D. / Florida State University
Florian Potra, Ph.D. / University of Maryland Baltimore County

Guest Researchers (Name, Degree / Home Institution)
David Gilsinn, Ph.D. / NIST (retired)
Yu (Jeff) Lei, Ph.D. / University of Texas at Arlington
Itzel Dominquez Mendoza / Centro Nacional de Metrología, Mexico
Christoph Witzgall, Ph.D. / *NIST Scientist Emeritus*

Mathematical Software Group

Michael Donahue, *Leader* Ph.D. (Mathematics), Ohio State University, 1991
Javier Bernal, Ph.D. (Mathematics), Catholic University, 1980
Howard Cohl, Ph.D. (Mathematics), University of Auckland, 2010

Stephen Langer, Ph.D. (Physics), Cornell University, 1989
Daniel Lozier, Ph.D. (Applied Mathematics), University of Maryland, 1979
Marjorie McClain, M.S. (Mathematics), University of Maryland College Park, 1984
Bruce Miller, Ph.D. (Physics), University of Texas at Austin, 1983
William Mitchell, Ph.D. (Computer Science), University of Illinois at Urbana-Champaign, 1988
Donald Porter, Ph.D. (Electrical Engineering), Washington University, 1996
Bonita Saunders, Ph.D. (Mathematics), Old Dominion University, 1985
Barry Schneider, Ph.D. (Physics), University of Chicago, 1969

Faculty Appointees (Name, Degree / Home Institution)
G.W. Stewart, Ph.D. / University of Maryland College Park
Abdou Youssef, Ph.D. / George Washington University

Guest Researchers (Name, Degree / Home Institution)
Gunay Dogan, Ph.D. / Theiss Research
Adri Olde Daalhuis, Ph.D. / University of Edinburgh
Leonard Maximon, Ph.D. / George Washington University
Mark Pederson, Ph.D. / DOE Office of Science
Jianwei Sun, Ph.D. / Temple University
Qiming Wang / NIST (retired)

Computing and Communications Theory Group

Ronald Boisvert, *Acting Leader,* Ph.D. (Computer Science), Purdue University, 1979
Isabel Beichl, *Project Leader,* Ph.D. (Mathematics), Cornell University, 1981
Brian Cloteaux, Ph.D. (Computer Science), New Mexico State University, 2007
*Scott Glancy, Ph.D. (Physics), University of Notre Dame, 2003
Barry Hershman, A.A. (Electronics Engineering), Capitol College, 1979
Stephen Jordan, Ph.D. (Physics), Massachusetts Institute of Technology, 2008
*Emanuel Knill, *NIST Fellow,* Ph.D. (Mathematics), University of Colorado at Boulder, 1991
Paulina Kuo, Ph.D. (Physics), Stanford University, 2008
Yi-Kai Liu, Ph.D. (Computer Science), University of California, San Diego, 2007
Lijun Ma, Ph.D. (Precision Instruments and Machinery), Tsinghua University, 2001
Vladimir Marbukh, Ph.D. (Mathematics) Leningrad Polytechnic University, 1986
James Shook, Ph.D. (Mathematics), University of Mississippi, 2010
Oliver Slattery, Ph.D. (Physics), University of Limerick, 2015
Xiao Tang, *Project Leader,* Ph.D. (Physics), Chinese Academy of Sciences, 1985

NRC Postdoctoral Associates
*Charles Baldwin, Ph.D. (Physics), University of New Mexico, 2016

Faculty Appointees (Name, Degree / Home Institution)
James Lawrence, Ph.D. / George Mason University

Guest Researchers (Name, Degree / Home Institution)
*Peter Bierhorst, Ph.D. / University of Colorado
*Bryan Eastin, Ph.D. / Northrup Grumman
Assane Gueye, Ph.D. / University of Maryland
Richard La, Ph.D. / University of Maryland
Alan Mink, Ph.D. / Theiss Research
Francis Sullivan, Ph.D. / IDA Center for Computing Sciences

High Performance Computing and Visualization Group

Judith Terrill, Leader, Ph.D. (Information Technology), George Mason University, 1998
Yolanda Parker, Office Manager
William George, Ph.D. (Computer/Computational Science), Clemson University, 1995
Terence Griffin, B.S. (Mathematics), St. Mary's College of Maryland, 1987
Wesley Griffin, Ph.D. (Computer Science), University of Maryland Baltimore County, 2016
John Hagedorn, M.S. (Mathematics), Rutgers University, 1980
Sandy Ressler, M.F.A. (Visual Arts), Rutgers University, 1980
Steven Satterfield, M.S. (Computer Science), North Carolina State University, 1975
James Sims, Ph.D. (Chemical Physics), Indiana University, 1969

Faculty Appointees (Name, Degree / Home Institution)
Marc Olano, Ph.D. / University of Maryland Baltimore County

Guest Researchers (Name, Degree / Home Institution)
Jian Chen, Ph.D. / University of Maryland Baltimore County

Table 1. *Undergraduate and graduate student interns in ACMD.*

Name	From	Program		Mentor	Topic
Alhajjar, Eli	George Mason U.	G	FGR	J. Lawrence	Polytopes, matroids, greedoids
Jensen, Alathea	George Mason U.	G	DGR	F. Hunt	Polytopes, matroids, greedoids
Keith, Adam	U. Colorado Boulder	G	PREP	E. Knill	Quantum measurement analysis
Khrac, Katjana	U. Zagreb, Croatia	G	FGR	K. Sayrafian	Positioning metrology in the human body
Mayer, Karl	U. Colorado Boulder	G	PREP	E. Knill	Protocols for quantum optics
Sauer, Franz	U. California Davis	G	NPSC	J. Terrill	Visualization for HydratiCA
Van Meter, James	U. Colorado Boulder	G	PREP	E. Knill	Quantum measurement of space-time
Vazquez Lundrove, Marilyn	George Mason U.	G	FGR	S. Langer	Microstructure image analysis
Wills, Peter	U. Colorado Boulder	G	PREP	E. Knill	Statistical analysis for quantum info
Zhang, Lizhong	ISIMA	G	FGR	S. Langer	OOF software development
Cooper, Samuel	Fayetteville State U.	U	SURF	S. Langer	OOF software development
Deng, Myra	Columbia U.	U	SURF	Beichl	Monte Carlo for network measurements
Dougherty, Eric	Millersville U.	U	SURF	S. Ressler	Virtual reality on web pages
Dunkers, Dan	Drexel U.	U	SURF	J. Terrill	Virtual reality
Greiner-Petter, Andre	TU Berlin	U	FGR	H. Cohl	Computer algebra systems and semantic LaTeX
Laurenceau, Harry	Bowie State U.	U	SURF	J. Terrill	Virtual reality
Maass, Steffen	Jacobs U. Bremen	U	FGR	B. Miller	Digital Library of Mathematical Functions
Mayer, Justin	U. of DC	U	SURF	J. Terrill	Virtual reality
Schmoll, Felix	Jacobs U. Bremen	U	FGR	B. Miller	Digital Library of Mathematical Functions
Sriram, Vinay	Stanford U.	U	SURF	J. Terrill	Virtual reality

Legend *G* *Graduate student*; *U* *Undergraduate*; *PREP* *Professional Research Experience Program (Boulder)*; *FGR* *Foreign Guest Researcher*; *NPSC* *National Physical Sciences Consortium Fellow*; *DGR* *Domestic Guest Researcher*; *SURF* *Summer Undergraduate Research Fellowship*

Table 2. *High school interns in ACMD.*

Name	From	Pro-gram	Mentor	Topic
Amani, Ahmed	Wootton HS	SHIP	J. Terrill	Visualizing yield onset in thermoset polymers
Bang, Joon	Poolesville HS	SVP	H. Cohl	Digital Repository of Mathematical Formulae
Bian, Edward	Poolesville HS	SVP	H. Cohl	Digital Repository of Mathematical Formulae
Chen, Kevin	Poolesville HS	SVP	H. Cohl	Digital Repository of Mathematical Formulae
Fink, Zachary	Clarksburg, HS	SVP	H. Cohl	Definite integrals from density-potential pairs in spaces of constant curvature
Hu, Amanda	Poolesville HS	SVP	H. Cohl	Verifying traceability to proofs in DLMF
Kapoor, Yash	Clarksburg, HS	SVP	H. Cohl	Literature search for special function formulas
Lin, Raymond	Montgomery Blair HS	SHIP	J. Terrill	Virtual Reality
Ly, Adrian	Montgomrey Blair HS	SHIP	S. Satterfield	Audio Utilites for High End Visualization
Oza, Parth	Poolesville HS	SVP	H. Cohl	Digital Repository of Mathematical Formulae
Park, Justin	Poolesville HS	SVP	H. Cohl	Special functions and orthogonal polynomials
Prem, Jaga	Poolesville HS	SVP	H. Cohl	Incorporating semantics in LaTeX expressions
Shah, Rahul	Clarksburg, HS	SVP	H. Cohl	Digital Repository of Mathematical Formulae
Shen, Kevin	Poolesville HS	SVP	H. Cohl	Digital Repository of Mathematical Formulae
Tang, Grace	Poolesville HS	SVP	H. Cohl	Verifying traceability to proofs in DLMF
Tang, Nina	Poolesville HS	SVP	H. Cohl	Verifying traceability to proofs in DLMF
Tkach, Oksana	Poolesville HS	SVP	H. Cohl	Digital Repository of Mathematical Formulae
Van Gieson, Yusuf	Wootton HS	SHIP	S. Satterfield	Audio utilities for high end visualization
Vellala, Sourabh	Poolesville HS	SVP	H. Cohl	Digital Repository of Mathematical Formulae
Wang, Philip	Poolesville HS	SVP	H. Cohl	Digital Repository of Mathematical Formulae
Yoo, Seong Joon	Poolesville HS	SVP	H. Cohl	Digital Repository of Mathematical Formulae
Yu, Edwin	Wootton HS	SVP	J. Terrill	CAVE software tests
Zong, Kevin	Wootton HS	SHIP	O. Slattery	Automation of optical fiber pulling and power transmission setup
Zou, Claude	Poolesville HS	SVP	H. Cohl	Incorporating semantics in LaTeX expressions

Legend *HS High school* *SHIP Summer High school Internship Program* *SVP Student Volunteer Program*

Glossary of Acronyms

2D	two-dimensional
3D	three-dimensional
AAAS	American Association for the Advancement of Science
ACM	Association for Computing Machinery
ACMD	NIST/ITL Applied and Computational Mathematics Division
ACTS	Advanced Combinatorial Testing System
AIP	American Institute for Physics
ALCC	Advanced Leadership Computing Challenge
ANSI	American National Standards Institute
API	application programmer's interface
APS	American Physical Society
arXiv	preprint archive housed at Cornell University (http://arxiv.org/)
ASCR	Advanced Scientific Computing Research
BAN	body area network
BGP	border gateway protocol
BMP	Bateman Manuscript Project
BOF	Birds of a Feather session
BQP	bounded-error quantum polynomial time (complexity class)
CAIDA	Center for Applied Internet Data Analysis
Caltech	California Institute of Technology
CAVE	Cave Automatic Virtual Environment
CCM	Combinatorial Coverage Measurement
CCS	controlled-controlled-signflip
CENAM	Center for Metrology of Mexico
CI	configuration interaction
CICM	Conference on Intelligent Computer Mathematics
CMA	University of Antwerp Computational Mathematics Research Group
CMOS	complementary metal-oxide semiconductor
CNRS	Centre National de la Recherche Scientifique (France)
CNST	NIST Center for Nanoscale Science and Technology
COW	cell on wheels
CPA	cryoprotective agents
CPU	central processing unit
CS	component system
CSCAMM	Center for Scientific Computation and Mathematical Modeling, University of Maryland
CSH	calcium silicate hydrate
CT	combinatorial testing
CT	computed tomography
CTL	NIST Communications Technology Laboratory
CY	calendar year
DARPA	Defense Advanced Research Projects Agency
DC	direct current
DLMF	Digital Library of Mathematical Functions
DMC	diffusion Monte Carlo
DNA	deoxyribonucleic acid
DOC	Department of Commerce
DOE	U.S. Department of Energy
DPD	dissipative particle dynamics
DRMF	digital repository of mathematical functions
DSO	display shared object
ECHo	an experiment to estimate neutrino mass from ^{163}Ho electron capture using MMC measurement
EIT	electromagnetically induced transparency
EL	NIST Engineering Laboratory
EM	expectation maximization

ETSI	European Telecommunications Standards Institute
FEDVR	finite element discrete variable method
FEM	finite element method
FFT	fast Fourier transform
FWM	four wave mixing
FY	fiscal year
GPU	graphics processing units
GUI	graphical user interface
HEC	High End Computing
HEV	high end visualization
HMD	head-mounted display
HOLMES	an experiment to estimate neutrino mass from ^{163}Ho electron capture using TES measurements
HPCVG	ACMD High Performance Computing and Visualization Group
HTML	hypertext markup language
HVAC	heating, ventilation and air conditioning
Hy-CI	Hylleraas-Configuration Interaction technique
IBBR	UMD-NIST Institute for Bioscience and Biotechnology Research
ICN	information and communication network
ICST	International Conference of Software Testing
ICT	information and communication technologies
IDA	Institute for Defense Analysis
IDE	integro-differential equations
IDS	interdependent security
IEEE	Institute of Electronics and Electrical Engineers
IFIP	International Federation for Information Processing
IMA	Institute for Mathematics and Its Applications
IMACS	International Association for Mathematics and Computers in Simulation
IMS	NIST Innovations in Measurement Science program
IoT	Internet of things
IP	internet protocol
IPCMS	Institut de Physique et Chimie des Matériaux de Strasbourg
ISG	industry specification group
ISGG	International Society for Grid Generation
ISIMA	Institut Supérieur d'Informatique, de Modélisation et de leurs Applications (France)
ITL	NIST Information Technology Laboratory
IVE	immersive visualization environment
JILA	joint NIST-University of Colorado physics research institute
JMONSEL	simulation code used to model electron scattering in materials
JQI	Joint Quantum Institute
KLS	Koekoek, Lesky and Swarttouw
LaTeX	a math-oriented text processing system
LIGO	Laser Interferometer Gravitational-Wave Observatory
MAA	Mathematical Association of America
MathML	Mathematical Markup Language (W3C standard)
MCMC	Monte Carlo Markov Chain
MD	molecular dynamics
MIT	Massachusetts Institute of Technology
MMC	metallic magnetic calorimeters
MML	NIST Material Measurement Laboratory
MPI	Message Passing Interface
MRAM	magneto-resistive random access memory
MRI	magnetic resonance imaging
MS	mass spectroscopy
MSE	mean squared error
muMAG	Micromagnetic Activity Group
NASA	National Aeronautics and Space Administration
NBS	National Bureau of Standards

NIST	National Institute of Standards and Technology
NISTIR	NIST Internal Report
NITRD	Networking and Information Technology Research and Development
NMR	nuclear magnetic resonance
NRC	National Research Council
NSF	National Science Foundation
NYU	New York University
ODE	ordinary differential equation
OOF	Object-Oriented Finite Elements (software)
OOMMF	Object-Oriented Micromagnetic Modeling Framework (software)
OPSF	orthogonal polynomials and special functions
P2C	presentation to computation
PCA	principal components analysis
PDE	partial differential equation
PHAML	Parallel Hierarchical Adaptive Multi Level (software)
PIMC	path integral Monte Carlo
PML	NIST Physical Measurement Laboratory
PoCF	probability of cascading failures
POM	part of math
PPLN	periodically poled lithium niobate
PSNR	peak signal-to-noise ratio
QD	quantum dot
QDPD	quarternion-based dissipative particle dynamics
QIS	quantum information science
QKD	quantum key distribution
QuICS	UMD-NIST Joint Center for Quantum Information and Computer Science
R&D	research and development
RAW	Robert-Asselin-Williams filtering technique
RDF	radial distribution function
RF	radio frequency
SED	NIST/ITL Statistical Engineering Division
SEM	scanning electron microscope
SHIP	NIST Summer High School Internship Program
SIAM	Society for Industrial and Applied Mathematics
SIGGRAPH	ACM Special Interest Group on Graphics
SMC	spectral Monte Carlo
SPH	smoothed particle hydrodynamics
SPIE	International Society for Optical Engineering
SQUID	superconducting quantum interference device
SRM	standard reference material
SURF	NIST Student Undergraduate Research Fellowship program
TACC	Texas Advanced Computing Center
TES	transition edge sensor
TLS	transport layer security
UMBC	University of Maryland Baltimore County
UMD	University of Maryland
UMIACS	University of Maryland Institute for Advanced Computer Studies
UQ	uncertainty quantification
VR	virtual reality
VRML	virtual reality modeling language
W3C	World Wide Web Consortium
WebGL	Web-based Graphics Library
X3D	Extensible 3D
X3DOM	an open-source framework for integrating X3D and HTML5
XSEDE	NSF eXtreme Science and Engineering Discovery Environment
XML	Extensible Markup Language